I. MOLECULAR ASSEMBLY: CLATHRINS–AN INSPIRATION FOR THE GENERATION OF CLOSED MOLECULAR SURFACES BY NON-COVALENT SELF ORGANIZATION
PART II. MOLECULAR DISASSEMBLY BY ZINC EJECTION AS A STRATEGY AGAINST HIV MATURATION : A MODEL STUDY

THESIS SUBMITTED
TO THE UNIVERSITY OF KERALA
IN PARTIAL FULFILMENT OF THE REQUIREMENTS
FOR THE DEGREE OF
DOCTOR OF PHILOSOPHY
IN CHEMISTRY
UNDER THE FACULTY OF SCIENCE

BY

K. M. MURALEEDHARAN

BIOMOLECULAR RESEARCH UNIT
REGIONAL RESEARCH LABORATORY
THIRUVANANTHAPURAM-695 019, KERALA, INDIA

JANUARY, 2000

PART I. MOLECULAR ASSEMBLY: CLATHRINS–AN INSPIRATION FOR THE GENERATION OF CLOSED MOLECULAR SURFACES BY NON–COVALENT SELF ORGANIZATION
PART II. MOLECULAR DISASSEMBLY BY ZINC EJECTION AS A STRATEGY AGAINST HIV MATURATION : A MODEL STUDY

THESIS SUBMITTED
TO THE UNIVERSITY OF KERALA
IN PARTIAL FULFILMENT OF THE REQUIREMENTS
FOR THE DEGREE OF
DOCTOR OF PHILOSOPHY
IN CHEMISTRY
UNDER THE FACULTY OF SCIENCE

BY

K. M. MURALEEDHARAN

BIOMOLECULAR RESEARCH UNIT
REGIONAL RESEARCH LABORATORY
THIRUVANANTHAPURAM-695 019, KERALA, INDIA

JANUARY, 2000

INDIAN INSTITUTE OF CHEMICAL TECHNOLOGY
HYDERABAD- 500 007

DISCOVERY LABORATORY, ORGANIC III

Dr. Darshan Ranganathan, F.A.Sc.; F.N.A.
Deputy Director

CERTIFICATE

Certified that the work contained in this thesis entitled "**Part I. Molecular assembly: Clathrins - an inspiration for the generation of closed molecular surfaces by non-covalent self organization. Part II. Molecular disassembly by zinc ejection as a strategy against HIV maturation: A model study**", has been carried out by Mr. K. M. Muraleedharan under my supervision and the same has not been submitted elsewhere for any other degree.

Darshan Ranganathan

(Thesis Supervisor)

DEDICATED TO MY PARENTS

ACKNOWLEDGEMENTS

With great admiration and appreciation, I acknowledge my supervisor Dr. Darshan Ranganathan for her invaluable and stimulating suggestions and creative guidance, which greatly enhanced my interest in the subject. Her hard working nature and high will power has always been an inspiration for me. I am grateful and thankful to her with no words in dearth.

Words are inadequate to express my deep sense of gratitude to Prof. S. Ranganathan for his encouragement, valuable advice and prudent guidance throughout my work. I am most thankful to him for introducing me in to this challenging field of Chemistry, filled with powerful themes on the various aspects of Information - Function system. It is my immense fortune to be under his tutelage during this valuable period of my life. A special word of thanks to Dr. A. Ranganathan for his help in computational molecular modelling.

I am extremely grateful to Dr. A. D. Damodaran, our previous director and Dr. G. Vijay Nair, the present Director for providing all the infrastructural facilities in the laboratory.

I am highly indebted to Prof. M. V. George for the help he extended during the course of this work. I also thank Dr. Mangalam S. Nair, Dr. Suresh Das, Dr. A. Ajayaghosh and Dr. K. R. Gopidas of RRL, Trivandrum for their help during the course of this work.

I take great pleasure in acknowledging Dr. Dipankar Chatterjee, M.B.U, IISc, for kindly providing me the facilities to carry out part of the biological studies reported in this thesis. I am also thankful to Dr. Vijaya Gopal, C.C.M.B for the valuable help she extended during the course of this work. I also thank Mr. Anil, Ms. Pallavi, Sujatha and Prabhudhua of M.B.U, I.I.Sc for their help and cooperation. My sincere thanks are also due to Dr. V. L. Narayanan, NIH, USA, for kindly carrying out the cytotoxic studies reported in this thesis.

My sincere gratitude is also due to Prof. S. Chandrasekharan, IISc for his interest in my work and for kindly providing various instrumental facilities. I am thankful to Dr. Sampath, Inorganic and Physical Chemistry Division, IISc for kindly helping me in gold surface modification studies. A special word of thanks to Ms. Smita, IPC, IISc, for her help during the study.

I am thankful to Dr. K. P. Madhusudanan (CDRI, Lucknow) and Dr. Vairamani (IICT, Hyderabad) for providing the mass spectral data reported in this thesis. I am also thankful to Dr. Parimal. K. Bharadwaj (IIT Kanpur) and Dr. Isabella Karle (Naval Research

Laboratory, Washington, U.S.A), for providing the X-ray data of various compounds reported here.

I have great pleasure in acknowledging my labmates, Dr. N. Tamilarasu, Dr. Achamma Thomas, Dr. V. Haridas, Ms. Sunita Kurur, Ms. Lakshmi .C, and Mr. Sreekanth for their co-operation and cheerful company during the course of my work. A special word of thanks to Ms. Priya. E. P for her help during the work. I also thank my labmates in IICT for their help and co-operation.

I am thankful to N. Manoj, Sheeba, Uma, Soumini, Swaroop, Prasad, Robert Philip, Mathew George, CRC, Raju Francis and all other members of Photochemistry and Organic Chemistry divisions for their help and co-operation during various stages of this work.

I thank Mr. Sisupalan for his help during sealed tube experiments.

I have great pleasure in acknowledging the Malayali family at IICT, whose cheerful company and co-operation made my stay at Hyderabad homely.

I humbly thank my family members whose love and encouragement remain the source of inspiation behind all achievements.

Muraleedharan. K. M

CONTENTS

PREFACE

The main focus of the work described in this thesis is on the design of molecular systems that mimic key biological functions like molecular assembly and disassembly. The thesis is divided into two parts (Part I and Part II), each of which is again sub divided into, A. Introduction, B. Background, C. Present work, D. Biological studies, E. Experimental, F. Spectra and G. References, related to each topic.

Part I describes our endeavours to design clathrin models, where non-covalent self organization play an important role in the formation of polyhedral lattices. Various supramolecular synthons were envisaged for bringing about the assembly, which include i) the directed organization of N-amino maleimide, ii) mellitic tris-N-amino imide, iii) hydrocarbon analog of mellitic tris N-amino imide iv) ligand directed assembly of peripherally hydrogen bonded mellitic acid hexa amidated systems v) ionic assembly of mellitic acid salts and vi) the metal directed assembly of the cyclic hexa peptide, Cyclo-[Glu(γOMe)Gly]$_3$. Various experimental findings during the course of synthesis of these systems are described here. Even though the goal of 'self assembled polyhedral lattices' remained elusive, the idea of spherical assembly has been secured, although in a left handed manner, by the synthesis of methionine based

mellitic acid-hexa amidated system, and demonstrating its assembly on a gold electrode, thereby providing scope for creating a spheroidal surface on colloidal gold. This section also describes the cytotoxic studies on the RuVIII oxidation product of Trindane. All the compounds are characterized by detailed spectral studies.

Part II of the thesis demonstrates the concept of exchange mechanisms in bringing about molecular disassembly. Various redox systems of the type Ar-S-S-Ar, having different amino acid appendages (Ala, Val, Aib, Pro, Phe, Ser, Met, Trp, His etc.) were synthesized for zinc ejection from the active site of RNA polymerase, the key enzyme involved in gene expression. The synthesis and characterization of all compounds are described in detail. The fragmentation of Ar-S-S-Ar systems to isothiazolidene-3-ones were observed in the case of amino acids which have a proton source in the side chain (eg. Threonine, serine, tryptophan, histidine etc.). Tethered Ar-S-S-Ar systems based on cystine was also synthesized for understanding the steric factors which affect the exchange processes. The inhibitory action of these compounds on RNA polymerase were studied by evaluating the percentage loss of activity of the enzyme in gene expression, taking Calf thymus DNA as the template. Significant inhibition of transcription was observed with several of the compounds studied.

LIST OF PUBLICATIONS

1. One step transformation of tricyclopentabenzene (trindane) [$C_{15}H_{18}$] to 4 - [(1R, 2S, 4R, 5S) - 1, 2, 5-trihydroxy - 3 - oxabicyclo [3.3.0] octane - 4 spiro-1'- (2'-oxocyclopentan)-2-yl] butanoic acid [$C_{15}H_{22}O_7$], Subramania Ranganathan, **K. M. Muraleedharan**, Parimal Bharadwajaj and K.P. Madhusudanan, *J. Chem Soc.Chem. Commun.*, 1998, 2239.

2. The Preference Profiles in Ruthenium Tetroxide Oxidations, S. Ranganathan, **K. M. Muraleedharan**, D. Bhattacharyya and D. Kundu, *J. Indian Chem. Soc.*, 1998, 75, 10-12, 583 - 589

3. Templated molecular assemblies on gold surface: Complete monolayer coverage with Benzene hexa carbox-[hexa-L-carbomethoxy methionyl]-amide, Subramania Ranganathan, **K. M. Muraleedharan**, Sampath and Smitha (manuscript under preparation)

4. Anticancer activity of 4 - [(1R, 2S, 4R, 5S)-1, 2, 5-trihydroxy - 3 - oxabicyclo *[3.3.0]octane-4 spiro-1'- (2'-oxocyclopentan)-2-yl]* butanoic acid, Subramania *Ranganathan and* ***K. M. Muraleedharan***
(manuscript under preparation)

5. Successful design of RNA Polymerase inhibitors by removal of zinc from [CCXX] boxes by thiol-disulfide exchange, Subramania Ranganathan, **K. M. Muraleedharan**, Dipankar Chatterji, Parimal Bharadwaj and Isabella Karle (manuscript under preparation)

Review

Halo and Seleno Lactonization, S. Ranganathan, D. Ranganathan, N. K. Vaish, **K. M. Muraledharan**. (Accepted in *Organic Reactions*)

ABBREVIATIONS

(1) All amino acids are represented by the standard three letter codes (e.g. Glu-Gly represents a peptide formed from the amino acids, glutamic acid and glycine) or standard one letter codes (e.g. G for glycine and E for glutamic acid)

(2) Standard abbreviations, s, d, t, q, m, dd, represents singlet, doublet, triplet, quartet, multiplet, and doublet of doublet in the NMR spectral assignments

Other abbreviations used in the thesis are as follows:

aq	: aqueous
Ar	: aromatic ring
Boc	: tert-butyloxycarbonyl
BOP	: benzotriazol-1-yloxy-tris(dimethylamino)phosphonium hexafluorophosphate
Bzl	: benzyloxycarbonyl
DCC	: dicyclohexylcarbodiimide
DMF	: dimethyl formamide
DMSO	: dimethyl sulfoxide
EtOAc	: ethyl acetate
FAB MS	: fast atom bombardment mass spectroscopy
FT	: fourier transform
g	: gram
GC	: gas chromatography

GI 50	: cell growth inhibition by 50%
h	: hour
IR	: infra red
mCPBA	: meta chloro perbenzoic acid
MeOH	: methanol
mL	: millilitre
M.p.	: melting point
MS	: mass spectroscopy
NCp	: nucleocapsid protein
NEt_3	: triethylamine
NMR	: nuclear magnetic resonance
NOE	: nuclear overhauser effect
OMe/OCH_3	: O-methyl ester
PAF	: platelet aggregation factor
PG	: percentage growth
POPOP	: 1,4-bis(5-phenyloxazol-2-yl)benzene
ppb	: parts per billion
ppm	: parts per million
py	: pyridine
ROESY	: rotating frame overhauser effect spectroscopy
satd.	: saturated
TFA	: trifluoroacetic acid
TGI	: total cell growth inhibition
TLC	: thin layer chromatography

PART I.

MOLECULAR ASSEMBLY: CLATHRINS - AN INSPIRATION FOR THE GENERATION OF CLOSED MOLECULAR SURFACES BY NON-COVALENT SELF ORGANIZATION

I.A. INTRODUCTION

A decade before the discovery of fullerene [C-60], a system with identical topology, called clathrin was known to biologists. These, aggrandized by the simple module triskelion, consisting of three each of heavy and light chain proteins, play a pivotal role in endocytosis, a critical cell function. Clathrin assembly is a more exciting phenomenon, since the required spherical topology is created entirely by reversible , non covalent interactions. Endeavours reported here [Section I.C] pertains to the crafting of spherical surfaces by non covalent self assembly, as a first step towards the understanding of clathrin assembly. The goal remained elusive, though much interesting chemistry was generated. The goal has been secured, although in a left handed and serendipitous way.

The narration falls into four categories. In the initial design, the spherical assembly was conceived by the generation of a 18 atom equatorial region by the formation of 12 hydrogen bonds of constructs anchored on an aromatic core. This is followed by the crafting of systems that assemble on a gold surface through ligands that are anchored on a hydrogen bonded periphery. Several types of ionic self assembly are illustrated that are anchored on the mellitic acid core. Finally models were constructed that could mimic the formation of triskelion assembly that involves the congruence of 12 carboxylic groups,

I.B. BACKGROUND

The crafting of surfaces by self assembly involving non covalent bonds is an area that has received attention in the recent past and has led to profound developments in diverse areas and has enabled the simulation of highly complicated biological events. As a brief background to the present work, illustrative examples are presented, that would have a bearing on the work reported in the thesis pertaining to studies on the preparation of clathrin models .

Endeavours in this area can be summarized briefly as follows.1) General principles 2) Self assembling complexes 3) Intra molecular networks 4) Amide networks and 5) Selected illustrations. Only those macromolecular structures arising from the involvement of hydrogen bonds are presented.

1) General principles

During the past few years, a growing volume of information is available, pertaining to assembly by hydrogen bonding. Efforts have been made to arrive at broad guidelines that could lead to these assemblies. The situation is somewhat like that in organic synthesis, which became quite organized with the introduction of 'synthons' and 'retrosynthetic analysis'. Networks arising from hydrogen bonding or almost all its manifestations, can be analyzed in terms of modules **1** - **11** presented in Chart I.B.1.[1] The examples presented in Chart I.B.1 are

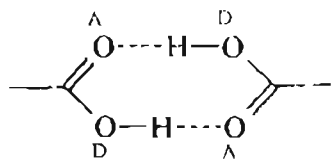

1

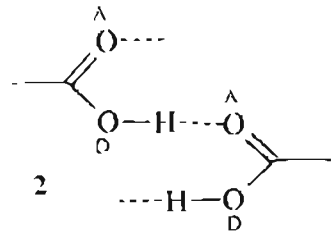

2

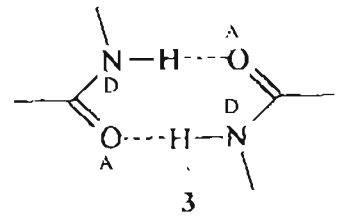

3

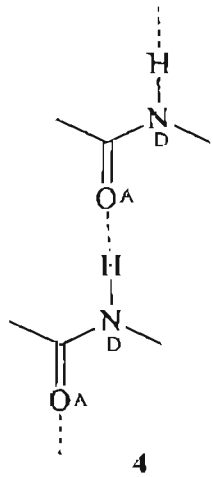

4

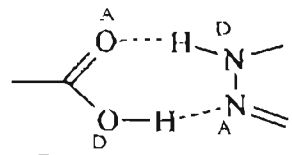

5

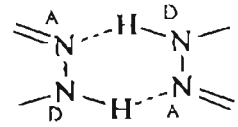

6

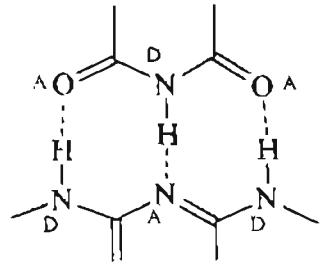

7

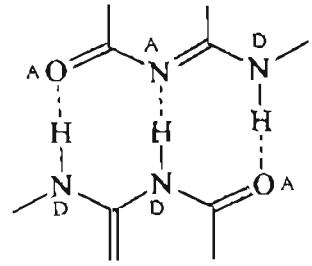

8

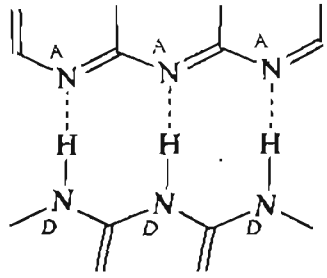

9

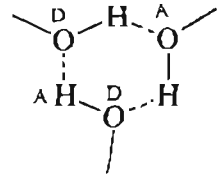

10

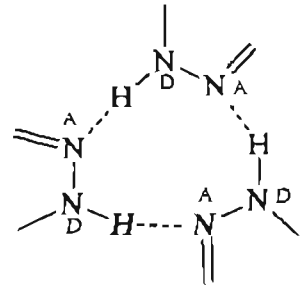

11

Chart I.B.1.

designated either as ligand donor (D) or ligand acceptor (A). In most cases, the ligand is H and here only established ligand donors (O, N) are listed. One could see from Chart I.B.1 that, with a donor - acceptor criteria, a primary ordering of hydrogen bonded structures can be achieved. For example, the complex from melamine and barbituric acid,[1] shown in Chart I.B.2 is of [D A D] melamine [A D A] barbituric acid type. The melamine cyanuric acid system presented in Chart I.B.3 could be used as an illustration as to how such hydrogen bonded noncovalent assemblies can be regulated to produce a desirable type of surface.[2] The assembly involved here is of the D A D melamine, A D A cyanuric acid type. The dimer unit in **12** (Chart I.B.3) can be

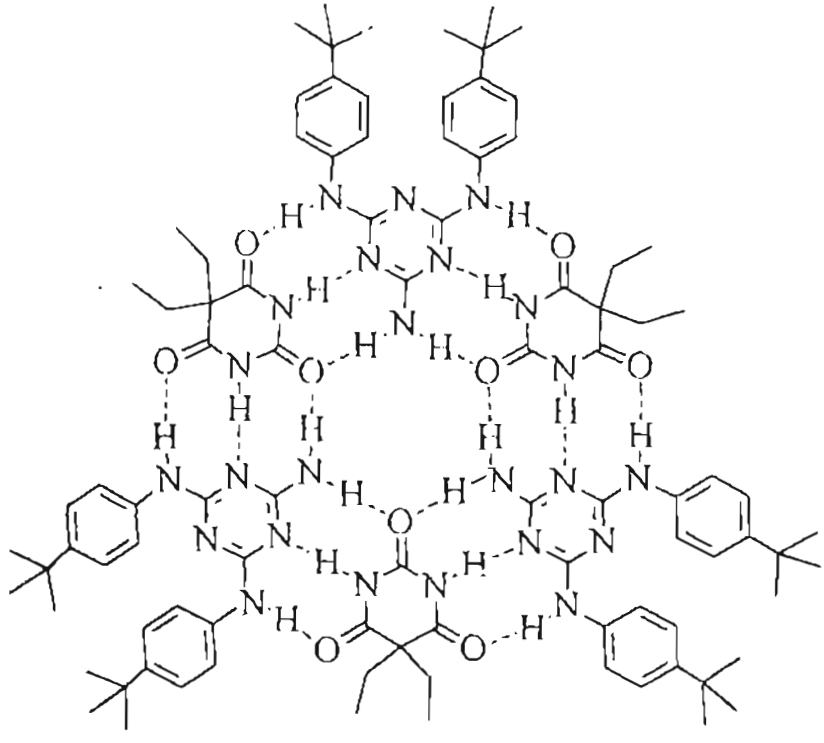

Chart I.B.2.

abbreviated in terms of discs as shown. The concept of such disc assembly has led to methodologies for designing and crafting of a desired surface based on the fundamental [D A D] - [A D A] assembly. An excellent illustration of this is shown in **13** (Chart I.B.3) where a tethered melamine unit is elegantly recognized by cyanuric acid to provide a three dimensional surface.[2]

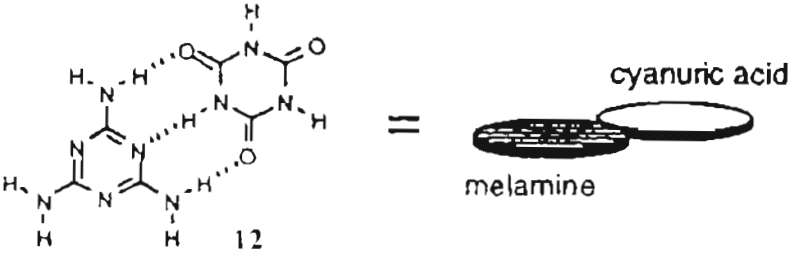

12

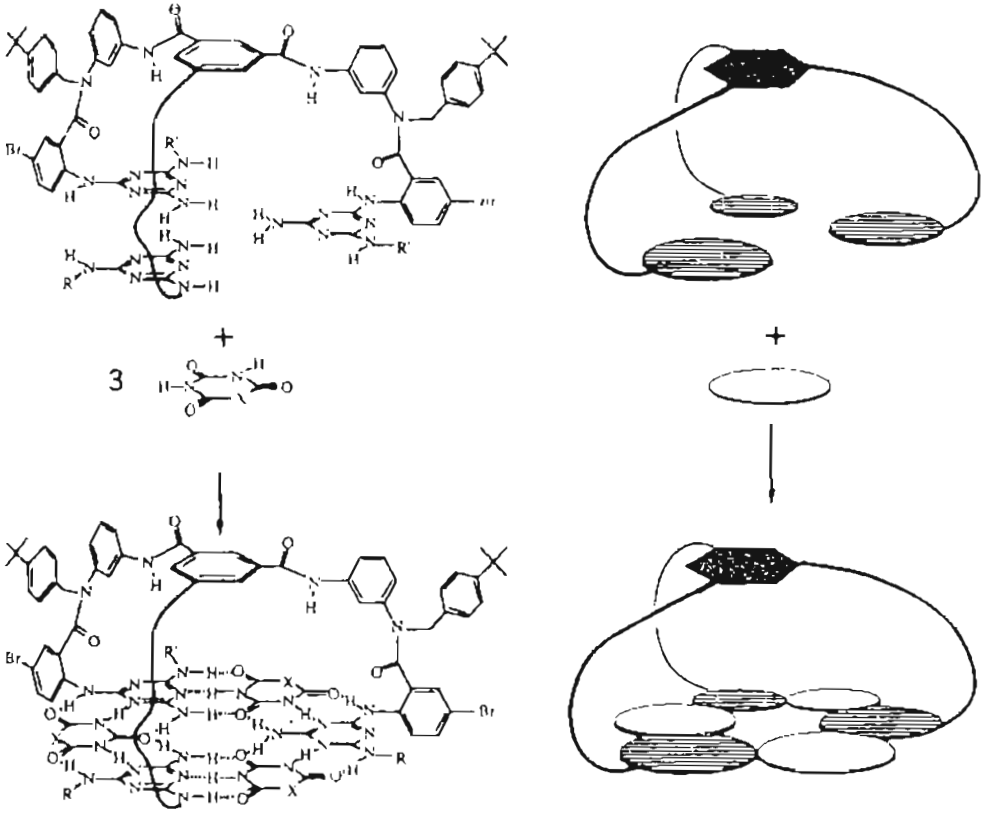

13

Chart I.B.3. R' = $(CH_2)_2C(CH_3)_3$. X = NR' (neo-hexylisocyanuric acid)

2) Self assembling complexes

The design possibilities whereby carefully placed hydrogen bonds form assemblies leading to surfaces of various profiles is a challenging and useful exercise. In one of the early illustrations,[3] compound **14** was shown to form a dimeric molecule **15**, promoted principally by the formation of 8 hydrogen bonds as shown in Chart I.B.4. The resulting supramolecule produces an open cavity, which has been shown capable of harbouring small molecules like

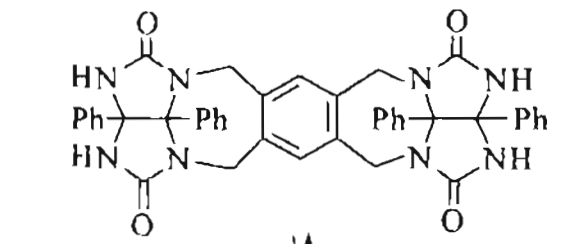

14

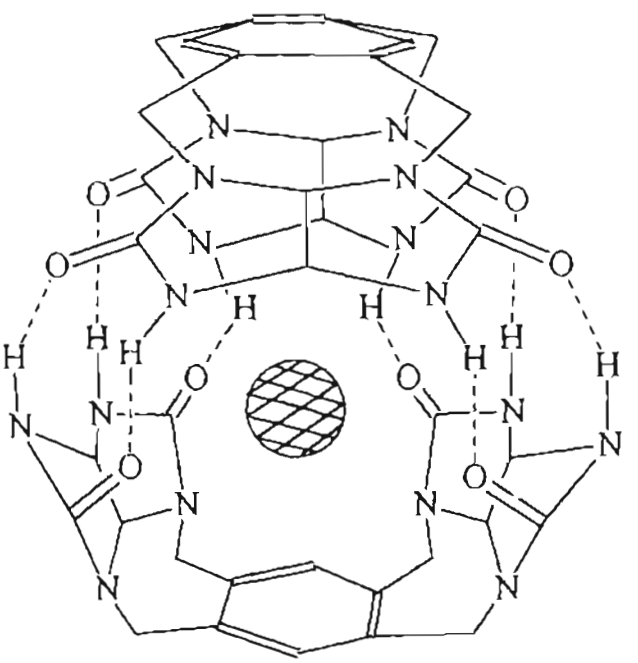

15

Chart I.B.4. Self assembled molecular Tennis ball. Phenyl groups are not shown in **15** for clarification. The sphere represents guest molecule like methane

methane. This provides sufficient evidence to show that a small number of hydrogen bonding interactions can, if carefully chosen, offset the disadvantages imposed by entropy, pertaining to ordering of molecules which are tuned for dimerization. The work presented here also is based along these expectations

The turning point in the design of these structures, leading to a better comprehension of their potential, came from the proton triggered self assembly process of the cyclic peptide cyclo-[-(D-Ala-Glu-D-Ala-Gln)$_2$-] (**16**, Chart I.B.5).[6] Here, the proton triggered assembly is highly convergent, where numerous ring shape peptides are stacked through an extensive network of hydrogen bonds, to form nanotube structures. The design has been so made that, the presence of the glutamic acid side chains makes the triggering of the assembly process possible by adjustment of pH. In alkaline solution, the glutamate side chains, move against each other by electrostatic repulsion, thus not making the thing favourable for intermolecular interactions. However, lowering of the pH, makes these glutamic acid side chains reach for each other and in this process, provide a splendid opportunity of the sub units to stack in an anti parallel fashion and participate in a back bone to back bone intermolecular hydrogen bonding to produce a contiguous β sheet structure as shown in Chart I.B.5. Indeed, under acid conditions, the assembly leads to rod shaped crystals. Subsequent developments have enabled the demonstration of such nanotubes in

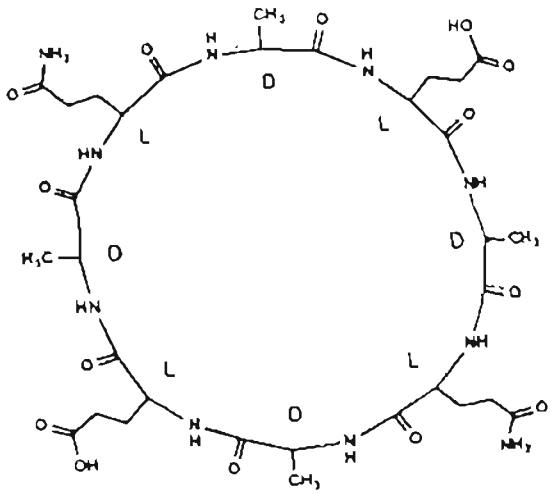

16

Self assembly

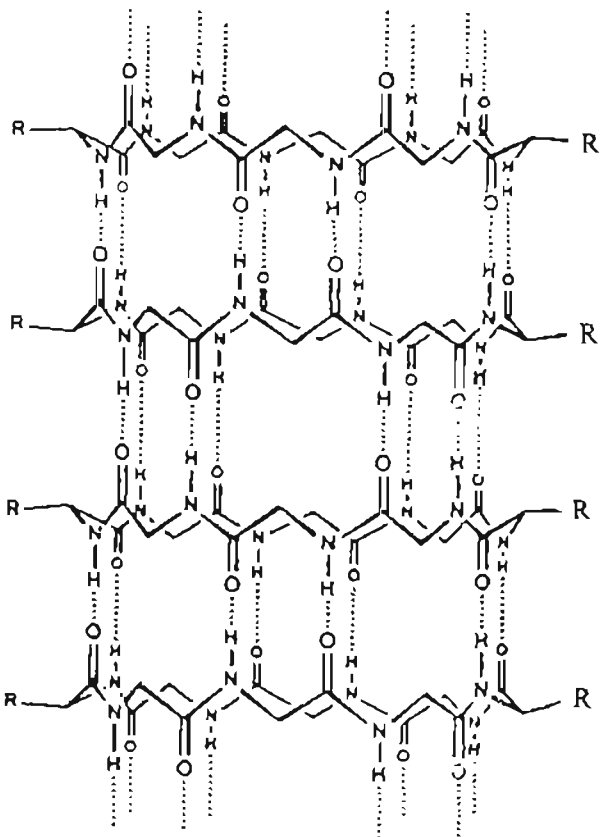

Chart I.B.5.

specific transport of small biomolecules like glucose and that, related designs could be embedded in membranes to generate transmembrane channels.[4b-f]

More recently, the design of such nanotubes has been exceptionally simplified by crafting them from cystine diOMe and methylene chain 1,ω–isocyanates (**17**).[5] X-ray crystallographic studies have shown that they form elegant channels as shown in Chart I.B.6. Thus, the molecular assembly by such stacking interactions, generate a wide range of possibilities enabling crafting of surfaces of designed description.

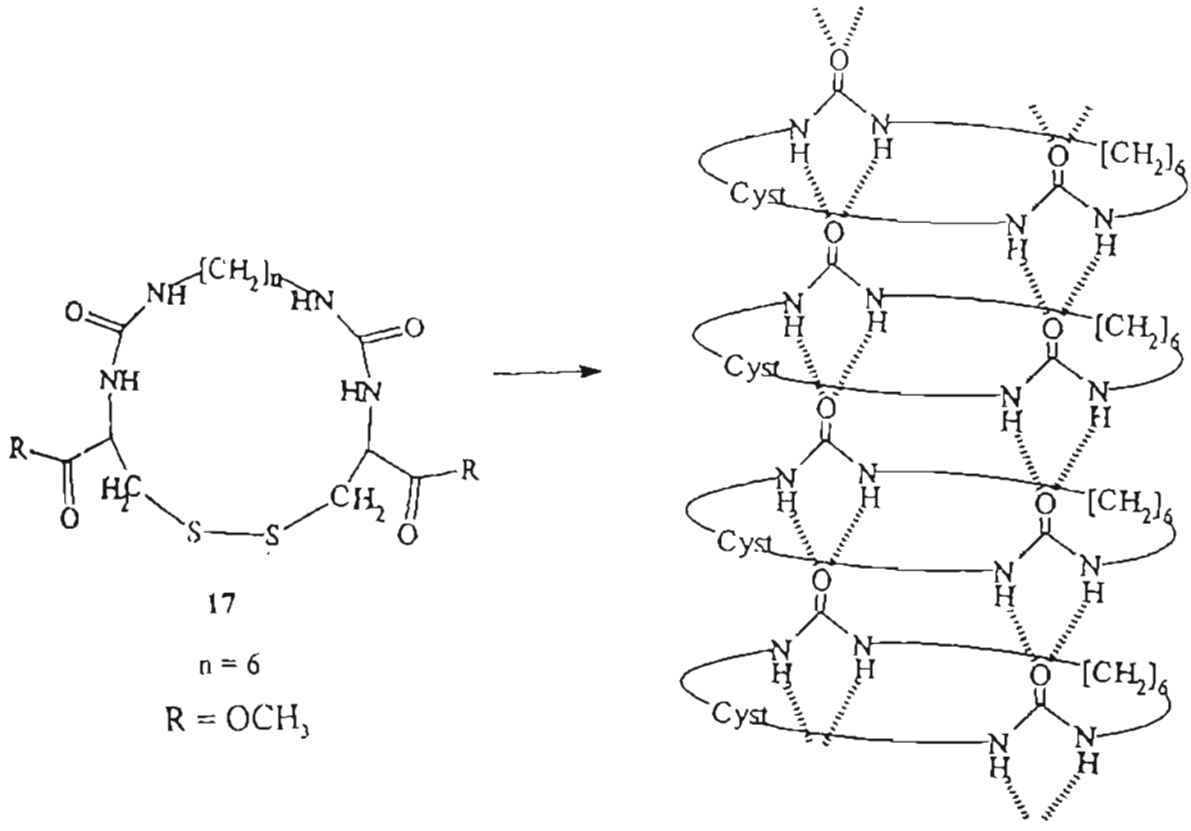

Chart I.B.6.

3) Intramolecular networks

An area in self assembly using hydrogen bonding which still needs attention is that pertaining to intramolecular hydrogen bonding. The concept of the addition of aromatic ring created by hydrogen bonding in o-hydroxy acetophenone, when extended, can lead to a variety of arrays and facets of this are related to the present work.

Placement of appropriate contiguous donor - acceptor pairs around a pericycle would be the simplest mode for the generation of surfaces by hydrogen bonding. This is best illustrated with the symmetrical three fold acceptors of a substituted triamino benzene[6] (Chart I.B.7, **18-23**).

18

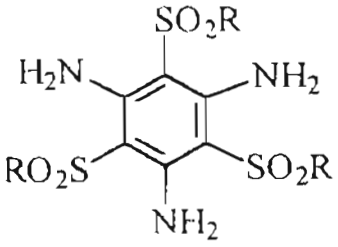

R = CF_3: **19**
R = CH_3: **20**
R = Et : **21**

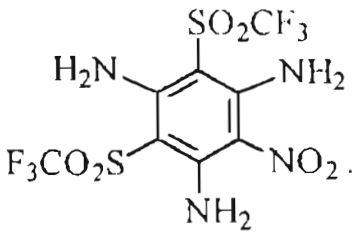

22

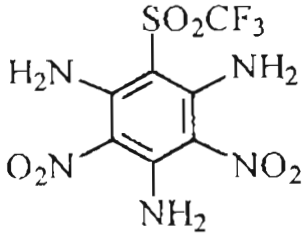

23

Chart I.B.7.

A basic property of such system is that, due to the stabilization arising with substitution, the 3 donor-3 acceptor system have their π electron density shifted from the benzene core as shown in Chart I.B.8.

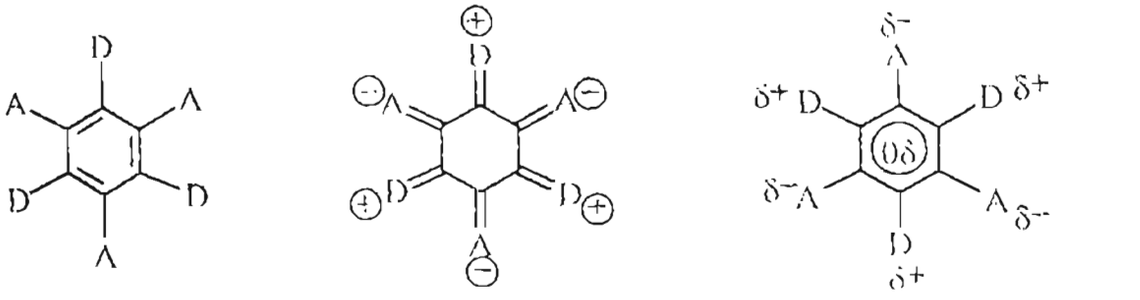

Benzenoid Radialenoid Octapolar charge distribution

Chart I.B.8.

The substitution of the acceptor moiety in these systems can be used as a control in engineering the crystal structures. In simply alkyl substituted sulfonyl compounds, like **20** and **21**, no layer structure was observed, with the molecules as dimers orthogonally arranged. In sharp contrast, substitution of the hydrogen with fluorine leads to layer structure, the tilting of which can further be controlled by substitution. In general, a characteristic feature of donor - acceptor arrays around a benzene pericycle leads to compounds where one sees intra as well as intermolecular arrangements as shown in Chart I.B.9. An element of control in their arrangement can be introduced by appropriate substitution. The crystal structure of **18** has been studied by two groups.[6,7] In the earlier version,

the notable feature was reported as one where the π charge of the aromatic ring was totally taken outside, resulting in a radialene type of structure and the periphery consisted of the expected 6 hydrogen bonded pattern as shown in Chart I.B.9. A more recent examination of this compound have further revealed that the compound **18** exist as two polymorphs,[h] of which one is noncentrosymmetric. They form graphite like structures of approximate trigonal symmetry of the pattern shown in Chart I.B.9.

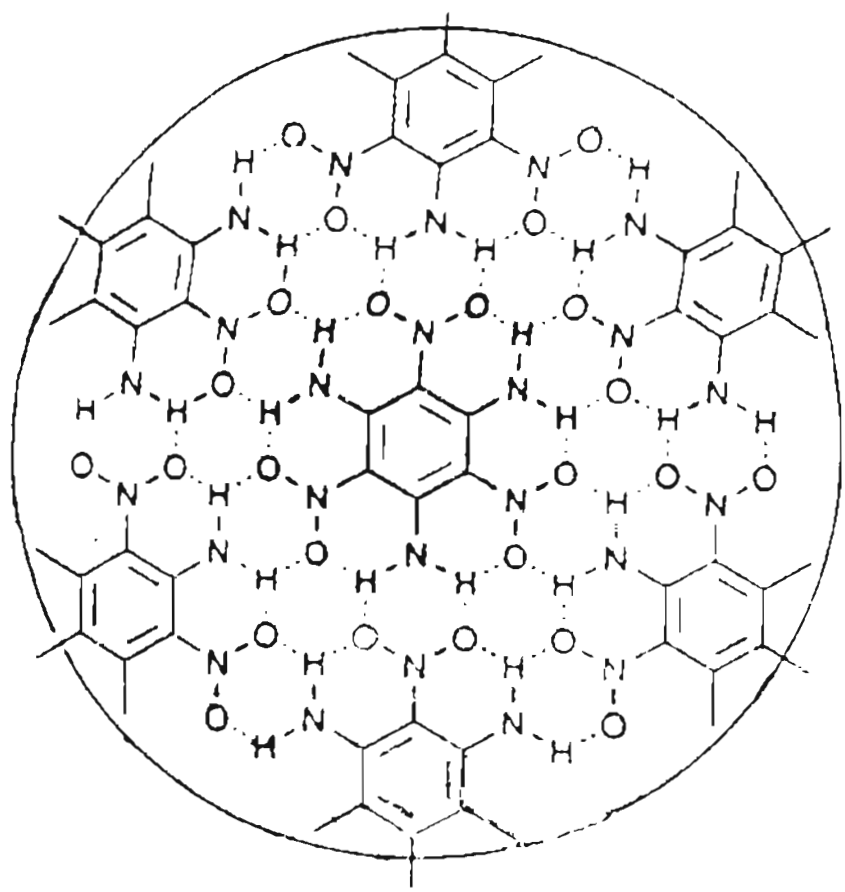

Chart I.B.9.

The comparison of this compound with that of graphite brings out above all, that the intramolecular hydrogen bondings that constitute the layer is like the covalent bonds in graphite that surround an aromtic ring. The stacking in these, as seen in graphite structures arises from interaction between layers which is substantially weaker.

The strong intramolecular hydrogen bonding in ortho-hydroxy nitro benzene is also seen in the case of 4,6 dinitro resorcinol (24, Chart I.B.10). Here the donor acceptor pairs are symmetrically arranged around the vertical axis of the benzene ring. The structure determined by gas phase electron diffraction brings out the significant result of very strong resonance assisted intramolecular hydrogen bonding.[8] The compound is highly symmetrical and planar and in some ways could be considered as a hetero analogue of anthracene.

Dimethyl-3,6-dichloro-2,5-dihydroxy terephthalate presents an interesting case of possibilities with reference to the formation of intramolecular hydrogen bonded networks[9] (Chart I.B.10). The compound exist in two crystallographic forms, the yellow one, which on heating goes to the white form. Detailed crystallographic studies have shown that the yellow form could be represented as 25 where the expected intramolecular hydrogen bonding of the hydroxyl to the proximate ester group is seen. On the other hand, the white compound is one

where hydrogen bonding exist between the phenolic hydroxyls and the chlorine atoms (**26**).

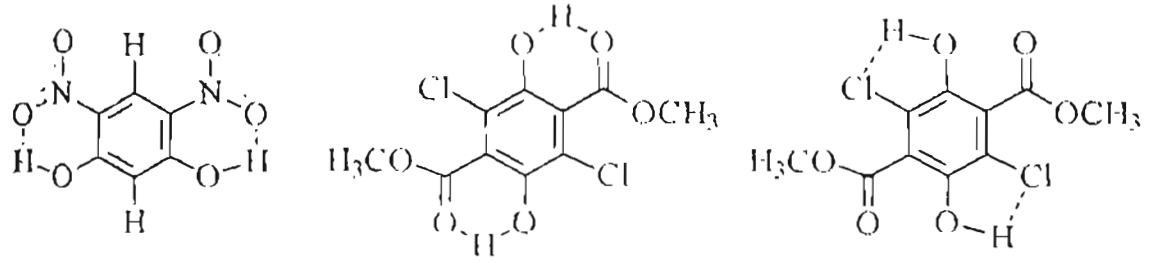

24 **25** **26**

Chart I.B.10.

The concept of crafting core anchored hydrogen bonded surfaces presents infinite possibilities Thus simple dissolution of tris(4,5-dihydroimidazo-2yl)-benzene (**27**) with three equivalents of trifluoroacetic acid provides compound **28**, whose X ray structure clearly shows the peripheral hydrogen bond networking (Chart I.B.11).[10] In this concept, a peripheral hydrogen bond networking is achieved by using an auxiliary such as trifluro acetic acid. Such approaches can, not only lead to greater flexibility in design but also could make the synthetic procedures easier.

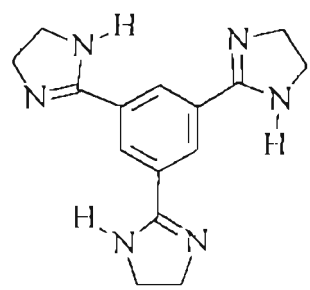

27

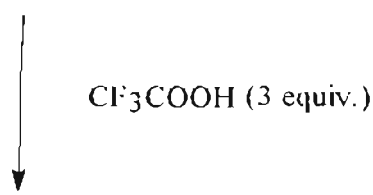

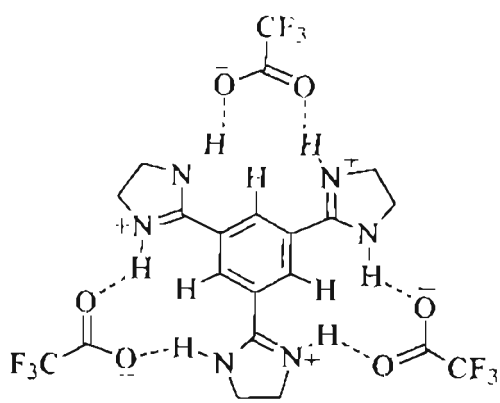

28

Chart I.B.11.

4. Amide networks

Historically, the transformation of ammonium isocyanate to urea marked the preparation of naturally occurring substances by synthesis. Indeed, in the context of formation of hydrogen bonding networks, the corner stone is still the urea molecule whose hydrogen bonding possibilities as well as its very numerous analogs have been extensively studied. The networking formed by amide bonds have been examined from diverse perceptions. Basic to this unit is the presence of a donor - acceptor pair. As has been pointed out earlier, even with such a simple unit, it is possible to craft with confidence, a variety of intricate structures. The possibilities in this direction have been extensively covered[11] and in this section, only highlights pertaining to the present work are presented.

A very elegant example which shows that highly hydrogen bonded surfaces can be crafted from very simple amides is that shown in Chart I.B.12 relating to oxalamide.[12] The hydrogen bonded networking as shown in **29** extends in two planes, making maximum opportunity for the hydrogen bonding possibilities. Recent studies on the telomeric ends of chromosomes have shown that they are composed of quadricolumnar stacks of G4 surfaces that could keep potassium and sodium ions, thus performing a very key biological function, namely, the sealing of the chromosomal ends. As could be seen from **30** (Chart I.B.12), the amide type of hydrogen bonding is the core of the G4 motif which is

peripherally stabilized by N-H---N hydrogen bonding, forming exquisite frame work, which could well be a model for the design of other complex structures. [13]

An excellent example where illustrations can be made for predictable properties in crystal and solution structures is provided by the simple amides arising from linking of the pyridone unit with an acetylene. It was predicted, as shown in Chart I.B.13, that the anti compound would form a hydrogen bonded surface as shown in **31**, and that the syn compound would not be able to form such a compound and therefore it would lead to a linear polymer (**32**). Interestingly, these expectations were shown to be true both in the crystal state as well as in solution[13].

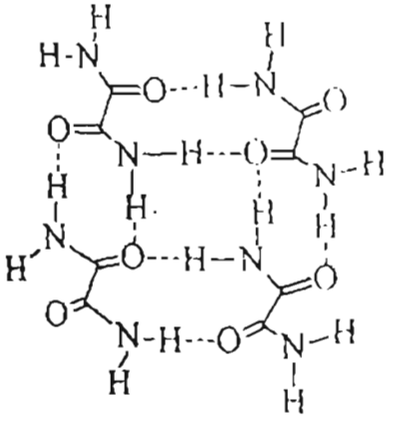

29

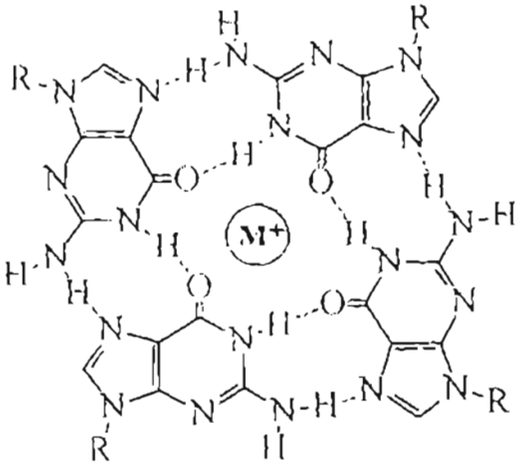

30

Chart I.B.12.

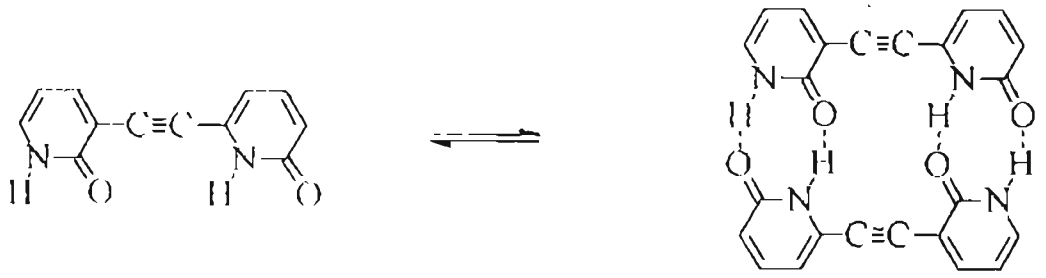

31

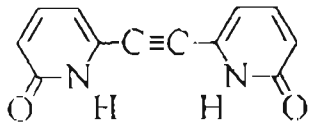

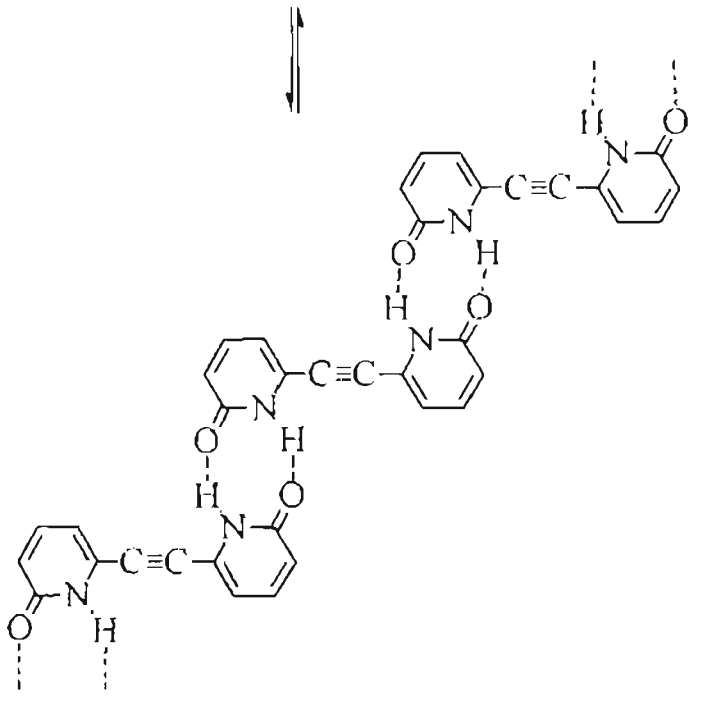

32

Chart I.B.13.

5. Selected illustrations

Amphiphilic hydrogen bonding networks consisting of alkylated melamines and ammonium head group appended cyanuric acids are stably dispersed in water as supramolecular membranes[14] (**33**, Chart I.B.14).

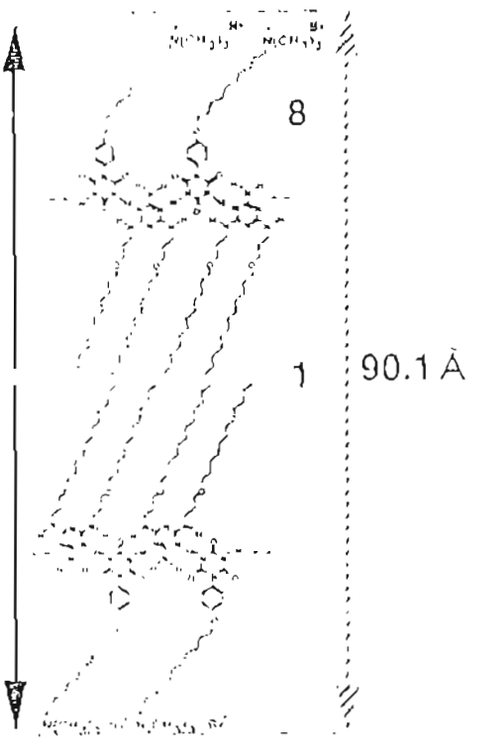

Chart I.B.14.

33

In the course of sacharide metabolism, the sugars are transported through cellular membranes. Nature has evolved elaborate proteins for this transport, a notable one being the L-Arabinose binding protein (ABP) whose crystal structure clearly showed that the recognition mainly arises from interaction of each of the sugar hydroxyls and indeed, this recognition is generally brought about by the side chains of planar amino acids like arginine, asparagine, aspartic acid and

glutamic acid[15]. A profile of this interaction is shown in Chart I.B.15, **34**. That invitrosystems can be crafted based on this concept is demonstrated by the fact, complexation of Phloroglucinol can be achieved by a designed receptor as shown in Chart I.B.15, **35**.

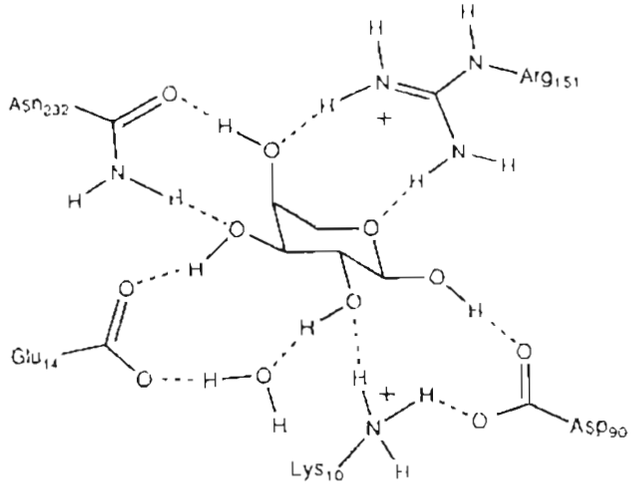

34

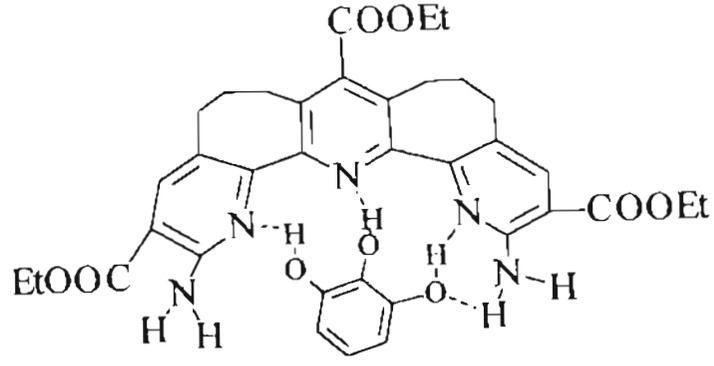

35

Chart I.B.15.

Metal ion anchored hydrogen bonded networking can lead to materials which could have properties similar to zeolites and this aspect has been illustrated in Chart I.B.16 (**36**, **37**).[36] 1,3,5-benzenetricarboxylic acid (BTC) on reaction with metal acetates (Co, Ni, Zn) leads to tetra hydrate coordinated benzenetricarboxylates that are hydrogen bonded to give a tightly held 3D networks, which, as shown in Chart I.B.16, on heating, gives up loosly held water ligands. The voids thus created produces channels which have sufficient pore diameter close to that observed in zeolites and molecular sieves. The particular arrangement shown in Chart I.B.16 can include ammonia. The uptake and loss of water are reversible.

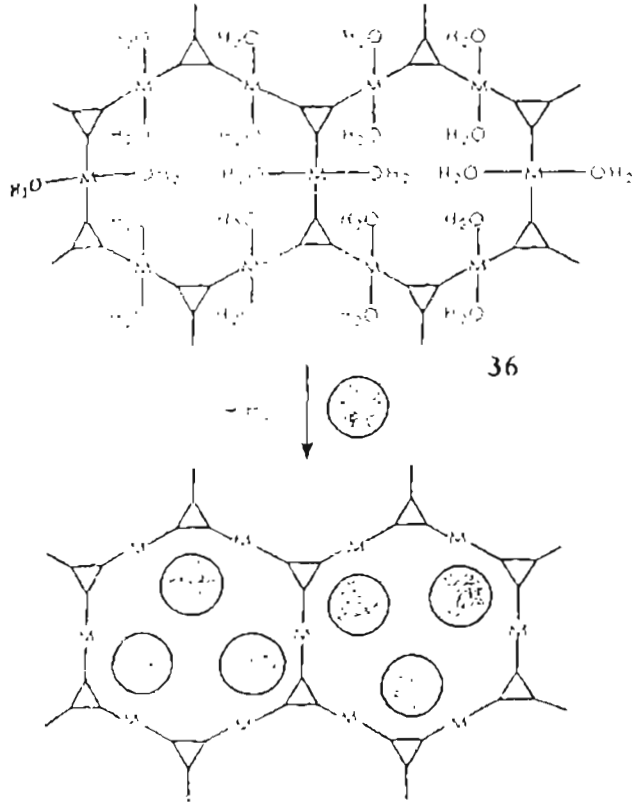

36

37

Chart I.B.16

- 1,3,5-benzene tricarboxylic acid

M = Metal

Compound **37** represents an interesting situation where an aromatic template and a metal core are held to produce macromolecules whose design can be widely varied to produce channels that could have simple or complex properties.

The two arms of amide arising from benzene 1,3 dicarboxylic acid and 2-amino 6,methyl pyridine lie at an angle to each other. This aspect has been very elegantly taken advantage of, to craft a self assembling hydrogen bonded helix using a 1,ω–dicarboxylic acid like pimelic acid which could comfortably complex with alternating arms of the amide (**38**) as shown in Chart I.B.17. Thus crystallization of a mixture of **38** and heptane dioic acid (pimelic acid) afforded crystals composing of alternating units of **38** and pimelic acid linked by a netwotrk of hydrogen bonds (**39**). Interestingly, the U turn shape of **38** enforces an overall helical arrangement on to the strand[17].

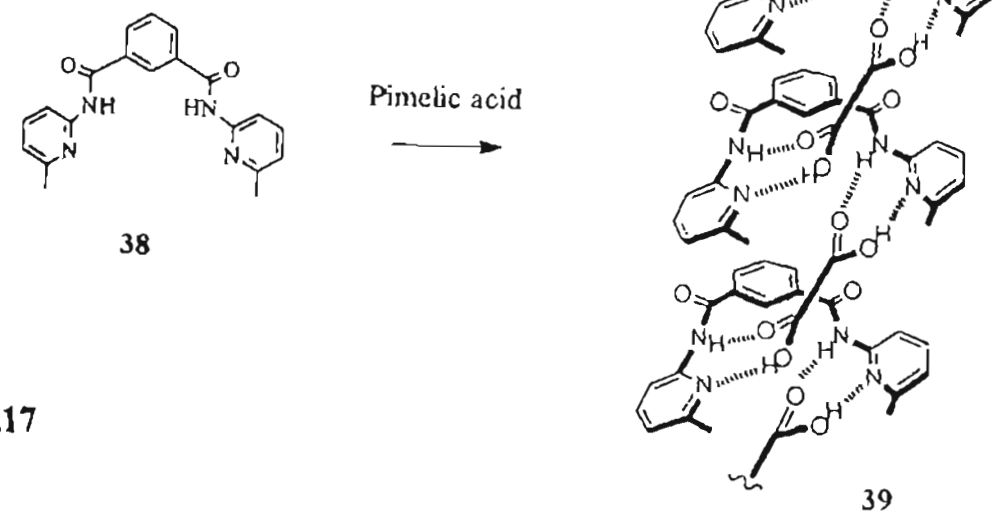

38 **39**

Chart I.B.17

I.C. PRESENT WORK

A decade before the discovery of fullerene, a system with identical topology, called clathrin was known to biologists [Fig. I.C.1(a,b)]. These, aggrandized by the simple module, triskelion, consisting of three each of heavy and light protein chains [Fig. I.C.1(c-g)], play a pivotal role in endocytosis, a critical cell function.[9] Clathrin assembly is a more exciting phenomenon, since the required spherical topology is created entirely by non covalent interactions. A comparison of the profiles of fullerene and clathrin presented in Table I.C.1 dramatically illustrates the complexity of clathrin assembly. The triskelions assemble at pH 5 - 6 and disassemble above pH 9. The crafting of spherical surfaces by non covalent assembly would be an appropriate starting point in the understanding of much more complex clathrin assembly.

A 3 dimensional retrosynthetic strategy was developed towards the construction of spherical surfaces by non covalent assembly, the cornerstone of which was the formation of the spherical equatorial girdle consisting of 18 atoms in one step motivated by the genesis of 12 hydrogen bonds. Starting from simple N-aminomaleimide, aggrandization of six units of which can generate a spherical assembly, entropy constraints were increasingly imposed to promote the critical assembly.

a. Clathrin cage (21A° resolution)

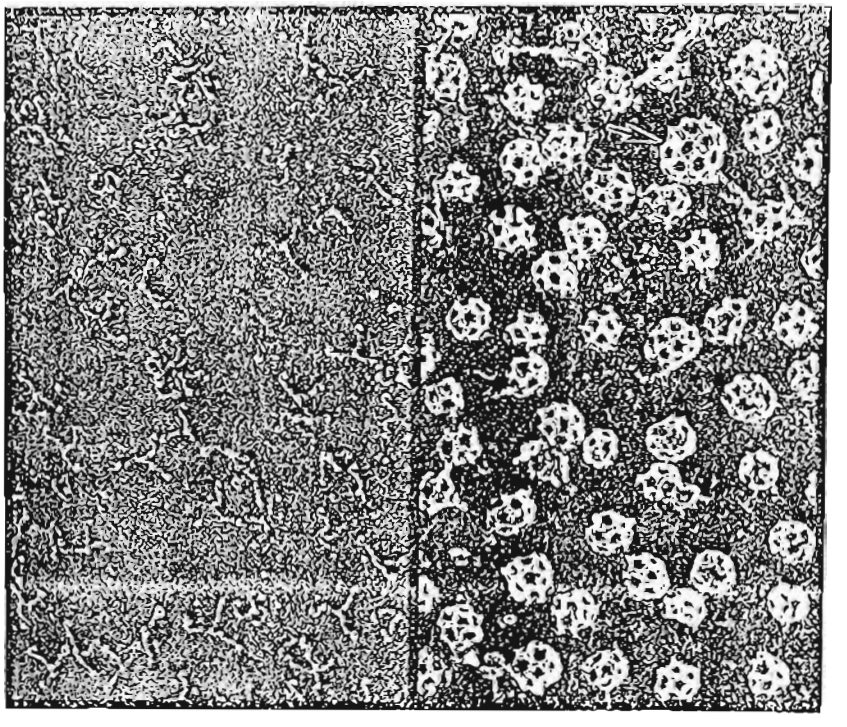

b. SEM pictures of Clathrin formation from triskelions

Fig. I.C.1

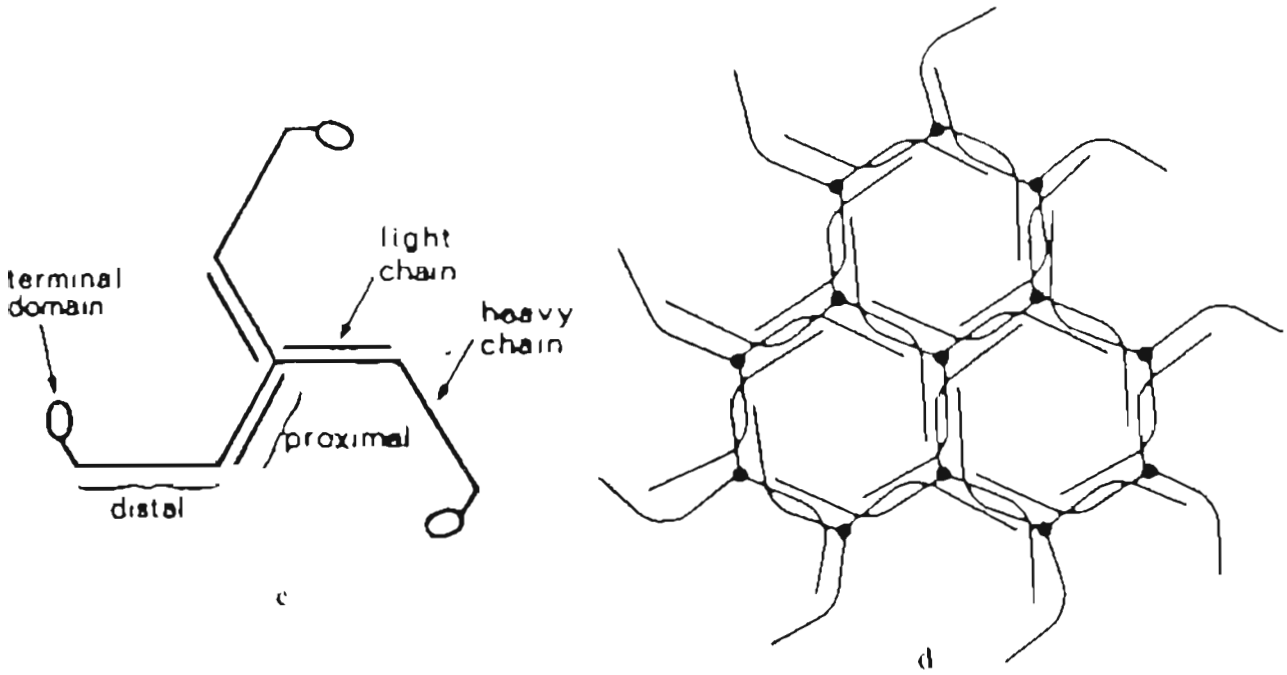

Packaging of triskelions (c) to hexagonal lattices (d)

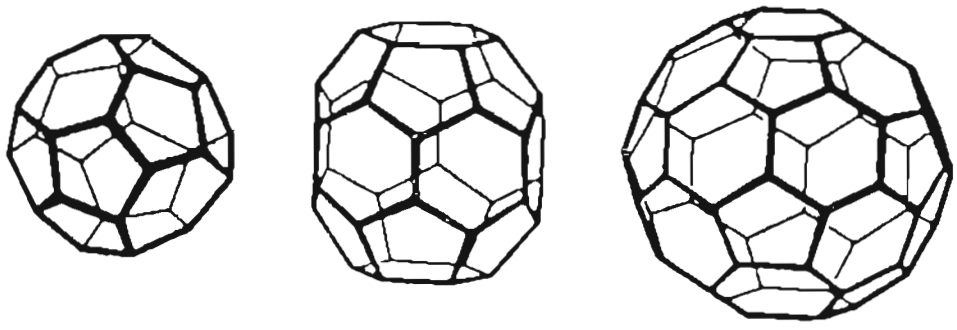

Examples of the geometry of clathrin cages. Each cage has 12 pentagons in the polyhedron. **Structures e, f,** and g contain 4, 8, and 20 hexagons and are built from 28, 36, and 60 **triskelions,** respectively, thus giving shells of increasing size. Structure g is probably the **smallest** polyhedron likely to be able to accommodate a vesicle

Fig. I.C.1 Continues....

Table I.C.1. Comparison of Clathrin with fullerene

	FULLERENE	CLATHRIN
NODES	60	60
HEXAGONS	20	20
PENTAGONS	12	12
"BOND"	C-C	$\{[\text{-NH-CH(R)-CO-}]_{800}\}_6$
"BOND LENGTH"	1.34 Å	~ 3000 Å
"BOND ENERGY"	5×10^2 kJ/mol	5×10^6 kJ/mol

Initial endeavours at the crafting of spherical surfaces by non covalent assembly were based on a three dimensional retrosynthetic analysis of such models wherein the equatorial region is assembled by the formation of twelve hydrogen bonds. The simplest example that surfaced from such an analysis is the directed alignment of six N-amino maleimide units as shown in Chart I.C.1 to provide potential for formation of a closed spherical surface. Thus, this simplest approach envisaged the preparation of N-amino maleimide and its assembly, including those directed by the metal directed complexation of π bonds as shown in Chart I.C.1.

The preparation of N-amino maleimide has been reported in literature by reaction of Boc carbazate with maleic anhydride, followed by deprotection by methanolic HCl.[20] However, monitoring the reaction by NMR clearly showed that the expected N-Boc maleimide **1** was absent as evidenced by the appearance of the olefinic protons as doublet. Subsequent experiments showed that the product reported earlier was not **1**, but the ring opened carboxylic acid (vide infra). This suggested that the water formed in the reaction was leading to the rapid decomposition of **1**. This was confirmed by performing the reaction in presence of molecular sieves, where the expected **1** was obtained in 52% yields (Chart I.C.2). The structural assignment for **1** is fully supported by spectral data including X-ray structure. The suggested reference [20] - deprotection with

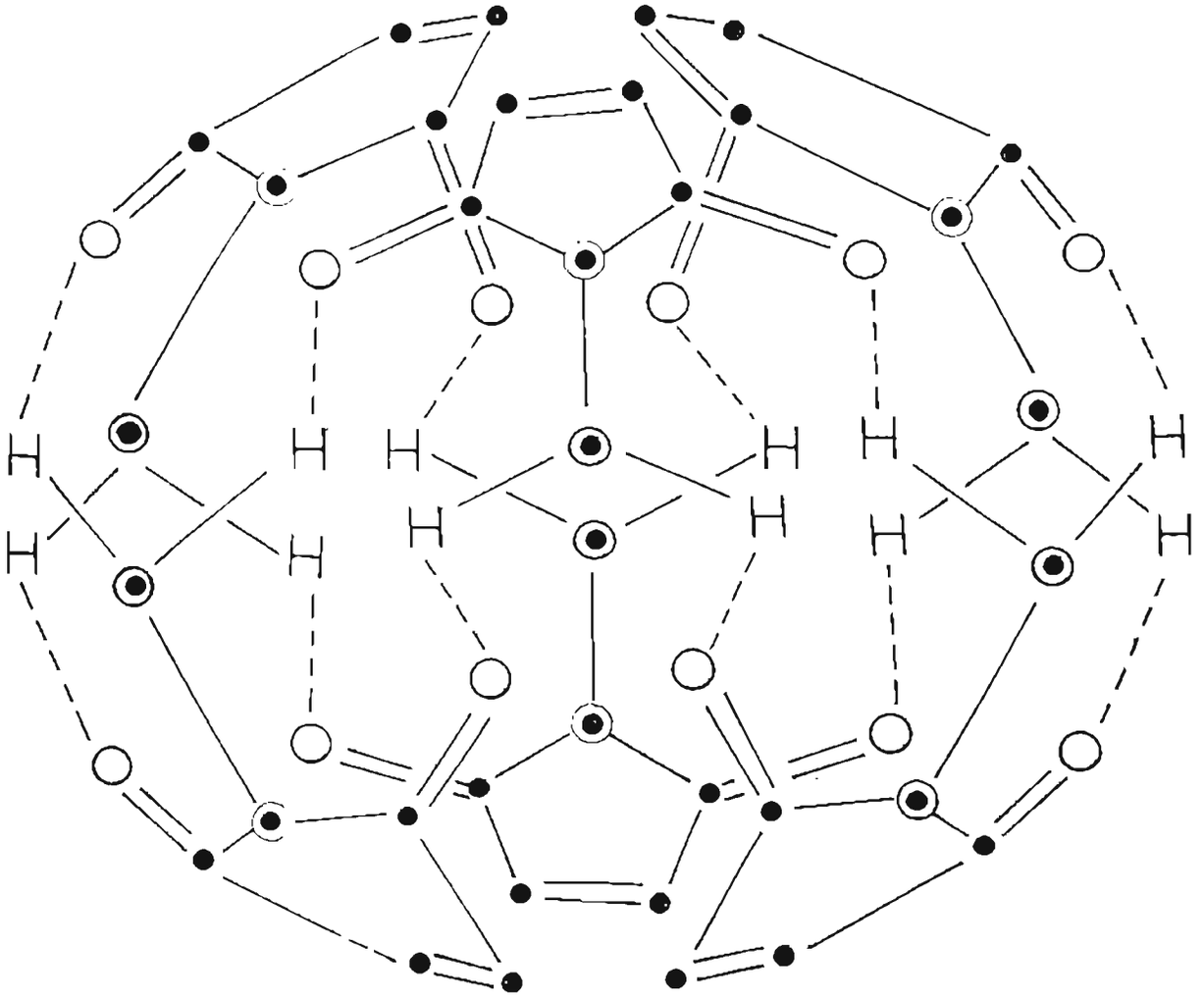

Carbon

Nitrogen

Oxygen

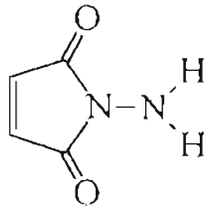

Chart I.C.1.

methanolic HCl, in fact led to the methanolysis of **1**, followed by deprotection to compound **2**, whose structure is fully in agreement with the spectral data (Chart I.C.2)

Unusual properties of the compound **1** were revealed by a detailed study of its FAB mass spectra. The FAB mass(+ ve) spectrum showed presence of the parent ion at m/z 213 and a dimer at 425 as well as a trimer at 637. In addition, the fragmentation of **1** by loss of isobutylene and CO_2 was also seen in the mass spectra. The formation of dimeric and trimeric species was confirmed by mass spectrometric doping experiments using lithium perchlorate, which led to strong presence of lithium complexed monomer, dimer and trimer at respectively 219, 431 and 643, with the complete absence of the parent species, thus indicating total metal ion complexation as shown in Chart I.C.2.

Compound **1** crystallized from EtOAc-hexane to afford rod shaped crystals whose single crystal X-ray analysis, presented in Fig. I.C.2, was unexceptional in the sense that the expected intermolecular and intramolecular hydrogen bonds involving the amide bonds were absent. However, the unit cell packed two molecules, which highlighted the close proximity of the hydrophobic Boc groupings. The selected interatomic parameters from the crystal data of **1** are presented in Table I.C.2.

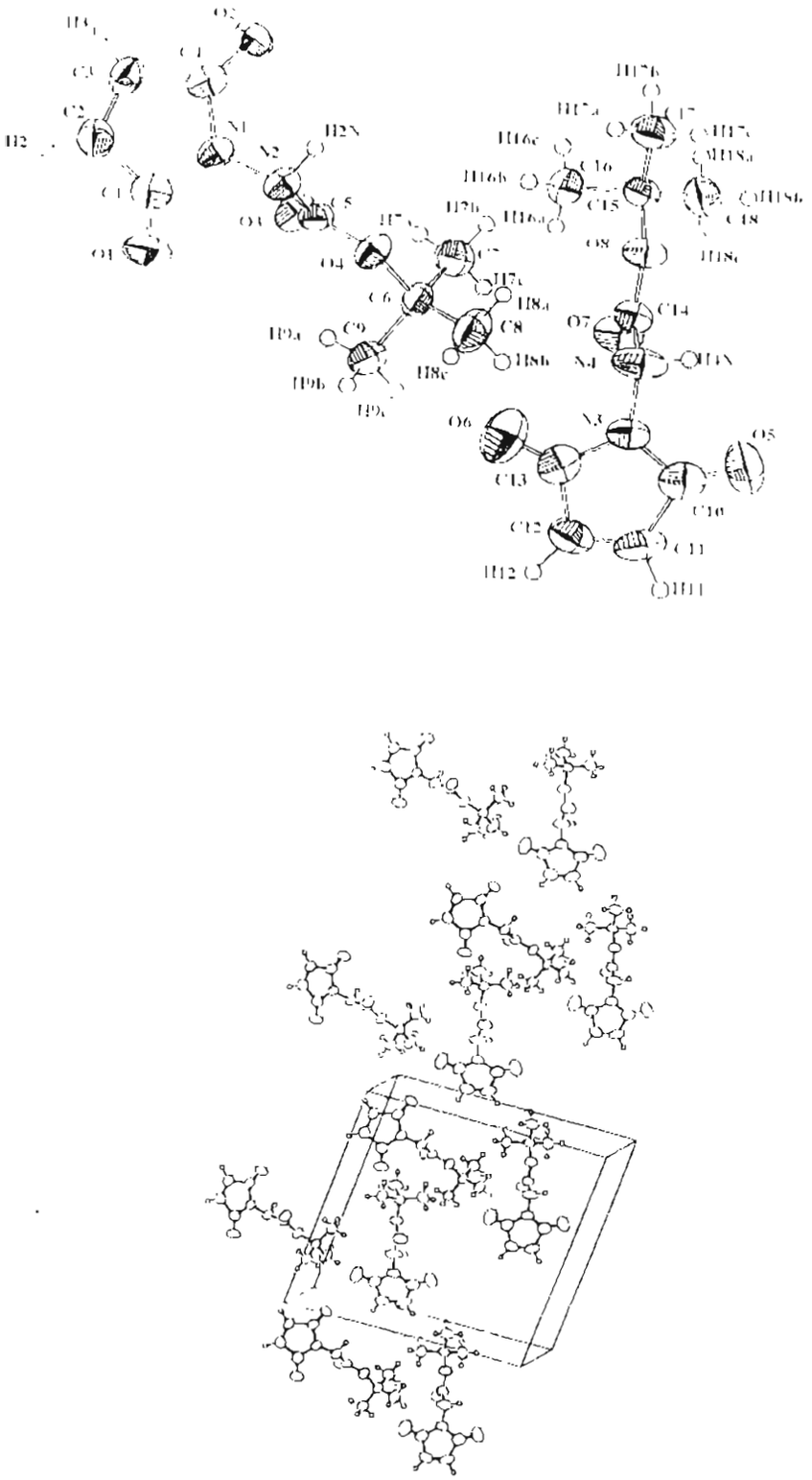

Fig. I.C.2. Crystal structure of N-N-Boc maleimide (**1**)

Table I.C.2 Inter atomic parameters from the crystal data of **1**

Bond Distances	(Angstroms)	Bond Angles	(degrees)
O1-C2	1.[illegible]	[illegible]	120.5(5)
O2-C4	1.189(9)	N2-N1-C1	123.4(6)
O3-C5	1.[illegible]	N2-N1-C4	122.6(5)
O4-C5	1.[illegible]	C1-N1-C4	113.1(5)
O4-C6	1.[illegible]	N1-N2-C5	117.2(5)
N1-N2	1.391(8)	O1-C1-N1	126.3(7)
N1-C1	1.[illegible]	O1-C1-C2	131.4(7)
N1-C4	1.40(1)	N1-C1-C2	102.3(6)
N2-C5	1.370(9)	C1-C2-C3	110.9(6)
C1-C2	1.51(1)	C2-C3-C4	109.1(7)
C2-C3	1.52(1)	O2-C4-N1	125.2(7)
C3-C4	[illegible]	O2-C4-C3	130.4(7)
C6-C7	[illegible]	N1-C4-C3	104.3(6)
C6-C8	1.51(1)	O3-C5-O4	128.6(6)
C6-C9	1.52(1)	O3-C5-N2	123.8(6)
O5-C10	1.19(1)	O4-C5-N2	107.6(6)
O6-C13	1.18(1)	O4-C6-C7	109.6(5)
O7-C14	1.205(9)	O4-C6-C8	101.8(5)
O8-C14	1.327(8)	O4-C6-C9	108.7(5)
O8-C15	1.489(8)	C7-C6-C8	111.7(6)
N3-N4	1.396(8)	C7-C6-C9	113.7(6)
N3-C10	1.41(1)	C8-C6-C9	110.7(6)
N3-C13	1.40(1)	C14-O8-C15	121.0(5)
N4-C14	1.365(9)	N4-N3-C10	123.8(7)
C10-C11	1.49(1)	N4-N3-C13	122.6(6)
C11-C12	1.31(1)	C10-N3-C13	113.0(6)
C12-C13	1.48(1)	N3-N4-C14	118.6(6)
C15-C16	1.52(1)	O5-C10-N3	126.3(7)
C15-C17	1.53(1)	O5-C10-C11	131.8(8)
C15-C18	1.51(1)	N3-C10-C11	101.9(7)
		C10-C11-C12	111.4(7)
		C11-C12-C13	109.1(7)
		O6-C13-N3	126.7(7)
		O6-C13-C12	128.8(8)
		N3-C13-C12	104.4(7)
		O7-C14-O8	128.7(6)
		O7-C14-N4	123.7(6)
		O8-C14-N4	107.6(6)
		O8-C15-C16	102.2(5)
		O8-C15-C17	109.4(5)
		O8-C15-C18	109.7(5)
		C16-C15-C17	110.5(6)
		C16-C15-C18	111.3(6)
		C17-C15-C18	113.1(6)

The difficulties in the preparation of N-aminomaleimide should be contrasted with the ease with which the N-amino phthalimide could be prepared most easily from phthalimide and Hydrazine.[21] Alternately, it was shown in the present work that the reaction of phthalic anhydride with Boc carbazate gave the expected Boc protected N-aminophthalimide (**1a**, Chart I.C.2) in excellent yields.

In view of the difficulties relating to the preparation of N-aminomaleimide, the replacement of the three units of N-aminomaleimide, whose alignment is envisaged in Chart I.C.1, with an aromatic anchor appeared attractive. Thus, the bridging of the three π bonds would naturally lead to system where the three units of N-aminomaleimide are locked. An analysis like this shown in Chart I C.3 led to the identification of benzene- hexacarboxylic acid (mellitic acid) tris-N-amino imide, whose dimerization could lead to closed surfaces as could be seen.

Benzene hexa carboxylic acid (**4**) is reported to undergo transformation to the tris anhydride on refluxing with Ac_2O.[22] Following this procedure, the putative tris anhydride was reacted with Boc carbazate with the anticipation that the desired amino protected compound would be formed. In the event, careful chromatographic analysis followed by mass spectrometry revealed the formation of the compound **5**, arising from imide formation involving the 1-2 & 4,5 carboxylic acids (Chart I.C.4). In view of this result, it is proposed that the

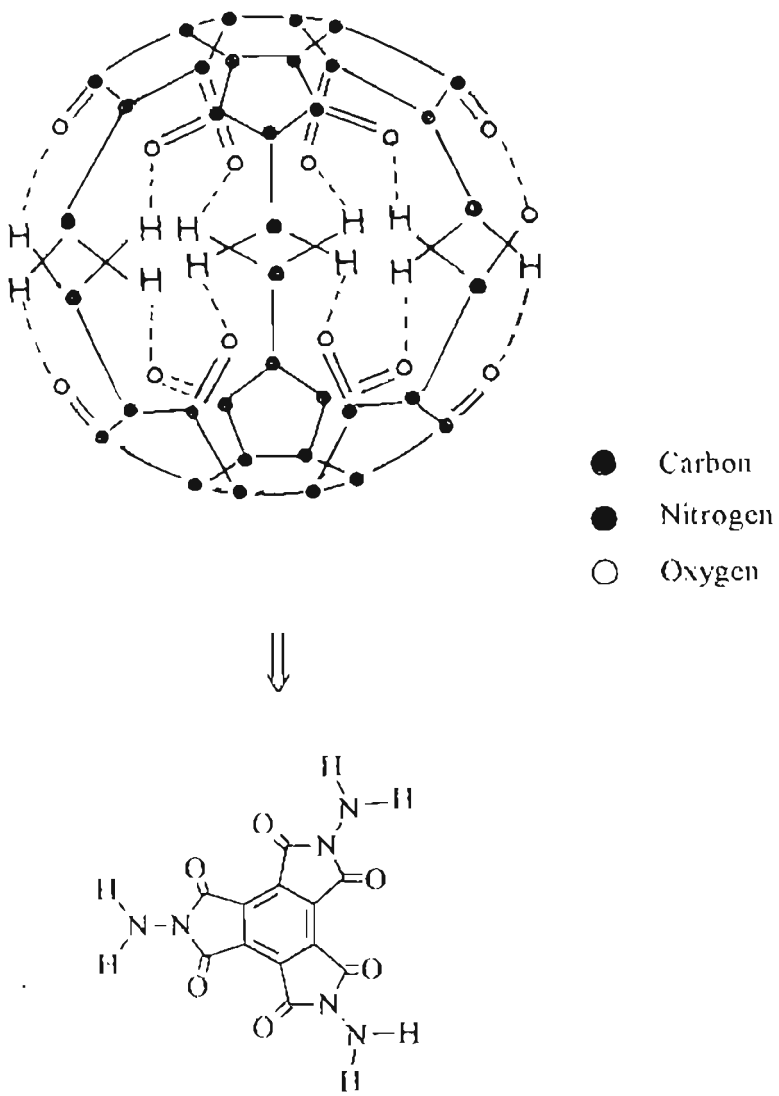

Chart I.C.3.

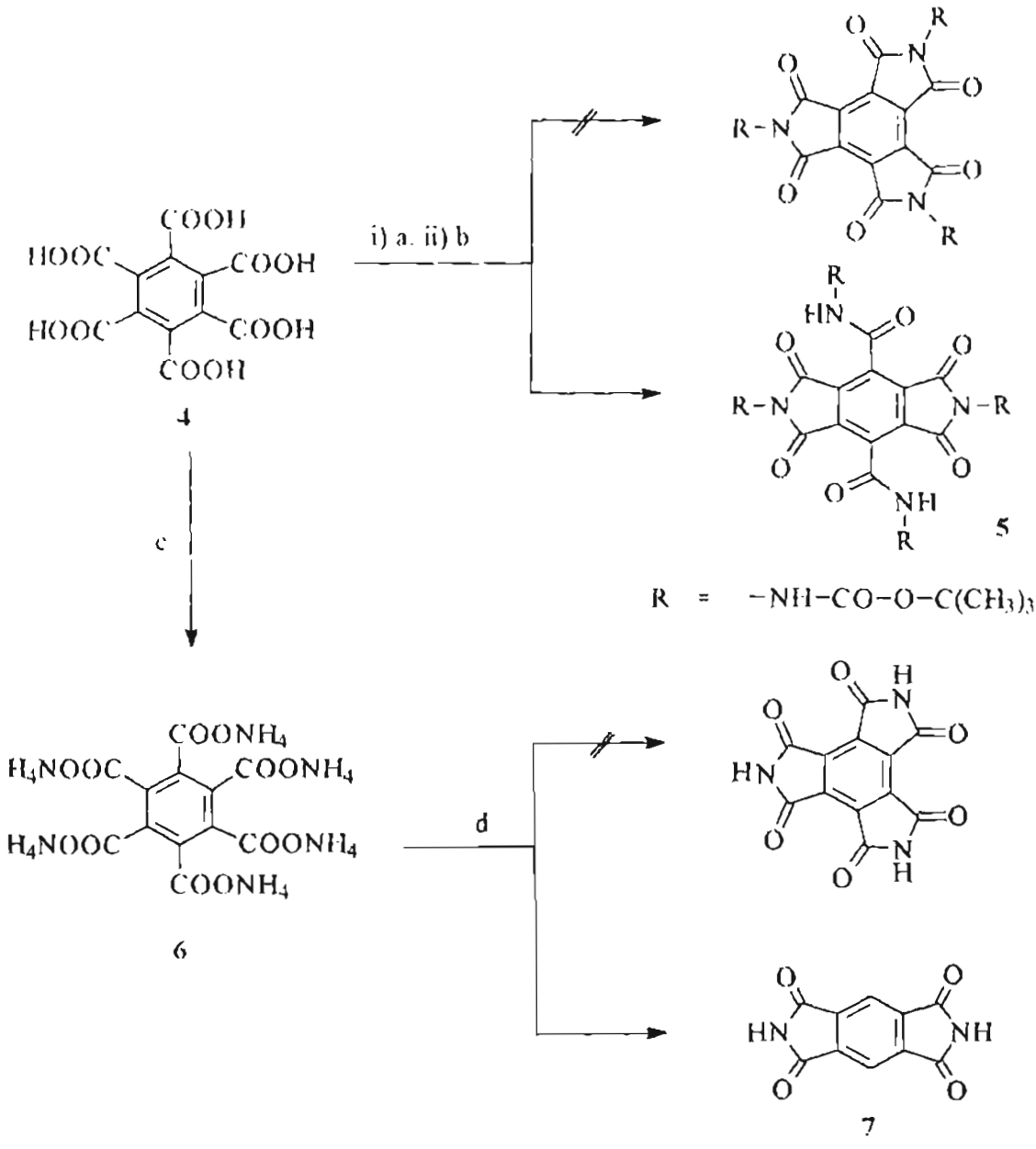

a) Ac_2O, reflux. b) Boc carbazate, $CHCl_3$, reflux. c) NH_3, THF. d) thermolysis

Chart I.C.4.

reaction of **4** with Ac_2O does not lead to the tris anhydride, but to a bis anhydride with two carboxyl groups in the peri positions activated as mixed anhydride with Ac_2O.

An alternate route to the mellitic acid tris N-aminoimide envisaged pyrolysis of the hexa ammonium salt to the tris imide as reported in the literature [23], followed by amination with hydrazine. The reaction of mellitic acid with ammonia in THF led to precipitation of the ammonium salt (**6**), which decomposed on heating, in contrast to the reported transformation to the trisimide at 144 - 150°C. In the event, the reaction afforded the sole product diimide **7** arising from decarboxylation of the pericarboxyl groups (Chart I.C.4). These results again indicate a non sequential preference for the second imide / anhydride, thus making the formation of the tris imide by this approach not feasible.

To obviate the above problems, a hydrocarbon equivalent of the mellitic acid tris N-aminoimide was envisaged. Thus trindane, tris cyclopentanobenzene **8**, (Chart I.C.5) could, in principle be restructured by sequence - oxidation of the six benzylic positions, oximination of the bridge methylenes and reduction, to provide the carbon analog of benzotris N-amino maleimide, that could dimerize to a spheroidal surface. Detailed MNDO-5 calculations showed that such dimerization is feasible, leading to the closed surface envisaged in Chart I.C.6.

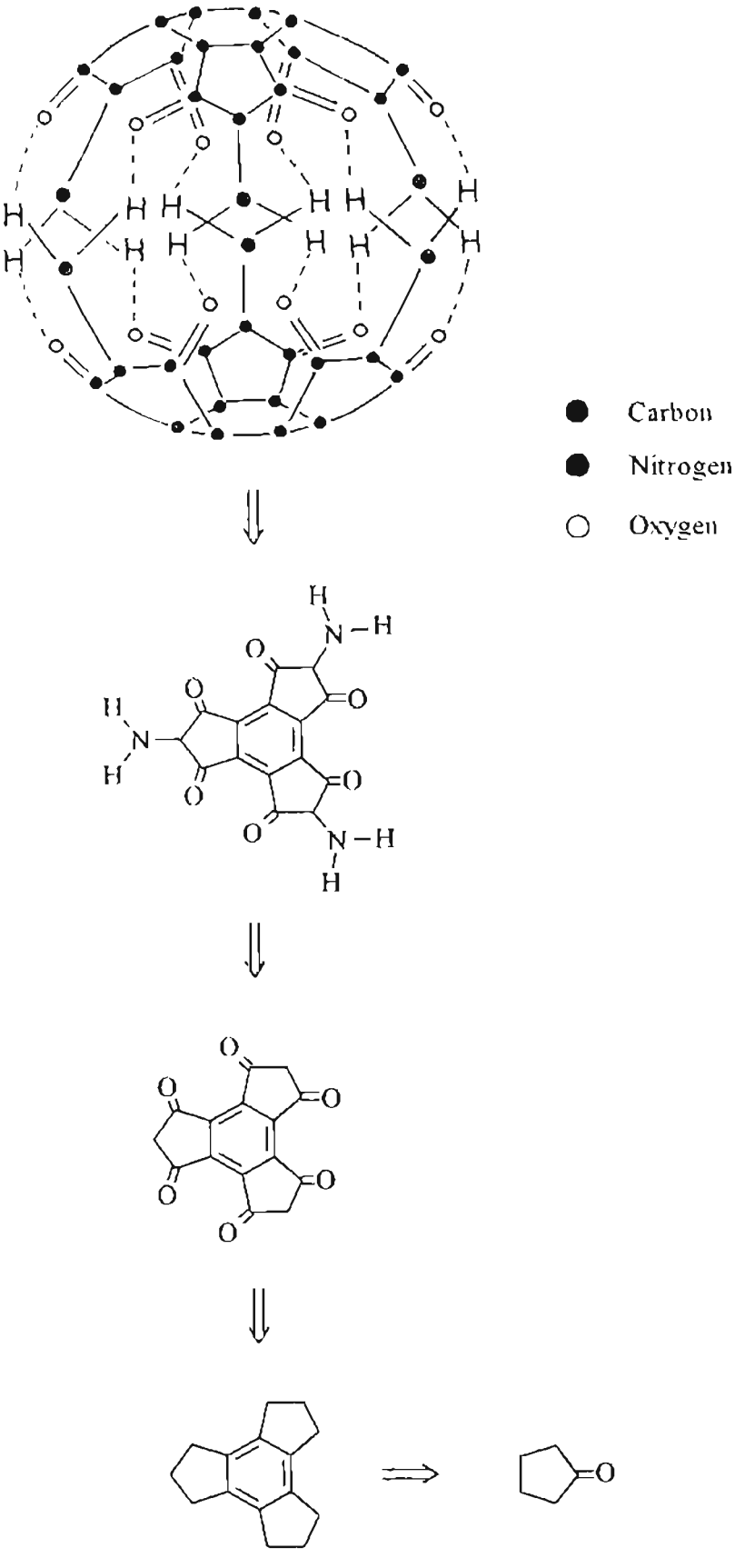

Chart I.C.5.

8

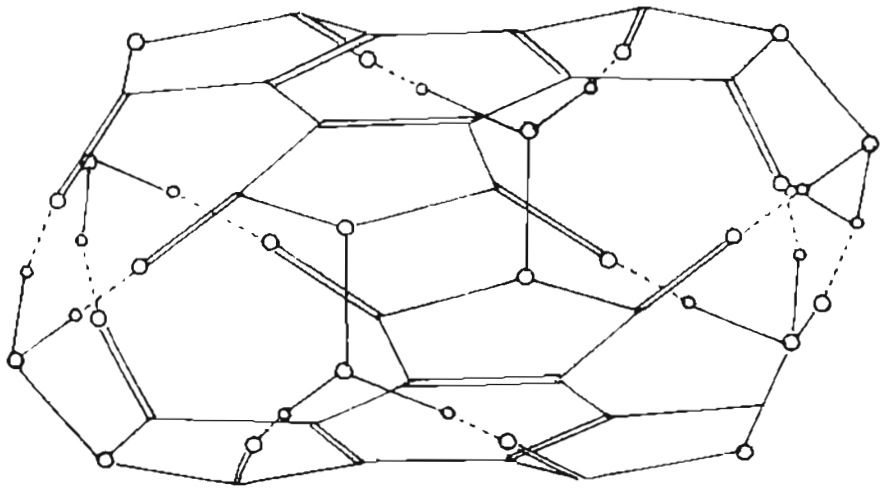

Chart I.C.6. 'MNDO' Picture of the dimeric assembly shown in Chart I.C.5

Cyclopentanone on reflux with ethanol containing con. H_2SO_4 afforded trindane in ~35% yields. This unusual reaction, though reported earlier,[24] has been standardized in the present work to give optimum yields. The reaction proceeds by tandem aldol condensation as shown in Chart I.C.7.

The reaction of **8** with bromine under illumination afforded the hexabromide **9** in 68% yields whose properties were similar to that reported earlier.[25] In connection with studies on the synthesis of multi iron ferrocene, harboured on a single anchor, **9** has been converted to trindene (**10**) as a mixture of isomers,[25] by reaction with zinc in DMF. In the event, this reaction was capricious, offering a modest yield of the desired product **10**. The **9** → **10** transformation most likely proceeds through a 1 - 4 elimination mediated by zinc followed by tautomerization. As shown in Chart I.C.7, it was envisaged that compound **10** could be transformed to the tris epoxide **11**, which on an electrophilic rearrangement ought to afford the desired non-conjugated trione, which could be further elaborated. In the event, the reaction of **10** with mCPBA in CH_2Cl_2 afforded the desired tris-epoxide (NMR) which was treated with $BF_3.Et_2O$ in dry benzene. The IR spectrum of the resulting compound suggested the presence of a conjugated carbonyl group, thereby demonstrating that a conjugated carbonyl compound **12** was formed (Chart I.C.7).

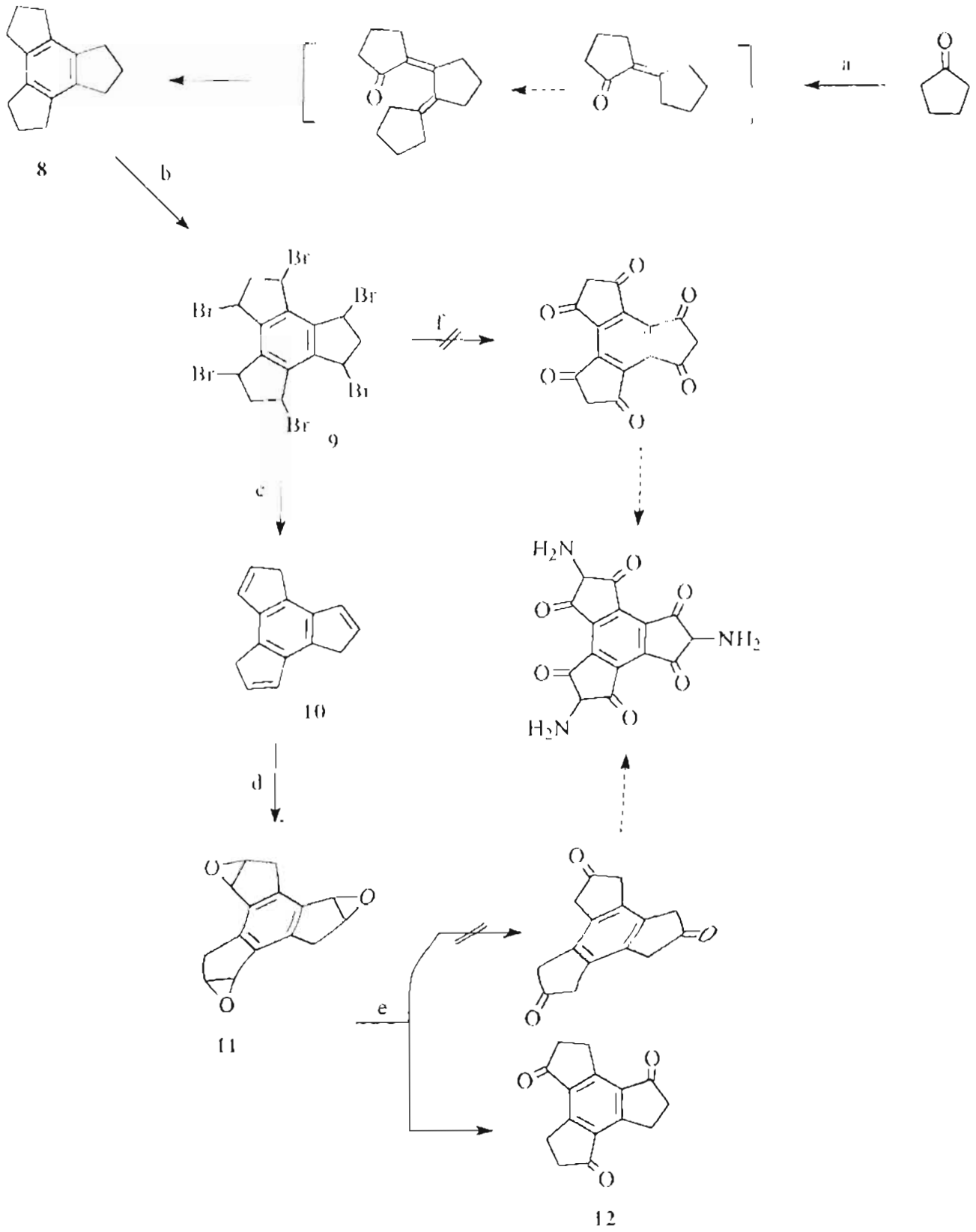

a) EtOH, Conc. H_2SO_4, reflux. b) Br_2, CCl_4. c) Zn, Et_3N, DMF. d) mCPBA, CH_2Cl_2. e) BF_3. Et_2O, C_6H_6. f) DMSO, reflux.

Chart I.C.7.

Initially, it was envisaged that the compound **9** having six bromines in benzylic positions could be subjected to treatment with DMSO, leading to, in one step, the corresponding ketone (Chart I.C.7). The reaction in the event led to intractable mixtures

Numerous attempts were made to effect the oxidation of trindane (**8**) at the benzylic positions. These included photosensitized oxidation (methylene blue), Fe/Ni - isopropyl aldehyde oxidizing system etc. The reaction gave complex mixtures of small amounts of oxidized products, which, as per GC MS indicated the presence of only upto three carbonyl groups.

In view of the inability of the usual oxidizing agents to bring about the desired transformation of trindane, the use of more powerful oxidizing agents were explored. In terms of volt equivalents RuO_4 is next only to ozone in terms of oxidizing properties. The former reagent has been extensively used in the oxidation of a wide range of substrates.[26] It was hoped that RuO_4 would be able to bring about the desired oxidation of trindane in the benzylic positions. The reaction of **8** with *in situ* generated RuVIII species (Chart I.C.8) afforded no product arising from benzylic oxidation, but consistently gave in ~ 15% yields a crystalline compound, mp. 148-150°C. The ^{13}C NMR spectrum coupled with DEPT studies suggested that the methylenes were intact and showed presence of two types of carbonyls. The FAB (normal and negative ion) mass spectrum

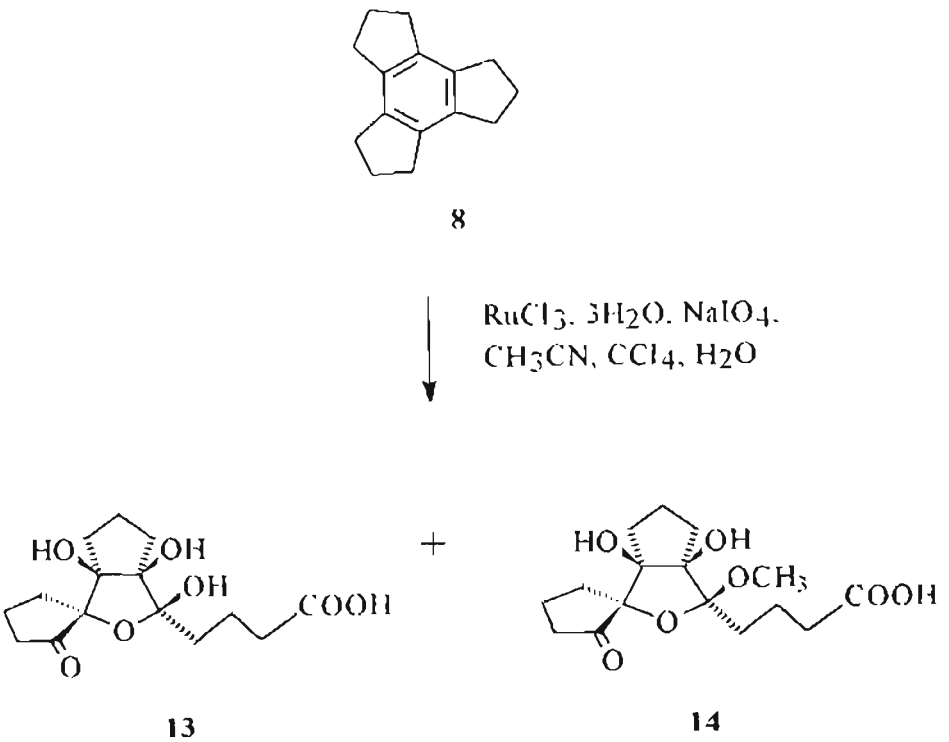
8
RuCl3. 3H2O. NaIO4.
CH3CN, CCl4, H2O
HO
OH
OH
COOH
O
13
+
HO
OH
OCH3
COOH
O
14

Chart I.C.8.

showed a molecular weight of 314. Elemental analysis was consistent with a molecular formula $C_{14}H_{22}O_7$ which when compared to the starting trindane ($C_{14}H_{18}$) amounts to introduction of seven oxygens. The FT IR indicated presence of hydroxyl groups, cyclopentanone and another carbonyl peak at 1709 cm^{-1}.

Single crystal X - ray analysis revealed the structure of the oxidation product as **13**. The crystal structure of **13** and the selected inter atomic parameters are presented in Fig. I.C.3 and Table I.C.3 respectively. All the bond distances and angles are within normal statistical errors. The three five membered rings are puckered.[27]

A plausible rationalization of the **8** $\rightarrow$**13** change, where the oxidation has been contained by the peripheral methylenes, is presented in Chart I.C.9.

The basic frame work of **13** is similar to that of ginkgolides [28], a class of cytotoxic substances having therapeutic value. The one step transformation of hydrocarbon trindane to such condensed, highly oxygenated systems is noteworthy.

The resemblance of **13** to sugars was highlighted by simultaneous isolation of **14**, by replacement of the anomeric hydroxyl group during workup.

The nature of **13** would need the oxidation of each carbon centre of the aromatic ring. However, the sequence of events envisaged in Chart I.C.9 is largely notional. The step leading to *cis* hydroxylation, envisaged as the first step,

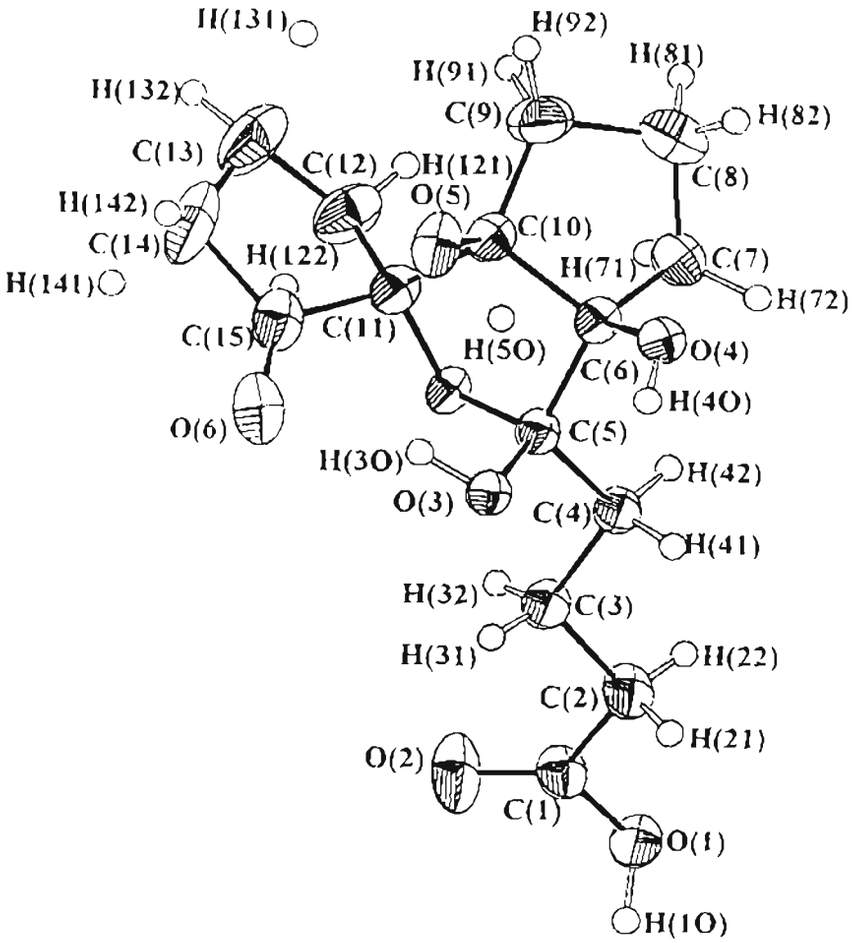

Fig. I.C.3. Crystal structure of the RuVIII oxidation product of Trindane (13)

Table I.C.3. Inter atomic parameters from the crystal data of 13

Bond lengths (Å)

O1-C2	1.314(7)
O2-C1	1.20(1)
O3-C5	1.385(7)
C4-C5	1.426(7)
C5-C10	1.435(8)
O6-C15	1.202(8)
O7-C5	1.419(7)
O7-C11	1.435(6)
C1-C2	1.50(1)
C2-C3	1.523(8)
C3-C4	1.520(9)
C4-C3	1.524(7)
C5-C6	1.550(8)
C6-C7	1.468(9)
C6-C10	1.554(7)
C7-C8	1.520(9)
C8-C9	1.54(1)
C9-C10	1.53(1)
C10-C11	1.59(1)
C11-C12	1.514(8)
C11-C15	1.54(1)
C12-C13	1.53(1)
C13-C14	1.51(1)
C14-C15	1.509(9)

Bond angles (deg)

C5-C7-C11	110.5(4)
O1-C1-O2	122.6(6)
O1-C1-C2	112.5(6)
O2-C1-C2	124.5(5)
C1-C2-C3	113.5(6)
C2-C3-C4	111.2(6)
C3-C4-C5	111.7(5)
O3-C5-O7	110.9(5)
O3-C5-C4	108.1(4)
O3-C5-C6	110.5(5)
O7-C5-C4	109.2(5)
O7-C5-C6	102.1(4)
C4-C5-C6	116.0(5)
O4-C6-C5	110.0(4)
O4-C6-C7	109.3(5)
O4-C6-C10	112.7(5)
C5-C6-C7	116.8(5)
C5-C6-C10	104.2(5)
C7-C6-C10	103.6(4)
C6-C7-C8	104.6(5)
C7-C8-C9	103.3(6)
C8-C9-C10	106.3(5)
O5-C10-C6	112.9(4)
O5-C10-C9	112.9(5)
O5-C10-C11	104.9(5)
C6-C10-C9	105.6(5)
C6-C10-C11	101.8(4)
C9-C10-C11	118.4(5)
O7-C11-C10	106.3(4)
O7-C11-C12	110.5(5)
O7-C11-C15	110.2(5)
C10-C11-C12	117.8(5)
C10-C11-C15	110.6(5)
C12-C11-C15	101.4(5)
C11-C12-C13	104.2(6)
C12-C13-C14	102.7(6)
C13-C14-C15	106.9(7)
O6-C15-C11	124.6(5)
O6-C15-C14	127.9(8)
C11-C15-C14	107.2(6)

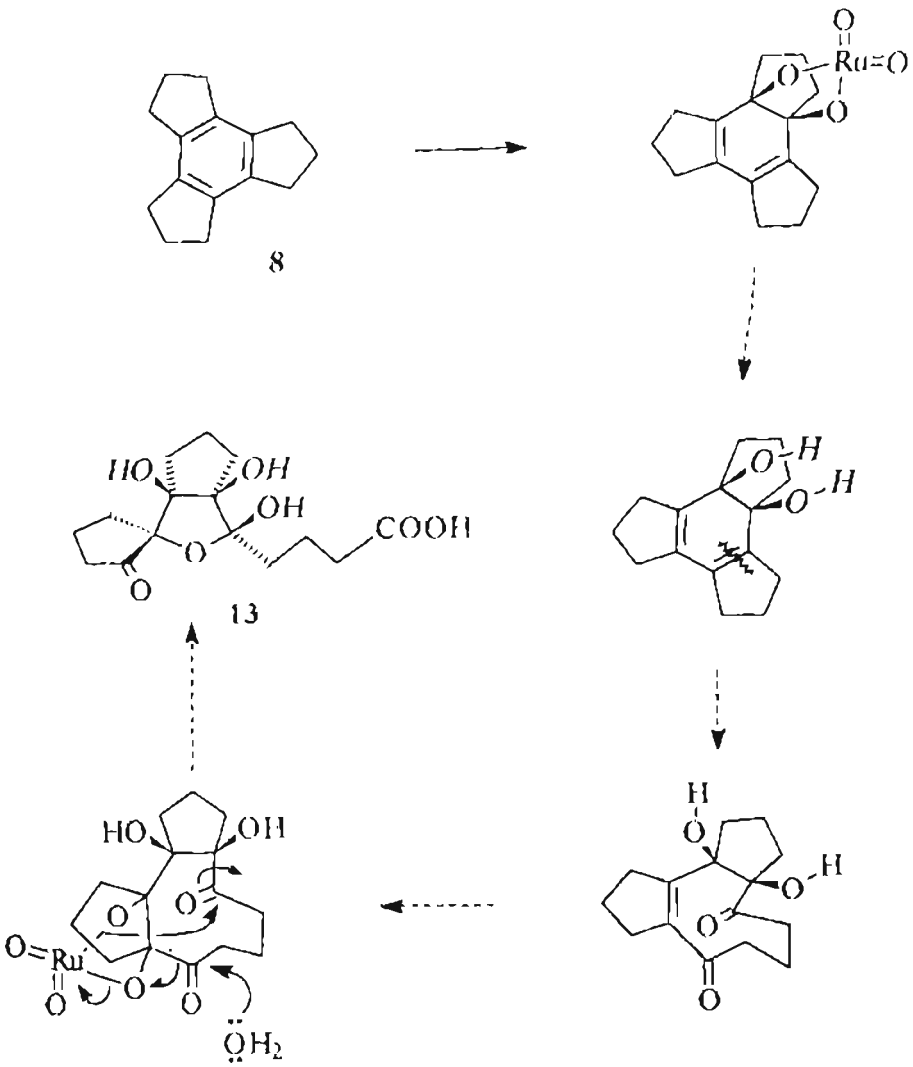

Chart I.C.9.

is required to control the stereochemical outcome of the reaction. Preference, if any, of the reagent addition in the second step is obliterated since the process leads to oxidative C-C scission. Molecular models clearly show that the critical third step requires addition of the reagent from side *anti* to the *cis* hydroxyl grouping - which seem to be dictated by steric factors - to enable the generation of the oxabicyclo octane unit in **13** by transannular addition with correct stereochemical disposition at centres 2 and 4.

The formation of **14** (Chart I.C.8), which was isolated as a gum, in ~7% yield has been traced to the use of small amounts of methanol as a co-eluent. A spectral comparison of **13** with this compound indicated a simple replacement of hydroxyl group with a methoxyl, which was confirmed by detailed spectral studies.

The exclusive π oxidation of Trindane with RuO_4 at once suggested that the π strain imposed by the cyclopentane periphery could impart a high activity for the double bonds. In the event, this was experimentally found to be true (vide infra). The results made it necessary to reexamine the reaction of ozone with Trindane, which had earlier reported to yield glutaric acid.[29] The reaction of Trindane with ozone gave, in addition to glutaric acid (25%), neutral compounds **15** and **16** in 14% and 13% yields respectively (Chart I.C.10). The structural assignments of **15** and **16** are fully supported by spectral data. The formation of

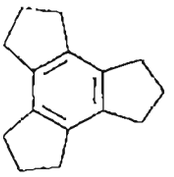

8

i) O_3, CH_2Cl_2, -70-80°C
ii) Me_2S

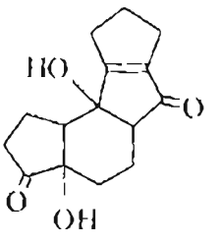

15

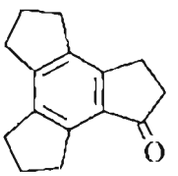

16

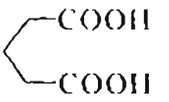

17

CH_2N_2

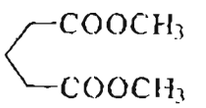

17a

Chart I.C.10.

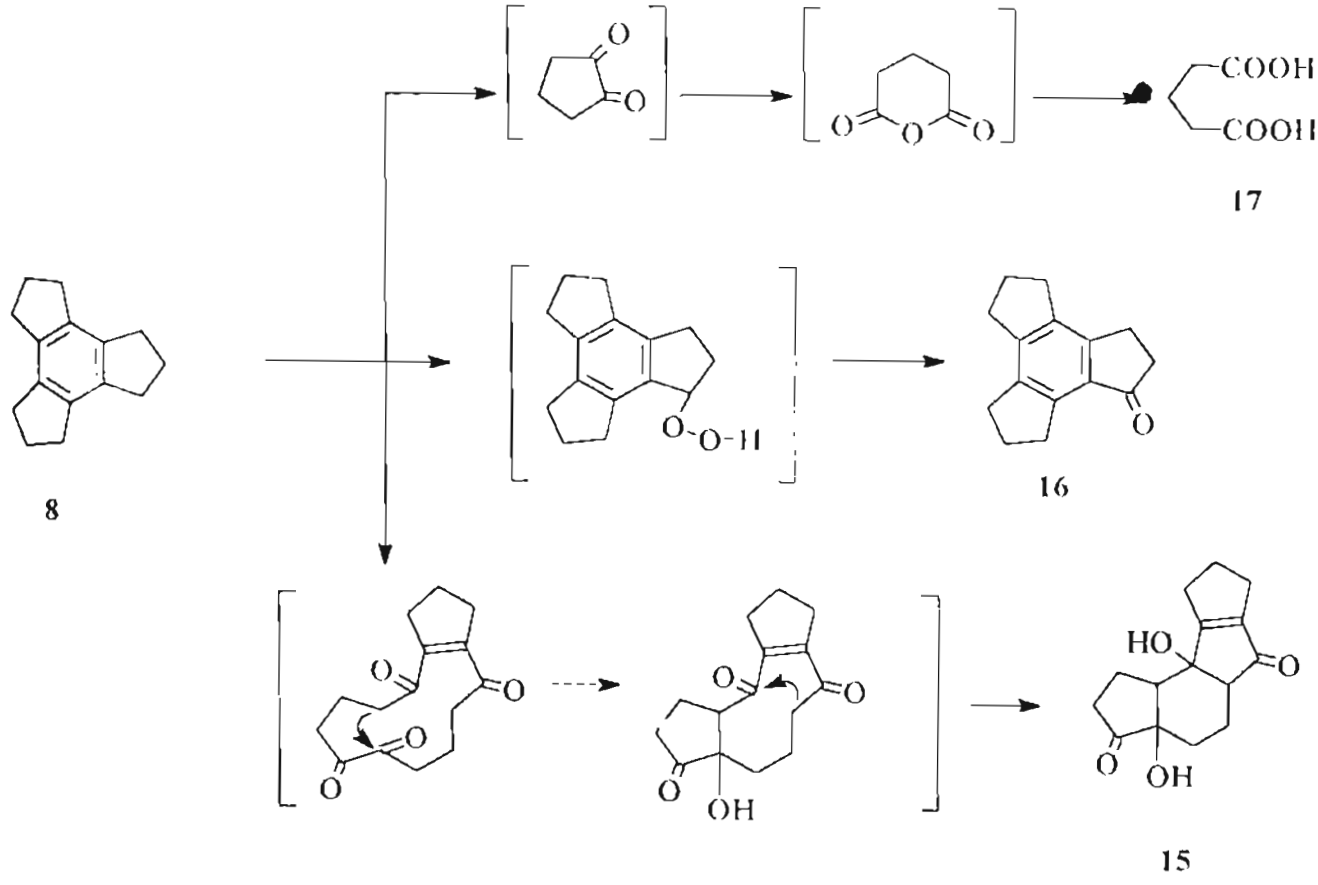

Chart I.C.11.

15, **16** and **17** is rationalized in Chart I.C.11. The one step transformation of **8** to **15**, with incorporation of four oxygens is noteworthy and represents the transformation of a hydrocarbon to a protosteroid, involving cleavage of double bonds and aldol condensations.

As anticipated, the homologue of tricyclopentanobenzene, namely, tricyclohexanobenzene (**18**), on treatment with RuVIII species afforded products solely from benzylic oxidation compared to that of Trindane. Tricyclohexanobenzene was readily prepared from cyclohexanone by procedure same as that used for Trindane (**8**). The reaction of **18** with ruthenium tetroxide exclusively afforded products from benzylic oxidation, namely **19** and **20** (Chart I.C.12). The structural assignment of **19** and **20** is supported by detailed spectral studies. The proximal positioning of two carbonyl groups in **20** is supported by the presence of base peak in mass spectra at 253, indicating loss of one oxygen to give species **20a**.

The divergence in behaviour of **8** with **18** towards oxidation by the same RuVIII species under similar conditions is striking. The fact that Trindane underwent exclusively π bond oxidation and the cyclohexane analog gave only products from benzylic oxidation highlights the alteration in the preference profile of RuVIII species to the substrates. In both cases, steric considerations pertaining to the formation of the cyclic intermediates involving the ruthenium

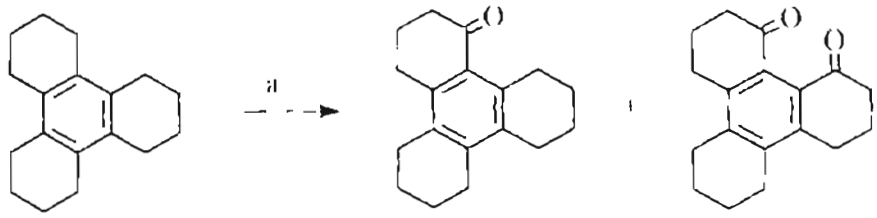

18 19 20

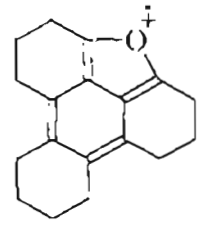

20a

a) $RuCl_3$. $3H_2O$, $NaIO_4$, CH_3CN:CCl_4:H_2O

Chart I.C.12.

tetroxide and the π bonds would be about the same and consequently, it is likely that the reactivity of the π bonds in Trindane is higher. Recently, there has been considerable interest in the identification of benzenoids whose π bonds are frozen by extraneous manipulations.[30] However, although Trindane is considerably more strained than that of its cyclohexane homologue, all evidences point to a normal delocalized π framework for trindane. It is thus logical to conclude that the reason for preference for the π oxidation here can be attributed to the relief from the marginal π bond strain that exist in Trindane as clearly demonstrated by spectroscopic measurements.[30d] The subtle factors, that govern this is illustrated by the fact that attempted easy addition of hydrogen (Pd/C, H_2) was not successful.

Another strategy explored in the present work, for closed surfaces pertained to the prior preparation of anchored constructs, that could derive stabilization from a hydrogen bonded periphery. This could dimerize to closed surfaces by intermolecular hydrogen bonding stabilization by a staggered arrangement. This is illustrated in Chart I.C.13 and Chart I.C.14.

Target molecule **24a** (Chart I.C 13), which could be expected to derive stabilization by peripheral hydrogen bonding network and even more so by dimerization to **24b** was sought from 2,5-dihydroxy teryphthalic acid **21**. Treatment of **21** with diazomethane, followed by chlorination afforded the

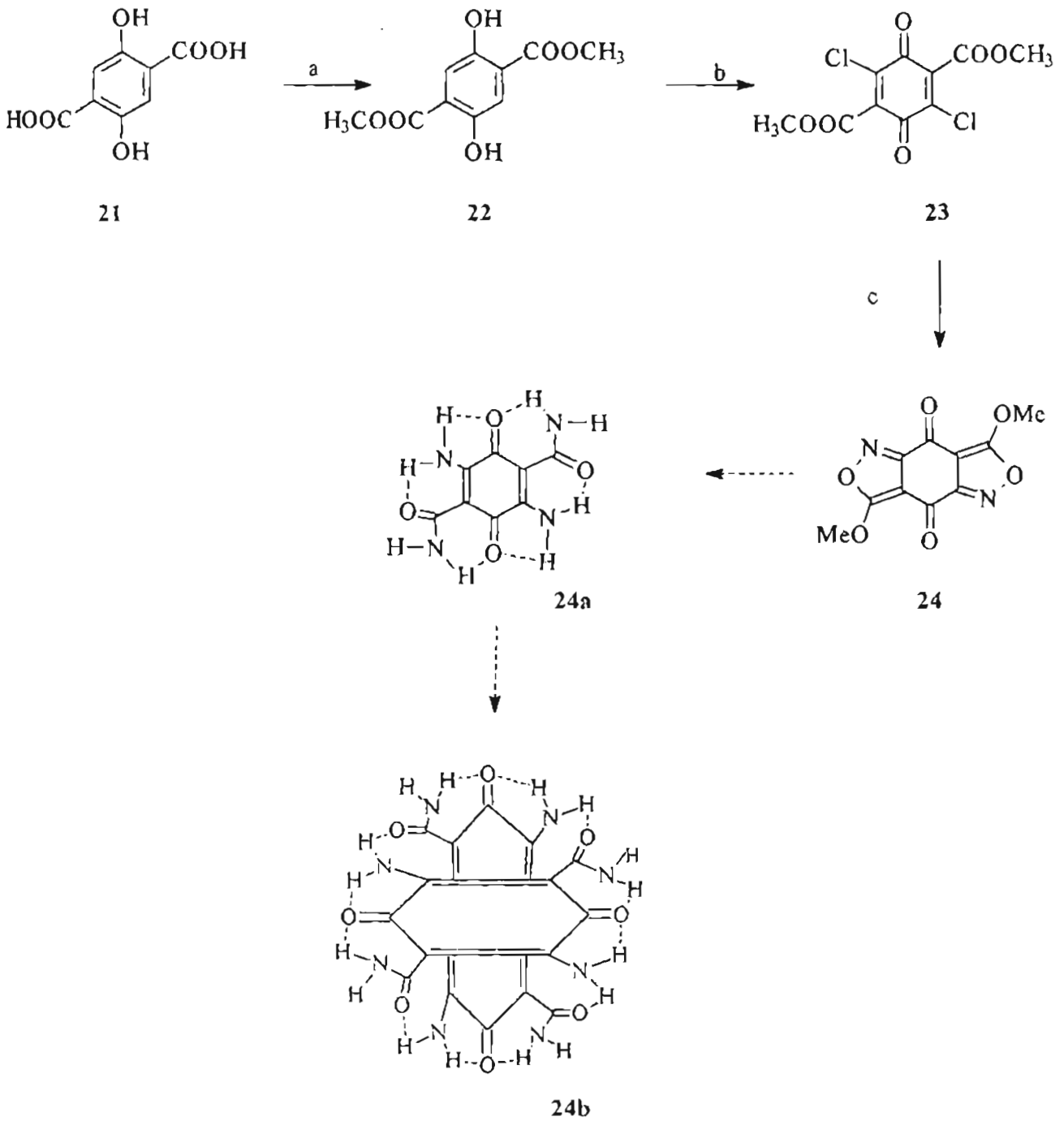

21 22 23

24

24a

24b

a) CH_2N_2, MeOH. b) Cl_2, $FeCl_3$, CCl_4. c) NaN_3, MeOH

Chart I.C.13.

expected quinone **23** in good yields. All attempts to oxidize **22** to the quinone by means that would obviate the introduction of chlorine did not succeed, possibly due to the presence of strong intramolecular hydrogen bonding that exist in **22**. The transformation of **23** to **24** by sodium azide proceeded as reported,[31] but in poor yields. The difficulties experienced in transforming **23** to **24** suggested that this would not be a viable route to **24a**.

Another strategy pertained to the possible preparation of the peripherally hydrogen bonded system shown in Chart I.C.14, that could also derive additional hydrogen bonded stabilization by dimerization to closed surfaces.

A simple approach to this system would be the diketopiperazine formation of protected C-hydrazino malonic acid methylester monoamide. In the event, this compound eluded synthesis. A pathway repeatedly tried was the displacement of bromine from a precursor with Boccarbazate as shown in Chart I.C.14.

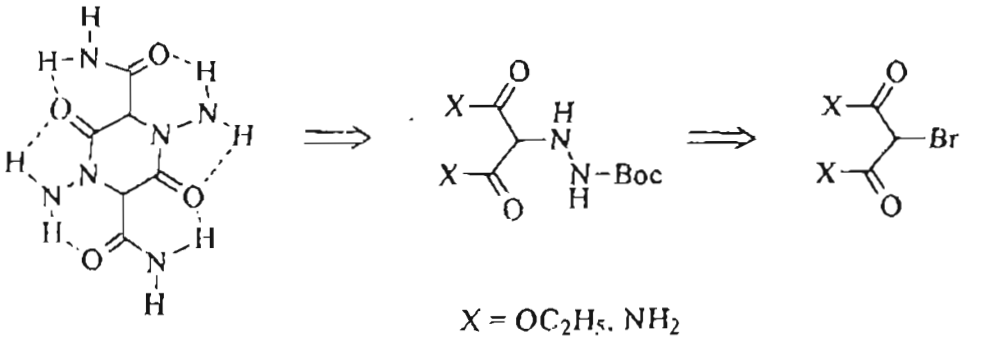

Chart I.C.14.

In the event, the consideration of such peripherally hydrogen bonded systems as precursors could be illustrated in a novel and unanticipated manner, where the principle of self assembly to spheroid surfaces could be achieved based on metal promoted interactions.

The potential for such a design came from studies on mellitic acid hexaamide (**26**), prepared by ammonolysis of mellitic acid hexamethyl ester (**25**) prepared by reaction of **4** with diazomethane (Chart I.C.15).

In the present work, hexa mellitoyl chloride **27** has been found to be an excellent compound for attachment of various ligands. Amongst the many procedures reported for the preparation of hexa substituted mellitic acid derivatives, most of them were found to be not correct, excepting fortunately the case of **27**, which could be prepared in good yields as reported by the digestion of mellitic acid with phosphorous pentachloride at 150°C for 24 h. The structural assignment for the hexa acid chloride is supported by its ready transformation to the hexamethyl ester (**25**) by methanolysis. The availability of hexa mellitoyl chloride (**27**) made it possible to explore alternate strategies, whereby non covalent assemblies to give spheroidal surfaces could be crafted, taking advantage of the ligand. This strategy has given promising results. It was envisaged that the ligands attached to the aromatic anchor of mellitic acid could form an assembly on a spherical surface which would lead to spheroidal surfaces

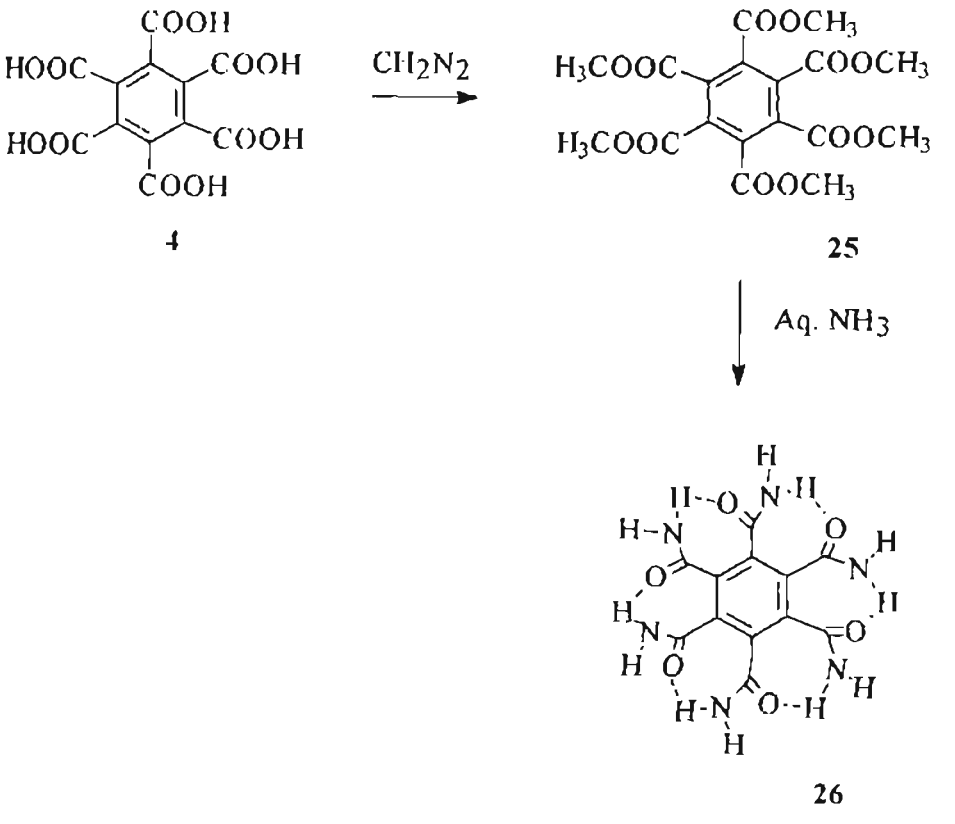

4 **25** **26**

Chart I.C.15

by metal ligand interactions, whereby the aromatic anchor would be projecting outwards. The appropriate ligand that was considered practical was the sulfur containing α amino acid, methionine. Experiments have shown that they could be expected to deposit on a colloidal gold surface.

To test this, hexamellitoyl chloride was reacted with methionine methyl ester (Chart I.C.16). Careful analysis of the reaction mixture afforded three compounds, which were identified based on their spectral and analytical data as the design, hexaamide **28**, monoimide **29** and the diimide **30**. The structural assignments of these three compounds are fully supported by their ^{1}H NMR, ^{13}C NMR, FAB mass spectra and elemental analysis. The mass spectral fragmentation in the FAB mass spectrometer of this family was quite interesting. With reference to the hexa amide **28**, the parent peak was that arising from uptake of sodium ions and the mass spectrum clearly showed the successive loss of the ligands to form the monoimide **29**, diimide **30** and the triimide (**30a**), which was not formed in the reaction. Indeed, this unique fragmentation pattern was a positive way for assigning the structures easily for these class of compounds.

The tris imide to hexa amide in systems like these represents an uptake of ligands from 3 to 6, and the conditions of formation of these could be controlled by the extent of ligands used and this aspects merits investigation.

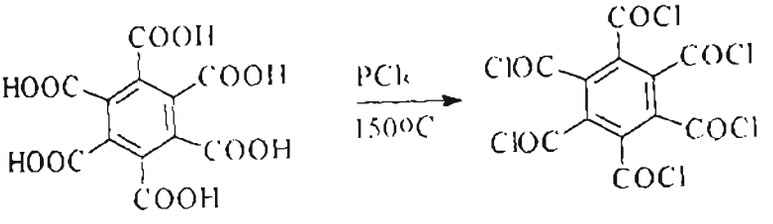

4 27

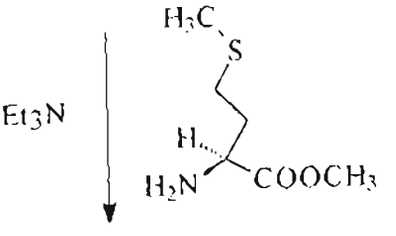

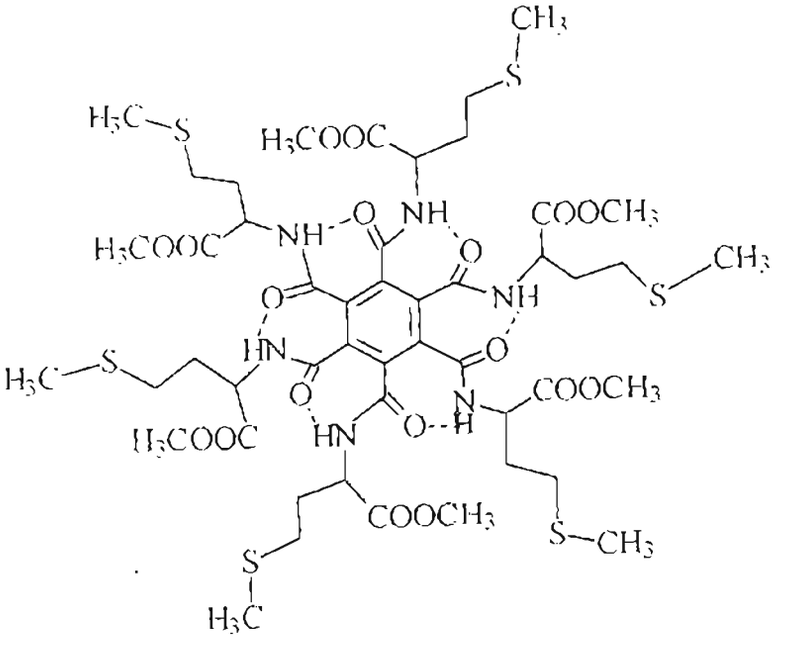

28

+ Continues.....

Chart I.C.16.

Chart I.C.16 continues....

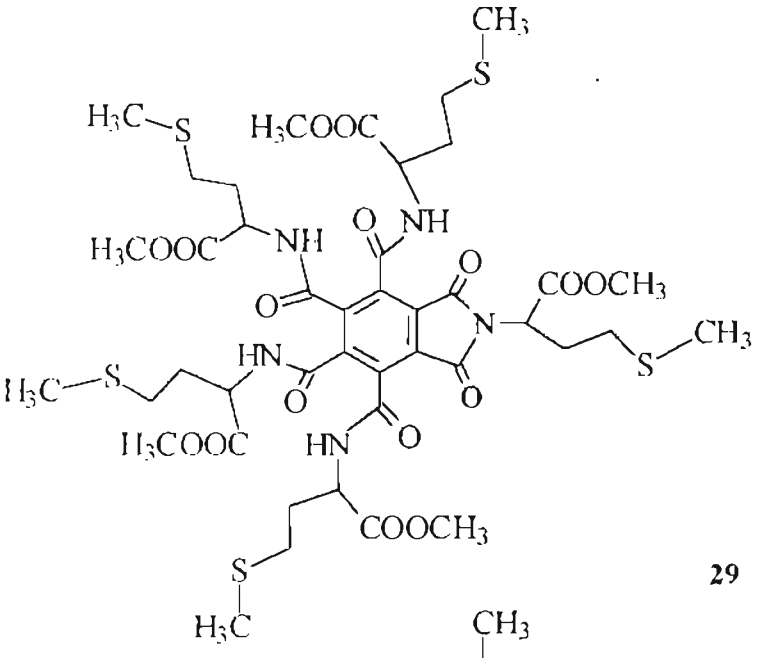

29

+

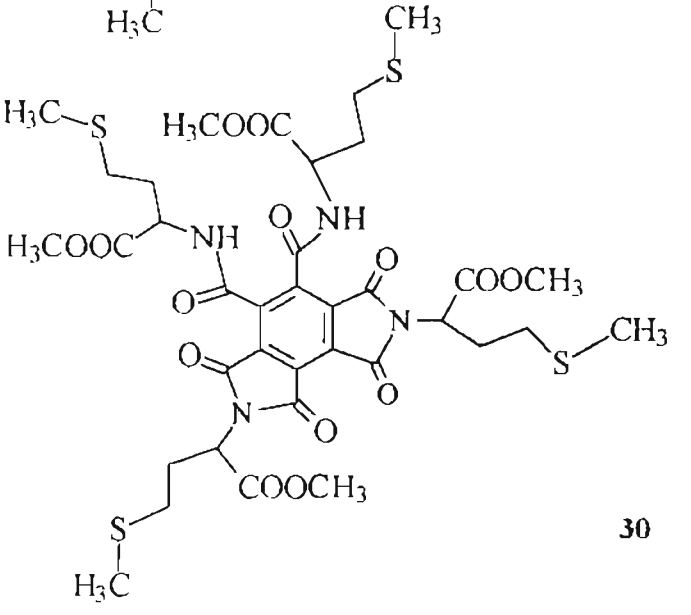

30

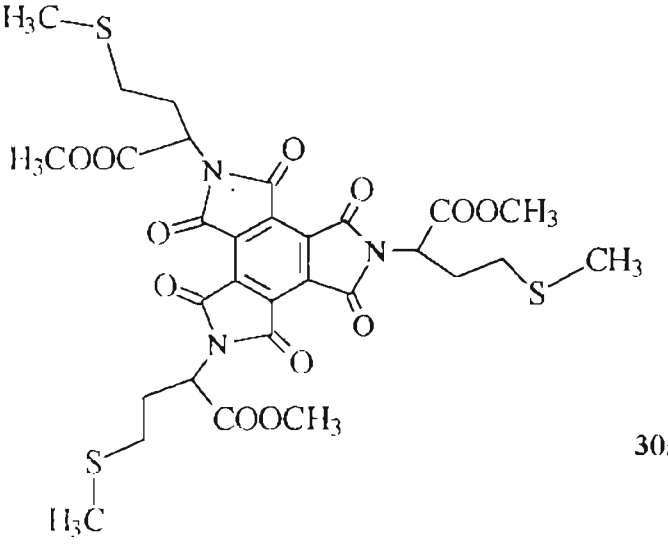

30a

The FT IR spectra of the hexa amide in chloroform clearly showed band at 3273 cm^{-1}, even at 1 mM concentration, indicating an intramolecular hydrogen bonded network (Fig. I.C.4). The core structure of the hexa amide therefore consists of an array of the methionine side chain on a rigid seven membered periphery, which is anchored in the benzenoid unit (Chart I.C.16). Energy minimization studies provided several almost equivalent energy conformations, suggesting the randomization of the side chains. This aspect was encouraging in making all the six sulfur atoms to touch the metal surface (vide infra).

The monolayer of hexa amide was prepared by immersing a clean gold electrode in 3.3 mM methanol solution of the hexa amide (**28**) for 12 h. The homogeneity of the monolayer was examined by cyclic voltammetry by monitoring the current increase at ~ -0.28 eV corresponding to oxygen reduction at the electrode. The cyclic voltammogram presented in Fig. I.C.5 clearly shows the significant effect of monolayer formation with the hexa amide on the electrode surface as monitored by the virtual stoppage of oxygen and the resultant reduction at the electrode. From a comparison of oxygen reduction peak before and after monolayer formation, it can be estimated that ~98% of the electrode surface is covered by the monolayer of the hexa amide (**28**).

An explanation for the near total absence of oxygen approach, when the electrode is covered by a monolayer of **28** would be that, the expected six sulfur

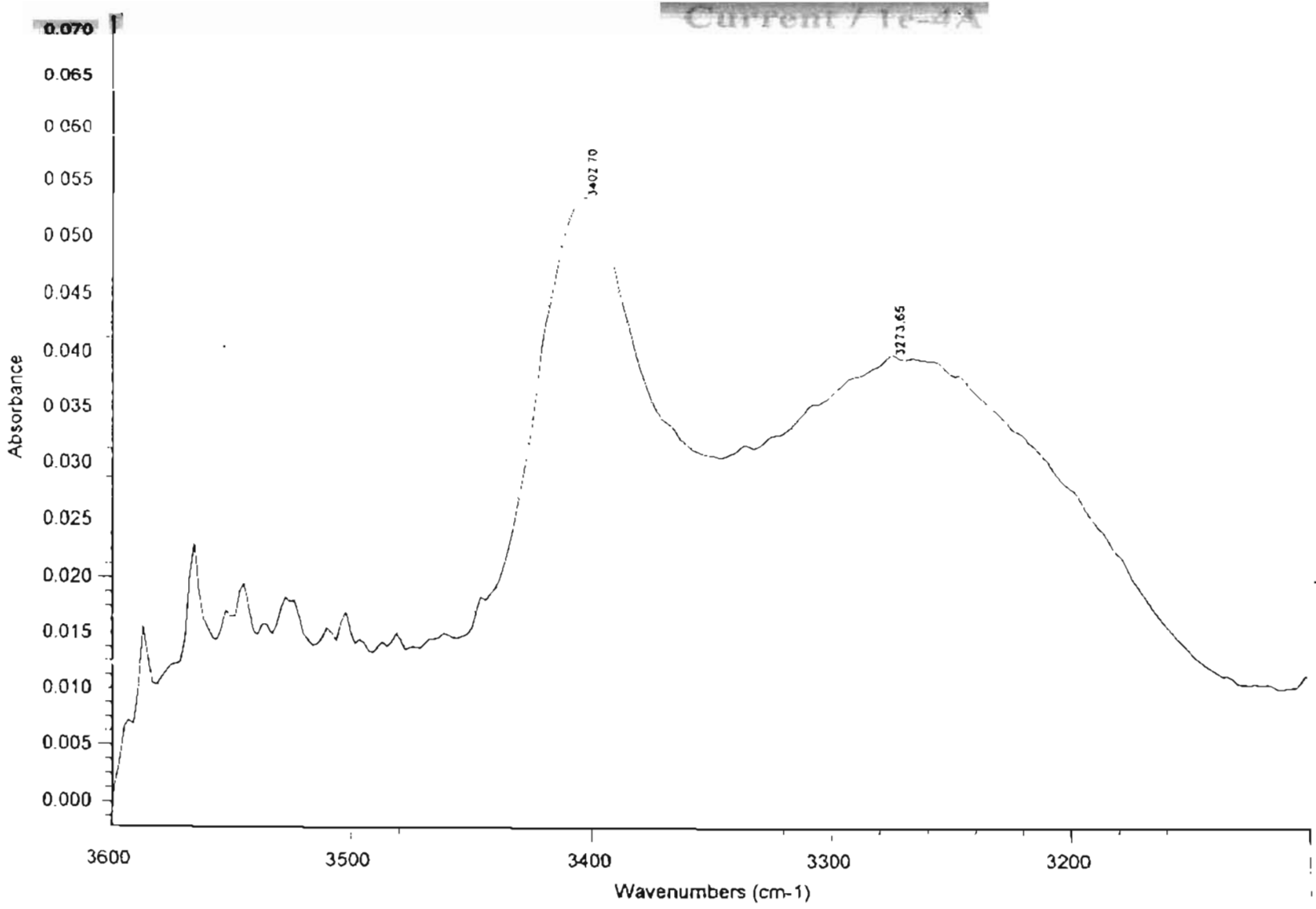

Fig. I.C.4. FT IR spectra of a 1 mM solution of **28** in chloroform, showing significant population of intramolecular H bonding

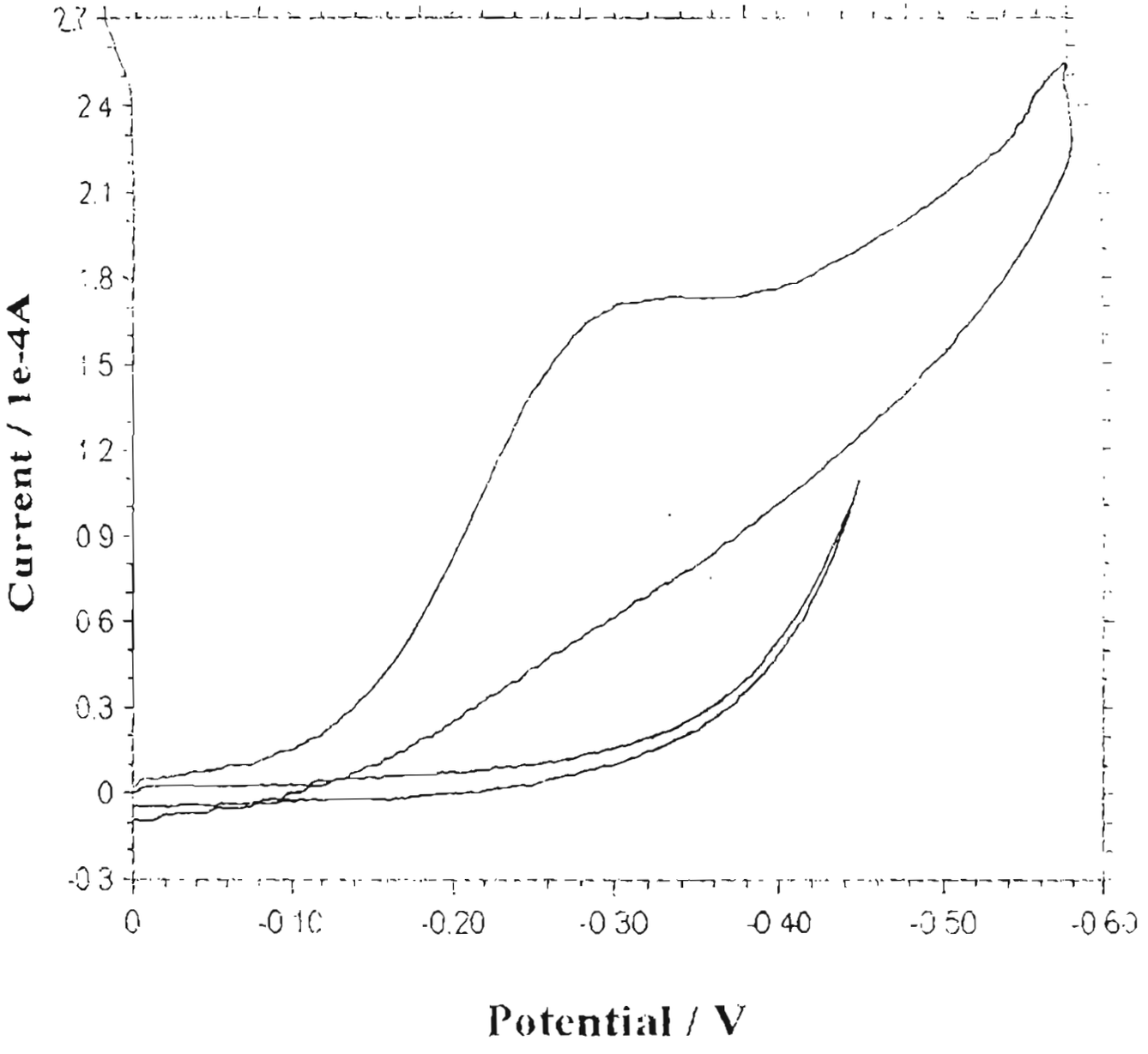

Fig. I.C.5. Cyclic voltammogram showing the change in Oxygen reduction peak, when the gold electrode is modified with a monolayer of **28.** The cyclic voltammetric experiment was done in phosphate buffer at pH 7.2

atoms contact with the electrode could be best accomplished by keeping the ligands as far away as shown in Fig. I.C.6(a).

The deposition of the hexa amide on a spheroid surface like that in colloidal gold would lead to an assembly wherein the ligands would be, in principle, distributed spherically around the gold as shown in Fig. I.C.6(b). The resulting would be an assembly quite similar in some respects to that of clathrins. The systems in "clathrin mimics" envisaged earlier were conceived as arising from assembly of appropriate molecules having the basic principle of the structuring of the equatorial surface from hydrogen bonds. Here, we have a converse of the situation, where the spherical gold directs the assembly, in a non covalent manner around, using its strong affinity to sulfur and based on the principle that the extraneous ligands are kept as far away as possible to secure the spheroid surface.

The preparation and characterization of the hexa amide has shown a strategy for the crafting of peptide bundles. The formation of such macromolecules have attracted much attention in terms of design from vantage of catalytic activity and ion transport. Thus, peptide segments can be grown on mellitic acid, which could have very interesting material and mechanical properties. The ready hexa amidation of the mellitic acid with methionine has been extended to tryptophan and phenyl alanine, giving rise to the hexa

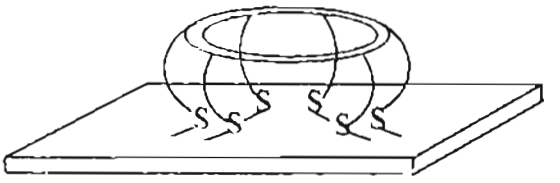

(a)

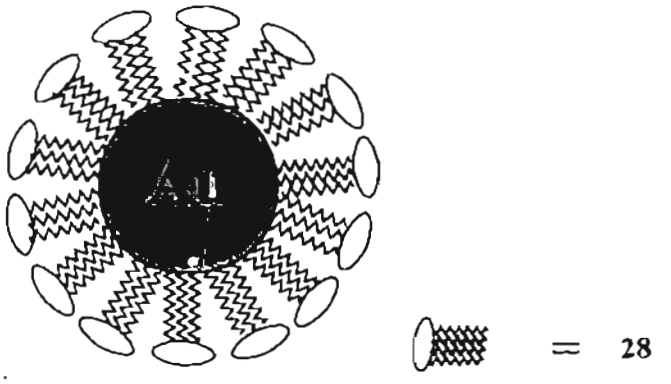

(b)

Fig. I.C.6. a) Expected assembly of **28** on gold electrode

b) Assembly as envisaged on colloidal gold

substituted compounds **31** and **32**, whose structures have been established completely on the basis of detailed spectral studies (Chart I.C.17 & 18). Here also, the FAB mass spectrum was revealing, in the sense that, the hexa amide gradually lost one ligand at a time, to form the mono imide, the bisimide and the tris imide. An interesting aspect of the mass spectra of **31** was that it showed a peak at 1525 arising from loss of water, which could be readily explained on the basis of the formation of the tetrahedral intermediate (**31a**) which is also common to ligand loss-followed by loss of water to **31b** (Chart I.C.17).

The steric consequences in such hexa amidation were dramatically brought out in attempts to prepare the hexa amide from α amino isobutyric acid (Aib) methyl ester. The hexa amide was very desirable, since molecular models showed that the placement of the gem dimethyl groups in a periphery could lead to hydrogen bonded bowl like structures. In the event, the only compound formed in the reaction was the mono imide-tetra amide **33** (Chart I.C.19) whose structure was conclusively established by spectral properties particularly by the typical FAB MS fragmentation pattern (vide infra). Compound **33** could be transformed in to a hexa amide by treatment with another equivalent of Aib methyl ester. Attempts to prepare the corresponding glycine amide were not successful because of the rapid polymerization of the glycine methyl ester resulting in depletion of its concentration. However, the reaction afforded the

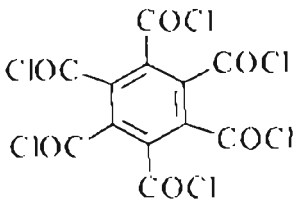

27

$H_2NTrpOMe, Et_3N$

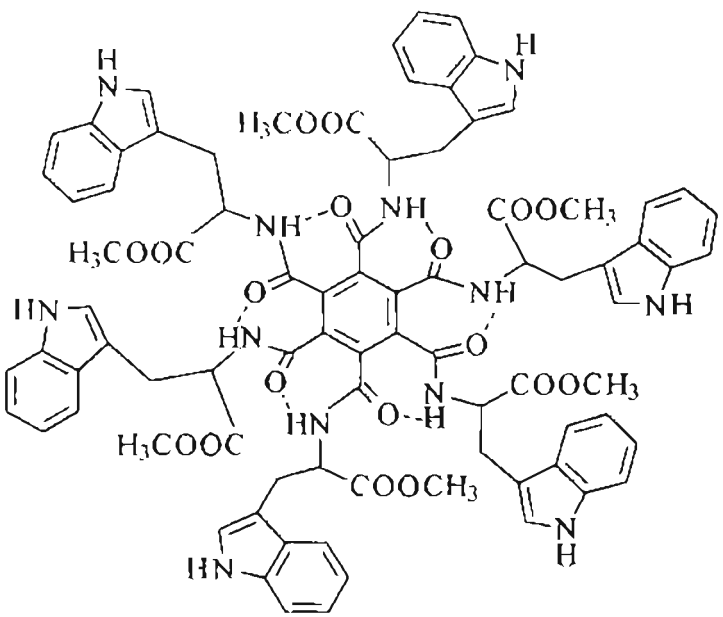

31

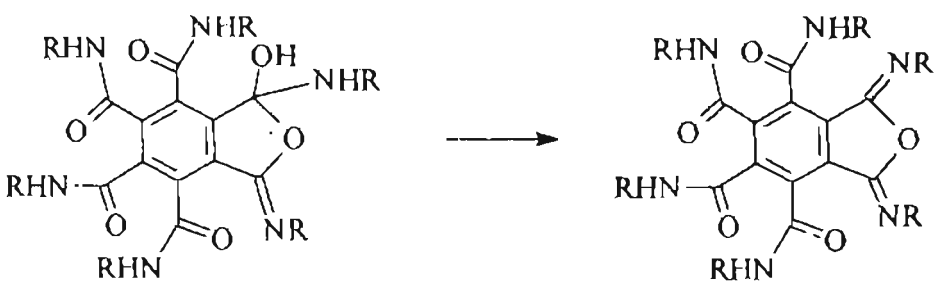

31a 31b

R = TrpOMe

Chart I.C.17

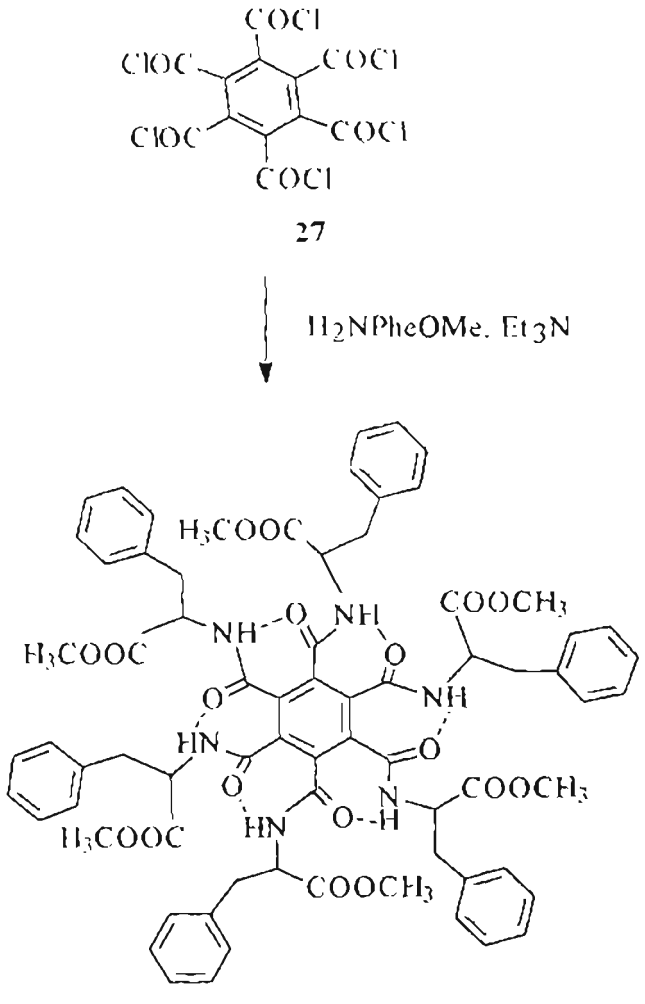
COCl
ClOC
COCl
ClOC
COCl
COCl
27
H2NPheOMe. Et3N
H3COOC
COOCH3
H3COOC
NH
O
NH
O
O
NH
HN
O
O
N
COOCH3
H3COOC
HN
O--H
COOCH3
32

Chart I.C.18

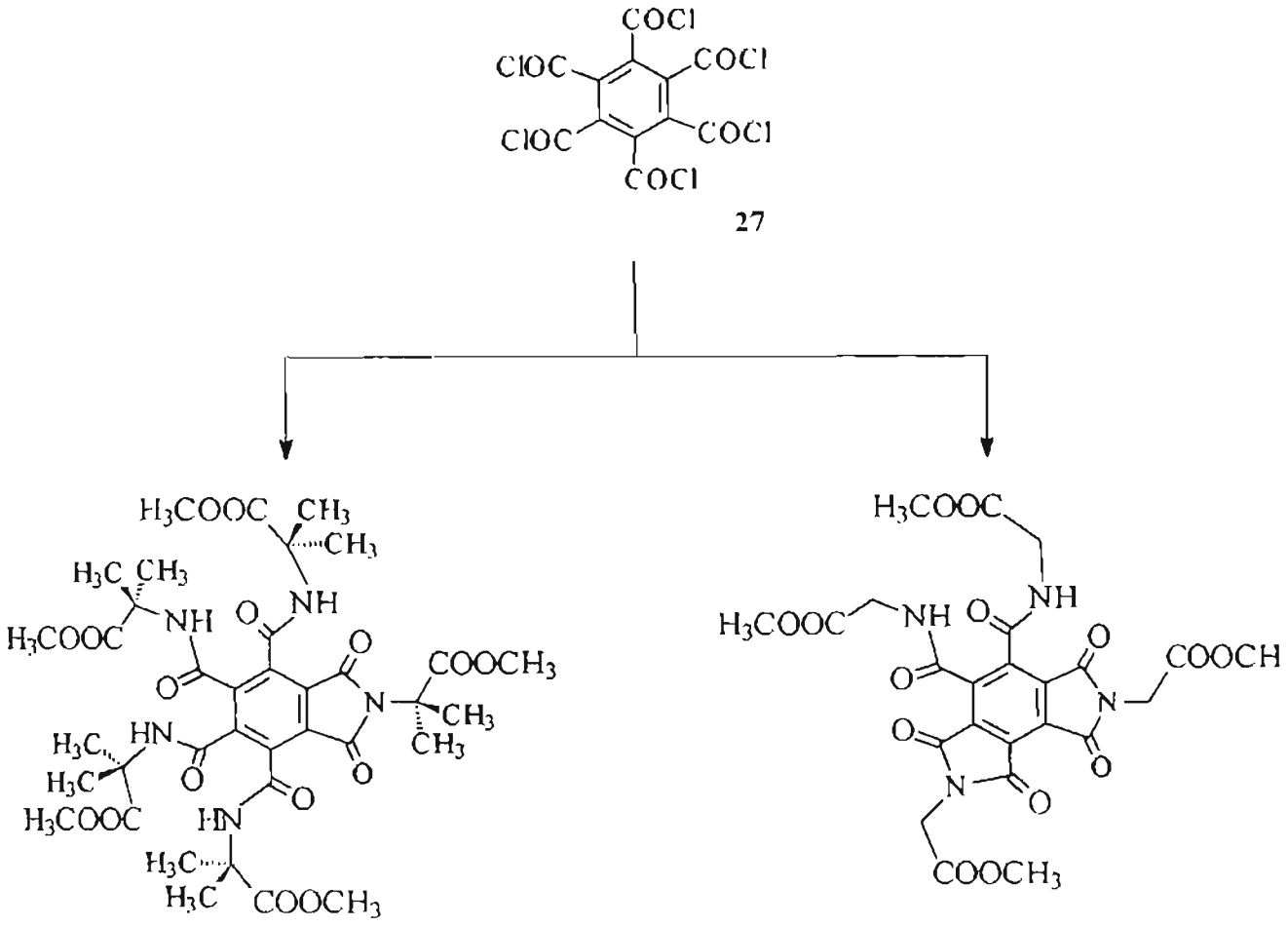
COCl
ClOC
COCl
ClOC
COCl
COCl
27
H3COOC
CH3
CH3
H3C
CH3
NH
H3COOC
O
NH
O
O
COOCH3
N
CH3
CH3
O
O
H3C
HN
H3C
O
H3COOC
O
HN
H3C
CH3
COOCH3
33
H3COOC
NH
H3COOC
O
NH
O
O
COOCH
N
O
O
N
O
COOCH3
34

Chart I.C.19.

bisimide-diamide **34** (Chart I.C.19). As stated previously, the transformation of this compound to the hexa amide should be possible by treatment with excess ligand.

In conclusion, the concept of hexa amidation of mellitic acid has afforded new avenues in the design of peptide models assembled on surfaces, having desirable properties and unusual structures.

The utility of mellitic acid as an anchor for crafting surfaces was further elaborated by the synthesis of a novel class of compounds where the assembly is directed by ionic interactions.

Methanolic solutions of mellitic acid (**4**) and orthophenylene diamine (OPDA) with ratio of 1:3, on admixing, precipitated salt **35** (Chart I.C.20). The structural assignment is supported by analytical data and solution studies.

The molecular weight of **35** at different concentrations were determined by size exclusion chromatography. In the range of 1 - 10 mM concentration, the observed molecular weight remained the same, indicating the presence of discrete species **35**, rather than assemblies arising from association

Fig I.C.7 shows the plot of molecular weight vs K_{av}, which is constructed using standard compounds of known molecular weight. K_{av} is the inner volume accessible to the compound in the column, which is given by

$$K_{av} = \frac{Ve - Vo}{Vt - Vo}$$ Where,

Ve = Elution time

Vo = Void volume

Vt = Bed volume

MAOPDA gave a K_{av} value of 0.75, which when extrapolated to the Y axis corresponded to an average molecular weight of 640, which indicates a 1: 3 type of aggregation as envisaged

As expected, (**4**) afforded, with three equivalents of ethylene diamine (EDA), salt, for which structure **36** has been assigned on the basis of analytical data and comparison with **35** (Chart I.C.20). Of the several [1ω] diamino complexes, that were reacted with mellitic acid (**4**), only the above two formed stochiometric salts.

The reaction of hexamethylene diamine (HMDA) and **4** under conditions described above gave salt (**37**), for which, the 1:1 structure (**37**) has been assigned on the basis of solution studies (Chart I.C.21). This compound showed a K_{av} value of 0.81, which corresponds to a molecular weight of 450 (Fig. I.C.7). Compound **37** is unassociated even at 10 mM concentration. The absence of formation of stochiommetric complex may be due to steric factors. The mellitic

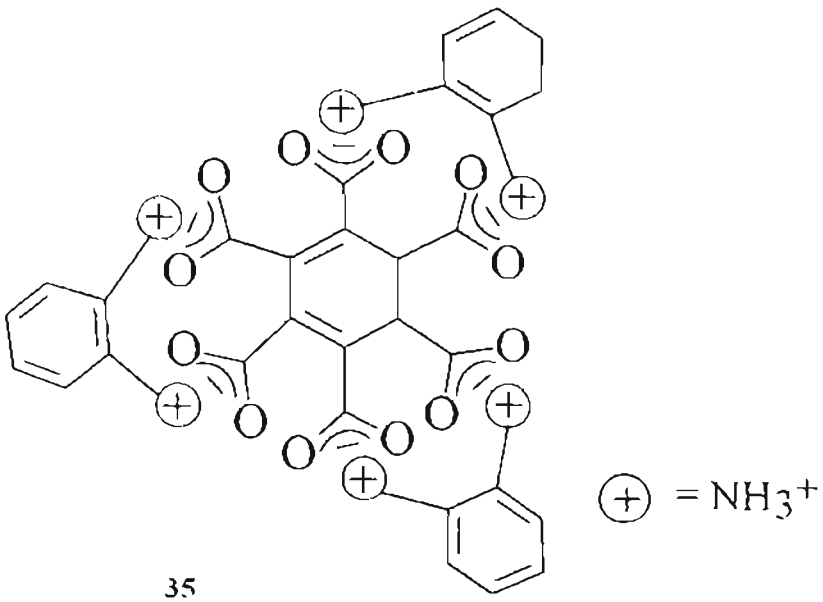

35

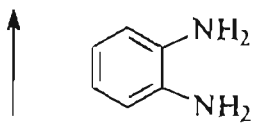

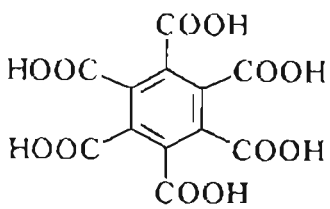

4

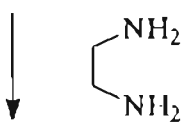

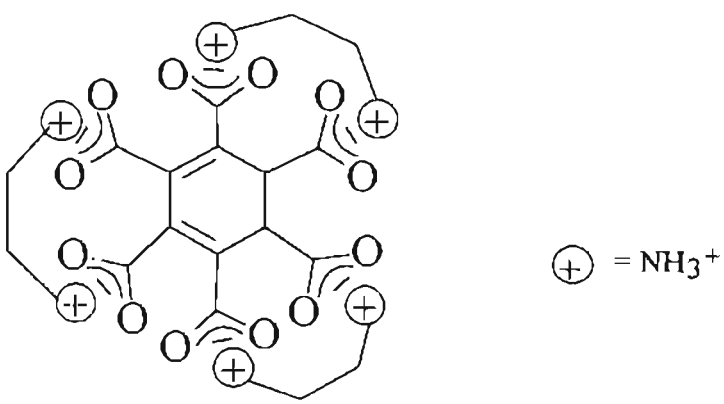

36

Chart I.C.20.

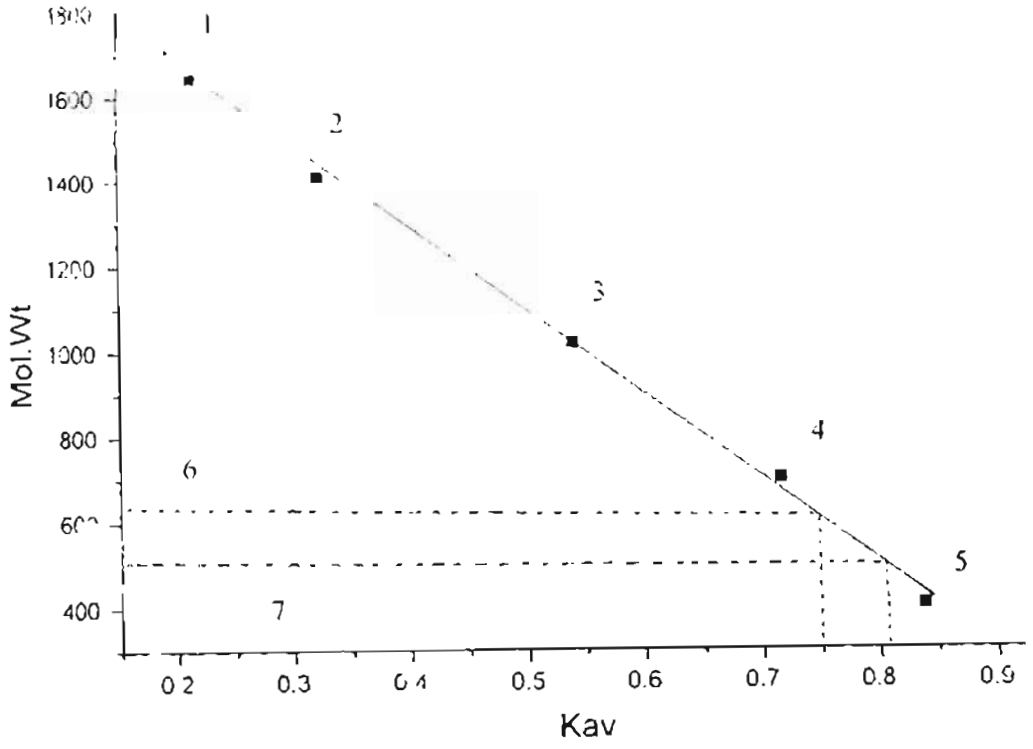

Fig. I.C.7. Size exclusion chromatographic results of mellitic acid salts **35** & **37**

Standard compounds used for comparison

1) Tetramer of Chromotropic acid
   Mol.wt. 1644; Kav. = 0.2162
2) Propyl astra blue iodide
   Mol.wt. 1408; Kav. = 0.3243
3) Rose bengal
   Mol.wt. 1017.65; Kav. = 0.5405
4) Bromocresol green
   Mol.wt. 698; Kav. = 0.7162
5) Chromotropic acid
   Mol.wt. 400.3; Kav. = 0.8378
6) Compound **35**
   Kav. = 0.75
7) Compound **37**
   Kav. = 0.81

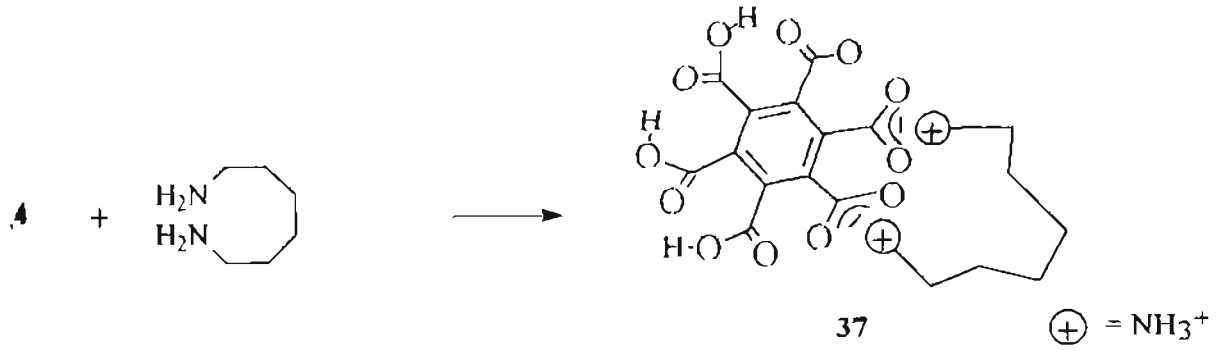

37

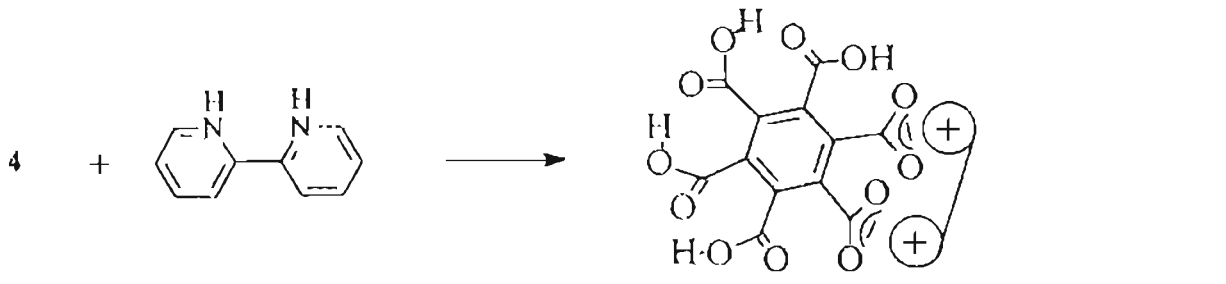

38

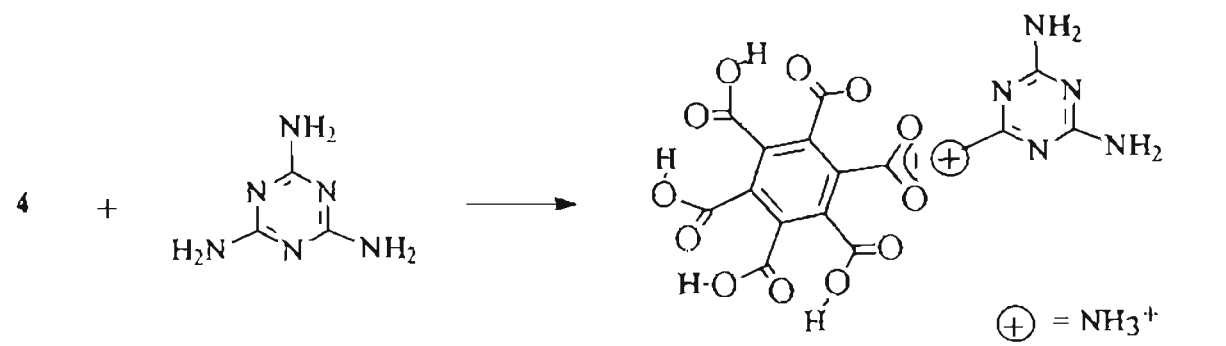

39

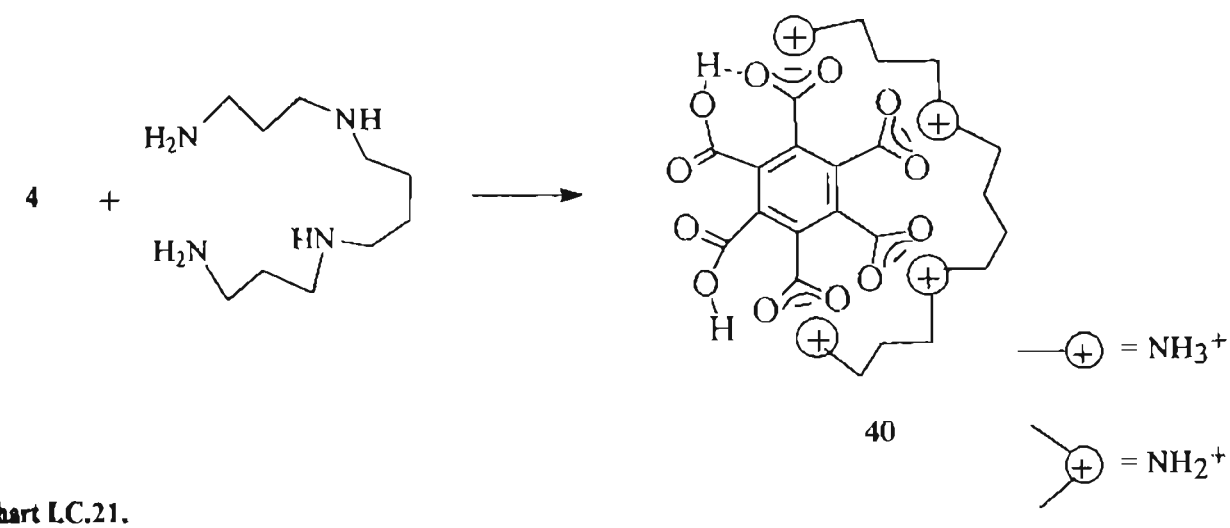

40

Chart I.C.21.

acid-bipyridyl complex is assigned also the 1:1 structure (**38**), based on ms data (Chart I.C.21). The compound has given beautiful crystals.

In a novel effort, the salt formation was monitored by FAB ms. Thus, quantities of mellitic acid and melamine on the one hand and mellitic acid and spermine on the other were mixed and analyzed. In each case, peaks corresponding to 1:1 complexes were observed, for which structures **39** and **40** have been assigned (Charts I.C.21).

In the only example of monoamine tried so far, hexadecylamine, was treated with mellitic acid in the ratio of 6:1. The resulting compound has been assigned the structure **41** on the basis of indirect, ion spray, ms and elemental data (Chart I.C.22). The ion spray ms of **41** clearly showed presence of a cluster of 6 units of hexadecylamine, which could arise only from a structure like **41**.

Mellitic acid salts described above presents a new class of compounds that presents diverse possibilities. Studies pertaining to the controls involved in their formation, solution and solid state studies, need to be undertaken to assess the potential of the design as a route for materials.

The clathrin assembly is directed by triskelions. Interestingly, a triskelion junction involves - in principle - the juxta positioning of 12 carboxyl ends, six from each triskelion. The obvious protocol for the simulation of this event is to

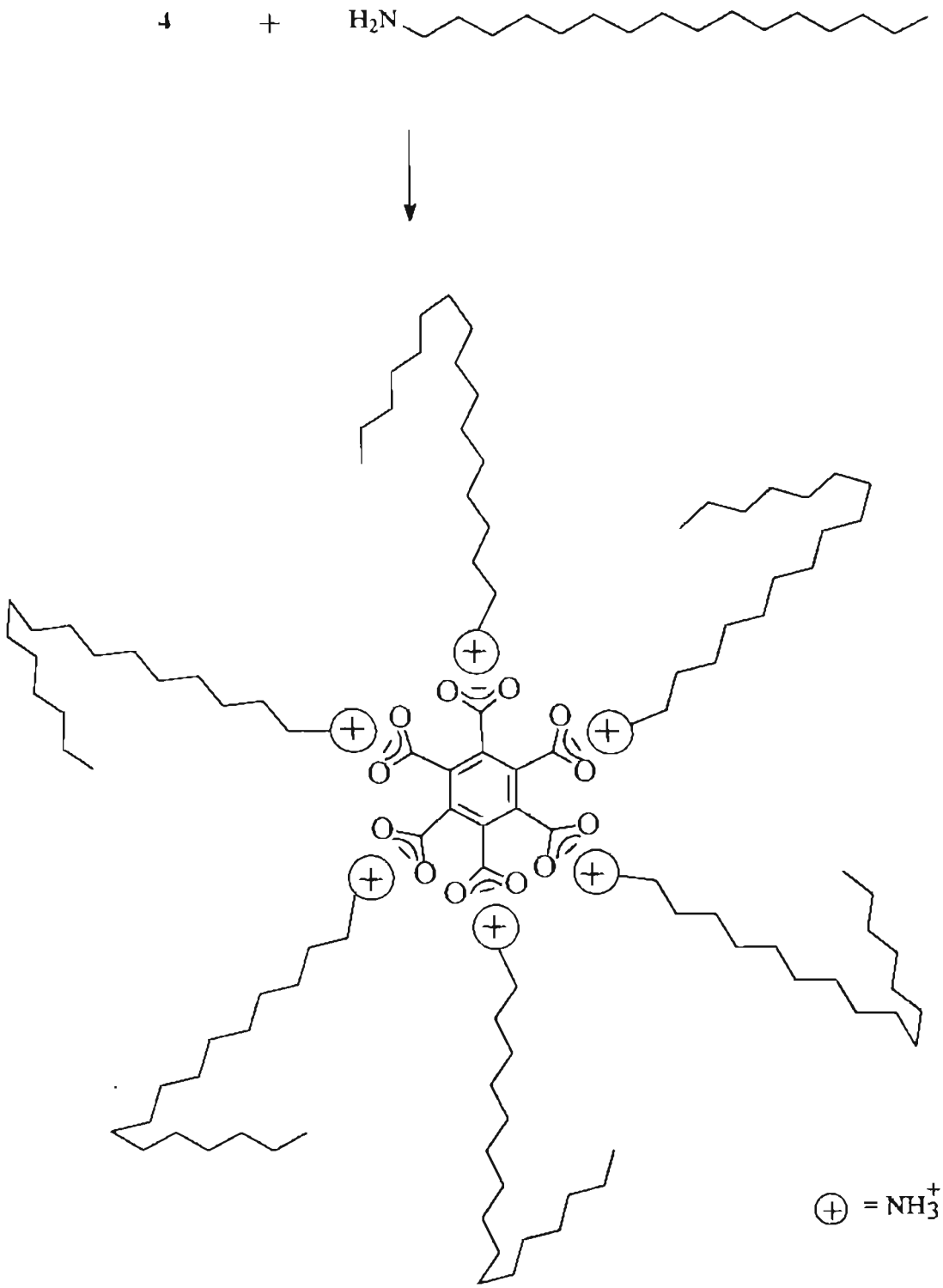

41

Chart I.C.22.

craft systems having directed carboxyl ends on a scaffold and study their assembling properties.

The cyclic hexa peptide $[Glu\text{-}Gly]_3$ was designed for this study. Molecular models clearly showed two patterns here for self assembly. One of these would be the six antiparellel organization of the backbone which will promote stacking interactions, which, in turn, would promote the proper positioning of the propionic acid side chains. The expected one would be the inter and intra association of the three directed carboxylic acids, either alone or in presence of metal ions. The hexa peptide was prepared by protocols presented in Chart I.C.23 & Chart I.C.24.

Glycine was transformed to Glycine benzyl ester hydrochloride (**42**) via reaction with benzyl alcohol/TsOH, deprotection of the p-toluenesulfonate salt with aq. NaOH and treatment with dry HCl.

Glutamic acid was converted to Boc Glu(γOMe)OH (**43**) via sequence, selective γ esterification [$SOCl_2$, MeOH] and N-Boc protection [di-^{t}butyl carbonate, Et_3N]. Coupling of the free base generated from **42** with **43** afforded the key dipeptide Boc-Glu(γOMe)-Gly-OBzl (**44**) in 92% yields. The structural assignment of **44** is supported by spectral data. Peptide **44** was C-deprotected (Pd/C, H_2) at one hand (**44a**) and N-deprotected (TFA / CH_2Cl_2) on the other (**44b**). Coupling of these two (DCC, HOSu) afforded the tetra peptide,

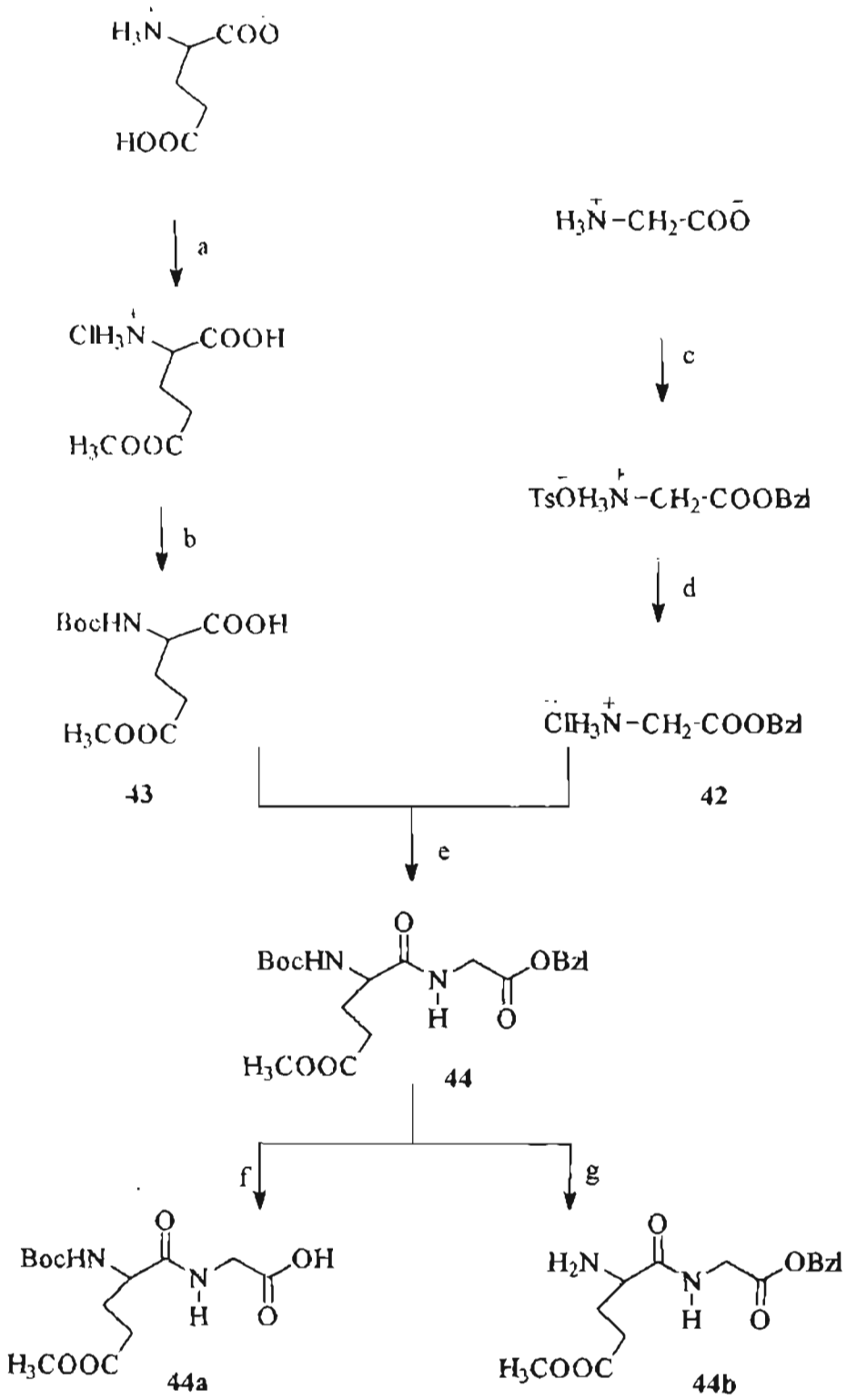

a) $SOCl_2$, MeOH b) i. Pyridine, MeOH; ii. Et_3N, Boc carbonate.

c) TsOH, Benzyl alcohol d) i. aqueous NaOH ii. Dry HCl, Et_2O.

e) Et_3N, DCC, HOSu, CH_2Cl_2. f) H_2/Pd, MeOH. g) i. TFA, CH_2Cl_2

ii. 5% Na_2CO_3

Chart I.C.23

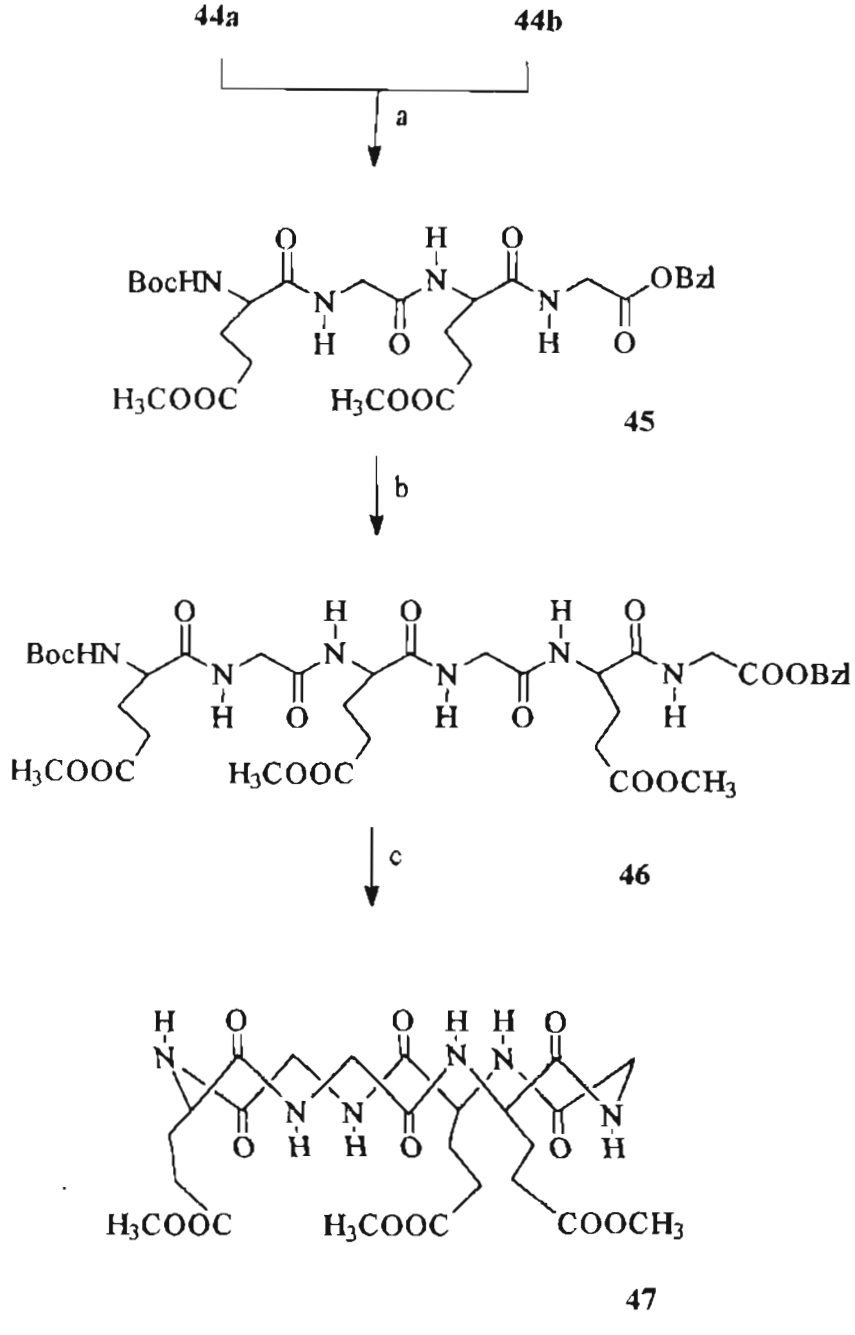

a) DCC, HOSu, CH_2Cl_2. b) i. H_2/Pd, MeOH. ii. **44b**, DCC, HOSu, CH_2Cl_2 :: DMF

c) i. H_2/Pd, MeOH. ii. TFA, CH_2Cl_2. iii. BOP, $NaHCO_3$, DMF

Chart I.C.24.

Boc-Glu(γOMe)-Gly-Glu(γOMe)-Gly-OBzl **45** in 82% yield. Peptide **45** was C-deprotected (Pd/C, H_2) and coupled with N-deprotected dipeptide (**44b**) to afford the hexapeptide Boc-Glu(γOMe)-Gly-Glu(γOMe)-Gly-Glu(γOMe)-Gly--OBzl (**46**) in 71% yield. The very low solubility of the hexapeptide in usual solvents, particularly in MeOH, necessitated the handling of large volume of solutions.

Having at one hand, dipeptide, tetrapeptide and hexapeptide, the solution conformation was studied by NMR methods. This permitted the monitoring of the development of a secondary structure in the above progression. Whilst, the conformation of the dipeptide was common, that of tetra and the hexa peptide showed clear spatial contacts. Table I.C.4 gives the significant ROE correlations observed for di, tetra and hexapeptides as evident from the ROESY spectra. Based on the detailed NMR studies, the hexapeptide (**46**) has been assigned conformation shown in Fig. I.C.8. The temperature dependent NMR of these compounds did not show any significant hydrogen bonded stabilization. The NH dependence on temperature is graphically represented in Fig. I.C.9.

The hexapeptide (**46**) was C-deprotected using Pd/C, H_2 in Methanol. N-deprotection was achieved with TFA. The resulting triflate acid was cyclized [BOP reagent, $NaHCO_3$, DMF] to cyclo[Glu(γOMe)-Gly]$_3$ (**47**). In spite of several attempts, the yield of **47** was quite poor. Further, the low solubility of **47**

Table I.C.4. NOE contacts observed for tetra and hexa peptides (45 &46)

Tetrapeptide (45)	Hexapeptide (46)
N_1 - N_2	N_1 - N_2
C_1 - N_2	N_3 - N_6
C_2 - N_2	C_1 - N_2
N_3 - N_4	C_2 - N_3
C_3 - N_4	N_3 - C_4
	N_4 - C_5
	C_2 - N_4
	C_3 - N_6

Ni and Ci represents proton connected to amide nitrogen and α carbon , respectively of the i^{th} aminoacid residue.

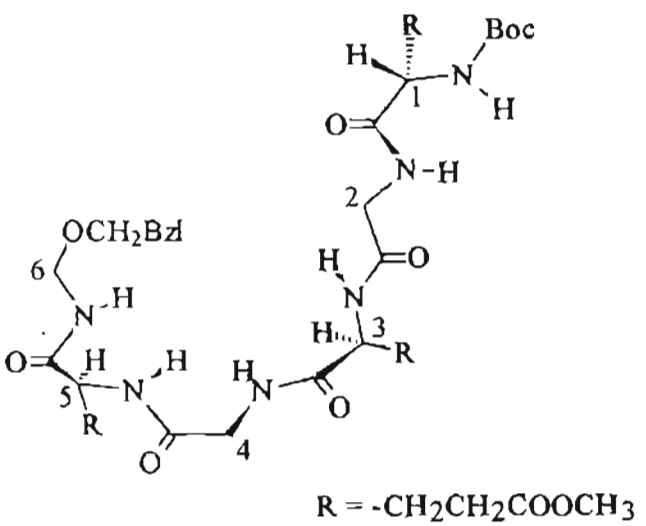

R = -$CH_2CH_2COOCH_3$

Fig. I.C.8. Conformation assigned to the hexapeptide 46 on the basis of NMR studies

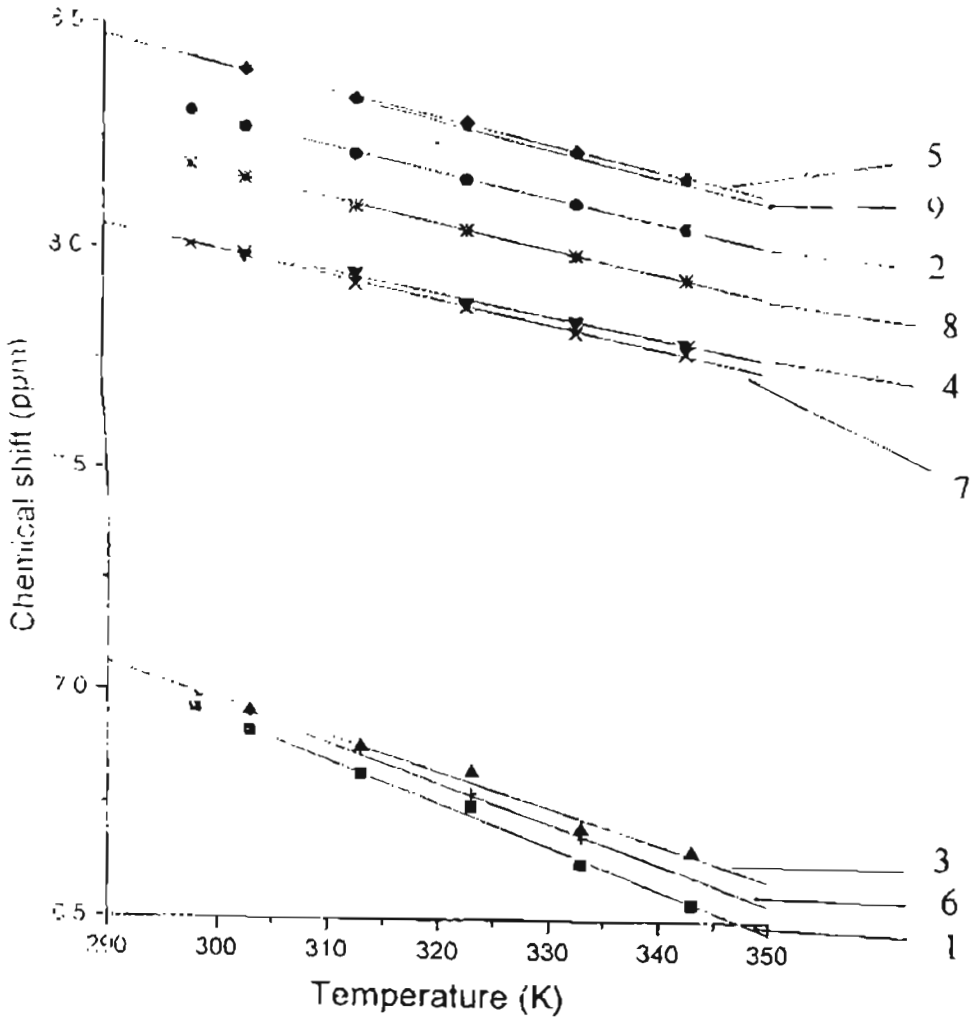

Fig. I.C.9. A plot showing the amide NH shift dependence on temperature (298 - 343K) of di, tetra and hexa peptides (**44**, **45**, and **46**). $d\delta/dt$ values obtained from the slopes did not give any indication of temperature dependence.

1) N_1H (**44**)

2) N_2H (**44**)

3) N_1H (**45**)

4) N_2H and N_3H (**45**)

5) N_4H (**45**)

6) N_1H (**46**)

7) N_2H, N_3H, and N_5H (**46**)

8) N_4H (**46**)

9) N_6H (**46**)

N_i (i = 1, 2, etc.) represents the proton connected to the amide nitrogen of the i^{th} amino acid residue

made purification of the sample extremely difficult. The 600 MHz NMR spectra obtained in DMSO-d6 completely matched with that expected for the cyclic peptide **47**. However, the mass spectrometric results were found to be very capricious and failed to show the expected mass at 600. In several cases, strong peak at 621 was observed. In view of these difficulties, particularly pertaining to the proper characterization of the cyclic hexapeptide **47**, coupled with low yields, further experiments involving **47** was differed.

The clathrin system has inspired efforts in the crafting of spherical surfaces by non covalent self assembly. The flexibility here is illustrated by the fact that success in this direction can be secured in a serendipitous manner using colloidal gold, by directing a spherical assembly from the core of the sphere than from the surface. In addition, the efforts have led to an understanding of subtle factors of aromaticity, unusual oxidation processes, the crafting of systems having hydrogen bonded periphery and facets of ionic self assembly.

I.D. CYTOTOXIC STUDIES WITH THE GINKGOLIDE ANALOG 13 - ARISING FROM ONE STEP TRANSFORMATION OF TRINDANE WITH RUTHENIUM TETROXIDE

The *in vitro* cytotoxic activity of the compound (**13**) was tested against a cell panel, consisting of 60 cell lines which fall under nine different sub-panels - leukemia, non-small cell lung cancer, colon cancer, CNS cancer, melanoma, ovarian cancer, renal cancer, prostate cancer and breast cancer. The overall assessment involved five different concentrations of **13** at ten fold dilutions. A 48 h continuous drug exposure protocol was used. The cell growth was estimated by Sulforhodamine B assay.[32]

The effect of the compound on cell lines are calculated according to one or other of the following two expressions.

If $(\text{Mean OD}_{test} - \text{Mean OD}_{tzero}) \geq 0$, then

$PG = 100 \times (\text{Mean OD}_{test} - \text{Mean OD}_{tzero}) / (\text{Mean OD}_{ctrl} - \text{Mean OD}_{tzero})$

If $(\text{Mean OD}_{test} - \text{Mean OD}_{tzero}) < 0$, then

$PG = 100 \times (\text{Mean OD}_{test} - \text{Mean OD}_{tzero}) / \text{Mean OD}_{tzero}$

Where:

PG = Percentage growth

Mean OD_{tzero} = The average of optical density measurements of SRB-derived colour just before the exposure of the cells to the test compound.

Mean OD_{test} = The average of optical density measurements of SRB derived colour after 48 hours exposure of cells to the test compound.

Mean OD_{ctrl} = The average of optical density measurements of SRB derived colour after 48 hours with no exposure of cells to the test compound.

Table I.D.1. presents the experimental data collected against each cell line. The first two columns describe the cell panel (e.g. leukemia) and the cell line (e.g. K-562) involved. The next two columns list the mean OD_{tzero} and mean OD_{ctrl}; the next five columns list the Mean OD_{test} for each of the five different concentrations. Each concentration is expressed as the $\log_{10}$ (molar). The next five columns list the calculated percentage growths for each concentration. The response parameters GI50, TGI, and LC50 are interpolated values representing the concentrations at which the PG is +50, 0, and -50 respectively. In the case of cell lines where the PG exceeded +50, it was not possible to get response parameters by interpolation. In such cases, the value given for each parameter is the highest concentration tested and is preceded by a > sign.

The variation of percentage growth with $\log_{10}$ of the sample concentration (molar) is presented in Fig.I.D.1 (a - i)

Table I.D.1 . In-vitro testing results

		Log10 Concentration												
		Mean Optical Densities					Percent Growth							
Panel/Cell Line	Tzero	Ctrl	-8.0	-7.0	-6.0	-5.0	-4.0	-8.0	-7.0	-6.0	-5.0	-4.0	GI50	TGI	LC50
Leukemia															
HL-60(TB)	[illegible]6	1.465	1.505	1.482	1.451	1.496	1.362	104	102	98	103	89	>1.00E-04	>1.00E-04	>1.00E-04
K-562	[illegible]18	1.254	1.215	1.217	1.044	1.105	0.980	96	97	81	86	75	>1.00E-04	>1.00E-04	>1.00E-04
MOLT-4	[illegible]5	1.197	1.228	1.136	0.998	0.964	0.895	103	94	80	76	69	>1.00E-04	>1.00E-04	>1.00E-04
RPMI-8226	[illegible]15	1.529	1.598	1.431	1.411	1.321	1.289	106	92	90	83	80	>1.00E-04	>1.00E-04	>1.00E-04
SR	[illegible]91	0.625	0.683	0.635	0.590	0.550	0.549	115	102	92	83	83	>1.00E-04	>1.00E-04	>1.00E-04
Non-Small Cell [illegible] Cancer															
A549/ATCC	[illegible]91	1.466	1.423	1.440	1.426	1.460	1.321	96	98	97	100	88	>1.00E-04	>1.00E-04	>1.00E-04
EKVX	[illegible]40	1.210	1.315	1.284	1.290	1.238	1.178	115	110	111	101	91	>1.00E-04	>1.00E-04	>1.00E-04
HOP-62	[illegible]71	0.550	0.517	0.543	0.543	0.566	0.477	91	98	98	104	81	>1.00E-04	>1.00E-04	>1.00E-04
HOP-92	[illegible]43	0.858	0.848	0.839	0.833	0.793	0.788	97	94	92	79	78	>1.00E-04	>1.00E-04	>1.00E-04
NCI-H226	[illegible]93	1.175	1.172	1.197	1.132	1.168	1.142	99	105	91	99	93	>1.00E-04	>1.00E-04	>1.00E-04
NCI-H23	[illegible]13	1.668	1.677	1.674	1.621	1.681	1.658	101	101	96	101	99	>1.00E-04	>1.00E-04	>1.00E-04
NCI-H322M	[illegible]15	1.904	1.856	1.876	1.861	1.818	1.784	96	98	96	93	90	>1.00E-04	>1.00E-04	>1.00E-04
NCI-H460	[illegible]91	1.114	1.110	1.134	1.138	1.159	1.105	100	102	103	105	99	>1.00E-04	>1.00E-04	>1.00E-04
NCI-H522	[illegible]15	0.467	0.420	0.383	0.008	0.016	0.002	74	54	-97	-95	-99	1.06E-07	2.28E-07	4.87E-07
Colon Cancer															
COLO 205	[illegible]41	0.950	0.899	0.895	0.870	0.907	0.912	94	93	90	95	95	>1.00E-04	>1.00E-04	>1.00E-04
HCC-2998	[illegible]04	1.965	1.998	1.962	1.892	1.895	1.837	102	100	96	96	92	>1.00E-04	>1.00E-04	>1.00E-04
HCT-15	[illegible]29	1.344	1.365	1.346	1.318	1.307	1.253	102	100	98	97	92	>1.00E-04	>1.00E-04	>1.00E-04
HT29	[illegible]46	1.651	1.593	1.589	1.557	1.530	1.503	96	95	93	91	89	>1.00E-04	>1.00E-04	>1.00E-04
KM12	[illegible]17	1.668	1.583	1.684	1.637	1.605	1.489	93	101	98	95	86	>1.00E-04	>1.00E-04	>1.00E-04
SW-620	[illegible]66	0.743	0.734	0.756	0.729	0.731	0.694	98	102	98	98	91	>1.00E-04	>1.00E-04	>1.00E-04
CNS Cancer															
SF-268	[illegible]14	0.789	0.780	0.783	0.775	0.768	0.760	98	99	97	96	94	>1.00E-04	>1.00E-04	>1.00E-04
SF-295	[illegible]13	1.232	1.287	1.280	1.140	0.842	0.396	107	106	89	27	-6	4.24E-06	6.44E-05	>1.00E-04
SF-539	[illegible]07	1.907	1.669	1.745	1.688	1.947	2.296	85	90	86	103	124	>1.00E-04	>1.00E-04	>1.00E-04
SNB-19	[illegible]42	1.692	1.742	1.785	1.709	1.739	1.612	104	108	101	104	93	>1.00E-04	>1.00E-04	>1.00E-04
SNB-75	[illegible]27	0.771	0.757	0.773	0.765	0.765	0.741	97	100	99	99	94	>1.00E-04	>1.00E-04	>1.00E-04
U251	[illegible]70	0.950	0.980	0.986	0.948	0.969	0.899	104	105	100	103	92	>1.00E-04	>1.00E-04	>1.00E-04
Melanoma															
LOX IMVI	[illegible]05	1.001	0.982	0.965	0.951	0.843	0.814	98	96	94	81	77	>1.00E-04	>1.00E-04	>1.00E-04
MALME-3M	[illegible]93	1.037	1.068	1.045	1.094	1.056	1.036	110	103	118	1[illegible]	100	>1.00E-04	>1.00E-04	>1.00E-04
M14	[illegible]50	1.169	1.129	1.147	1.136	1.115	1.102	95	97	96	94	92	>1.00E-04	>1.00E-04	>1.00E-04
SK-MEL-2	[illegible]488	1.539	1.592	1.587	1.538	1.553	1.486	107	107	100	102	93	>1.00E-04	>1.00E-04	>1.00E-04
SK-MEL-28	[illegible]47	1.085	1.077	1.098	1.037	1.056	0.969	99	102	93	96	84	>1.00E-04	>1.00E-04	>1.00E-04
SK-MEL-5	[illegible]41	1.926	1.885	1.809	1.750	1.742	1.513	98	93	90	89	75	>1.00E-04	>1.00E-04	>1.00E-04
UACC-257	[illegible]19	1.380	1.390	1.368	1.394	1.379	1.311	102	98	102	100	89	>1.00E-04	>1.00E-04	>1.00E-04
UACC-62	[illegible]02	1.870	1.830	1.858	1.786	1.783	1.710	101	103	97	96	90	>1.00E-04	>1.00E-04	>1.00E-04
Ovarian Cancer															
IGROV1	[illegible]42	1.151	1.149	1.119	1.137	1.071	1.099	99	95	98	89	93	>1.00E-04	>1.00E-04	>1.00E-04
OVCAR-3	[illegible]86	0.598	0.598	0.644	0.601	0.635	0.561	100	111	101	109	91	>1.00E-04	>1.00E-04	>1.00E-04
OVCAR-4	[illegible]04	1.206	1.192	1.272	1.146	1.153	1.148	98	109	91	92	92	>1.00E-04	>1.00E-04	>1.00E-04
OVCAR-5	[illegible]47	1.004	0.990	0.975	1.004	0.950	0.940	97	95	100	90	88	>1.00E-04	>1.00E-04	>1.00E-04
OVCAR-8	[illegible]71	0.683	0.666	0.675	0.672	0.621	0.625	97	98	98	88	89	>1.00E-04	>1.00E-04	>1.00E-04
Renal Cancer															
786-0	[illegible]19	1.261	1.260	1.221	1.197	1.206	1.158	100	96	93	94	90	>1.00E-04	>1.00E-04	>1.00E-04
A498	[illegible]68	1.377	1.393	1.393	1.395	1.391	1.368	103	103	103	103	98	>1.00E-04	>1.00E-04	>1.00E-04
ACHN	[illegible]65	1.473	1.480	1.513	1.448	1.465	1.476	101	104	98	99	100	>1.00E-04	>1.00E-04	>1.00E-04
CAKI-1	[illegible]69	0.784	0.605	0.708	0.585	0.594	0.317	71	88	68	69	24	2.66E-05	>1.00E-04	>1.00E-04
RXF 393	[illegible]76	0.970	0.991	1.024	0.976	0.979	1.007	104	109	101	101	106	>1.00E-04	>1.00E-04	>1.00E-04
SN12C	[illegible]60	1.709	1.638	1.639	1.630	1.668	1.504	94	94	93	96	82	>1.00E-04	>1.00E-04	>1.00E-04
TK-10	[illegible]64	1.311	1.304	1.297	1.349	1.336	1.309	99	97	107	105	100	>1.00E-04	>1.00E-04	>1.00E-04
UO-31	[illegible]65	1.026	1.022	1.019	1.027	1.046	1.027	100	99	100	103	100	>1.00E-04	>1.00E-04	>1.00E-04
Prostate Cancer															
PC-3	[illegible]51	1.004	1.061	1.074	1.039	1.038	0.984	109	111	105	105	97	>1.00E-04	>1.00E-04	>1.00E-04
DU-145	[illegible]69	0.893	0.906	0.881	0.849	0.873	0.911	102	98	94	97	102	>1.00E-04	>1.00E-04	>1.00E-04
Breast Cancer															
MCF7	[illegible]67	1.375	1.392	1.355	1.375	1.353	1.313	102	98	100	98	94	>1.00E-04	>1.00E-04	>1.00E-04
NCI/ADR-RES	[illegible]58	1.062	1.055	1.074	1.030	1.057	1.036	99	102	95	99	96	>1.00E-04	>1.00E-04	>1.00E-04
MDA-MB-231/ATCC	[illegible]54	1.054	1.053	1.034	1.022	1.064	1.038	100	96	94	102	97	>1.00E-04	>1.00E-04	>1.00E-04
HS 578T	[illegible]76	1.118	1.109	1.154	1.191	1.207	1.103	97	112	124	130	95	>1.00E-04	>1.00E-04	>1.00E-04
MDA-N	[illegible]46	1.824	1.816	1.777	1.759	1.758	1.576	100	97	95	95	82	>1.00E-04	>1.00E-04	>1.00E-04
BT-549	[illegible]59	1.334	1.393	1.412	1.382	1.377	1.351	108	110	106	106	102	>1.00E-04	>1.00E-04	>1.00E-04
T-47D	[illegible]19	0.677	0.718	0.731	0.679	0.695	0.721	114	118	101	106	115	>1.00E-04	>1.00E-04	>1.00E-04

a)

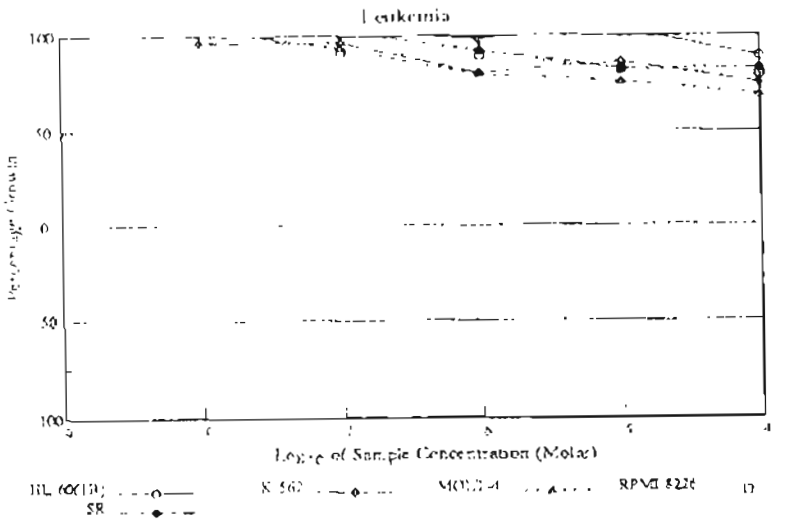

b)

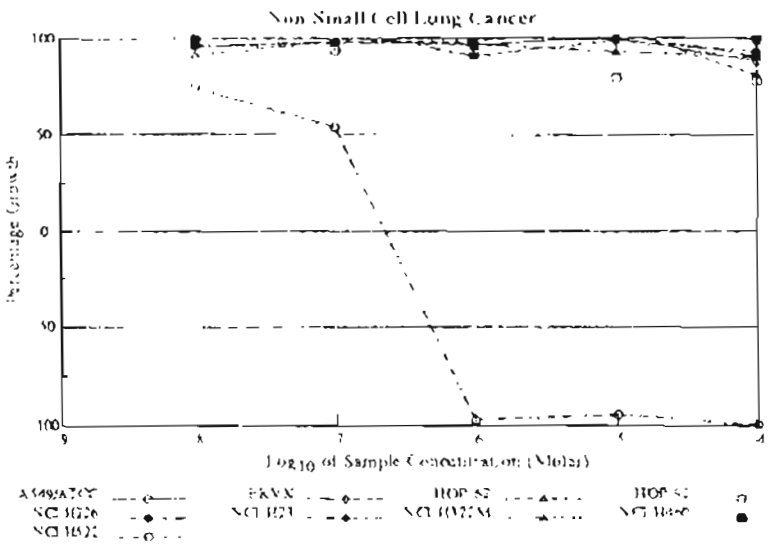

c)

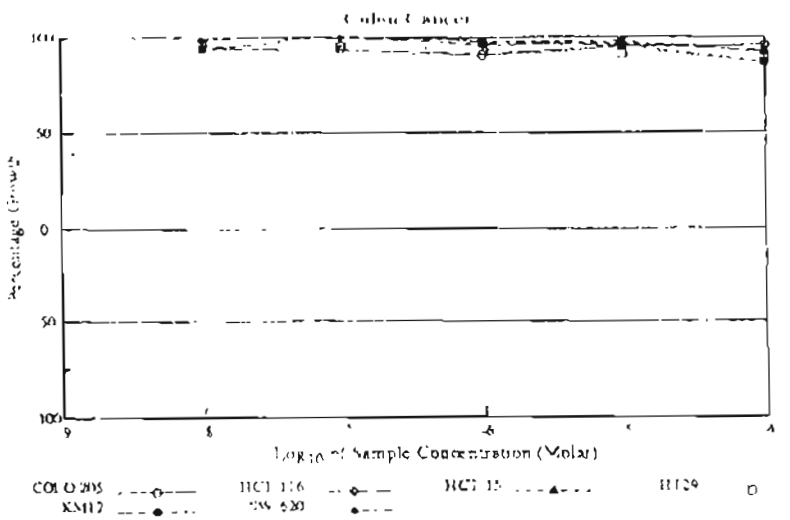

Fig. I.D.1. Dose response curves

d)

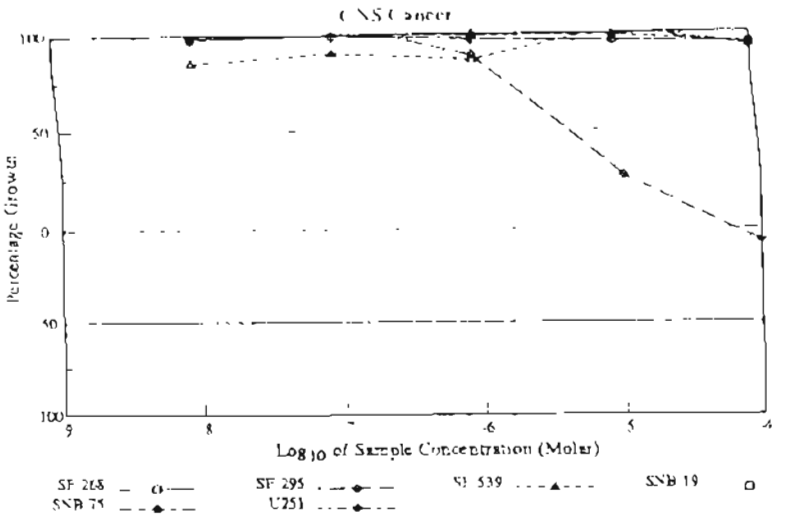

e)

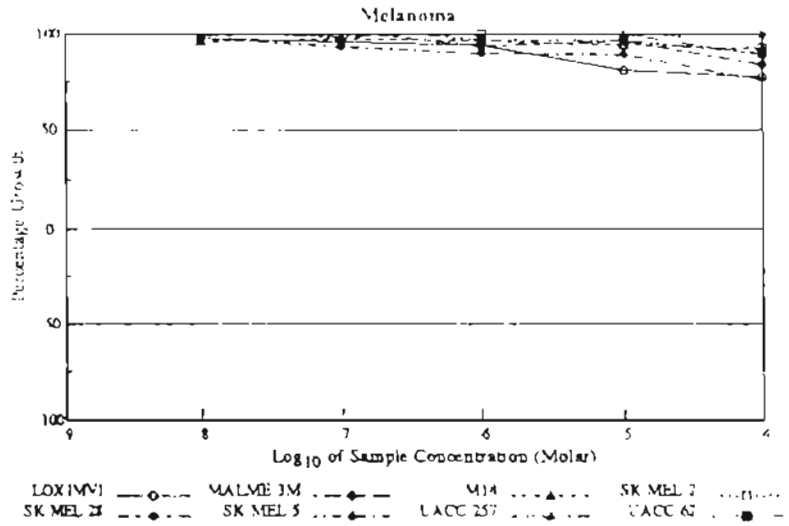

f)

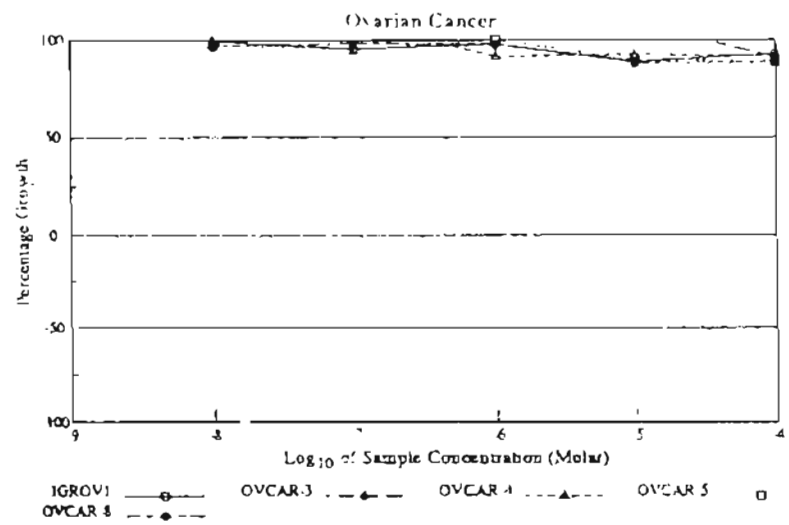

Fig. LD.1. Continues.....

g)

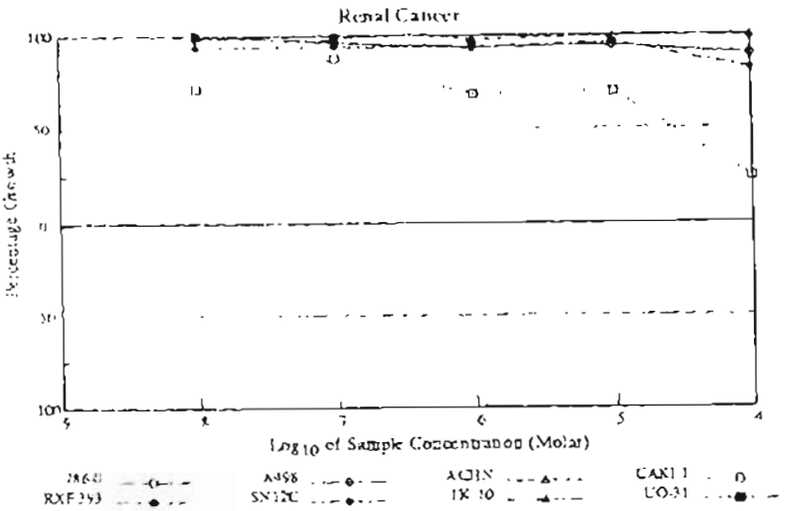

h)

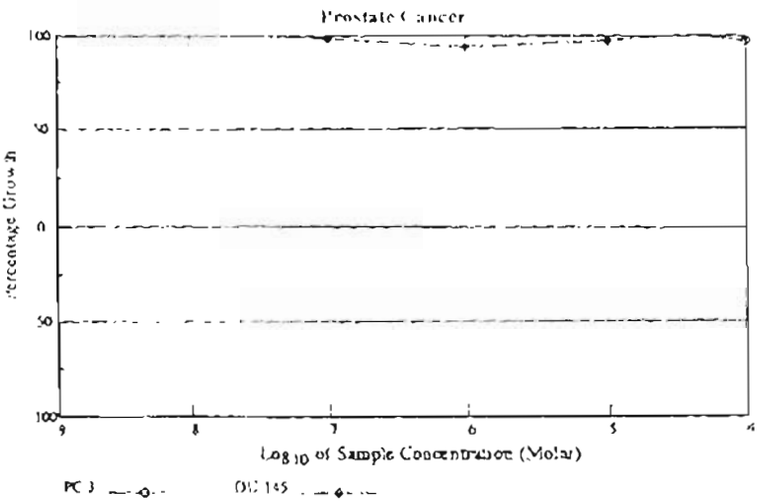

i)

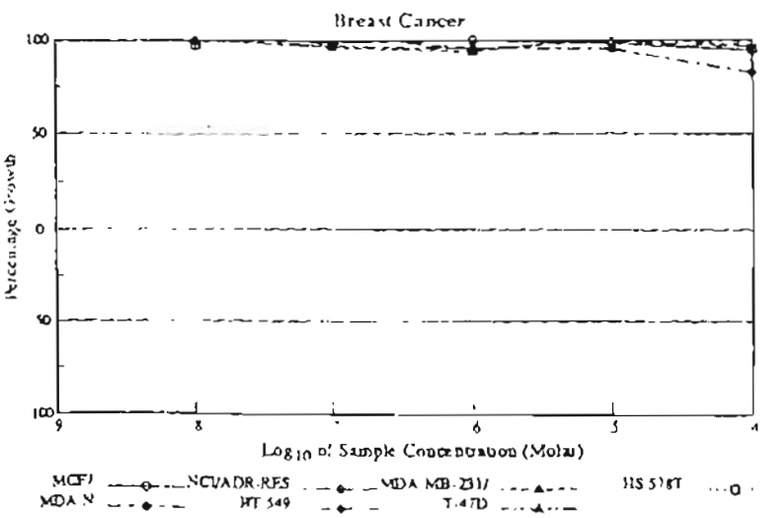

Fig. I.D.1. Continues.....

An examination of the dose response curves show that the compound **13** shows remarkable cytotoxic activity against NCI-H522 of non-small cell lung cancer, with $\log_{10}$ GI50, TGI and LC50 values -6.97, -6.64 and -6.31 molar respectively. Its activity towards SF-295 of CNS cancer was moderate with GI50 at -5.37 and TGI at -4.19 molar. CAKI-1 of Renal cancer showed a still lower response on drug administration with a GI50 of -4.58 molar. All other cell lines screened showed comparatively lower cytotoxic activity, where GI50 values exceeded -4.00 molar.

Conclusion

The selective inhibition shown by **13** against NCI H522 of non-small cell lung cancer is a novel finding, not reported thus far for this class of compounds. Thus, in addition to possible anti PAF activity expected for compound **13**, on the basis of such properties to the related ginkgolides, compound **13** or its analogs have been shown in the present work to posses cytotoxic activity as well.

I.E. EXPERIMENTAL

All amino acids used were of L-configuration. Melting points were recorded on a Fisher-Johns melting point apparatus and are uncorrected. Infra red spectra were recorded on a Perkin Elmer / 1600 - FT spectrometer either as neat liquids or as KBr pellets and prominent peaks are expressed in cm^{-1}. ^{1}H and ^{13}C NMR spectra were recorded on Bruker WM-300, Hitachi R-600 and JEOL 90 MHz instruments. The chemical shifts are expressed in δ (ppm) with TMS at 0.000 as the internal reference. FAB MS were obtained on a JEOL SX-120 / DA - 6000 instrument using m-nitrobenzylalcohol as the matrix. C, H, N analysis was carried out in Vario EL elemental analyzer. Optical rotation was measured with an automatic JASCO polarimeter; concentration is given in gram / 100 mL. The cyclic voltammetric experiment was done on CH1660A electrochemical work station, in phosphate buffer at Ph 7.2. Gold surface was used as the cathode, silver foil as anode and calomel electrode as reference. Reactions were monitored wherever possible by TLC. Silica gel / G (Merck) was used for TLC and column chromatography was done on silica gel (100 - 200 mesh) columns, which were generally made from a slurry in hexane or a mixture of hexane and ethyl acetate. Products were eluted with a mixture of ethyl acetate / hexane.

I. Preparation of N, N-Boc maleimide (1).

A mixture of maleic anhydride (2.45g, 25 mmol), tert-butyl carbazate (3.3g, 25 mmol) and activated molecular sieves (~1g) in chloroform (50 mL) was refluxed for 10 h, solvents evaporated and chromatographed on silica gel. Elution with hexane - EtOAc system (9:1) gave 2.73g of N, N-Boc maleimide (**1**).

Yield : (52%)

M.p. : 145 - 147°C

IR (KBr): 3312, 1744, 1712, 1520

^{1}H NMR ($CDCl_3$): δ 1.48 (s, 9H, Boc CH_3), 6.6 (s, 1H, NH), 6.8 (s, 2H, -CH=CH-)

FAB MS (neg) : $(M-H)^-$ 211; FAB MS : $(M+H)^+$ 213, $(2M+H)^+$ 425, $(3M+H)^+$ 637, $(M+Li)^+$ 219, $(2M+Li)^+$ 431, $(3M+Li)^+$ 643.

Phthalic anhydride (0.75g, 5 mmol), when reacted with boc-carbazate (0.66g, 5 mmol), under the conditions described above, gave 1.1g of N,N-Bocphthalimide (**1a**).

Yield : 84%

M.p. : 198-200°C

IR (KBr) : 3328, 3248, 1776, 1696, 1600, 1328

^{1}H NMR ($CDCl_3$) δ 1.5 (s, 9H, Boc CH_3s), 6.7 (brs, 1H, NH), 7.78, 7.91 (m, m, 4H, *ArHs*)

II. Attempted deprotection of (1): isolation of fumaric acid mono methyl ester hydrazide (3)

Compound **1** (0.5g, 2.35 mmol) in dry MeOH (10 mL), was cooled to 0 - 5°C and a steady stream of dry HCl was passed for 20 min. The resulting mixture was left to stand at 20°C for 2 h. diluted with 20 mL of dry ether, and the precipitated solid was filtered and dried to afford 0.148g of **2**.

Yield : (43%) ; M.p. : 148 - 150°C.

The above salt was dissolved in minimum amount of water, neutralized with cold saturated $NaHCO_3$, extracted with EtOAc (3 x 25 mL), dried ($MgSO_4$) and evaporated under reduced pressure to afford 0.049g of **3**.

Yield : (34%)

M.p. : 143 - 145°C

IR (KBr) : 3340 (br), 3000 (br), 1710, 1680, 1600, 1540, 1400

^1H NMR ($CDCl_3$) δ 3.8 (s, 3H, ester), 7.00 (d, 2H, -CH=CH-), 7.3 (brs, 3H, $-NHNH_2$)

FAB MS : $(M+H)^+$ 145

III. Attempted transformation of mellitic acid (4) to mellitic - N,N-Boc-triimide: isolation of 5.

Mellitic acid (0.5g, 1.46 mmol) was refluxed with dry acetic anhydride (15 mL) for 18 h.[22] The excess solvent was distilled out completely, the residue

triturated with 10 mL of dry xylene, evaporated, dried thoroughly in *vacuo* and used directly for the next step.

A mixture of the above and Boc carbazate (0.58g, 4.38 mmol) was refluxed in chloroform (20 mL) for 9 h. The reaction mixture was washed with cold saturated $NaHCO_3$ solution (2 x 10 mL), organic layer washed with distilled water (1 x 10 mL), dried ($MgSO_4$), evaporated under reduced pressure and the residue chromatographed on silica gel. Elution with hexane - EtOAc (1:1) afforded 0.068g (7%) of **5**.

IR (neat) : 3280 (br), 1730, 1610, 1380

^{1}H NMR ($CDCl_3$) 1.34 (s, Boc CH_3)

FAB MS (neg) : 762 (37%) $(M-H)^-$

IV. Attempted transformation of mellitic acid (4) to the mellitic tris-imide: isolation of the bis imide 7.

Ammonia was passed through a solution of mellitic acid (0.5g, 1.46 mmol) in THF for 0.5 h. The precipitated solid was washed with THF (2 x 10 mL) and dried to afford 0.6g (92%) of the hexa ammonium salt (**6**).

M.p. : >300 °C (dec)

IR (KBr) : 3191 (br), 1587 (br), 1431, 1337

Compound **6** (0.5g, 1.12 mmol) was gently heated in a test tube for 0.5 h, till the evolution of ammonia ceased. The residue was sublimed in vacuum at

270°C to afford 0.012g, (0.05 mmol, 5%) of 7. The residue unsublimed was acidic in nature, which, as per literature evidence, is euchroic acid[23]

7)

M.p. : > 310°C

IR (KBr) : 3204, 1775, 1728, 1391, 1317

GC MS : 216

V. Preparation of tris Cyclopentanobenzene (Trindane, 8).

Cyclopentanone (16 mL, 0.18 mol) in dry ethanol (18 mL) was admixed with, in drops, conc.H_2SO_4 (8 mL), refluxed for 15 h, poured on to ice (~70 g), neutralized with sodium carbonate and extr d with CH_2Cl_2 (3 x 30 mL), washed with water, dried ($MgSO_4$), evaporated and chromatographed on silica gel column. Elution with petroleum ether afforded 4.0 g of **8**

Yield : (33%)

M.p. : 92°C (lit.[29] 95-97°C)

IR (KBr) : 2956, 2845, 1450, 1431

^{1}H NMR (CDCl$_3$) δ 2.12 (m, 6H, CH_2s), 2.81 (t, 12H, benzylic CH_2s)

GC MS : 198

VI. Preparation of Trindane hexa bromide (9).

A stirred solution of Trindane (3g, 15.15 mmol) in CCl_4 (90 mL), cooled in ice-salt bath was illuminated with 200 W incandescent bulb and a solution of 4.8

mL of bromine (93 mmol) in CCl_4 (20 mL) was added in drops over a period of 4 h. The contents were stirred and illuminated for an additional 1 h and then gently refluxed for 1.5 h while flushing with nitrogen to remove traces of bromine and HBr. The reaction mixture was filtered, solvents evaporated and the residue precipitated from hot THF using ether to afford 7 g of trindane hexabromide,

Yield : (68%)

M.p. : > 180°C (dec)

IR (KBr) : 3413 (br), 2982, 1613, 1431, 1276, 1182, 933, 744

^{1}H NMR ($CDCl_3$) δ 2.6 - 4.00 (m, 6H, CH_2s), 5.00 - 6.00 (m, 6H, benzylic CH_2s)

VII. Preparation of Trindene (10)

To a stirred and ice cooled mixture of activated zinc dust (5g) and argon purged dry DMF (50 mL), was added Trindane hexabromide (8.3g, 12.3 mmol) and triethylamine (2 mL) simultaneously during 15 min. The resulting dark mixture was stirred at 0°C for 1 h and then at room temperature for 18 h. It was filtered and poured on to ~60g of ice. The precipitate was collected, washed with water and taken up in ether (4 x 30 mL). The washings was extracted with ether, the combined extracts dried ($MgSO_4$), evaporated under reduced pressure without applying heat and chromatographed on silica gel. Elution with hexane afforded 0.339 g of Trindene.

Yield : (10%)

M.p. : 104 - 105°C (lit[25] M.p. 108 - 110°C)

IR (KBr) : 3360 (br), 2900, 1700, 1610, 1390, 1270, 1080

^{1}H NMR ($CDCl_3$) δ 3.3 - 3.7 (m, 6H, CH_2s), 6.45 - 6.8 (m, 3H, =CH-), 6.9 - 7.2 (m, 3H, Ar-CH=)

VIII. Epoxidation of Trindene: isolation of 12

mCPBA (243 mg, 1.41 mmol) was added to a stirred solution of trindene (90 mg, 0.47 mmol) in dry CH_2Cl_2 (5 mL), the mixture stirred for 4 h, the solvent evaporated under reduced pressure and the residue chromatographed on silica gel. Elution with benzene - EtOAc (9:1) afforded 89 mg of the epoxide **11**.

^{1}H NMR ($CDCl_3$) : δ 3.00 - 3.5 (m, 6H, CH_2s), 4.6 - 5.00 (brs, 3H, CH), 6.2 - 6.5 (brs, 3H, CH)

To the above product in dry benzene (5 mL) was added ~ 0.3 mL of $BF_3.Et_2O$ and stirred for 8 h at room temperature. The reaction mixture was washed with water (2 x 5 mL), dried and evaporated under reduced pressure and chromatographed on silica gel using benzene. The IR of the product **12** clearly showed the presence of conjugated ketone

IX. Reaction of Trindane (8) with Ruthenium tetroxide: isolation of 13 and 14.

A mixture of trindane (0.495g, 2.5 mmol), CH_3CN : CCl_4 : H_2O [10 : 10 : 20 mL], $NaIO_4$ (9.7g, 45 mmol), $RuCl_3.3H_2O$ (2.2mol%, ~0.015g) was sealed,

shaken for 3h, cautiously opened, filtered, the residue washed with EtOAc (3 x 20 mL), the organic layers washed with water (2 x 10 mL), dried ($MgSO_4$), evaporated and chromatographed on silica gel. Elution with hexane - EtOAc (1:1) afforded **13** and **14**.

13) Yield : 0.120 g; ~15%

M.p. : 148-150°C

FT IR (KBr) 3396, 2972,1736, 1709, 1432, 1143

^{1}H NMR $CDCl_3$ - DMSO-d_6) δ 1.42 - 2.82 (brm, 9H, CH_2s), 3.99 - 4.44 (brs, merged with the water peak in DMSO, OHs), 5.9 (brs, OH), 7.75 (s, COOH).

^{13}C NMR ($CDCl_3$ - DMSO-d_6) δ 16.19 - 34.66 (9 x CH_2); 85.99, 87.32, 93.04, 103.78 (4 x ~C-O), 174.40 (CO), 221.01 (CO)

FAB MS (neg) (m/z) (%) : 313 (78%) $(MH)^-$, FAB MS (pos) (m/z) (%) : 337 (77%) $(M+Na)^+$

Anal. found C, 57.55; H, 7.33. Calc. for $C_{15}H_{22}O_7$; C, 57.3; H, 7.00.

14) Yield ; 0.06g (7%)

FT IR (neat) 3434, 2955, 1735, 1445, 1175

^{1}H NMR (300 MHz, $CDCl_3$) δ 1.4 - 2 5 (m, CH_2s), 3.48, 4.21, 6.42 (s, s, s, OH, COOH, exchangeable), 3.66 (OMe)

^{13}C NMR ($CDCl_3$) δ 17.05-38.05 (9 x CH_2), 51.48 (CH_3O), 85.95, 88.35, 95.17, 105.00 (4 x $-\overset{|}{\underset{|}{C}}-O-$); 174.00, 222.90 (2 x CO) | DEPT studies showed 9 x CH_2 and 1 x CH_3].

FAB MS (neg) (m/z) (%) : 327 (78%) $(M-H)^-$

X) Ozonolysis of trindane: isolation of steroid prototype (15), aromatic ketone (16) and glutaric acid (17)

Ozonized oxygen was bubbled through a solution of Trindane (0.495g, 2.5 mmol) in CH_2Cl_2 (30 mL) at ~ -70 - 80°C for 3 h, admixed with Dimethyl sulfide (0.8 mL), left stirred for 2h, treated with satd. $NaHCO_3$ (10 mL), and stirred for an additional 1 h. The organic layer separated, aqueous layer washed with additional CH_2Cl_2 (3 x 10 mL), organic layers combined, washed with distilled water (1 x 10 mL), dried ($MgSO_4$), evaporated and the residue chromatographed on silica gel. Elution with hexane-EtOAc (1:1) afforded **15** and **16** as gummy liquids.

The aqueous filtrate was acidified to pH 2 - 3 using citric acid, saturated with NaCl and extracted with EtOAc (3 x 15 mL). The EtOAc layer was washed with water (1 x 10 mL), dried ($MgSO_4$) and evaporated to get 213mg of a residue. This was dissolved in minimum amount of ether and esterified using an ether solution of diazomethane generated *in situ* from nitrosomethylurea. The mixture was then chromatographed using hexane - EtOAc (3:1) to afford 99 mg

(25%) of the glutaric acid methyl ester (**17a**) as a gummy liquid, the structure of which was confirmed by spectral comparison with an authentic sample.

15) Yield : 0.092g (14%)

IR (neat) : 3400 (br), 2944, 1752, 1680, 1440, 1040

^{1}H NMR ($CDCl_3$) δ 1.38 - 3.0 (m, m, CH_2s & CHs), 3.23 (m, 2H, -CH_2-C=O)

^{13}C NMR ($CDCl_3$) δ 17.93 - 35.3 (7 x CH_2), 58.36 (2 x CHs), 81.20, 98.50 (2 x HO-$\overset{|}{\underset{|}{C}}$ ---), *140.84, 154.60 (-C=C-), 198.58 (C=O, non-conjugated), 212.96* (C=O, conjugated)

FAB MS (m/z) (%) : 263 (56%) $(MH)^+$, 285 (30%) $(M+Na)^+$,

16) Yield : 0.066g (13%)

IR (neat) : 3424 (br, enolization), 2944, 1712, 1600, 1400, 1272, 1120.

^{1}H NMR ($CDCl_3$) δ 2.19 (m, 4H, 2 x CH_2), 2.64 - 3.00 (m, 10H, benzylic CH_2s), 3.2 (t, 2H, CH_2-CO).

^{13}C NMR ($CDCl_3$) δ 24.52 - 36.82 (8 x CH_2), 139.1 - 149.4 (6 x C aromatic), 207.67 (C=O)

FAB MS (m/z) (%) : 213 (100%) $(MH)^+$

17a)

Yield : 0.99g (25%)

IR (neat) : 2962, 1742, 1452, 1209, 1182

^{1}H NMR ($CDCl_3$) δ 1.82 - 2.0 (m, 2H, CH_2), 2.25 - 2.66 (m, 4H, 2 x CH_2s), 3.68 (s, 6H, 2 x $COOCH_3$)

XI) Preparation of tricyclohexanobenzene (18).

Cyclohexanone (37 mL, 0.36 mol) on acid catalyzed trimerization under the condition as described for Trindane (**8**) gave 7g, (~25%) of Tricyclohexanobenzene.

Yield : 25%

M.p. : 205°C (lit.[20] M.p. 229 - 231°C)

IR (KBr) : 2880, 2820, 1420, 1250

^{1}H NMR ($CDCl_3$) δ 1.78 (brs, 12H, nonbenzylic CH_2s), 2.57 (brs, 12H, benzylic CH_2s)

XII) RuVIII oxidation of 18: Isolation of benzylic oxidation products, *monoketone (19) and diketone (20)*

RuVIII oxidation of Tricyclohexanobenzene (1.2g, 5 mmol) was performed as described in experiment IX. The reaction, after 25 h afforded, besides starting material (0.56g, 47%), **19** and **20** in 25% and 11% yields respectively. Yields reported here are based on the amount of starting material recovered.

19)

Yield : 158mg (25%)

M.p : 230°C

IR (KBr): 2944, 2880, 1664, 1552, 1440.

^{1}H NMR ($CDCl_3$) : 1.50 - 2.0 (brm, 10H, nonbenzylic CH_2s), 2.07, 2.6, 2.78 (m, m, m, 10H, benzylic CH_2s), 3.14 (brs, 2H, -CH_2-CO-).

FAB MS (m/z) (%) 255 (100%) $(MH)^+$.

20)

Yield : 0.72g (11%)

M.p. : 196 - 198°C

IR (KBr) : 3440 (br), 2944, 2864, 1664, 1568, 1424.

^{1}H NMR ($CDCl_3$) δ 1.60 - 2.20 (brm, 8H, nonbenzylic CH_2s), 2.44 - 2.87 (brm, 10H, benzylic CH_2s + CH_2-CO), 4.86 (brs, 1H, -CH=C-), 5.2 (brs, 1H, enolic OH).

FAB MS (m/z) (%) : 269 (27%) $(MH)^+$, 253 (100%) $[(MH)^+-O]$

XIII) Preparation of 2,5-dihydroxy teriphthalic acid dimethyl ester (22).

An ice cooled solution of 2,5-dihydroxy teryphthalic acid (0.1g, 0.5 mmol) in methanol (3 mL) was admixed with an ether solution of diazomethane, generated *in situ* from nitrosomethyl urea (2.5 mmol). The mixture was shaken well for 2 min, excess CH_2N_2 quenched with ~3 drops of acetic acid, the mixture washed with satd. $NaHCO_3$, ether layer separated, dried ($MgSO_4$), and evaporated.

Yield : 0.086g (76%)

M.p. : 174°C

IR (KBr) : 3200, 1680, 1480, 1430, 1320, 1180

^{1}H NMR ($CDCl_3$) : δ 3.9 (s, 6H, $COOCH_3$), 7.5 (s, 2H, ArHs), 10.05 (s, 2H, OH)

XIV) Oxidation of 2,5-dihydroxy teriphthalic acid dimethyl ester: Preparation of quinone 23.

Dry chlorine was passed for 0.5 h, through a solution of **22** (0.1g, 1.77 mmol) in CCl_4 admixed with $FeCl_3$ (0.029g, 1.77 mmol). The reaction mixture was evaporated, the residue washed with water, extracted with EtOAc (3 x 25 mL), dried ($MgSO_4$), evaporated and the residue chromatographed on silica gel. Elution with Hexane - EtOAc (1:1) gave 0.08g of **23**.

Yield : 67%

M.p. : 243°C

IR (KBr) : 1740, 1690, 1610, 1440, 1310, 1130

^{1}H NMR ($CDCl_3$) d 3.9 (s, 6H, 2 x $COOCH_3$)

XV) The reaction of quinone (23) with sodium azide: isolation of isoxazole 24.

To a suspension of **23** (0.25g, 0.85 mmol) in methanol (100 mL), was added a solution of sodium azide (0.15g, 2.718 mmol) in methanol (5 mL). The

mixture was left stirred for 3 h, the solid washed with methanol and dried to afford 0.013g of **24**.

Yield : (6%)

M.p. : 198°C (lit.[31a] M.p. : 198 - 199°C)

IR (KBr) : 1690, 1580, 1514

^{1}H NMR ($CDCl_3$) : δ 4.2 (s, 6H, $-OCH_3$)

XVI) Preparation of mellitic acid hexamethyl ester (25)

a) Using diazomethane:

To an ice cooled solution of mellitic acid (0.3g, 0.877 mmol) in methanol (3 mL) was added an ether solution of diazomethane (generated *in situ* from nitrosomethyl urea), small quantities at a time with shaking until the yellow colour persisted. The solution was kept overnight, solvents evaporated, the residue triturated with 5 mL of saturated $NaHCO_3$ solution, extracted with EtOAc *(3 x 10 mL)*, dried ($MgSO_4$) and evaporated to afford 0.19g of the mellitic acid hexamethyl ester.

Yield : 51%

M.p. : 180°C (lit. Belstein 183-184°C)

IR (KBr) : 1742, 1433, 1228

^{1}H NMR ($CDCl_3$) δ 3.88 (s, 18H, 6 x $COOCH_3$)

GCMS : 426

b) By methanolysis of hexamellitoyl chloride:

To 0.1g (0.22 mmol) of hexamellitoyl chloride was added dry MeOH (10 mL) and left overnight. The solvents were evaporated, the residue triturated with satd. $NaHCO_3$ (5 mL), extracted with EtOAc, dried ($MgSO_4$) and evaporated to afford 0.77g (81%) of **25**, whose spectral properties were exactly similar to that described above.

XVII) Raction of mellitic acid hexamethyl ester (25) with liquor ammonia: isolation of mellitic acid hexa amide (26)

A mixture of mellitic acid hexamethyl ester (50mg, 0.11 mmol) and liquor ammonia (5 mL) was left aside for 2 days. The ester slowly dissolved, with the precipitation of the amide **26**.

Yield : 50mg.

M.p. : 240°C (dec)

FAB MS : 391 $(M+H)^+$ (as trihydrate)

XVIII) Preparation of hexamellitoyl chloride (27)

Mellitic acid (1.62 g, 4.73 mmol) was digested with PCl_5 (9.8g, 47 mmol) at 150°C for 24 h. $POCl_3$ was distilled out, the residue triturated with dry benzene (10 mL), decanted and the residue thoroughly dried in vacuo to afford 1.8g (84%) of the mellitic hexa acid chloride.

M.p. : 245 - 247°C

XIX) Reaction of hexamellitoyl chloride (27) with methionine methyl ester: isolation of hexaamide (28), monoimide (29), and bisimide (30)

A solution of hexamellitoyl chloride (0.48g,1.1 mmol) in dry CH_2Cl_2 (20 mL) and 1 mL of triethylamine (6.7 mmol) were simultaneously added dropwise over a period of 0.5 h, to an ice cooled and stirred solution of the free amine of the methionine methyl ester [generated *in situ* by the drop wise addition of triethylamine (6.7 mmol) to an ice cooled and stirred solution of the methionine methyl ester hydrochloride (6.7 mmol) in dry CH_2Cl_2 (65 mL)]. The reaction mixture was left stirred for two days at room temperature, washed successively with cold saturated $NaHCO_3$ solution (2 x 15 mL), 2N H_2SO_4 (2 x 15 mL), water (1 x 15 mL), dried ($MgSO_4$), evaporated and the residue chromatographed using Hexane - EtOAc (8:2) to afford **28**, **29** and **30**.

28; Yield : 0.152g (12%)

M.p. : 140 - 142°C

$[\alpha]_D^{29}$: -72.00 (c 0.5, $CHCl_3$).

IR (KBr) : 3220, 2900, 1740, 1670, 1540, 1420, 1200, 970

^1H NMR ($CDCl_3$) δ 2.12 (s, 18H, $-SCH_3$), 1.97 - 2.62 (m, 24H, $C\beta H_2$s & $C\gamma H_2$s), 3.72 (s, 18H, 6 x $COOCH_3$), 4.83 (brs, 6H, $C\alpha$Hs), 7.06 (brs, 6H, NHs)

^{13}C NMR ($CDCl_3$) δ 15.26 (6 x $-SCH_3$), 29.65 (6 x $C\gamma H_2$), 31.96 (6 x $C\beta H_2$), 52.1 (6 x $C\alpha H$), 52.43 (6 x $-OCH_3$), 134.7 (C aromatic), 164.80 (6 x -COO-), 171.4 (6 x -CO-NH)

FAB MS (m/z) (%) : 1235 (13%) $(M+Na)^+$, 1050 (7%), (M - H_2N-Met-OMe + $H)^+$, 887 (100%) (M - 2 x H_2N-Met-OMe + $H)^+$, 724 (29%) (M - 3 x H_2N-Met-OMe + $H)^+$.

Anal. Found: C, 46.78; H, 6.03; N, 6.43 . Calc. for $C_{78}H_{72}N_6O_{18}S_6$: C, 47.52; H, 5.94; N, 6.93.

29; Yield : 0.228g (20%)

M.p. : 145 - 147°C

IR (KBr) : 3248, 2944, 2912, 1744, 1712, 1696, 1560, 1440, 1200

^1H NMR ($CDCl_3$) δ 2.08, 2.11 &2.13 (s, s, s, 15H, 5 x $-SCH_3$), 2.20 - 2.67 (m, 20H, 5 x $C\beta H_2$s & $C\gamma H_2$s), 3.73 & 3.78 (s, s, 15H, 5 x $COOCH_3$), 4.76 - 4.95 (m, 5H, $C\alpha$Hs), 7.19, 7.3 (d, d, 4H, NHs)

^{13}C NMR ($CDCl_3$) δ 15.30 (5 x $-SCH_3$), 27.81 - 31.64 (5 x $C\beta H_2$ & $C\gamma H_2$), 51.41 - 52.95 (5 x $C\alpha H$ + 5 x $-OCH_3$), 128.86, 132.88, 139.49 (C aromatic), 162.74, 164.10, 164.18 (-COO-), 168.87, 171.14, 171.44 (-CO-NH-)

FAB MS (m/z) (%) : 1072 (17%) $(M+Na)^+$, 887 (100%) (M - H_2N-Met-OMe + $H)^+$, 724 (43%) (M - 2 x H_2N-Met-OMe + $H)^+$.

Anal. Found: C, 48.61; H, 5.66; N, 6.33 . Calc. for $C_{42}H_{59}N_5O_{16}S_5$: C, 48.04; H, 5.62; N, 6.67.

30; Yield : 0.085g (9%)

M.p. : 146 - 148°C

IR (KBr) : 3376, 2920, 1728, 1392, 1248

^1H NMR ($CDCl_3$) δ 2.06, 2.17 (s, s, 12H, $-SCH_3$), 2.18 - 2.74 (m, 16H, $C\beta H_2$s & $C\gamma H_2$s). 3.75, 3.8, 3.82 (s, s, s, 12H, 4 x $COOCH_3$), 4.9 - 5.3 (m, 4H, $C\alpha$Hs), 7.14, 7.27 (d, d, 2H ,NHs)

^{13}C NMR ($CDCl_3$) δ 15.37 (4 x $-SCH_3$), 27.33 - 31.52 (4 x $C\beta H_2$ & $C\gamma H_2$), 51.69 - 53.15 (4 x $C\alpha H$ + 4 x $-OCH_3$), 129.06, 130.6, 133.66, 137.39 (C aromatic), 160.65 - 163.87 (4 x -COO-), 168.6 - 171.64 (-CO-NH-)

FAB MS (m/z) (%) : 887 (48%) $(MH)^+$, 724 (100%) $(M - H_2N\text{-Met-OMe} + H)^+$

Anal. Found: C, 48.36; H, 5.22; N, 5.88 . Calc. for $C_{36}H_{46}N_4O_{14}S_4$: C, 48.75; H, 5.19; N, 6.32.

XX) Reaction of hexamellitoyl chloride (27) with Tryptophan methyl ester: isolation of hexaamide (31)

Hexa mellitoyl chloride (0.287g, 0.633 mmol) was reacted with free amine from TrpOMe.HCl (1g, 3.93 mmol) under the same conditions as described for methionine (XIX) to afford 0.07g of **31**.

Yield: 7%

M.p. : 158 - 160°C

IR (KBr) : 3360, 2900, 1720, 1660, 1530, 1420, 1220

^{1}H NMR ($CDCl_3$ - DMSO-d_6) δ 3.1 - 3.3 (brs, 12H, 6 x CβH_2s), 3.59 (brs, 18H, 6 x $COOCH_3$), 4.7 - 5.2 (m, 6H, CαHs), 6.46 (brs, 6H, amide NH), 6.53 - 7.4 (m, 30H, ArHs), 8.05 - 8.45 (m, 6H, Indole NHs)

ES$^+$ MS (m/z) (%) : 1525 (68%) $(M-H_2O+H)^+$, 1347 (36%) (M - [H_2NTrpOMe + Na)$^+$, 1107 (18%) (M - [2 x H_2NTrpOMe]+H)$^+$, 889 (41%) (M - [3 x H_2NTrpOMe]+H)$^+$.

XXI) Reaction of hexamellitoyl chloride (27) with Phenylalanine methyl ester: isolation of hexaamide (32)

Hexa mellitoyl chloride (0.4g, 0.883 mmol) was reacted with free amine from PheOMe.HCl (1.2g, 5.48 mmol) under the same conditions as described for methionine (XIX) to afford 0.19g of **32**.

Yield : 16%

M.p. : 139 - 141°C

IR (KBr) : 3340, 1730, 1660, 1450

^{1}H NMR ($CDCl_3$ - DMSO-d_6) δ 3.1 (brs, 12H, CβH_2s), 3.59 (brs, 18H, 6 x $COOCH_3$), 4.5 - 5.3 (m, 6H, CαHs), 7.19 (brs, ArHs), 8.25 (brs, CO-NH)

FAB MS (m/z) (%) : 1331 (13%) $(M+Na)^+$

XXII) Reaction of hexamellitoyl chloride (27) with α-amino isobutyric acid methyl ester: isolation of monoimide (33)

Hexa mellitoyl chloride (0.5g,1.1 mmol) was reacted with free amine from AibOMe.HCl (1.48g, 6.83 mmol) under the same conditions as described for methionine (XIX) to afford 0.1g of **33**.

Yield : 11%

M.p. : 203 - 205°C

IR (KBr) : 3280, 2900, 1720, 1670, 1540, 1450, 1290, 1150

^{1}H NMR ($CDCl_3$) δ 1.63, 1.77, 1.88 (s, s, s, 30H, CH_3s), 3.68, 3.73, 3.78 (s, s, s, 15H, $COOCH_3$s), 7.13 (s, 4H, NH)

FAB MS (m/z) (%) : 842 (77%) $(M+Na)^+$, 703 (100%) $(M - [H_2NAibOMe]+H)^+$, 586 (24%) $(M - 2 \times [H_2NAibOMe]+H)^+$

XXIII) Reaction of hexamellitoyl chloride (27) with Glycine methyl ester: isolation of bisimide (34)

Hexa mellitoyl chloride (0.5g,1.1 mmol) was reacted with free amine from GlyOMe.HCl (0.858g, 6.83 mmol) under the same conditions as described for methionine (XIX) to afford 0.01g of **34**.

Yield : 2%

M.p. : 210 - 212°C

IR (KBr) : 3260, 1730, 1660, 1400, 1220

^{1}HNMR ($CDCl_3$ - DMSO-d_6) : δ 4.1, 4.2 (s, s, 12H, $COOCH_3$), 4.4 (bd, 8H, GlyCαH_2s), 8.6 - 8.8 (bd, 4H, NH)

FAB MS (m/z) (%) : 591 (12%) $(M+H)^+$, 613 (11%) $(M+Na)^+$, 502 (79%) (M - $[H_2NGlyOMe]+H)^+$

XXIV) The reaction of mellitic acid with orthophenylene diamine: isolation of 1:3 adduct 35

To a solution of mellitic acid (0.2g, 0.584 mmol) in dry MeOH (5 mL) was added 0.19g, 1.75 mmol) of o-phenylenediamine in methanol (5 mL). The precipitated mellitic acid salt was washed with methanol (3 x 10 mL) and dried.

Yield : 0.307g (79%)

M.p. : 297 - 299°C

IR (KBr) : 3384, 2912, 2608, 1712, 1648, 1504, 1424, 1256.

Mol.wt (by size exclusion chromatography) : 640

Anal. found : C, 53.97; H, 4.48; N, 12.28; Calc for: $C_{30}H_{30}N_6O_{12}$, C, 54.05; H, 4.5; N, 12.61

XXV) The reaction of mellitic acid with Ethylene diamine: isolation of 1:3 adduct 36

Prepared from 171 mg (0.5 mmol) of mellitic acid and 90 mg (1.5 mmol) of ethylene diamine as per procedure XXIV

Yield : 0. 200 g (77%)

M.p 230°C (dec)

IR (KBr) 3440 (br), 3008 (br), 1568, 1424, 1328.

Anal found : C, 36.06; H, 5.80; N, 13.73; Calc for: $C_{18}H_{30}N_6O_{12}$ (as trihydrate), C, 37.50, H, 6.25; N, 14.58

XXVI) The reaction of mellitic acid with Hexamethylene diamine: isolation of 1:1 adduct 37

Prepared from 200 mg (0.584 mmol) of mellitic acid and 0.203g (1.75 mmol) of hexa methylene diamine as per procedure XXIV.

Yield : 0.180 g

M.p. : decomposes after 210°C

IR (KBr) : 3440, (br), 3056, 2944, 1584, 1424, 1328.

Mol.wt (by size exclusion chromatography) : 450

XXVII) The reaction of mellitic acid with Bipyridyl: isolation of 1:1 adduct 38

Prepared from 171 mg (0.5 mmol) of mellitic acid and 234 mg (1.5 mmol) of bipyridyl as per procedure XXIV.

Yield : 0. 180g

M.p. : 240-241°C

IR (KBr) : 3417 (br), 3084 (br), 1695, 1582, 1527, 1248.

FAB MS : 498 $(MH)^+$, 1:1 adduct.

FAB MS Detection of mellitic acid-amine adducts-General procedure:

Small amounts of mellitic acid and the amines were triturated in methanol and analyzed in FAB Mass spectrometer.

XXVIII) The reaction of mellitic acid with Melamine: isolation of 1:1 adduct 39

FAB MS showed peak at 469 $(MH)^+$, indicating a 1:1 adduct.

XXIX) The reaction of mellitic acid with Spermine: isolation of 1:1 adduct 40

FAB MS showed peak at 545 $(MH)^+$, indicating a 1:1 adduct.

XXX) The reaction of mellitic acid with Hexadecylamine: isolation of 1:6 adduct 41

Prepared from 86mg (0.25 mmol) of mellitic acid and 360mg (1.5 mmol) of hexadecylamine.

Yield : 0.360g

M.p. : 261 - 263°C

IR (KBr) : 3408, 2920, 2848, 1616, 1560, 1408, 1320.

Anal. found : C, 70.63; H, 12.35; N, 4.12; Calc for: $C_{108}H_{216}N_6O_{12}$ (as trihydrate), C, 70.3; H, 12.05; N, 4.56

XXXI) Preparation of glycine benzyl ester hydrochloride (42)[GlyBzl.HCl]

a) Glycine benzyl ester p-toluene sulfonate [GlyBzl.TsOH]

A mixture of glycine (18.8g, 0.25 mol), p-toluenesulfonic acid (47.5g, 0.25 mol), benzyl alcohol (100 mL) and dry benzene (50 mL) was refluxed over a Dean-Stark water separator for 5 h. The mixture was cooled to room temperature, diluted with ether (500 mL) and refrigerated overnight. The solid was filtered and the crude product crystallized from methanol : ether :: 150 : 400 mL).

Yield : 61.2 g (72%)

M.p. 128 - 130°C.

b) Preparation of **42**

A suspension of 61.2g (0.181 mol) of the glycine benzyl ester p-toluene sulfonate in water (185 mL) was transferred to a separating funnel and shaken with 450 mL of ether. Aqueous NaOH (30.6 mL, 8N) was poured in and the mixture vigorously shaken for 10 min. The ether layer was separated and the aqueous layer extracted with additional ether (300 mL). The combined ether extracts were dried over anhydrous K_2CO_3 and filtered. The ether layer was cooled in ice bath and subjected to the passage of dry HCl for 1 h. The mixture was allowed to stand for 0.25 h, filtered, the residue washed with ether and dried over P_2O_5 to afford 15.75g of **42**.

Yield : (43%)

M.p : 129 - 130°C.

XXXII) Prepararion of Boc-Glu(γOMe)OH (43)

a) Glu(γOMe).HCl

L - Glutamic acid (15g, 0.102 mol) was added to an ice cooled solution of $SOCl_2$ (10 mL) in dry MeOH (70 mL) and stirred vigorously for 5 min until most of the solid dissolved. The reaction mixture was set aside at ~ 20°C for 30 min. and 100 mL of ice cold ether added. The turbid solution up on cooling crystallized, which was filtered, washed with ether and dried in vacuo to afford 13g of the product.

Yield : (65%)

M.p 153°C

b) Glu (γOMe):

Glu (γOMe).HCl (13g, 65.8 mmol) was dissolved in dry MeOH (32 mL) and pyridine was added drop by drop until basic (pH 8-9). The reaction mixture was kept aside at room temperature for 2 h, the precipitated solid was filtered, washed with EtOH, ether and dried to afford 8.9g of γ--methylglutamate.

Yield : (84%)

M.p. 178°C.

IR (KBr) : 3447 (br), 3070 (br), 1735, 1694, 1479, 1216

c) Boc-Glu(γOMe)OH (**43**):

Glu (γOMe)OH (3.2g, 20 mmol) was dissolved in a mixture of DMF (40 mL) and water (20 mL), cooled in ice, stirred, admixed with, in drops, triethylamine (3.3 mL, 23.7 mmol), followed by, in small batches, Boc carbonate (4.8g, 22 mmol), left stirred at room temperature for 24 h, covered with EtOAc (100 mL), cooled in an ice bath and acidified with 5% $KHSO_4$ to pH 2-3, shaken well. EtOAc layer separated, the aqueous layer extracted with additional EtOAc (4 x 20 mL), the combined EtOAc layers washed with distilled water (1 x 10 mL), dried ($MgSO_4$) and evaporated under reduced pressure to afford 4g of Boc-Glu(γOMe)OH as a gummy liquid.

Yield : (76%)

IR (neat): 3337 (br), 2981 (br), 1727, 1686, 1659, 1523, 1215.

^{1}H NMR ($CDCl_3$) δ 1.4 (s, 9H, Boc CH_3s), 1.8 - 2.6 (m, 4H, Glu CβH_2 and CγH_2), 3.7 (s, 3H, $COOCH_3$), 4.25 (m, 1H, GluCαH), 5.3 (d, 1H, Glu NH), 7.15 (brs, COOH)

XXXIII) General procedure for the synthesis of peptides (44, 45 &46)

To a stirred and ice cooled solution of the N-protected amino acid or peptide (10 mmol) in dry dichloromethane (35 mL) [or CH_2Cl_2 : DMF :: 9:1] was added N-hydroxy succinimide (10 mmol) followed by DCC (12 mmol). The mixture was stirred for ~2 min and the carboxyl terminal protected amino acid or

peptide (12 mmol) in dry CH_2Cl_2 (15 mL) was added to it, keeping the mixture ice cold and then left stirred at room temperature for 48 h. The reaction mixture was filtered, the residue washed with CH_2Cl_2 (3 x 10 mL), the organic layers combined, washed successively with cold saturated $NaHCO_3$ (2 x 10 mL), 2N H_2SO_4 (2 x 10 mL) and distilled water (1 x 10 mL), dried ($MgSO_4$), evaporated under reduced pressure and the crude residue chromatographed on a silica gel column using hexane - EtOAc (1:1) [$CHCl_3$: MeOH, (1:2) for tetra and hexa peptides] to afford the products.

XXXIV) Boc-Glu(γOMe)-GlyOBzl (44)

Prepared from Boc-Glu(γOMe)OH (7g, 26.8 mmol) and H_2NGlyOBzl [generated in situ by the addition of triethylamine (5.0 ml, 32 mmol) to a suspension of GlyOBzl.HCl (6.5g, 32 mmol) in dichloromethane (75 mL) under ice cold condition] by general procedure XXXIII

Yield : 10.16g (92%)

M.p. : 64 - 65°C

$[\alpha]_D^{25}$: -7.00 (c 1, $CHCl_3$)

IR (KBr) 3326, 2942, 1770, 1751, 1688, 1669, 1556

^{1}H NMR (300MHz, DMSO-d6) δ 1.37 (s, 9H, Boc CH_3s), 1.71 - 1.92 (bd, 2H, Glu CβHs), 2.35 (t, 2H, Glu CγHs), 3.58 (s, 3H, $COOCH_3$), 3.81 - 4.00 (m, 2H,

GlyCH$_2$ & GluCαH)., 5.12 (s, 2H, benzyl CH$_2$), 6.96 (d, 1H, J = 9Hz, GluNH), 7.36 (s, 5H, ArHs), 8.31 (t, 1H, J = 12Hz, GlyNH).

FAB MS (m/z) (%). 409 (81%) (MH)$^+$, 431 (34) (M+Na)$^+$, 309 (96) M-Boc+H)$^+$

XXXV) Deprotection of N, C protected peptides

a) Removal of the Boc group - general procedure.

The Boc protected peptide (1 mmol) was dissolved in dry CH_2Cl_2 (~3 mL), cooled in an ice bath, admixed with CF_3COOH (1 mL) and stirred at that temperature till the starting material was consumed (~2h). Trifluoroacetate salt was neutralized with an ice cooled 5% sodium carbonate solution, extracted with EtOAc (2 x 30 mL), dried ($MgSO_4$), evaporated under reduced pressure without the application of heat, and dried in vacuo. The resulting amine was immediately used for the peptide coupling.

b) Removal of the Benzyloxy carbonyl group..

The peptide benzyl ester (5 mmol) in dry MeOH (30 mL) was admixed with palladized charcoal (10% w/w, 0.5g) and subjected to hydrogenolysis (under a positive pressure of hydrogen) in a Parr hydrogenation set up. The progress of the reaction was monitored by tlc (~12 h). The reaction mixture was filtered, the filtrate evaporated under reduced pressure and the acid used for the peptide coupling.

XXXVI) Boc-Glu(γOMe)-Gly-Glu(γOMe)-GlyOBzl (45)

Prepared from Boc-Glu(γOMe)-GlyOH (2.64g, 8.3 mmol) [prepared in 99% yield from Boc Glu(γOMe)-GlyOBZl as per procedure XXXVb] and H_2N-Glu(γOMe)-GlyOBZl (3g, 9.93 mmol) [prepared in 90% yield from Boc-Glu(γOMe)-GlyOBZl (4.4g, 10.7 mmol) as per procedure XXXVa] as per general procedure XXXIII

Yield : 4.12g (82%)

M.p. : 139 - 141°C

IR (KBr) 3317, 2947, 1750, 1694, 1647, 1537

^{1}H NMR (300MHz, DMSO-d6) δ 1.36 (s, 9H, Boc CH_3s), 1.70 - 1.98 (bd, 4H, GluCβH_2s), 2.33 (t, 4H, GluCγH_2s), 3.57 (s, 6H, 2 x $COOCH_3$), 3.64 - 3.96 (m, 5H, Glu1CαHs, Gly2 & Gly4CH_2s), 4.32 (m, 1H, Glu3CαH) 5.12 (s, 2H, benzyl CH_2), 6.96 (d, 1H, J = 9Hz, Glu1NH), 7.35 (s, 5H, ArHs), 7.97 - 8.00 (brs, Gly2NH & Glu3NH), 8.41 (brs, 1H, Gly4NH).

FAB MS (m/z) (%): 609 (33%) $(MH)^+$, 631 (38) $(M+Na)^+$, 509 (100) $(M-Boc+H)^+$

XXXVII) Boc-Glu(γOMe)-Gly-Glu(γOMe)-Gly-Glu(γOMe)-GlyOBzl (46)

Prepared from Boc-Glu(γOMe)-Gly-Glu(γOMe)-GlyOH (2.52g, 4.86 mmol [prepared in 97% yield from Boc-Glu(γOMe)-Gly-Glu(γOMe)-GlyOBzl (3.04g, 5 mmol) as per procedure XXXVb] and H_2N-Glu(γOMe)-Gly-OBzl

(1.693g, 5.496 mmol) [prepared in ~90% yield from Boc-Glu(γOMe)-GlyOBZl (2.48g, 6.1 mmol) as per procedure XXXVa] as per general procedure XXXIII.

Yield : 71%

M.p. 193 - 195°C

IR (KBr) 3468, 3316, 2945, 1745, 1692, 1635, 1537

^{1}H NMR (300MHz, DMSO-d6) δ 1.36 (s, 9H, BocCH$_3$s), 1.73 - 1.97 (bd, 6H, Glu βH$_2$s), 2.33 (t, 6H, Glu CγH$_2$s), 3.56 (s, 9H, 3 x COOCH$_3$), 3.71 (brs, 4H, Gly2 & Gly4CH$_2$s), 3.8 - 3.96 (m, 3H, Glu1CαH & Gly6CH$_2$), 4.31 (m, 2H, Glu3CαH & Glu5CαH), 5.12 (s, 2H, benzyl CH$_2$), 6.98 (d, 1H, J = 9Hz, Glu1NH), 7.35 (s, 5H, ArHs), 7.98 - 8.04 (m, 3H, Gly2NH, Glu3NH & Glu5NH), 8.19 (brs, 1H, Gly4NH), 8.43 (t, 1H, Gly6NH).

FAB MS (m/z) (%): 809 (33%) $(MH)^+$, 831 (66) $(M+Na)^+$, 709 (100) $(M\text{-}Boc+H)^+$

XXXVIII) Preparation of the cyclic hexapeptide (47)

a) C terminal deprotection of **46**

The hexapeptide Boc-Glu(γOMe)-Gly-Glu(γOMe)-Gly-Glu(γOMe)-Gly-OBzl (0.46g, 0.569 mmol) was hydogenolysed (as per procedure XXXVb) using Pd/C (10% w/w, 0.3g) in dry MeOH (50 mL) to afford 0.372g (91%) of the debenzylated product.

b) N terminal deprotection of the above hexapeptide:

The above debenzylated hexapeptide (0.372g, 0.518 mmol)) was admixed with dry CH_2Cl_2 (2 mL), cooled in ice bath and 0.4 ml of CF_3COOH was added to it. The reaction was left stirred for 2.5 h, solvent evaporated under vacuo, the residue triturated with dry ether and the solid dried thoroughly *in vacuo* to afford 0.325 (85%) of the triflate salt which was directly used for cyclization.

c) Cyclization of the N,C deprotected hexapeptide:

To a stirred solution of the above triflate salt (0.28g, 0.38 mmol) in dry DMF (40 mL), was added $NaHCO_3$ (0.17g, 2 mmol) followed by BOP reagent (0.18g , 0.41 mmol). The mixture was left stirred at room temperature for 48 h in the dark, solvent evaporated in vacuo under reduced pressure, the residue triturated with EtOAc (2 x 10 mL), 5% $KHSO_4$ (2 x10 mL), saturated $NaHCO_3$ (2 x 10 mL), distilled water (2 x 10 mL) and finally with methanol (3 x 10 mL). The ethyl acetate and methanol washings did not contain the expected cyclic hexapeptide. The residue left behind after washings was reasonably pure and gave the spectra characteristic of the expected cyclic peptide. Purification of the residue for further studies was difficult because of its insolubility in almost all organic solvents except DMF and DMSO.

Yield : 30mg (13%)

M.p. : 230°C (dec)

IR (KBr) : 3292, 2962, 1755, 1640, 1539, 1445.

^{1}H NMR (600 MHz, DMSO-d6): δ 1.65 - 1.9 (bd, 6H, GluCβH_2s), 2.28 (brs, 6H, GluCγH_2s), 3.6 (s, 9H, 3 x $COOCH_3$), 3.61 - 3.8 (m, 3H, GluCαH), 4.25 (d, 6H, GlyCH_2), 8.00 (d, 3H, GluNHs), 8.17 (brs, 3H, GlyNHs).

I.F. SPECTRA

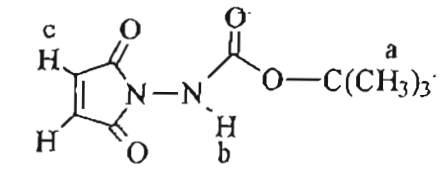

1

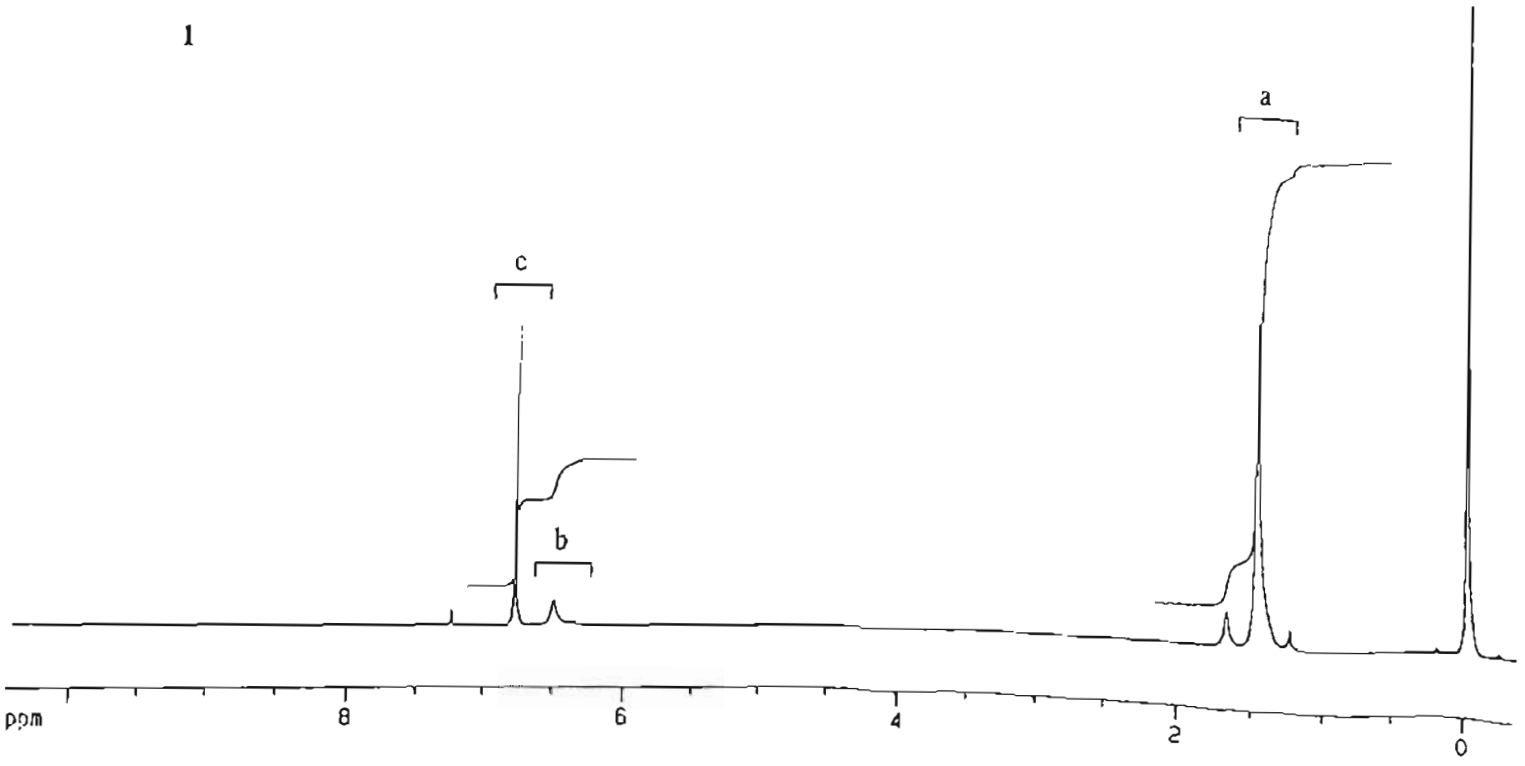

δ (300 MHz, $CDCl_3$)

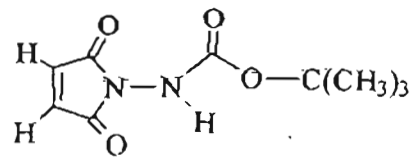

1

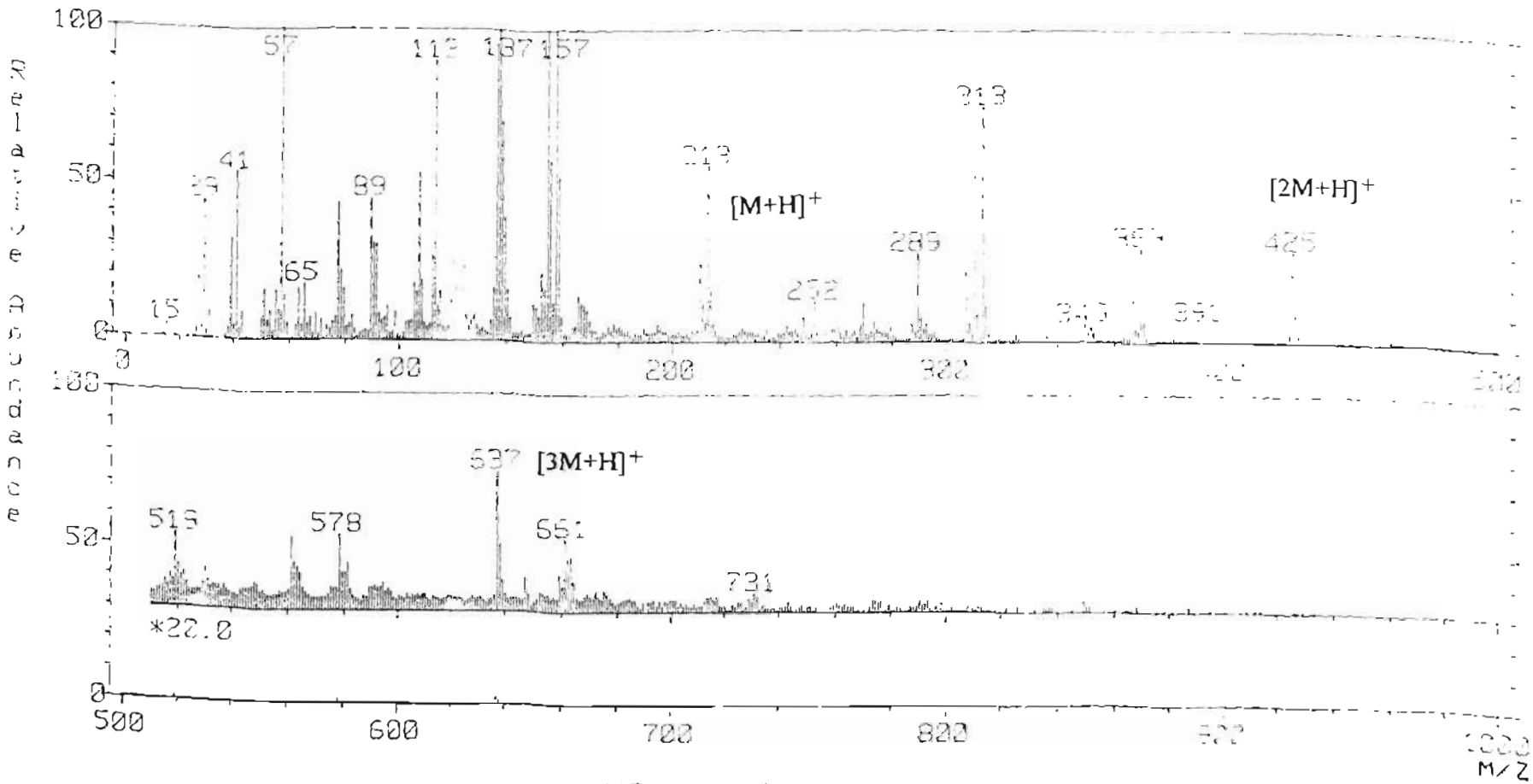

FAB mass spectrum

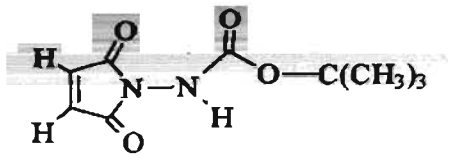

1

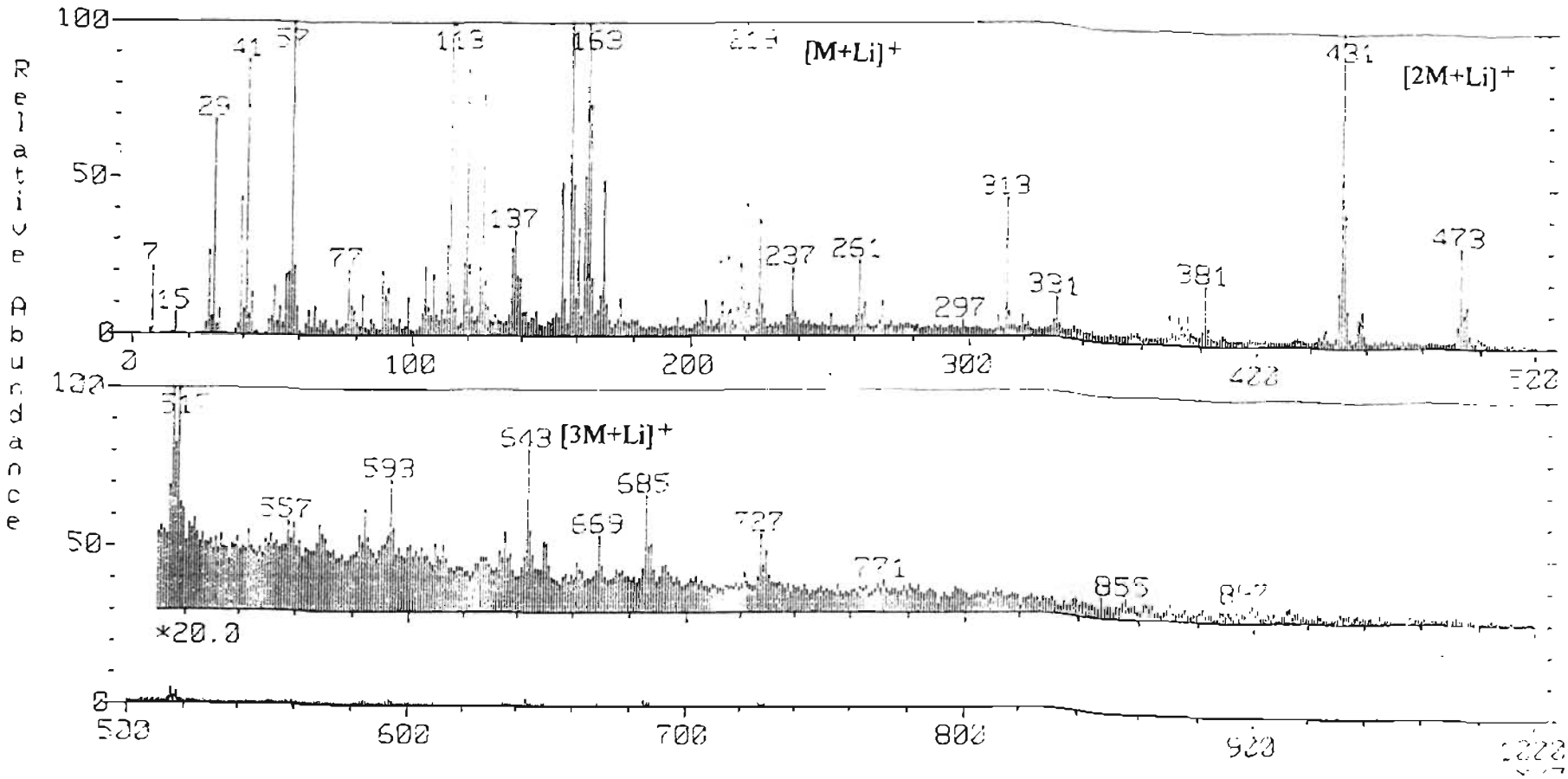

FAB mass spectrum

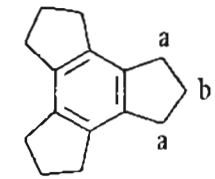

8

δ (300 MHz, $CDCl_3$)

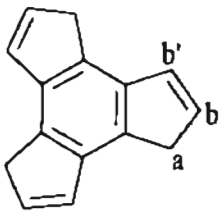

10

δ (60 MHz, $CDCl_3$)

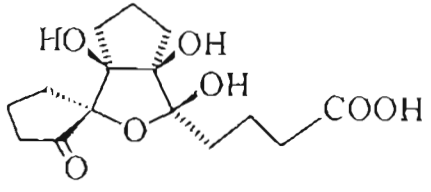

13

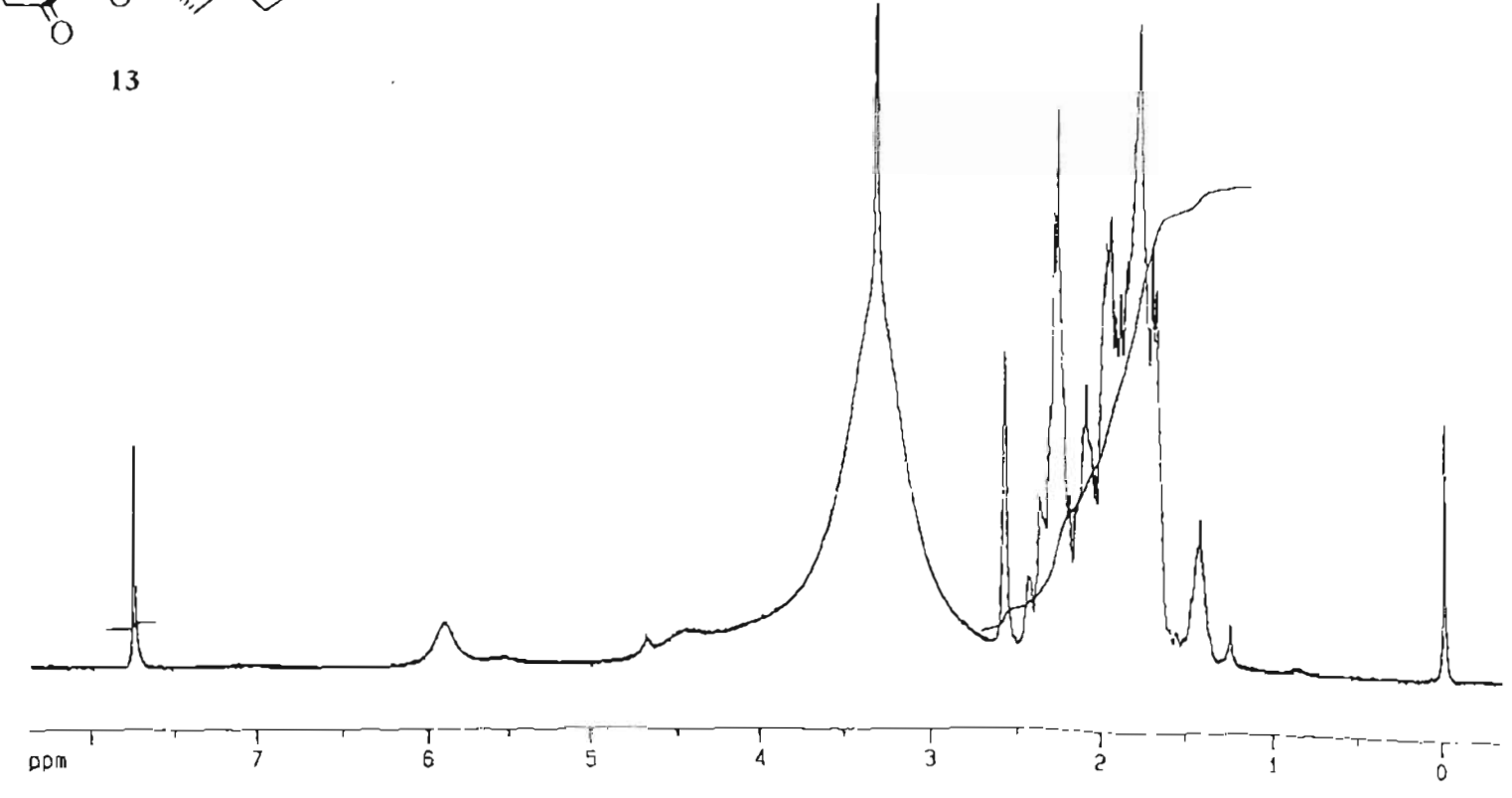

δ (300 MHz, $CDCl_3$ - DMSO-d_6)

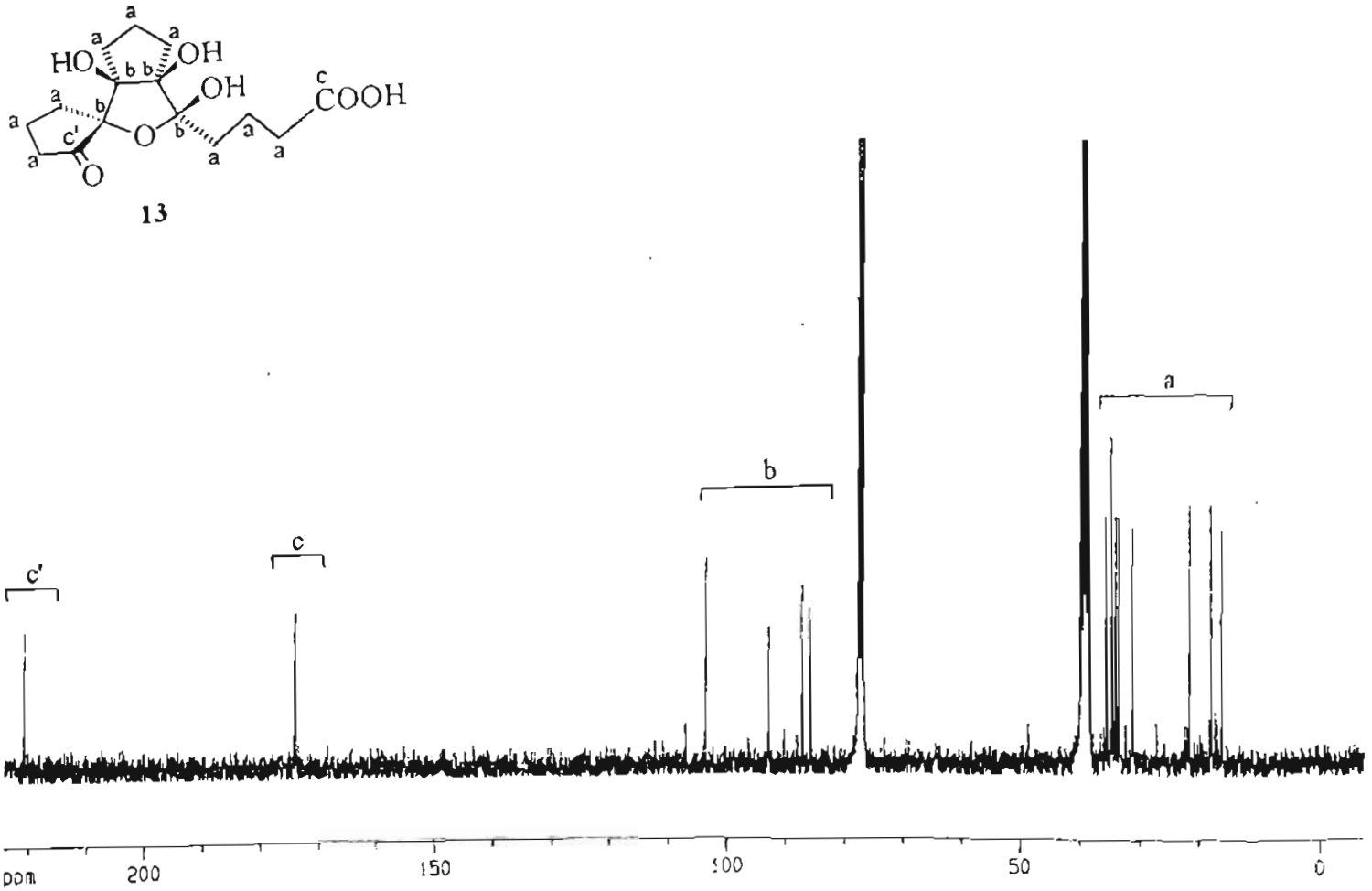

13

δ (300 MHz, $CDCl_3$ - DMSO-d_6)

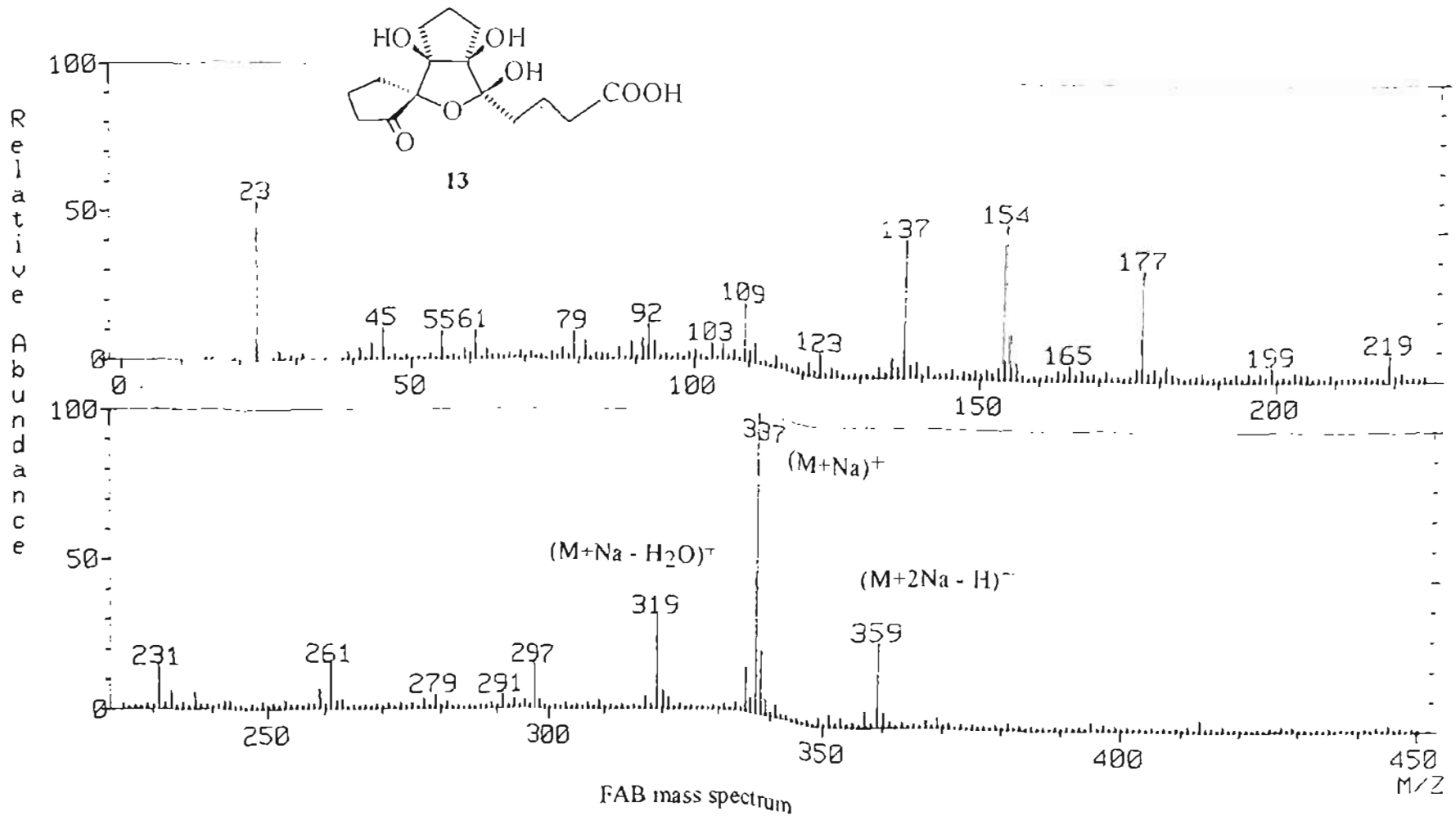

FAB mass spectrum

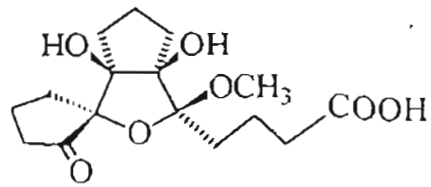

14

δ (300 MHz, $CDCl_3$)

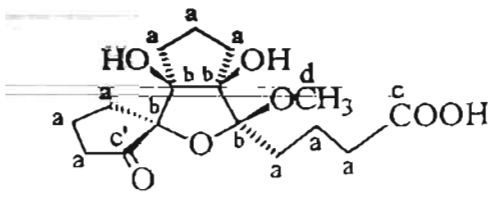

14

δ (300 MHz, $CDCl_3$)

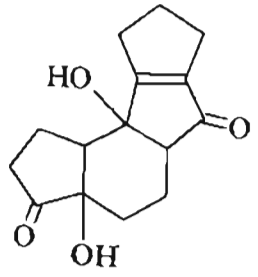

15

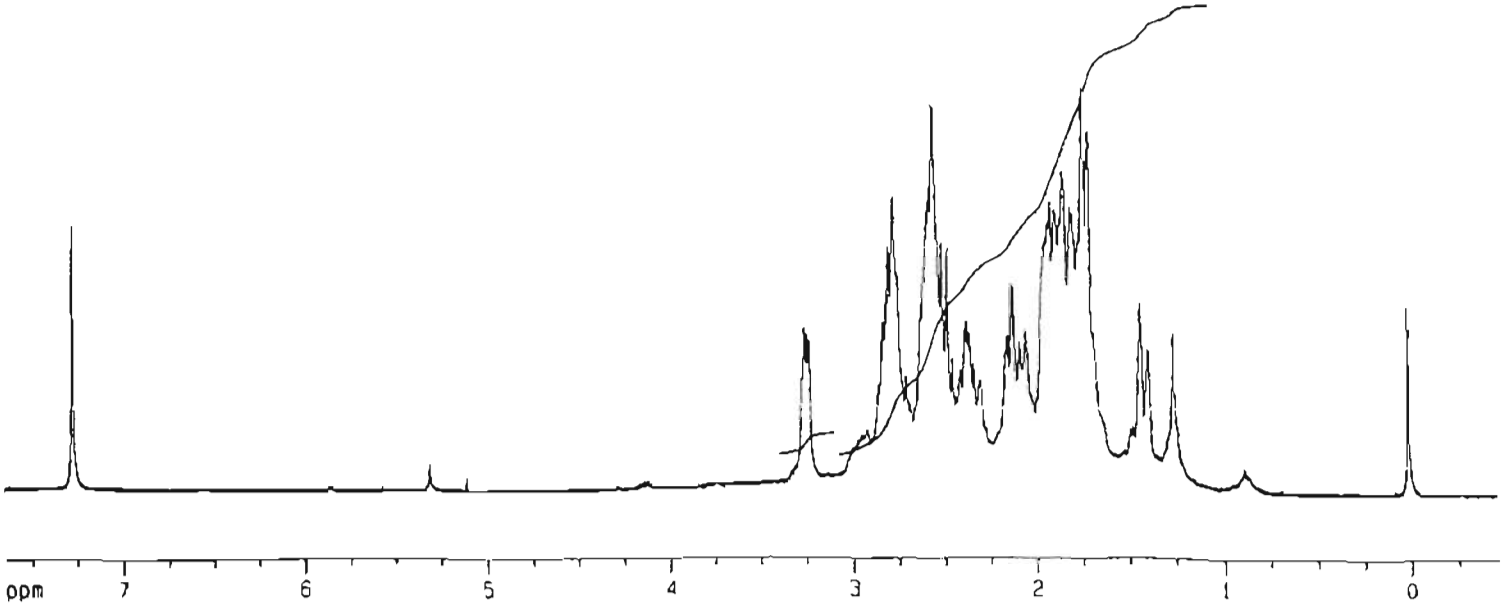

δ (300 MHz, $CDCl_3$)

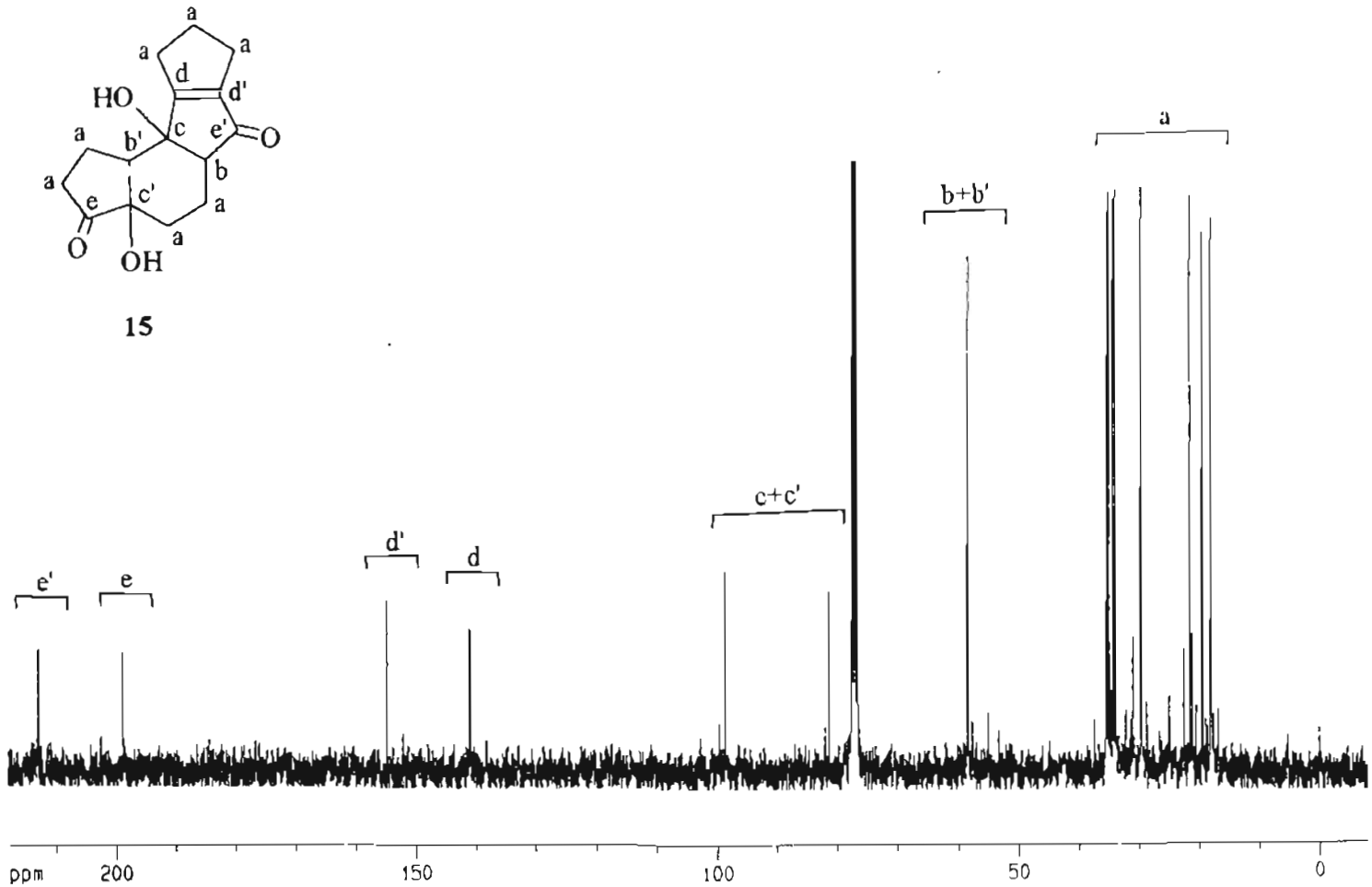

δ (300 MHz, $CDCl_3$)

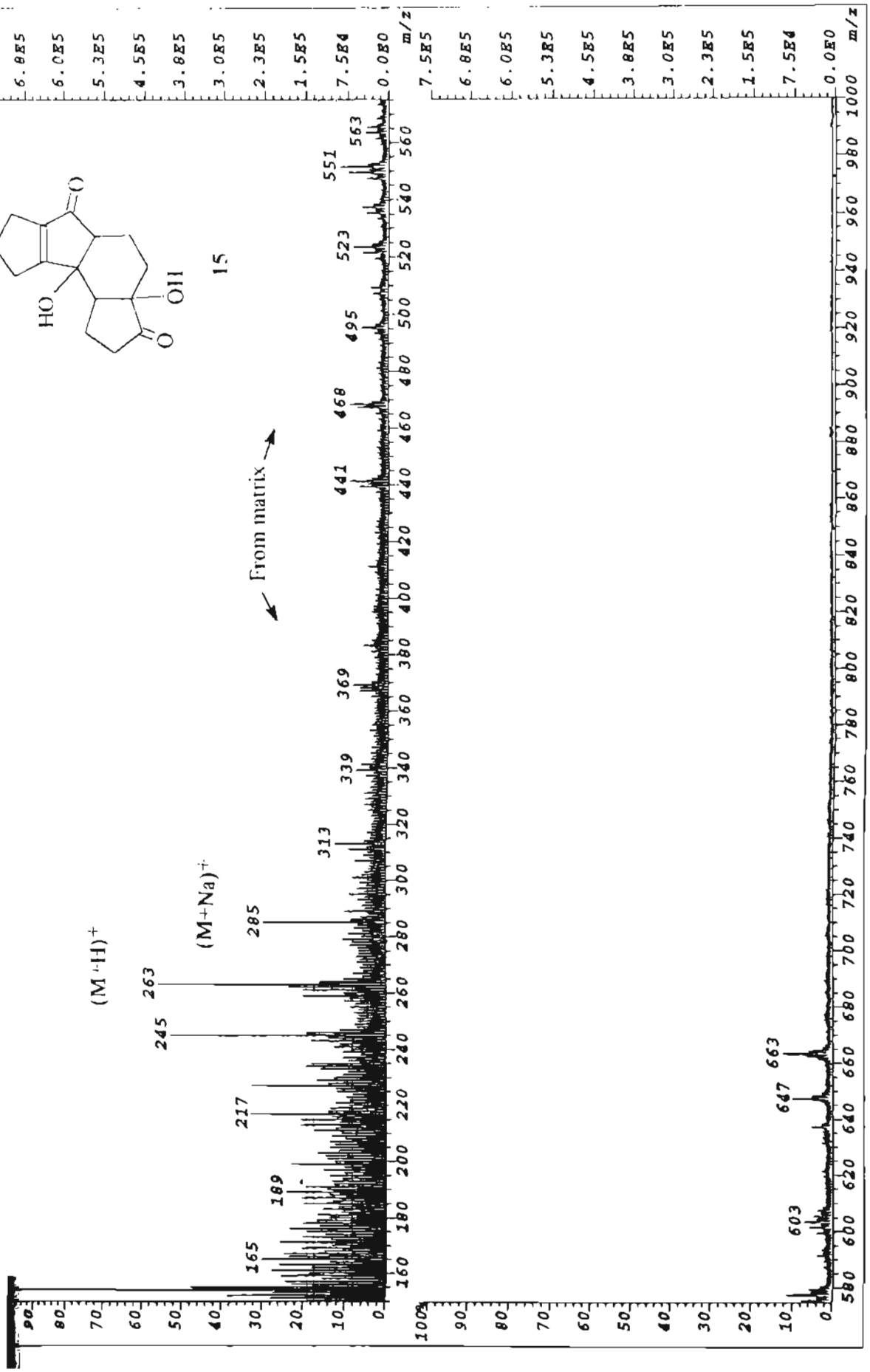

FAB mass spectrum

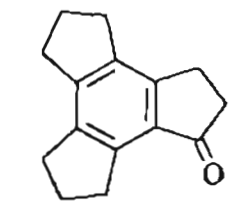

16

δ (300 MHz, $CDCl_3$)

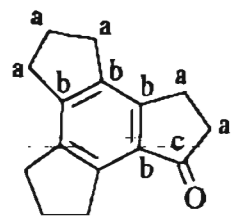

16

δ (300 MHz, $CDCl_3$)

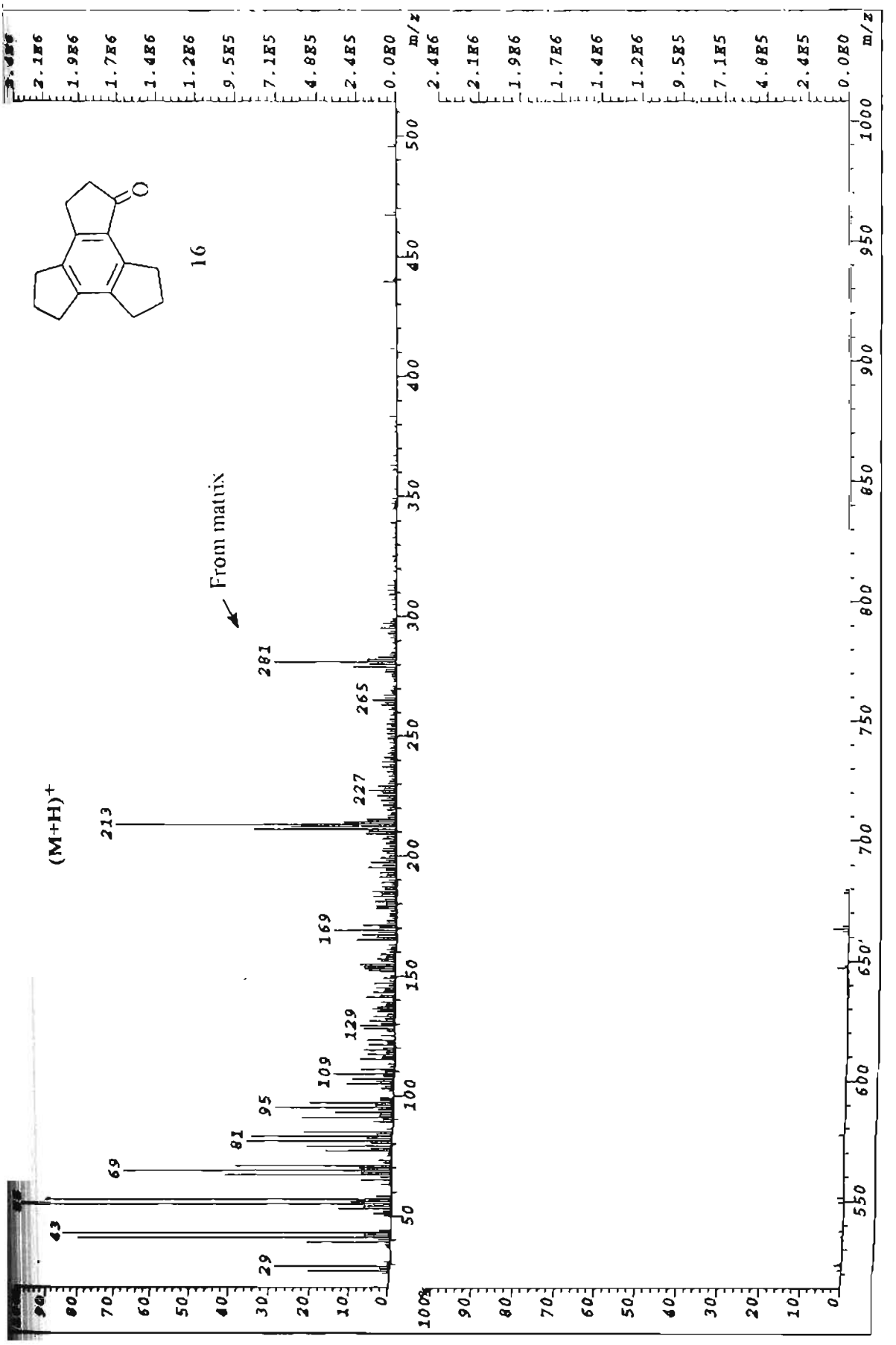

FAB mass spectrum

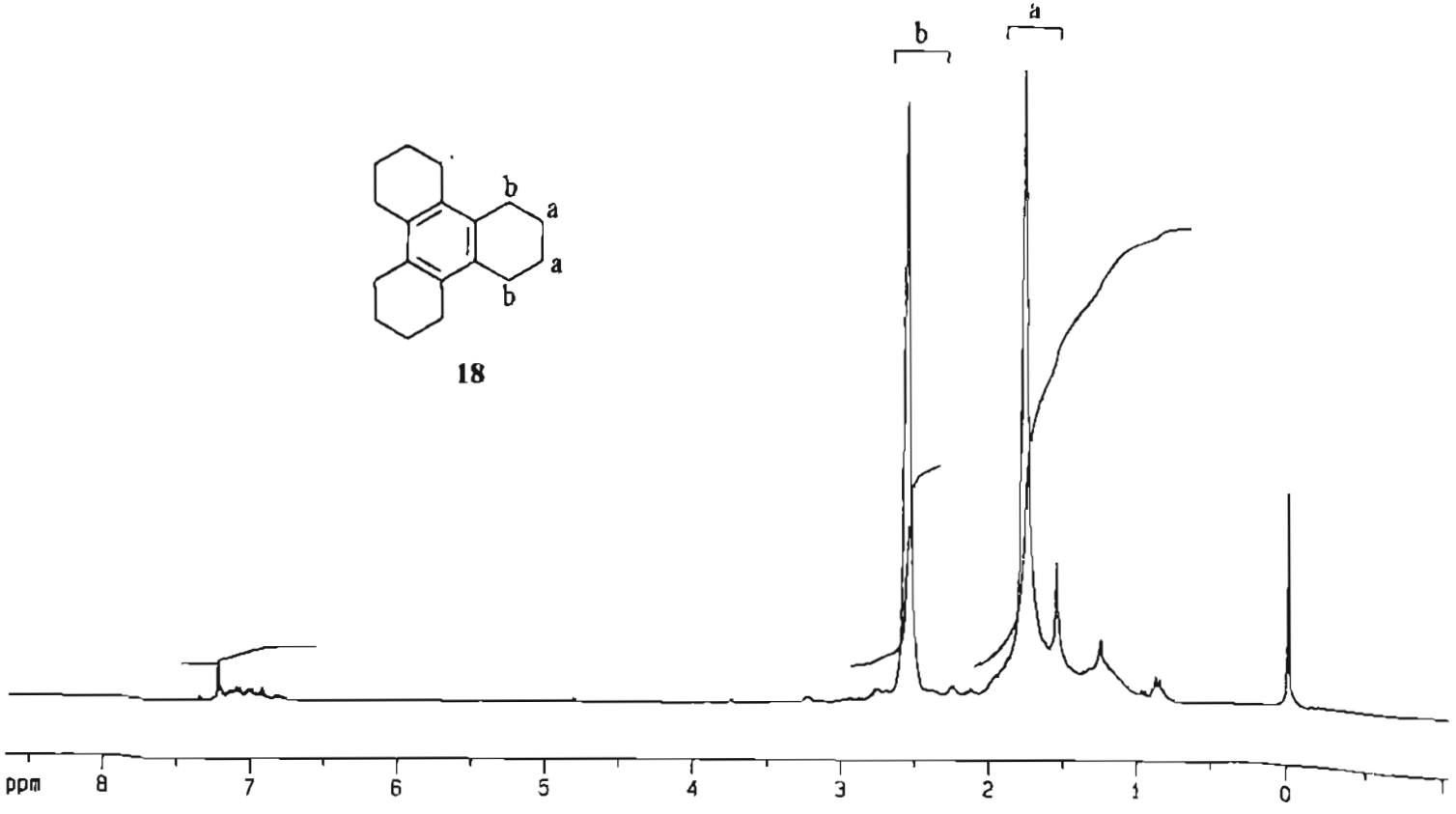

18

δ (300 MHz, $CDCl_3$)

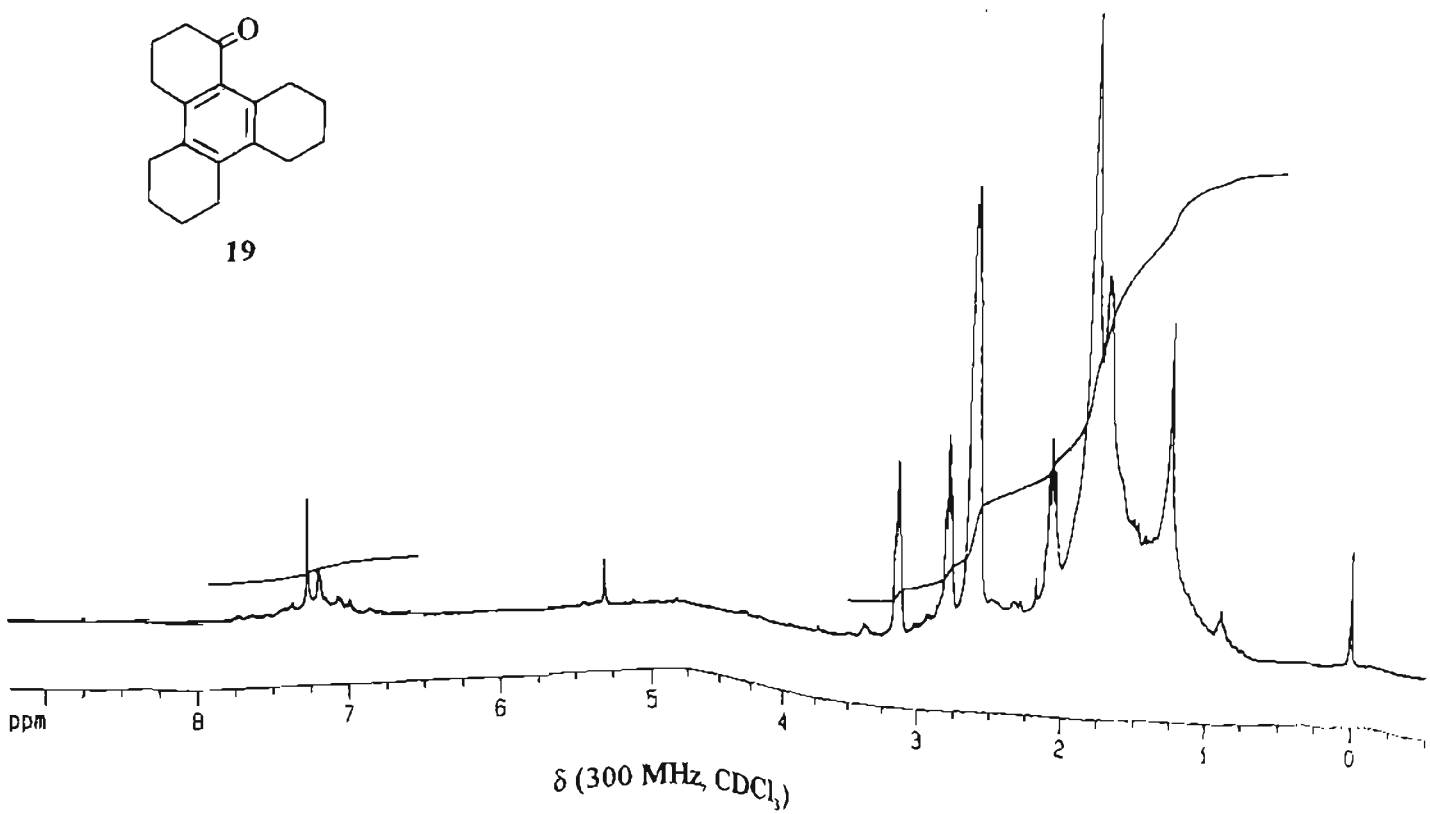

19

δ (300 MHz, $CDCl_3$)

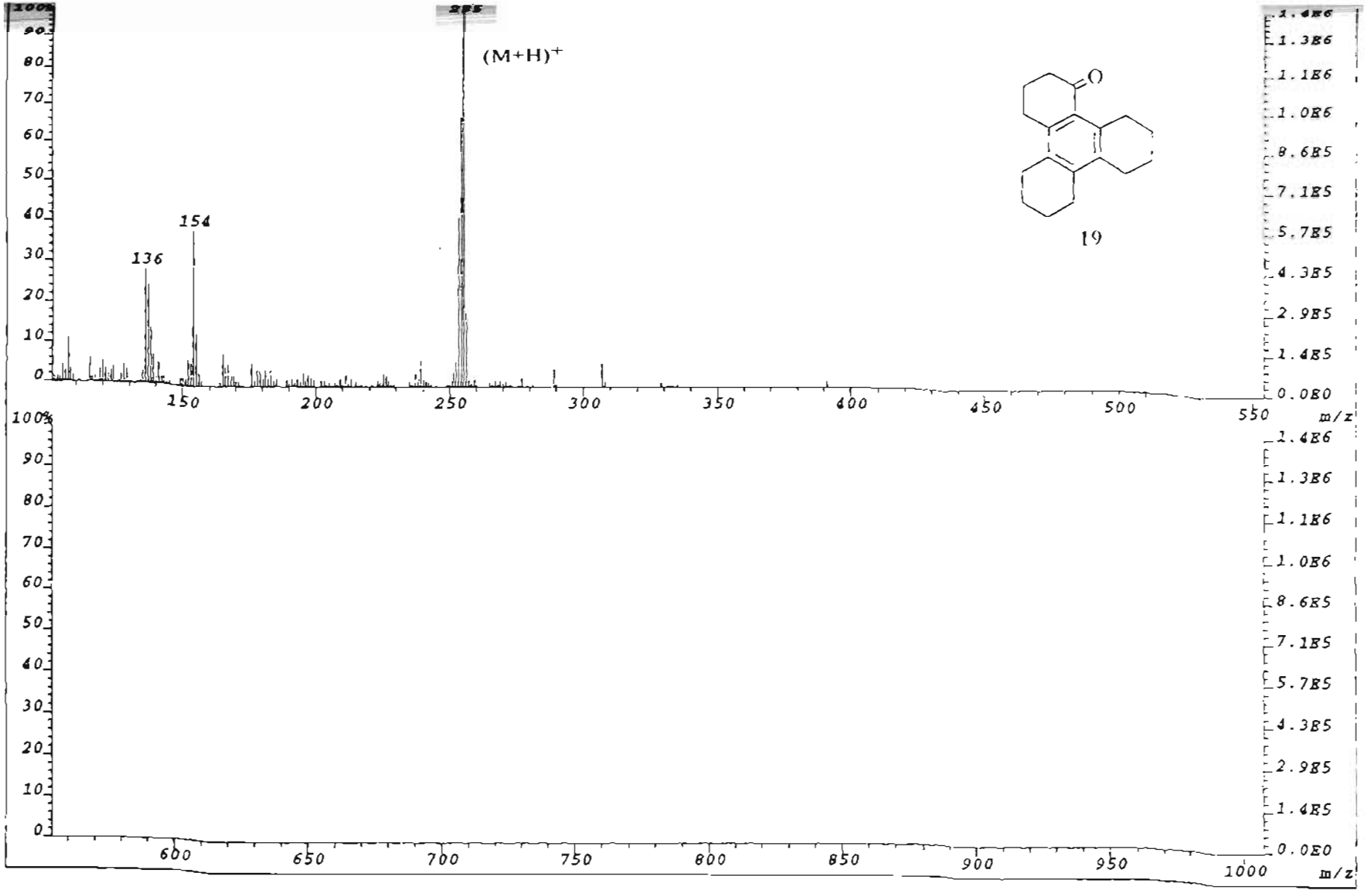

FAB mass spectrum

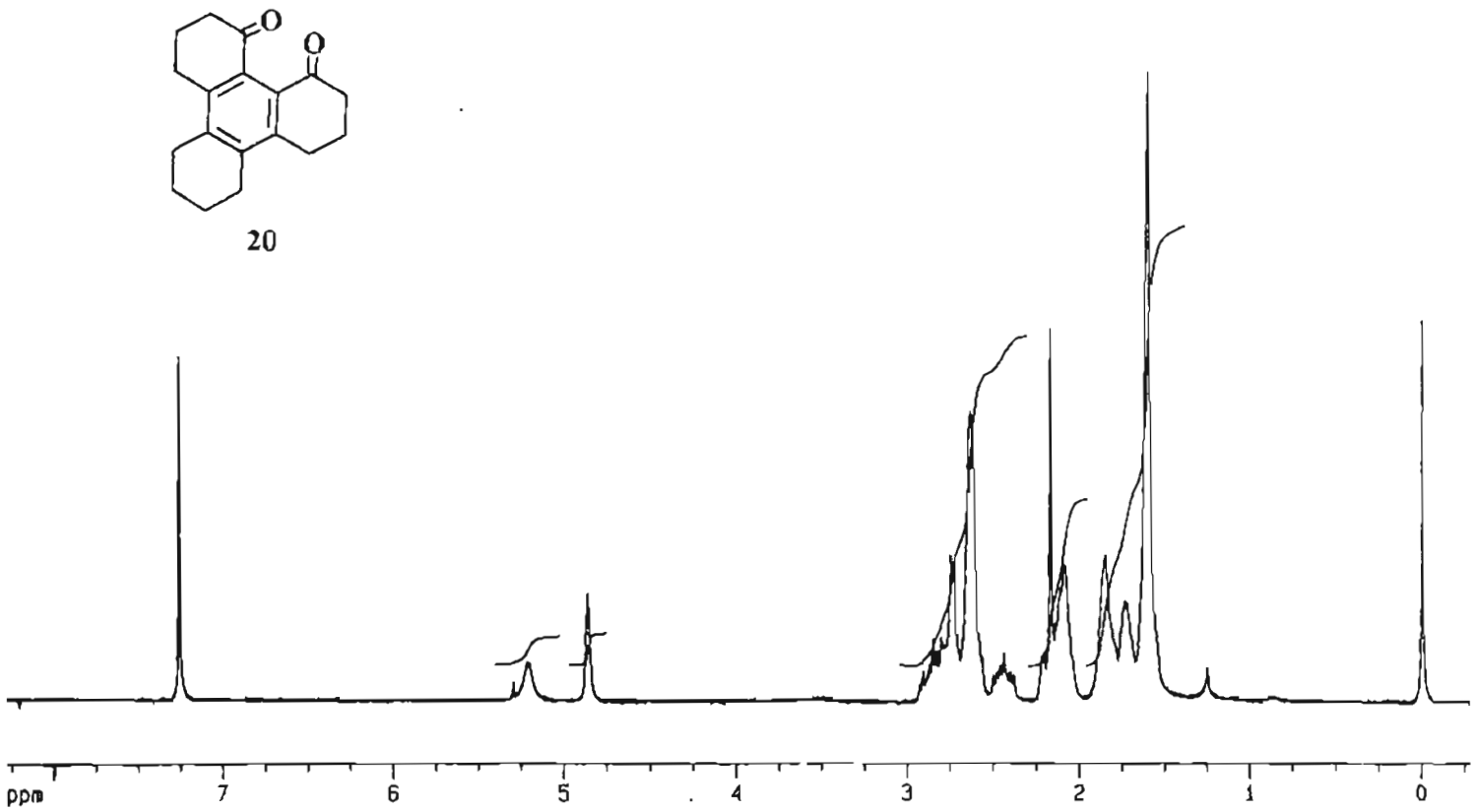

20

δ (300 MHz, $CDCl_3$)

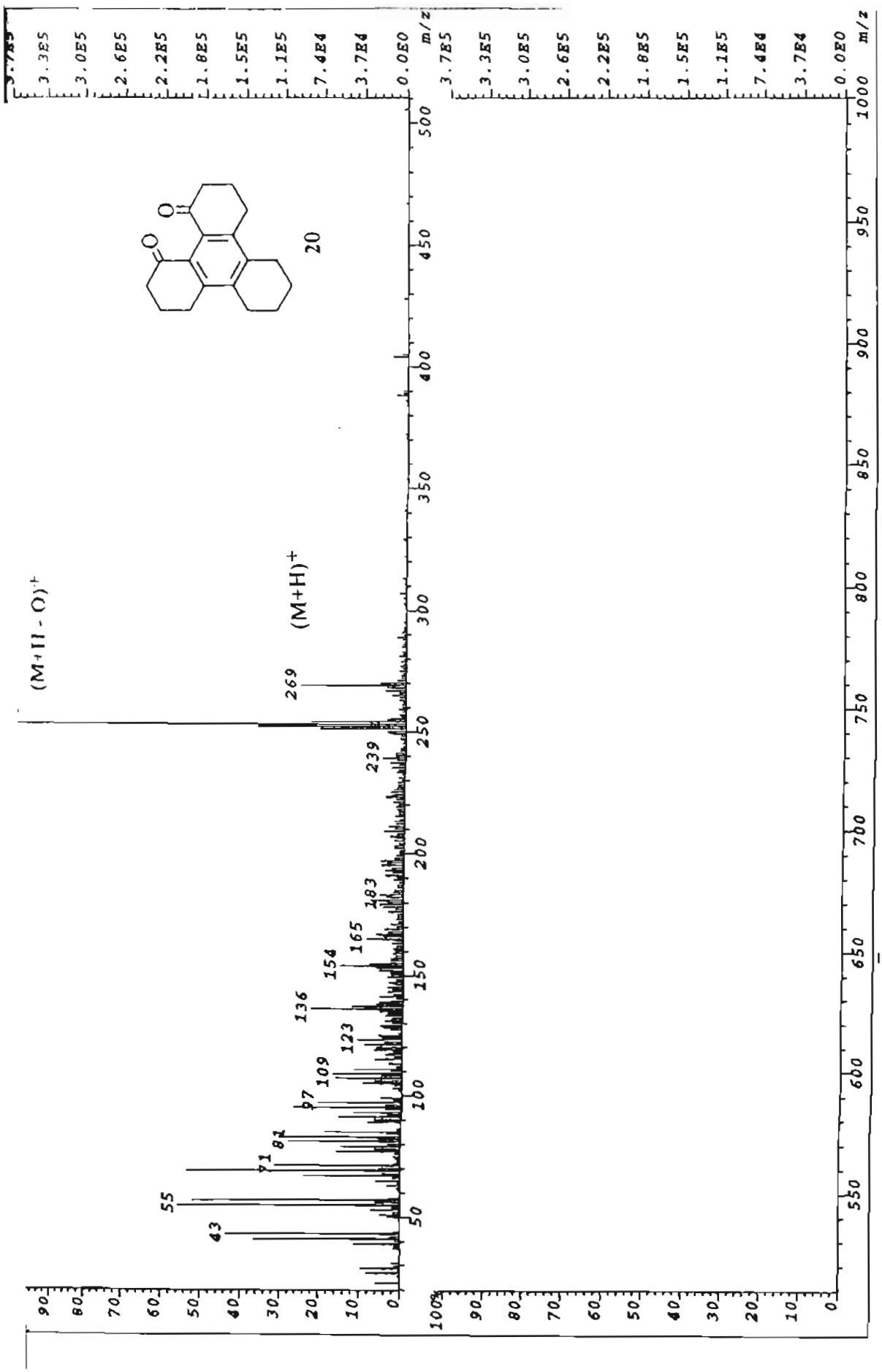

FAB mass spectrum

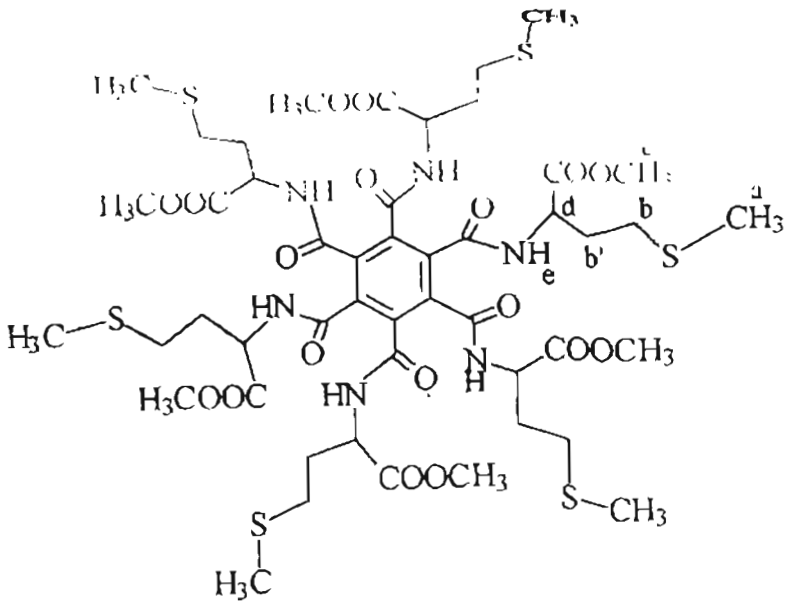

28

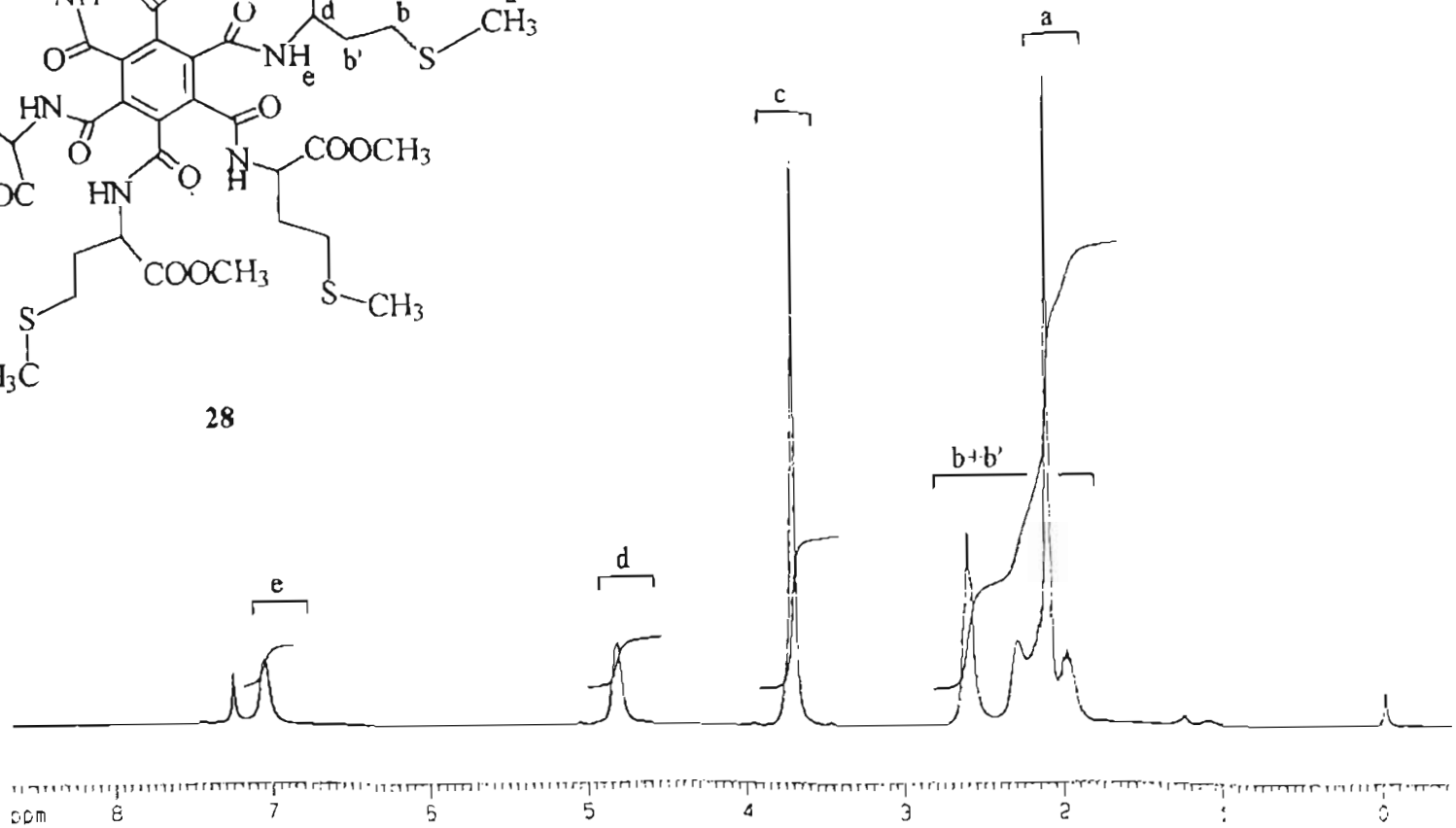

δ (300 MHz, $CDCl_3$)

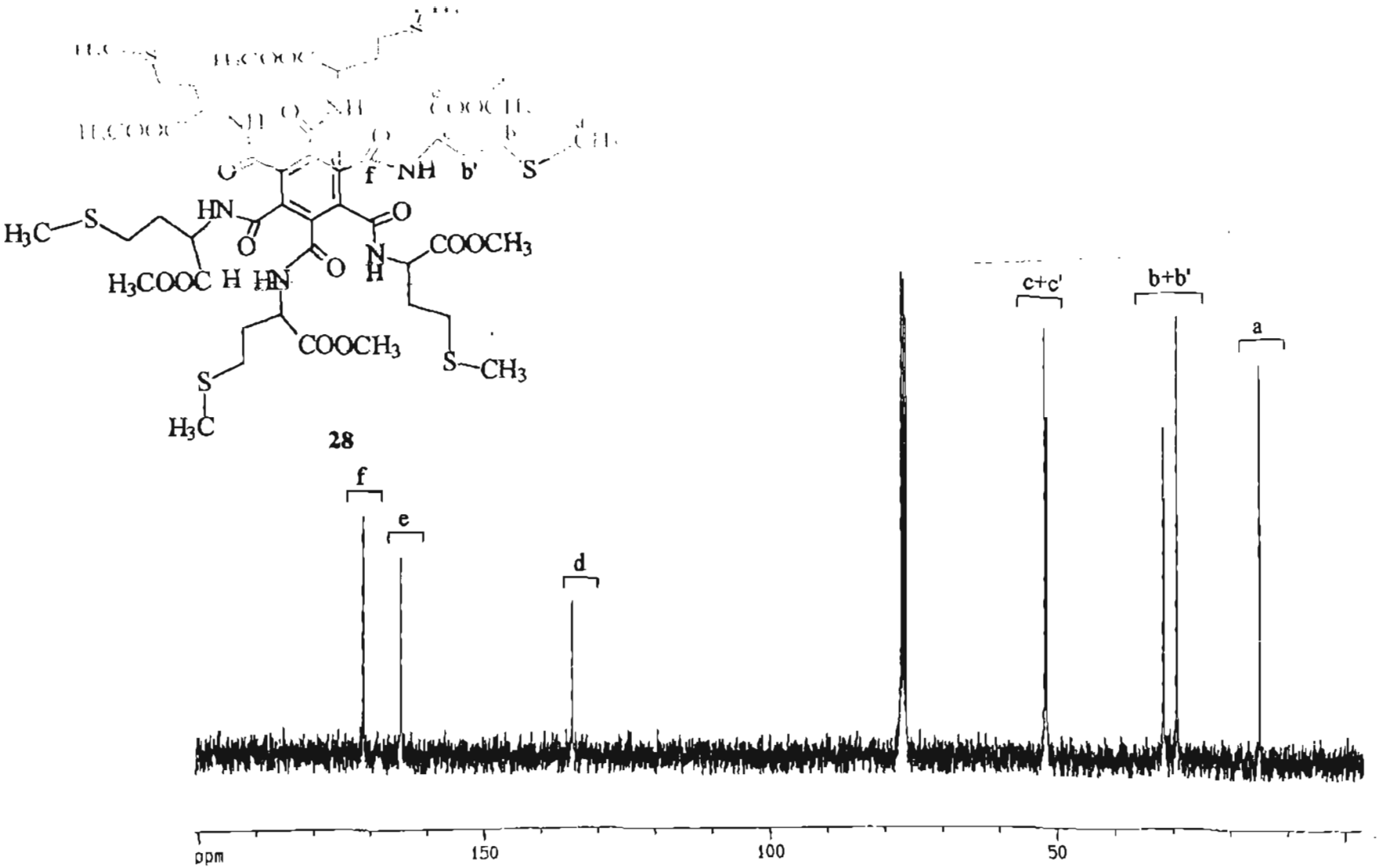

δ (300 MHz, $CDCl_3$)

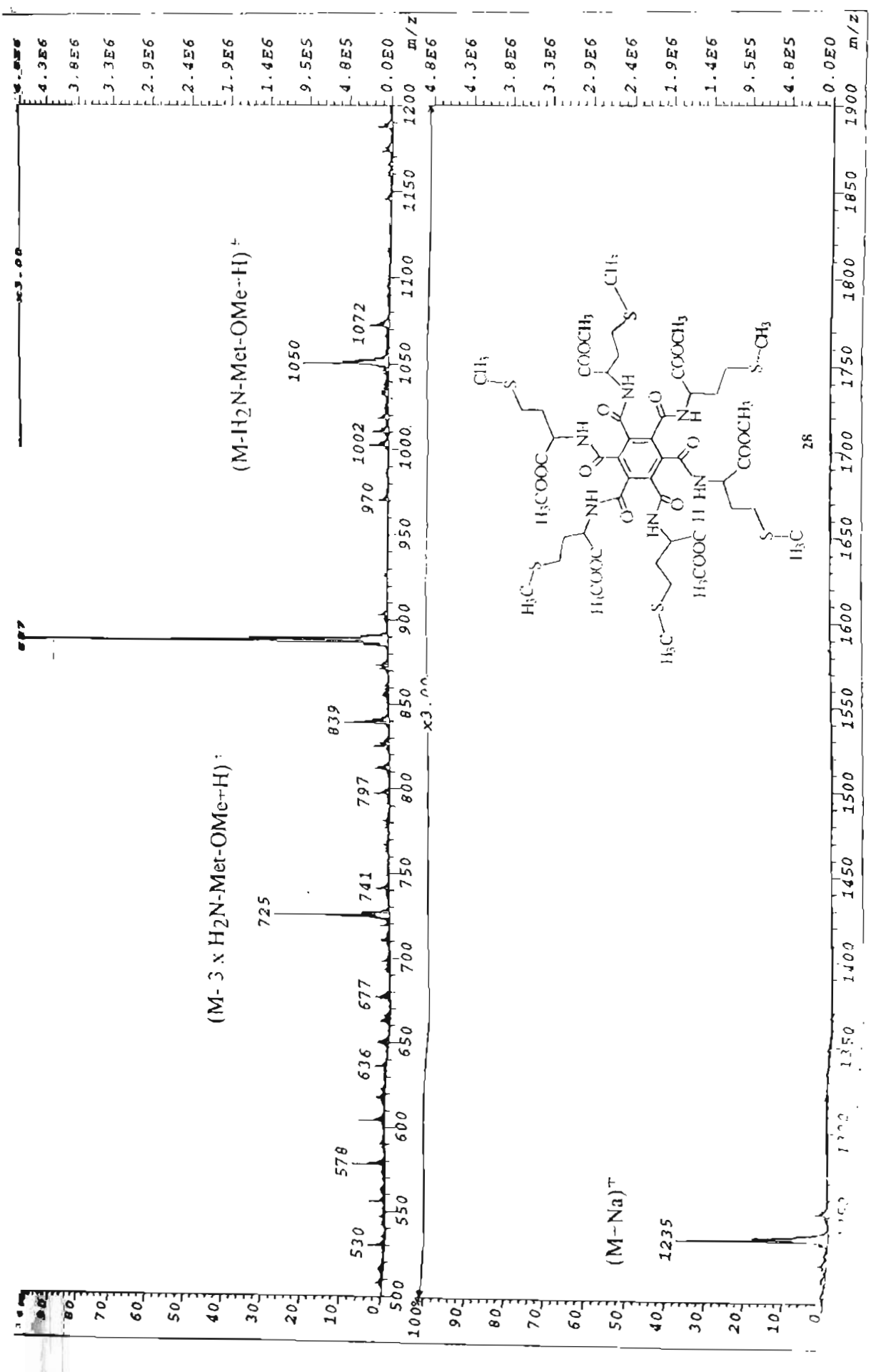

FAB mass spectrum

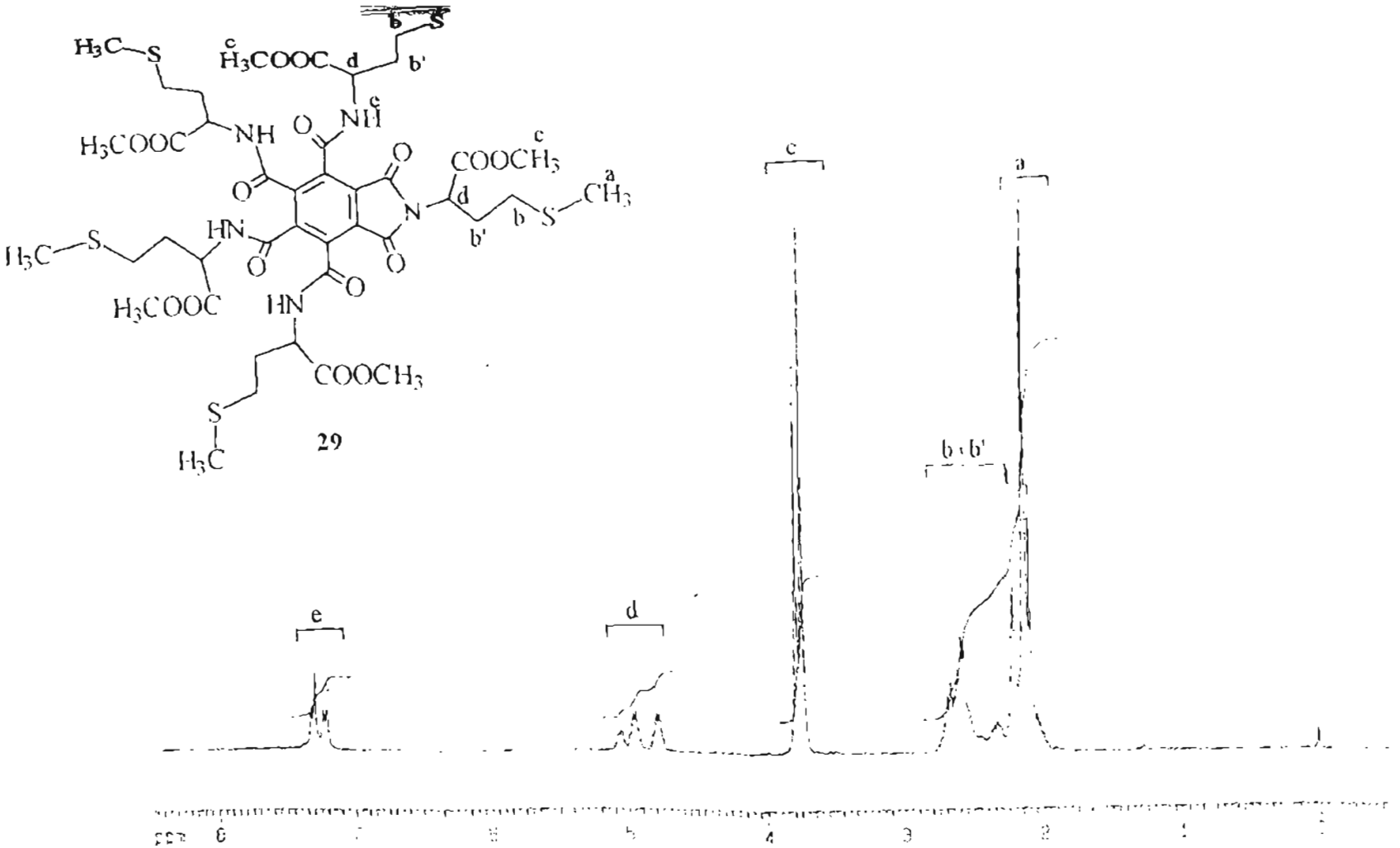
H3C
S
c
H3COOC
d
b'
NH
O
NH
c
H3COOC
O
O
COOCH3
c
a
CH3
d
b
S
b'
N
HN
O
O
H3C
S
H3COOC
HN
O
O
COOCH3
S
H3C
29
e
d
c
a
b + b'
δ (300 MHz, CDCl3)

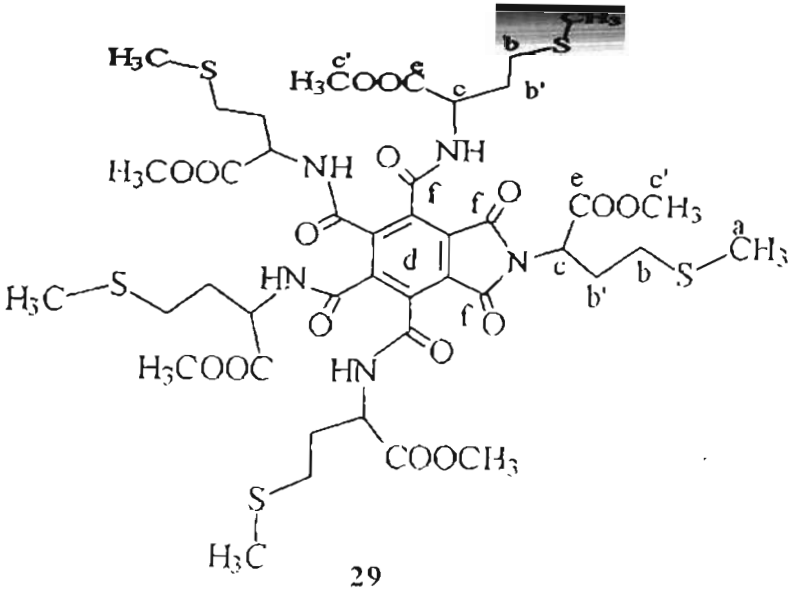

29

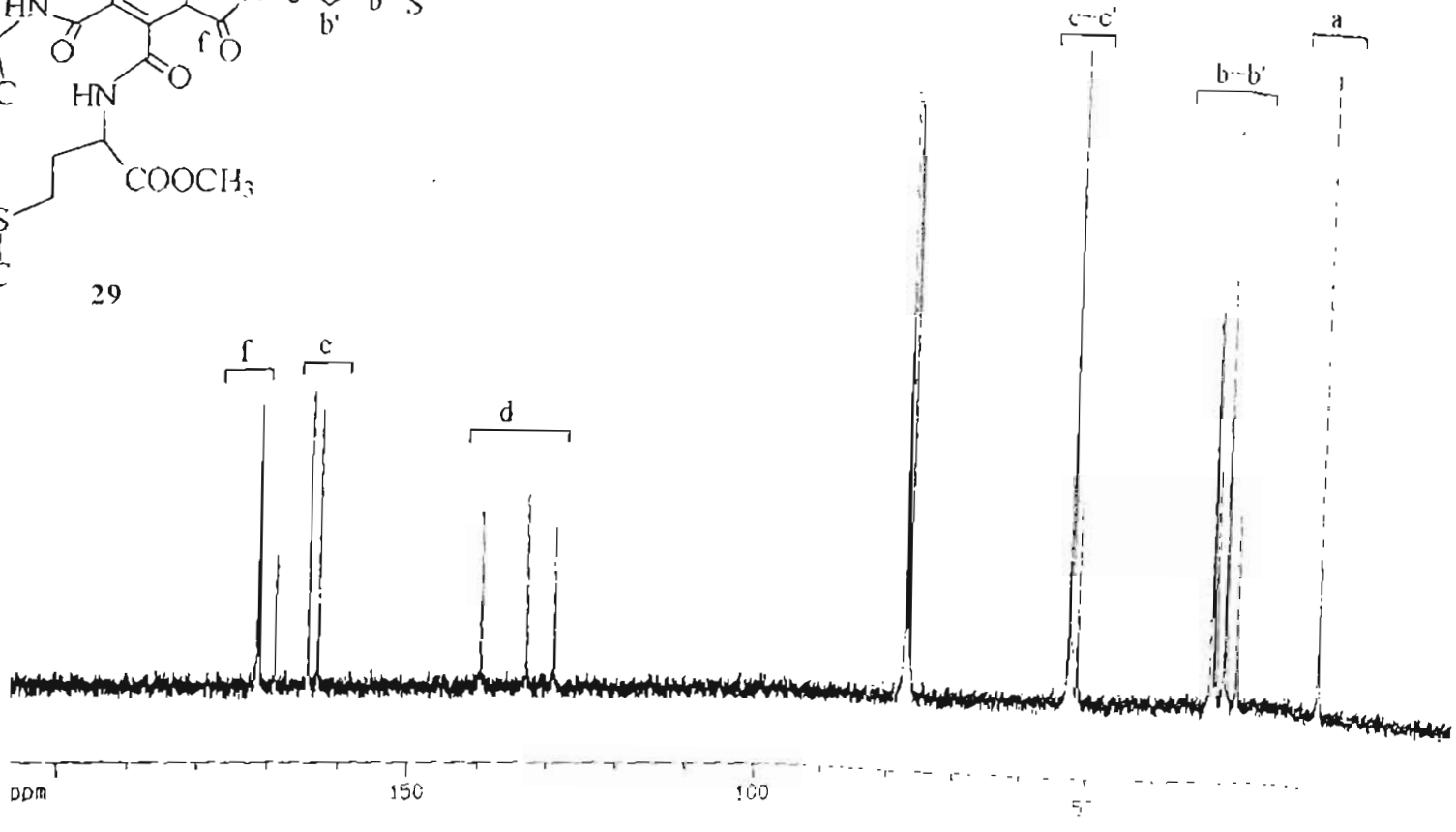

δ (300 MHz, $CDCl_3$)

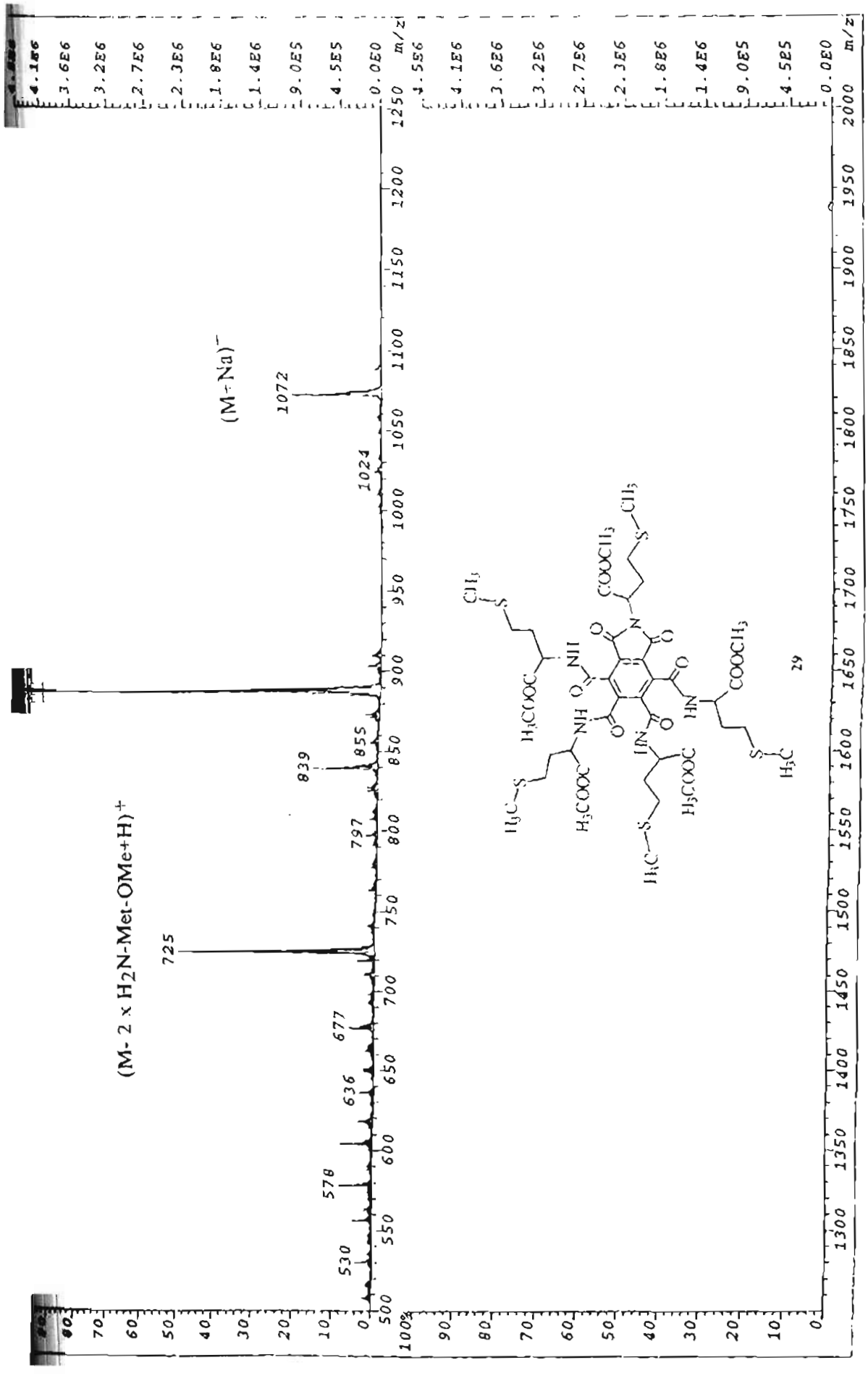

FAB mass spectrum

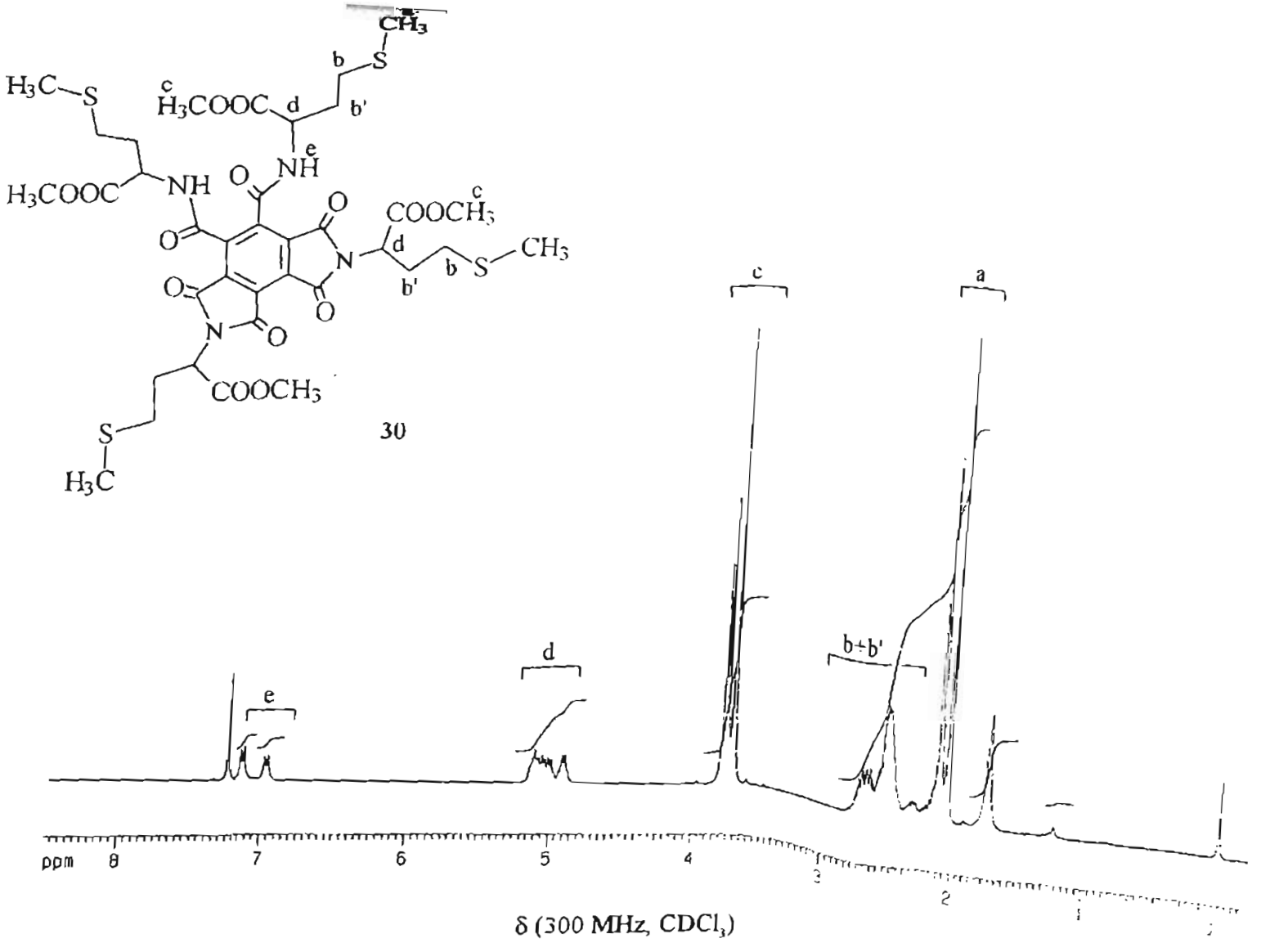

δ (300 MHz, $CDCl_3$)

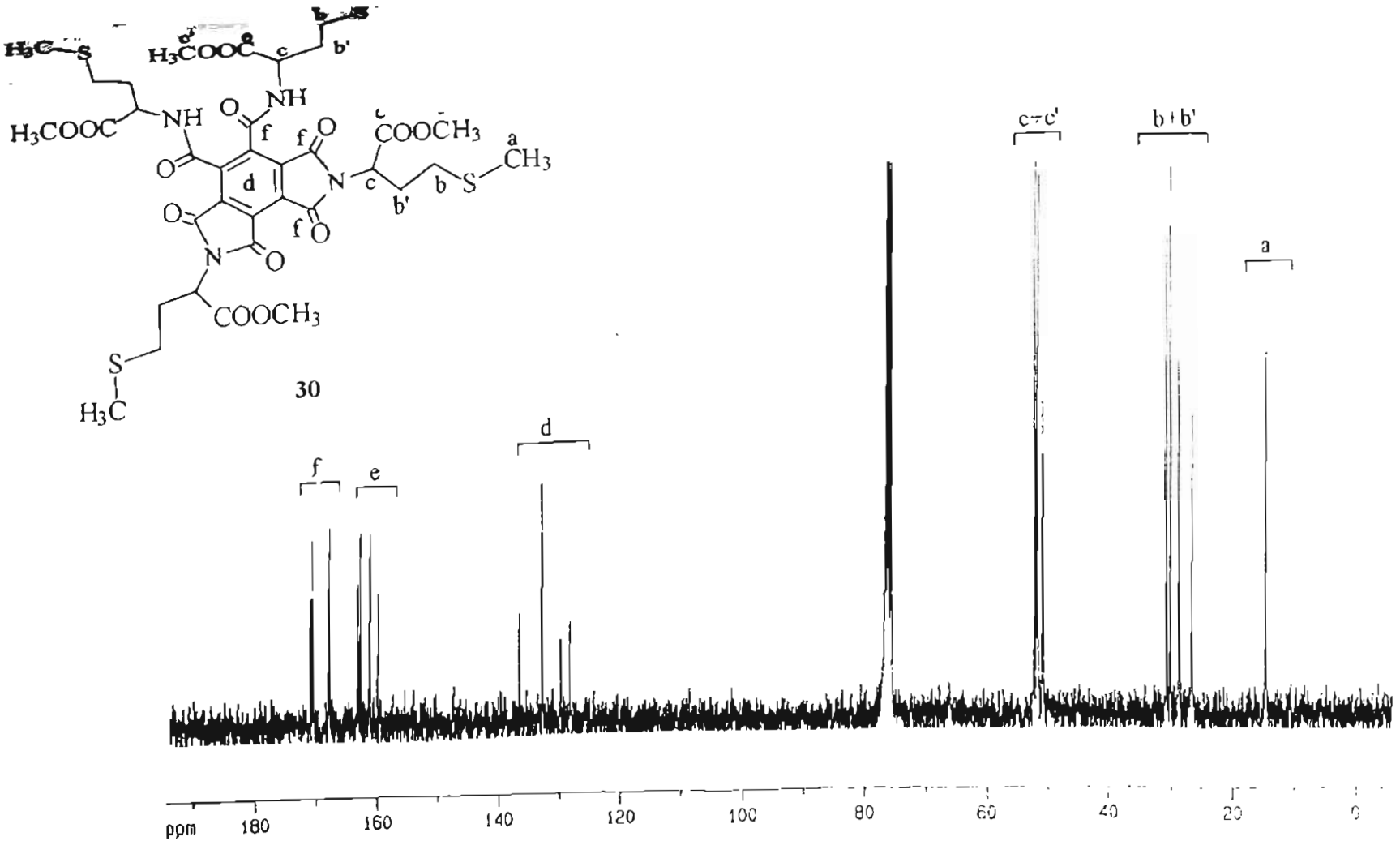

δ (300 MHz, $CDCl_3$)

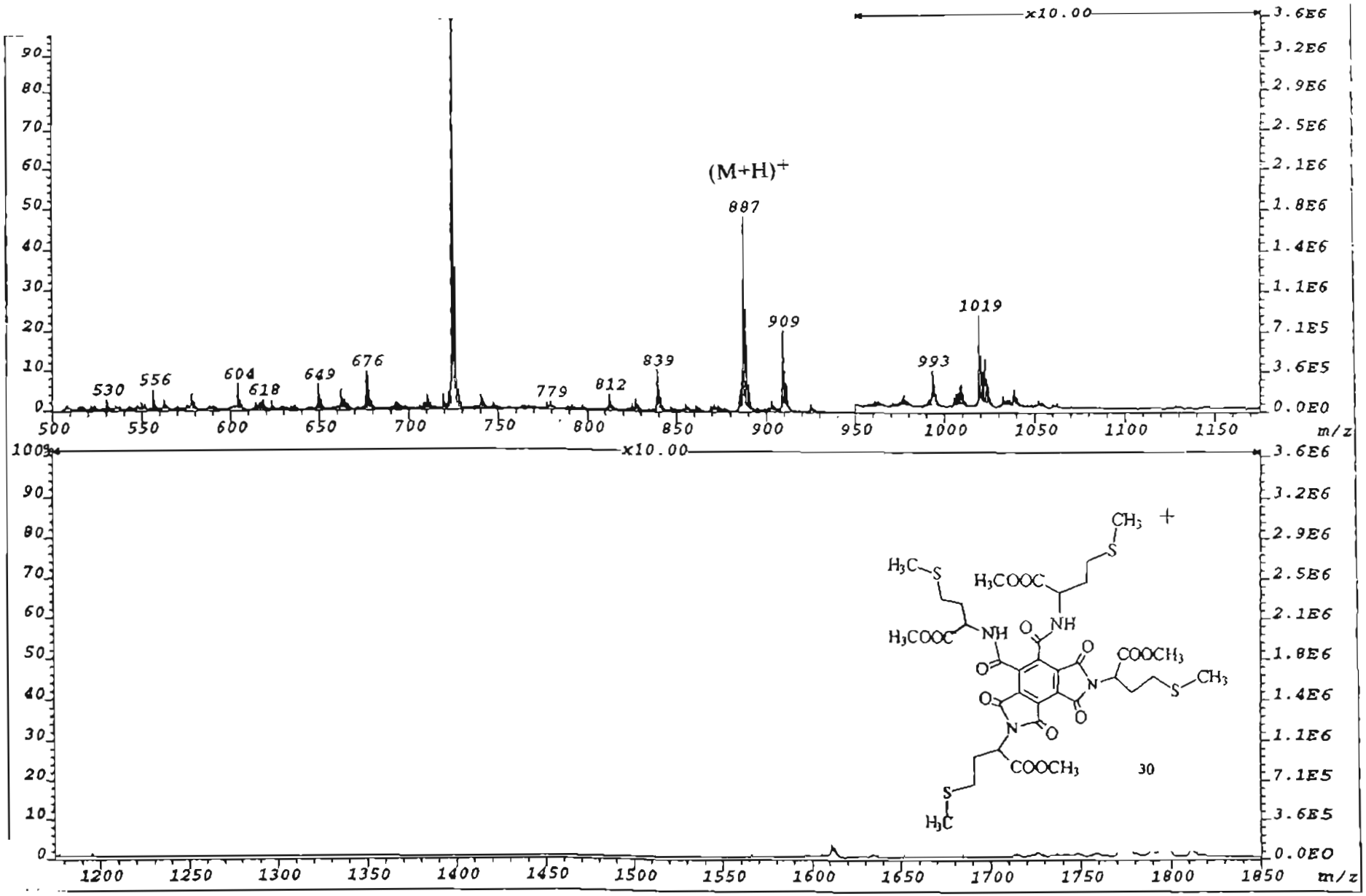

FAB mass spectrum

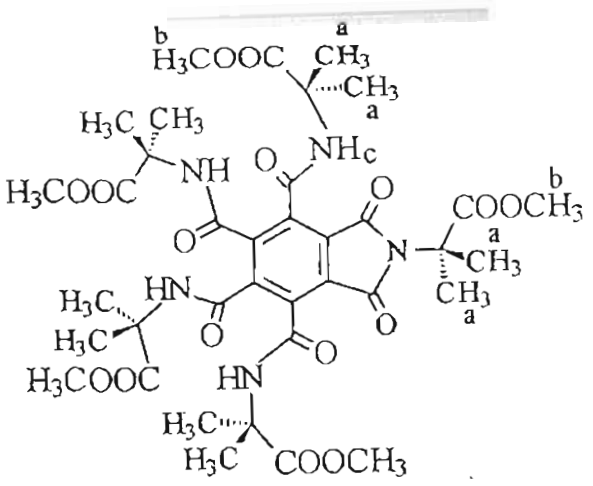

33

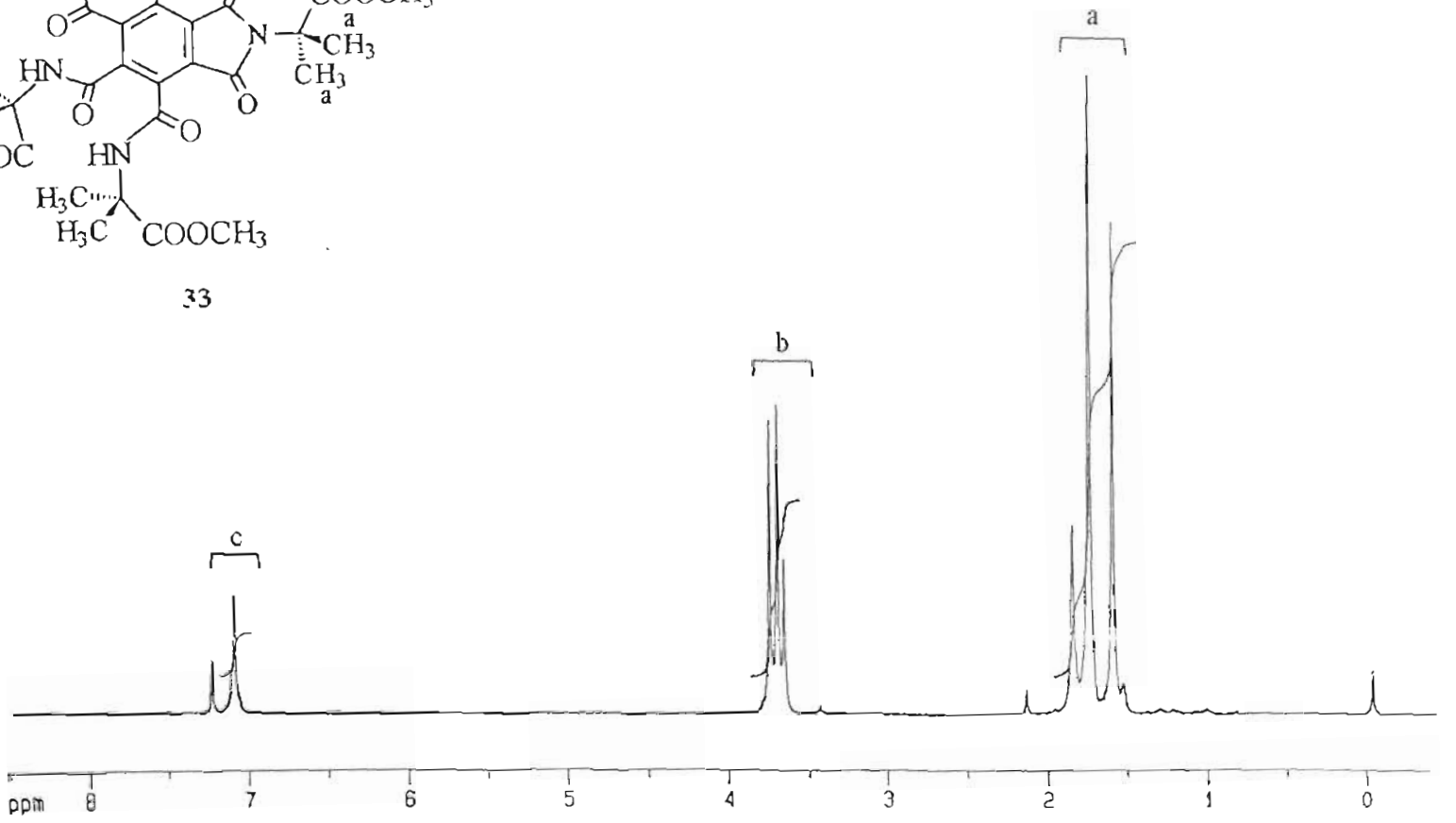

δ (300 MHz, $CDCl_3$)

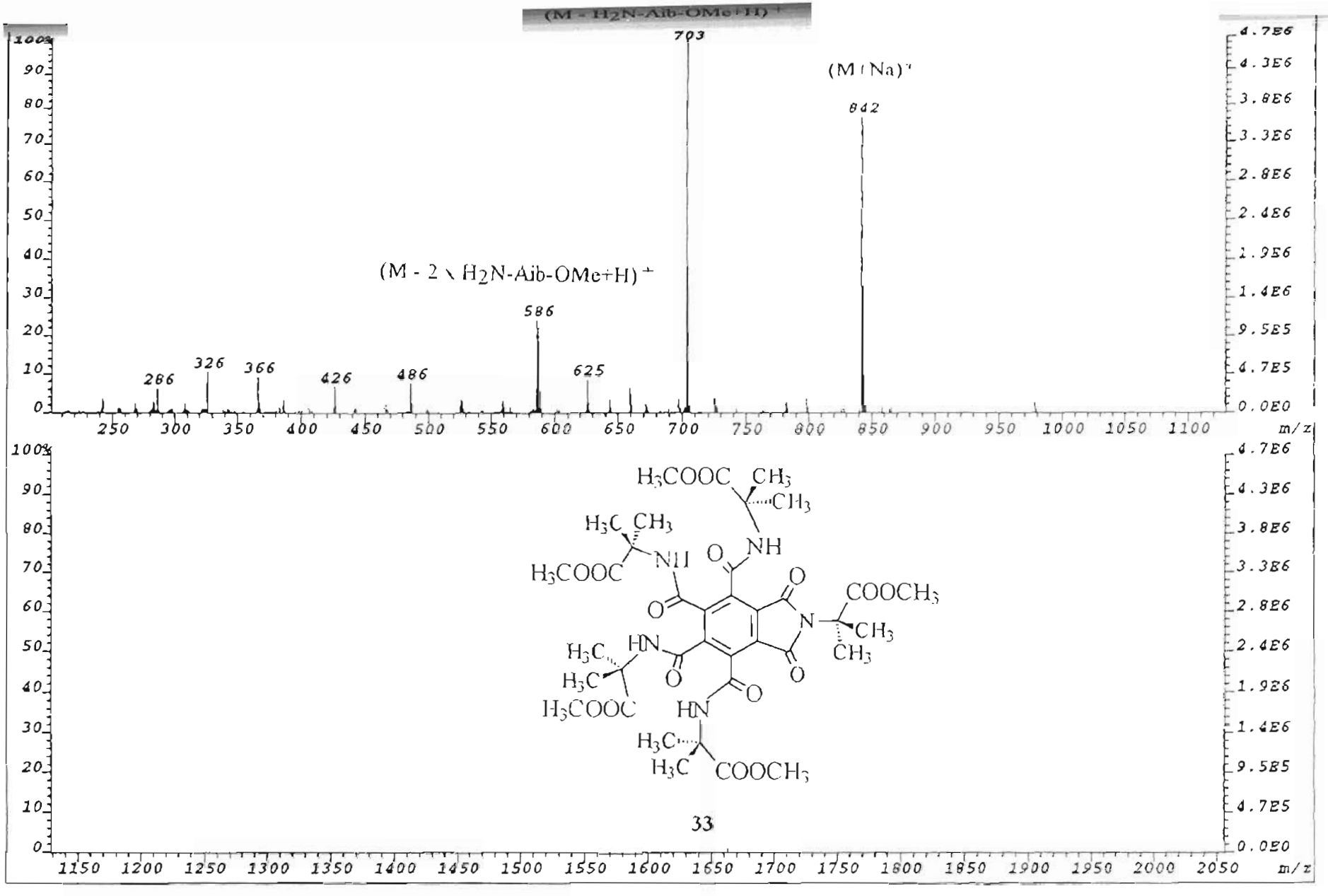

FAB mass spectrum

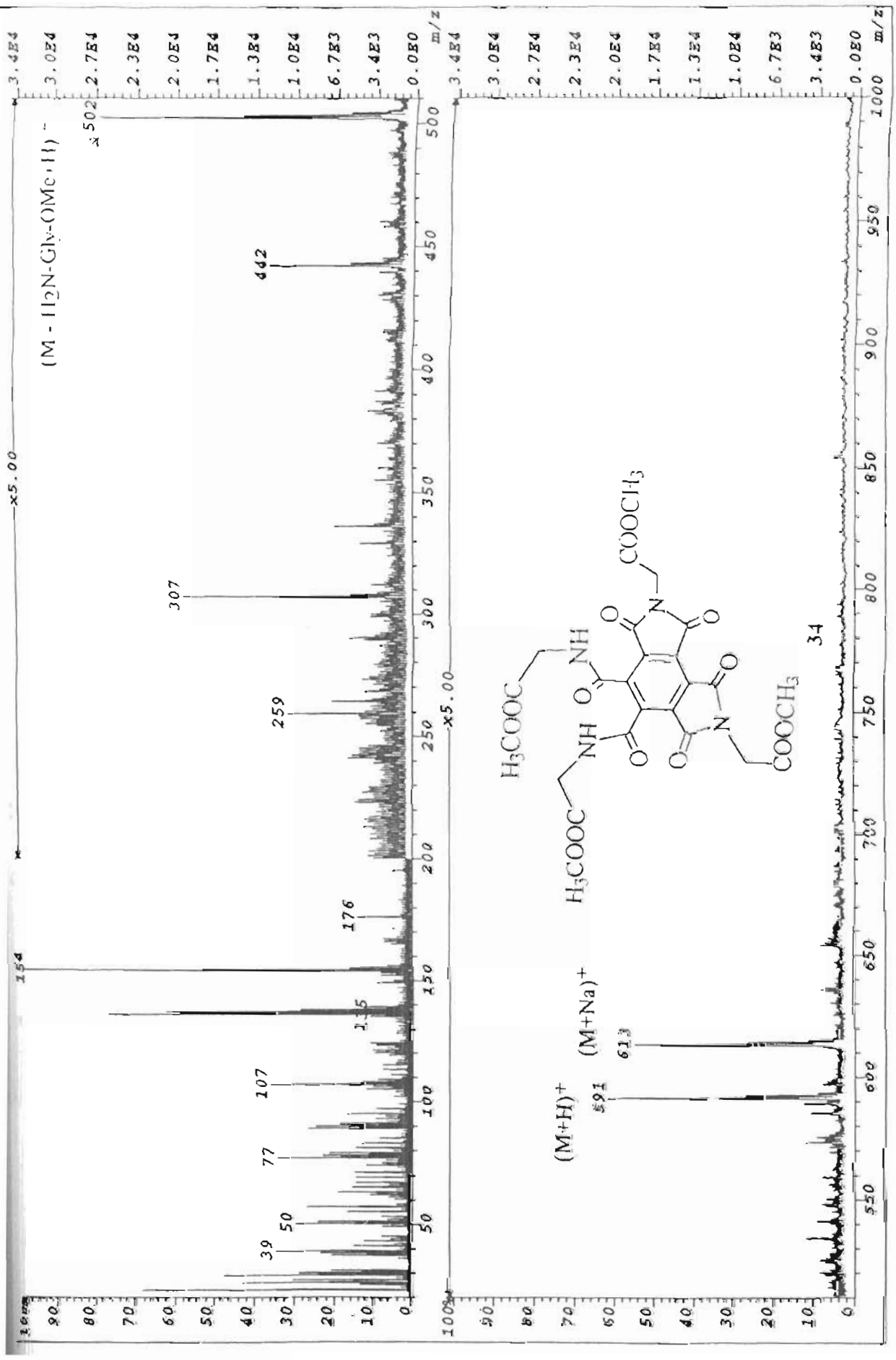

FAB mass spectrum

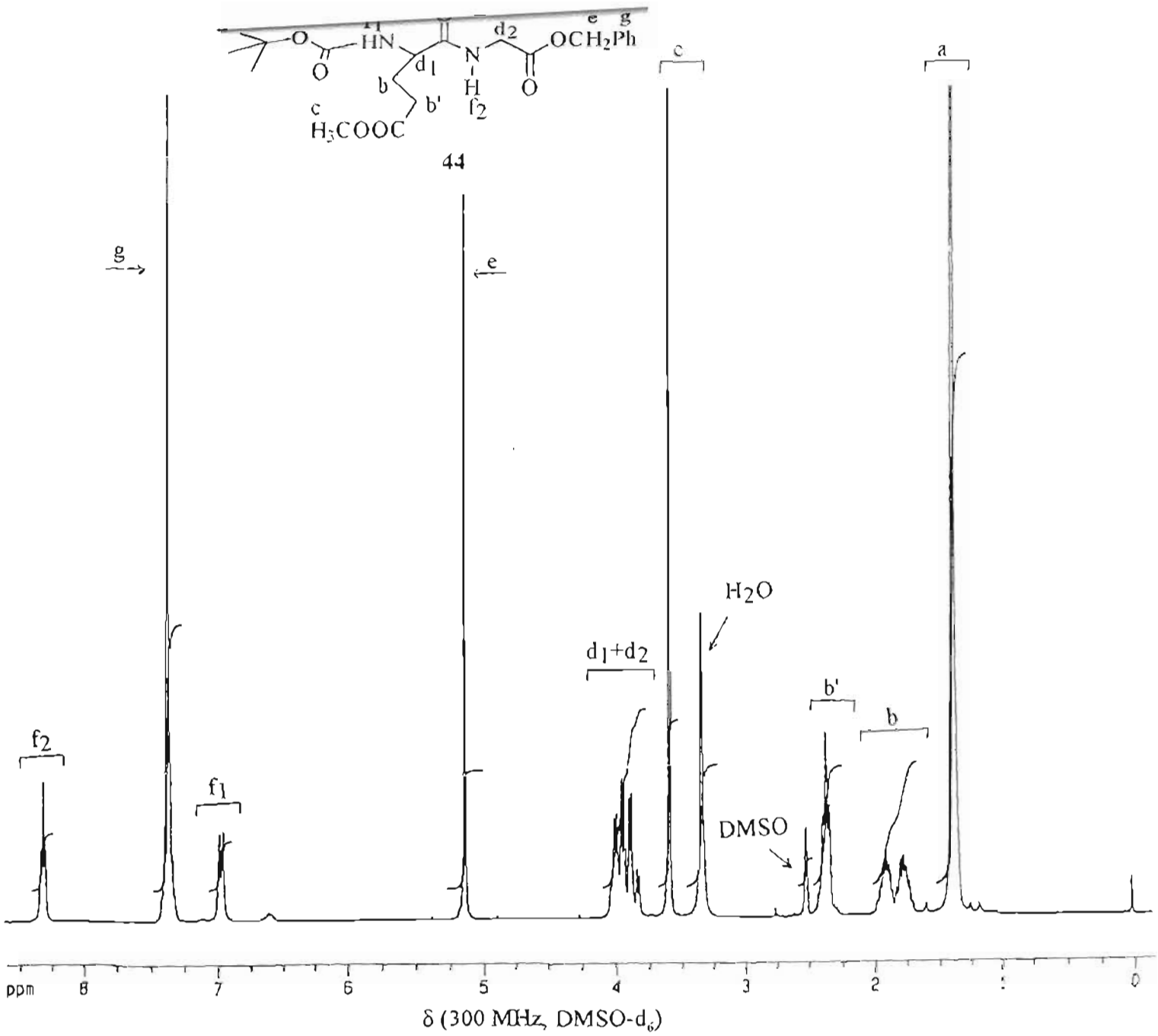
44
g
e
c
a
H_2O
d_1+d_2
b'
b
f_2
f_1
DMSO
ppm
δ (300 MHz, DMSO-d_6)

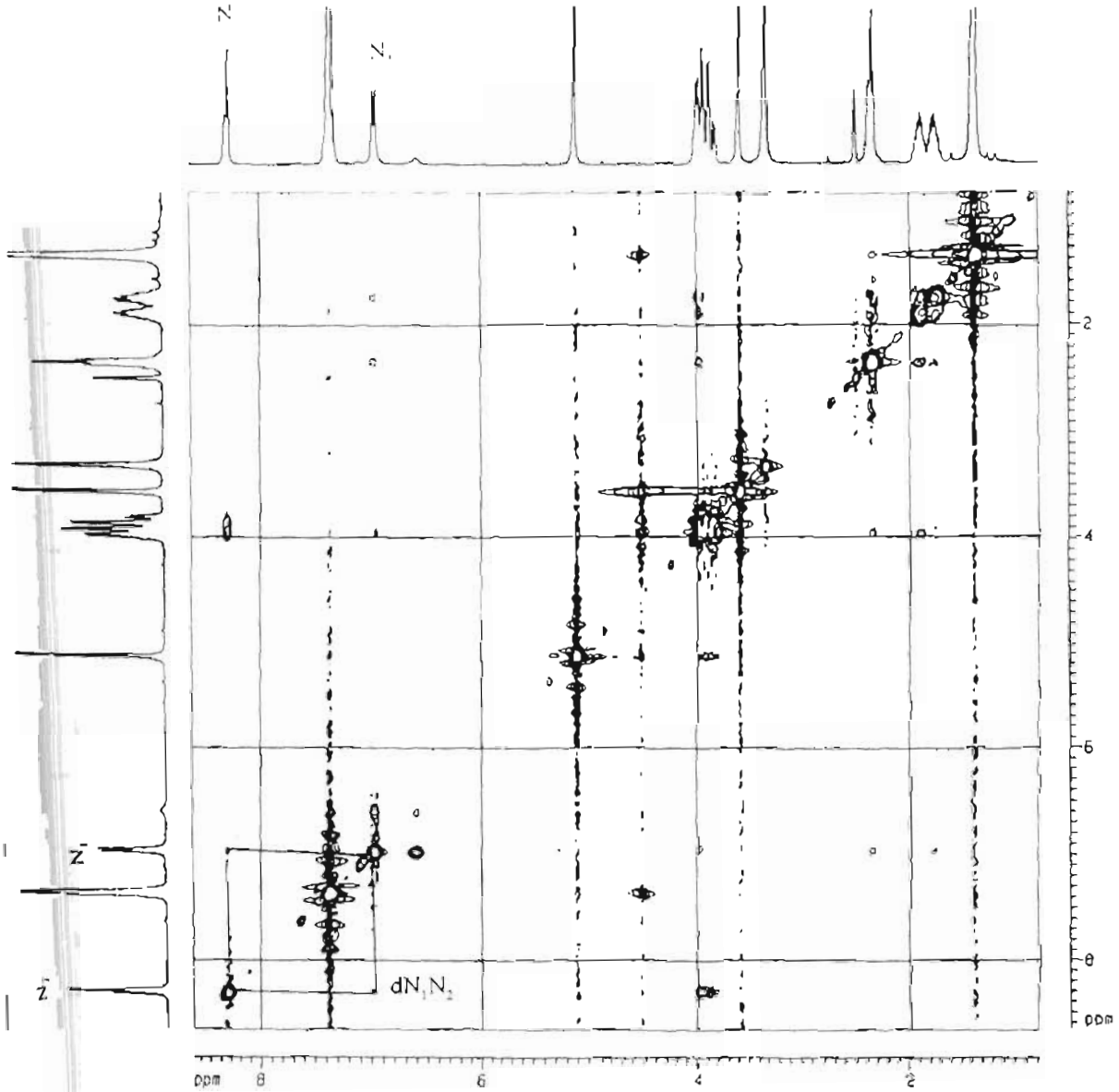

ROESY Spectra of the dipeptide (**44**), showing $d_{N,N}$ coupling. N_1 and N_2 designates protons connected to the amide groups of first and second amino acid residues respectively

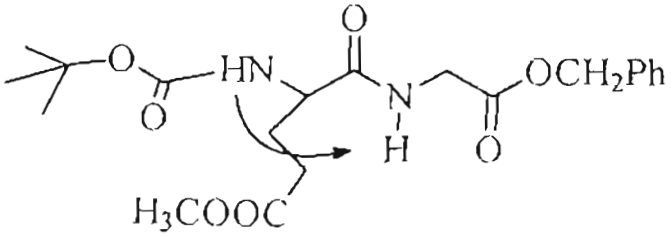

44

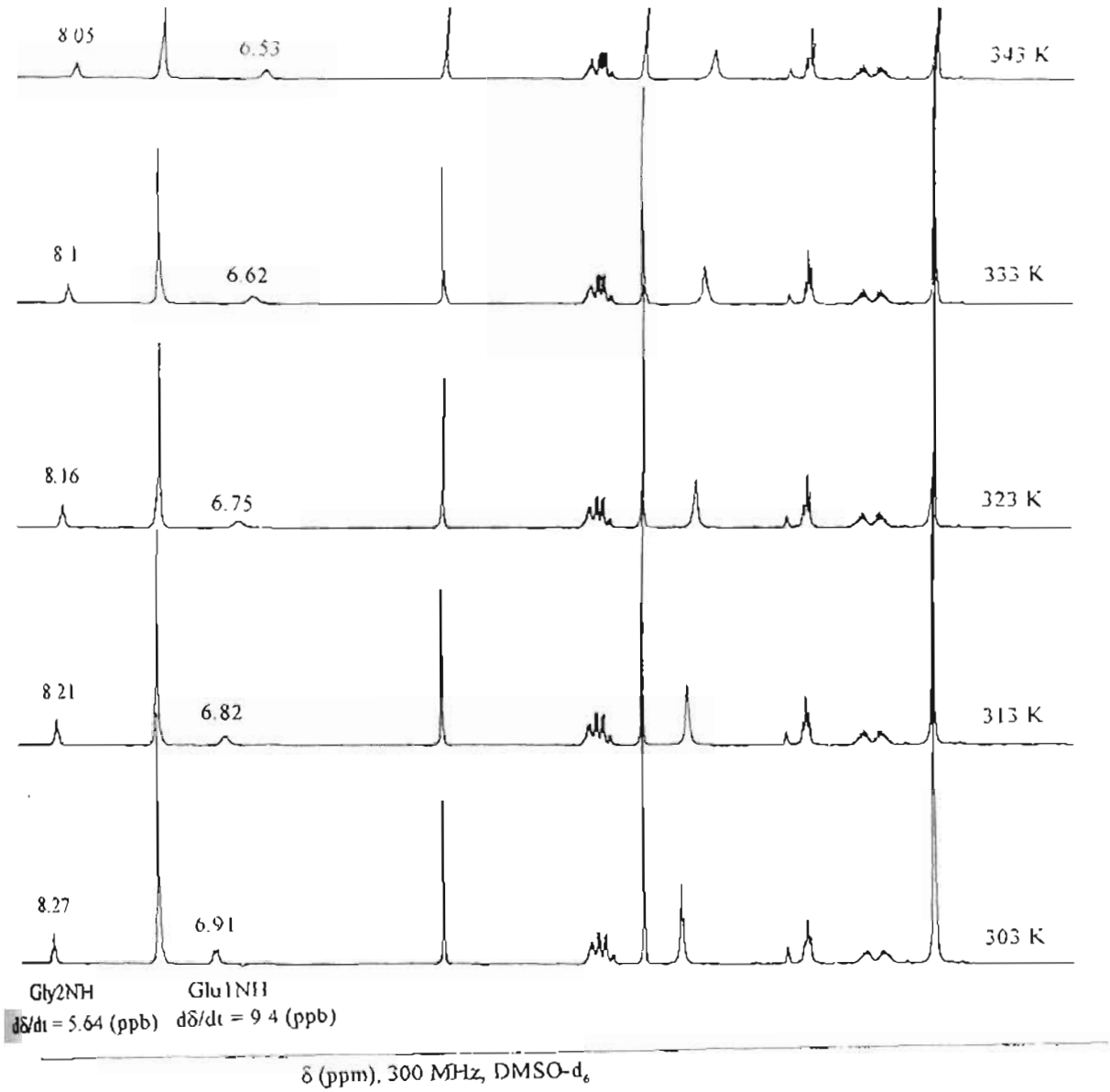

Variable temperature NMR plots of the dipeptide (44)

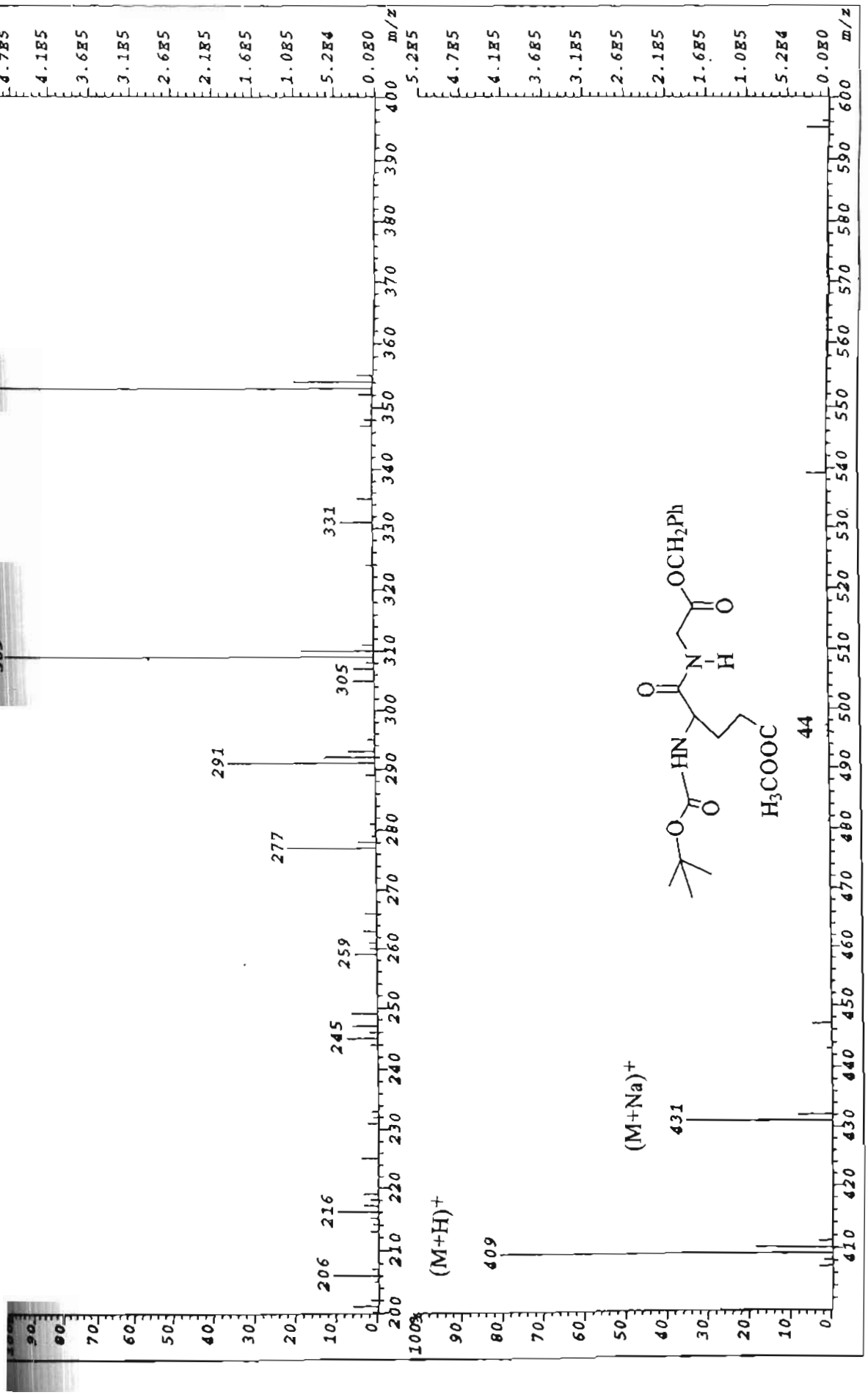

FAB mass spectrum

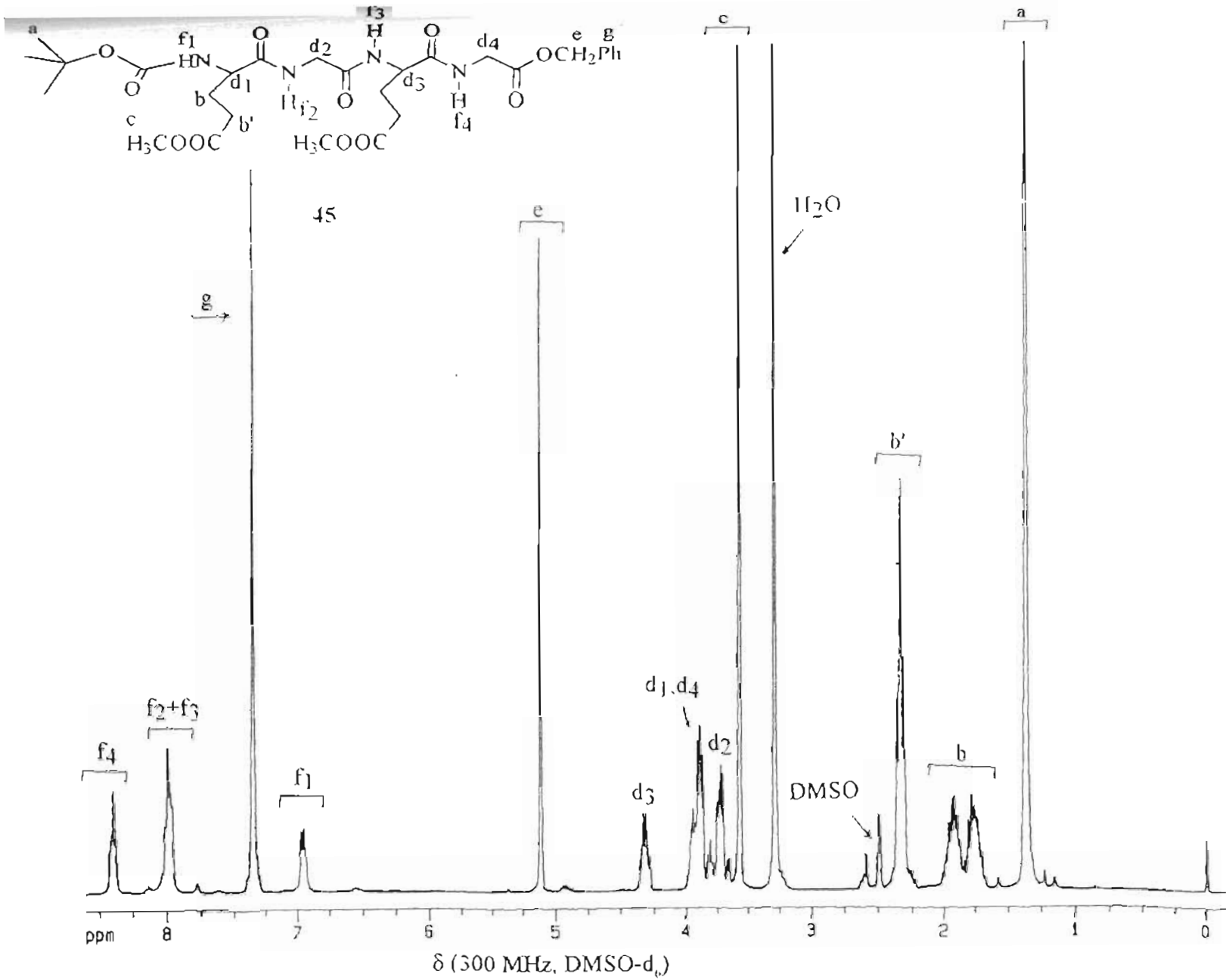

δ (300 MHz, DMSO-d_6)

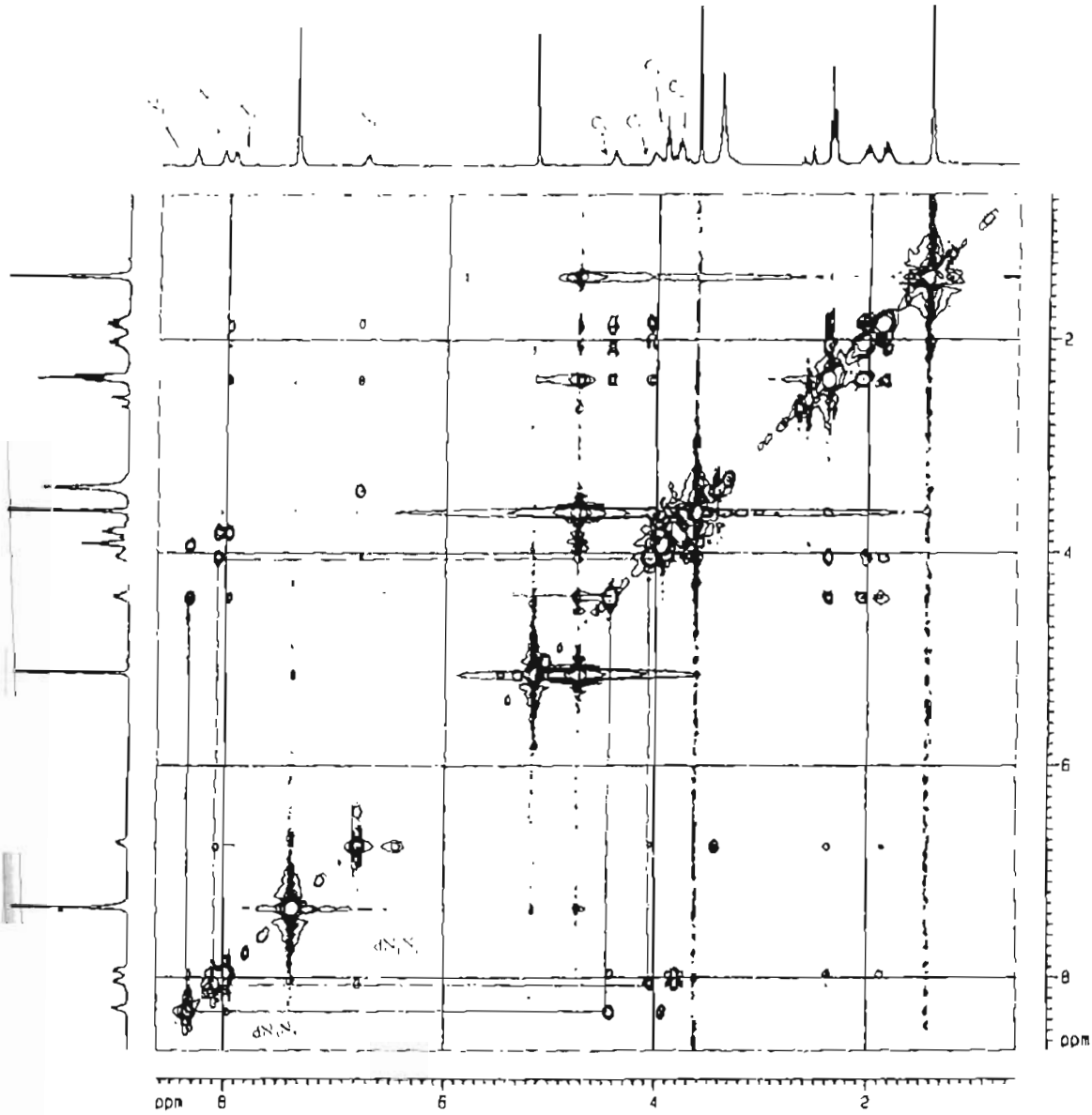

ROESY spectra of the tetrapeptide (**45**). N_i and C_i designates the proton connected to the amide nitrogen or Cα respectively of the i^{th} aminoacid residue

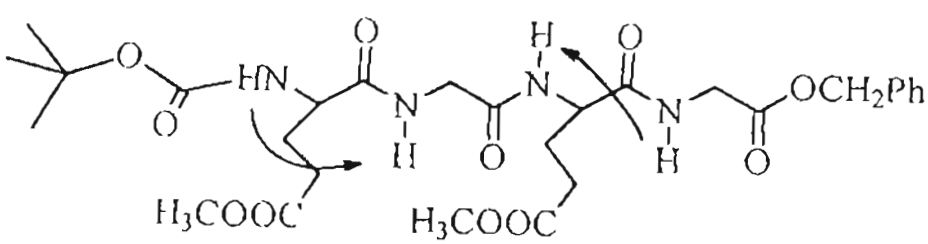

45

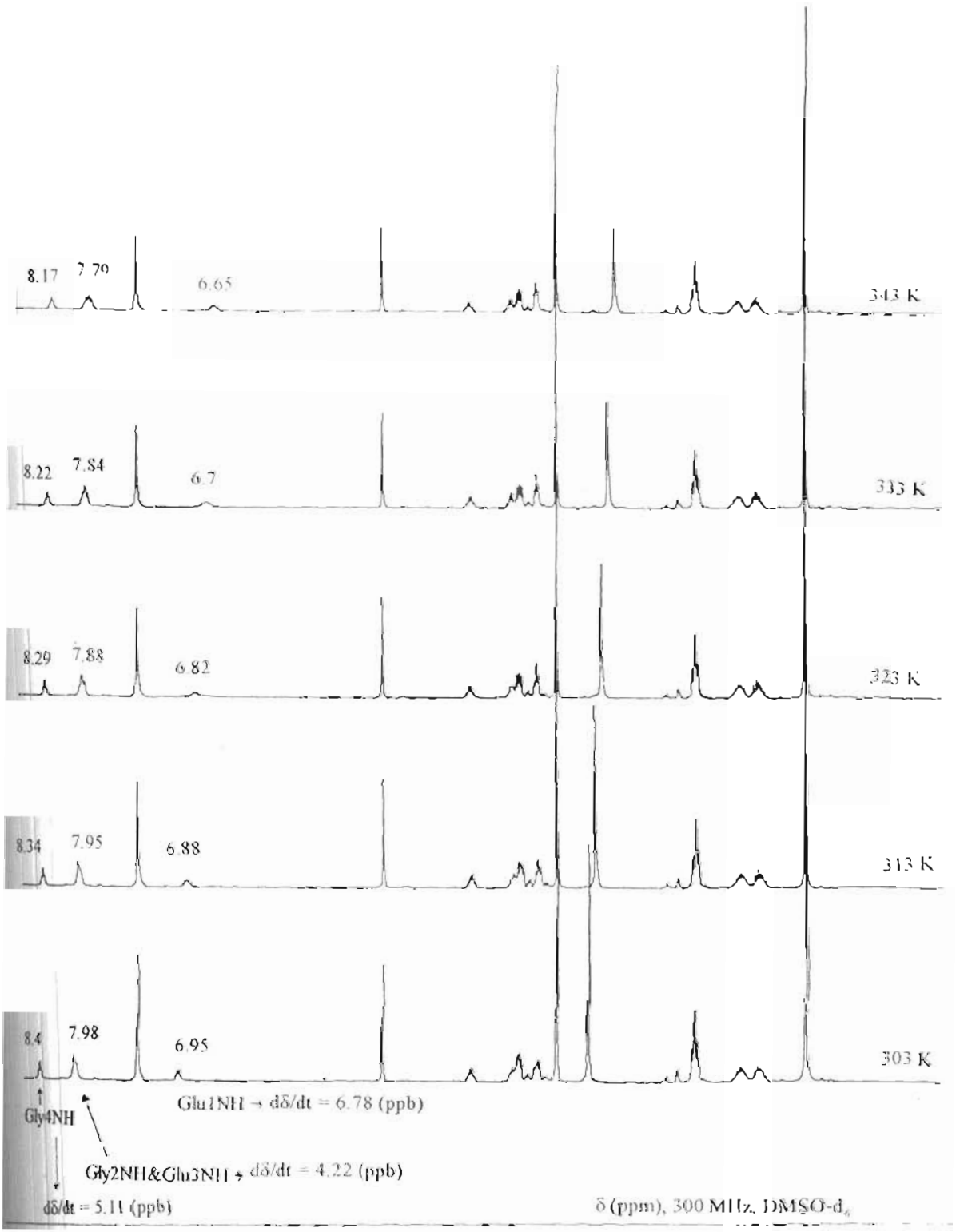

Variable temperature NMR plots of the tetrapeptide (45)

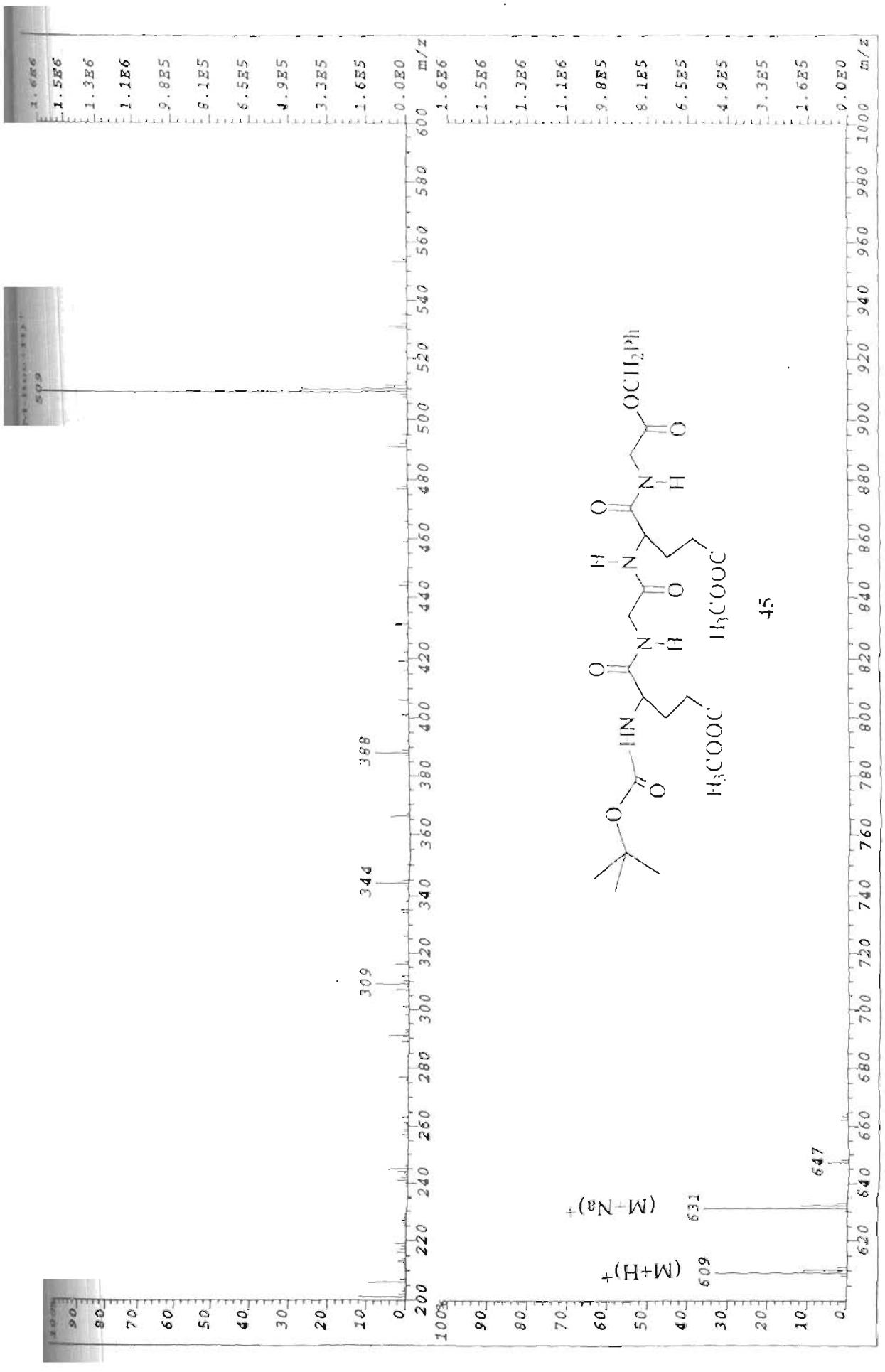

FAB mass spectrum

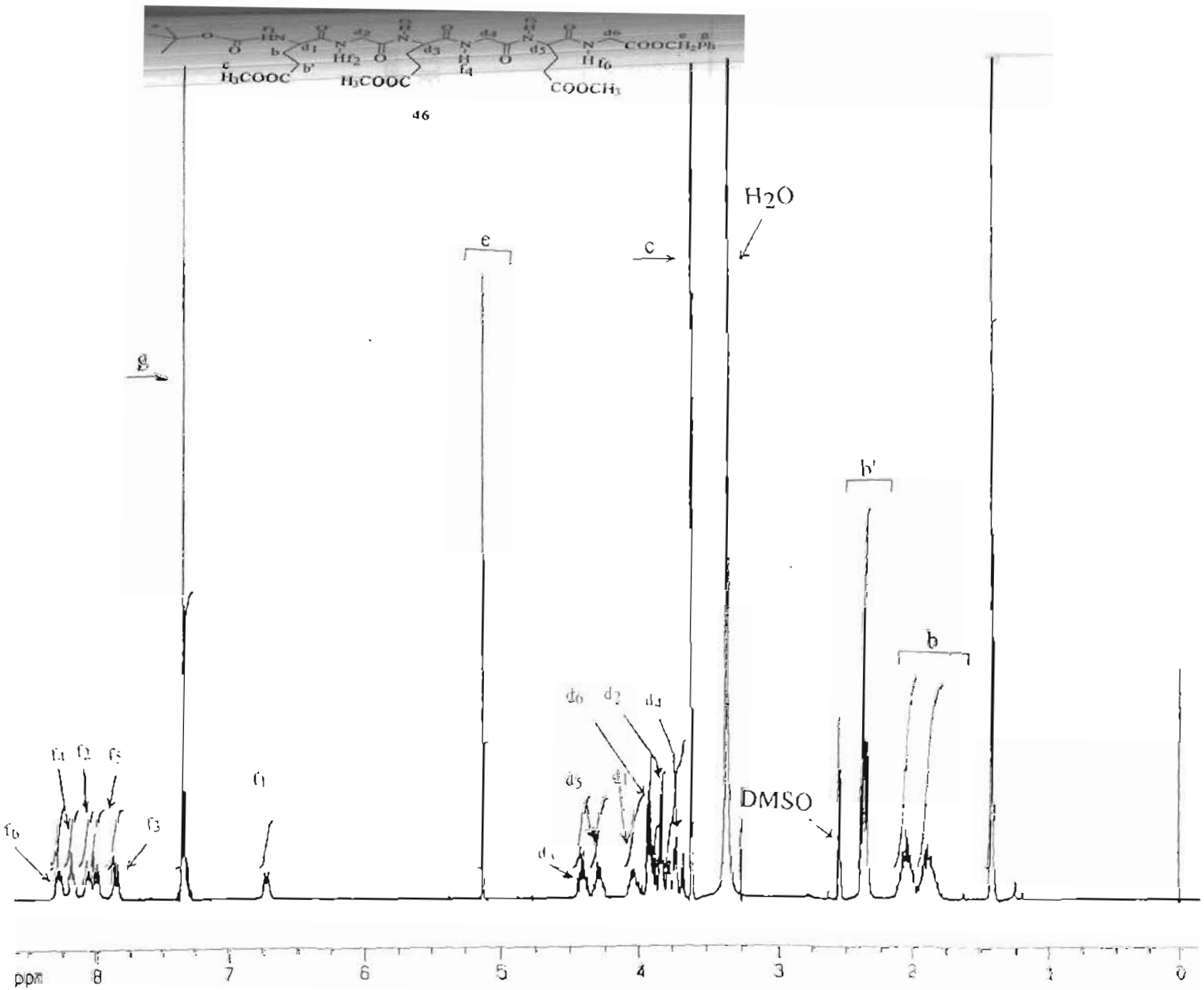

δ (300 MHz, DMSO-d_6)

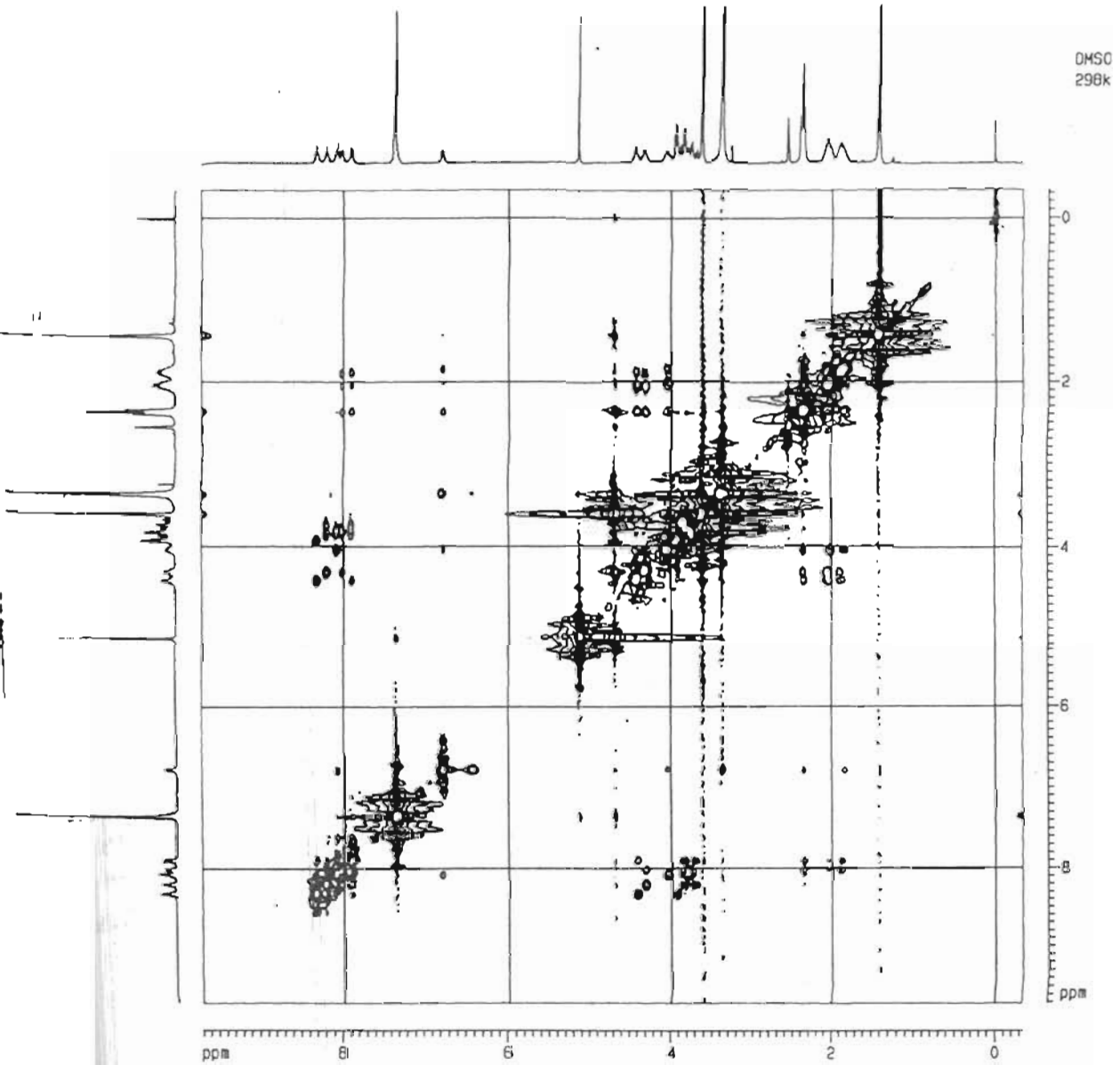

ROESY spectra of the hexapeptide (**46**). Expanded regions from this, showing spatial correlations are provided in the next two pages.

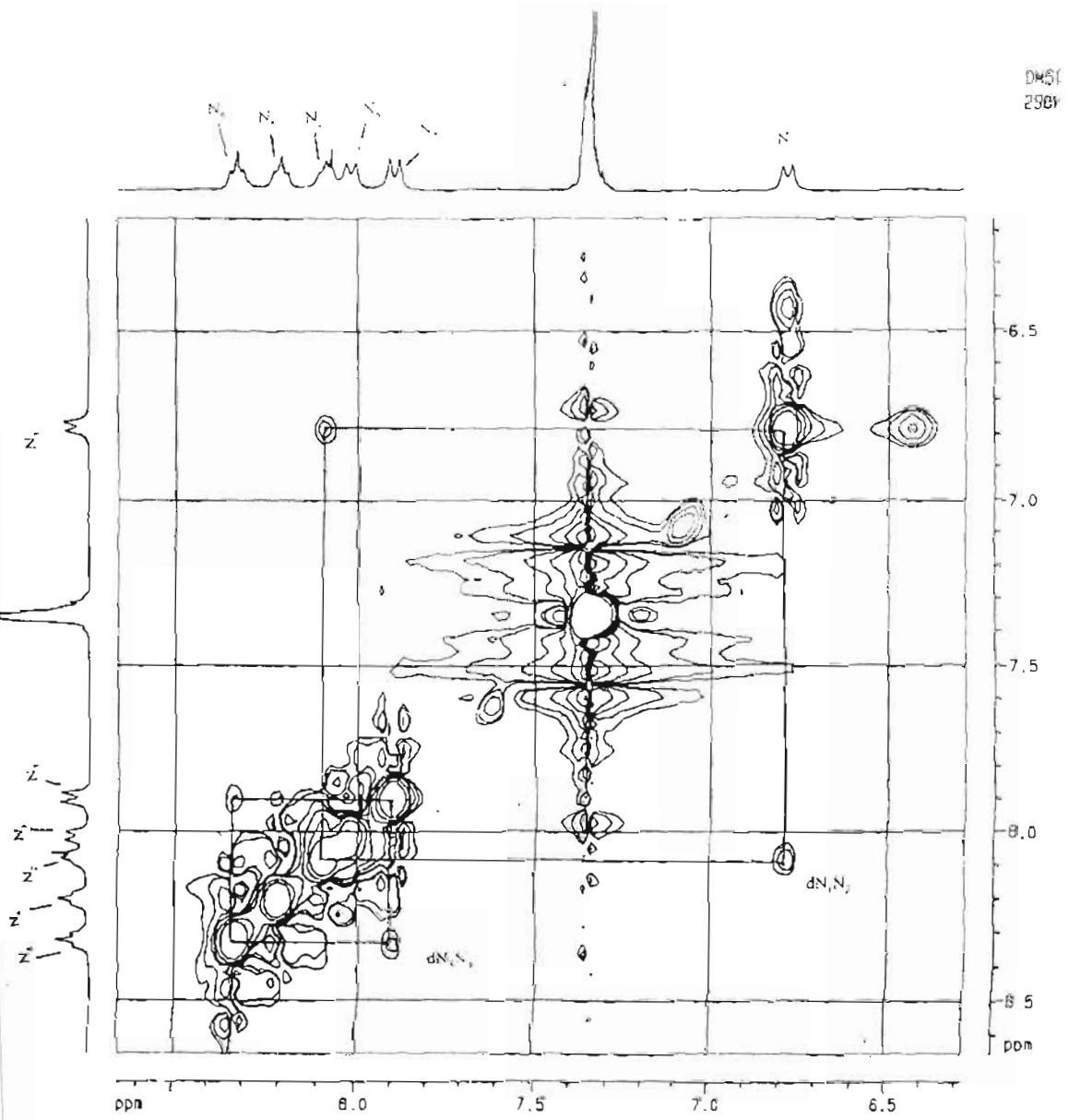

ROESY spectra of the hexapeptide (**46**). dN,N cross peaks are shown. N_i designates the proton connected to the amide nitrogen of the i^{th} amino acid residue.

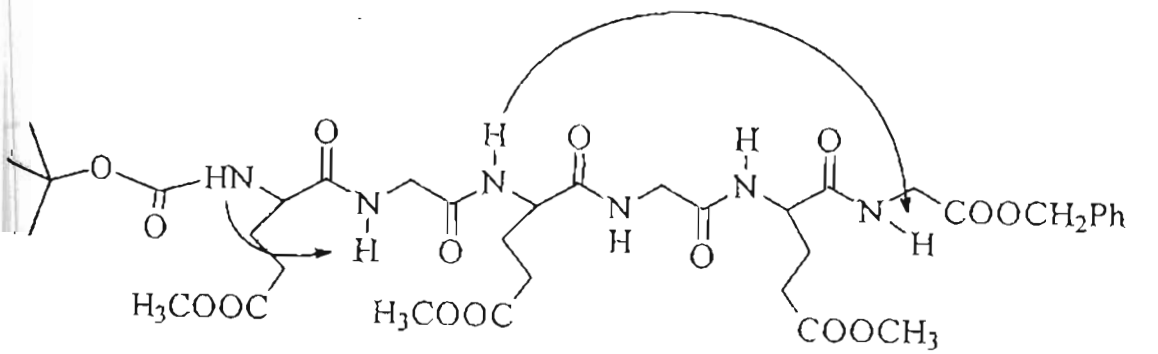

46

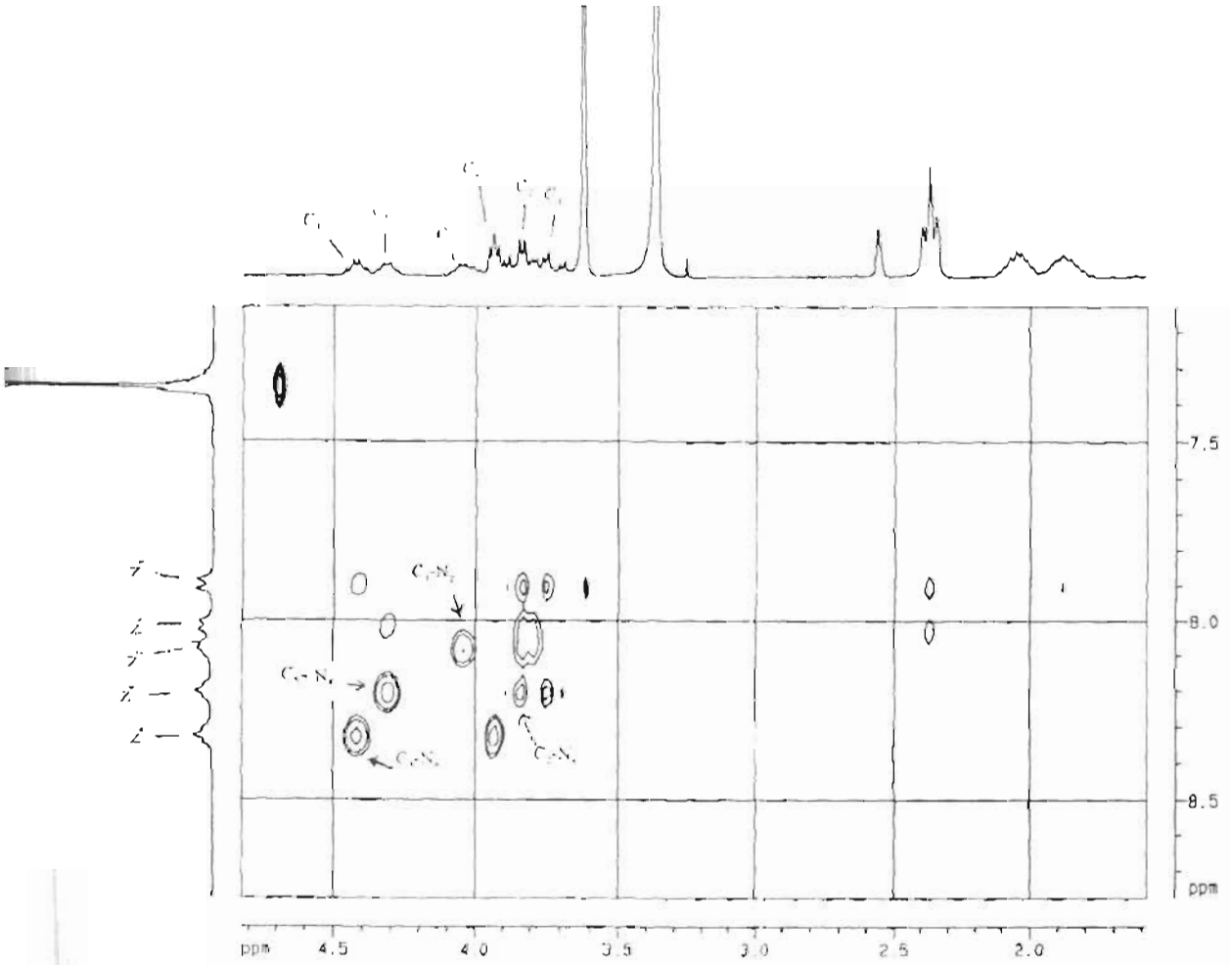

ROESY spectra of the hexapeptide (**46**) N_i and C_i designates the proton connected to the amide nitrogen or Cα respectively of the i^{th} amino acid residue

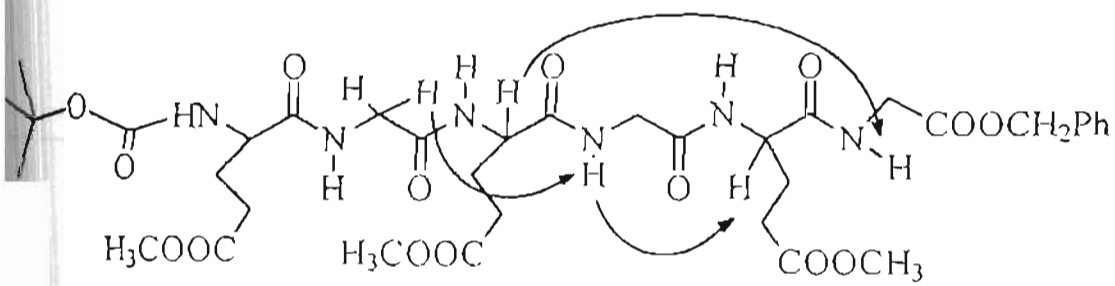

46

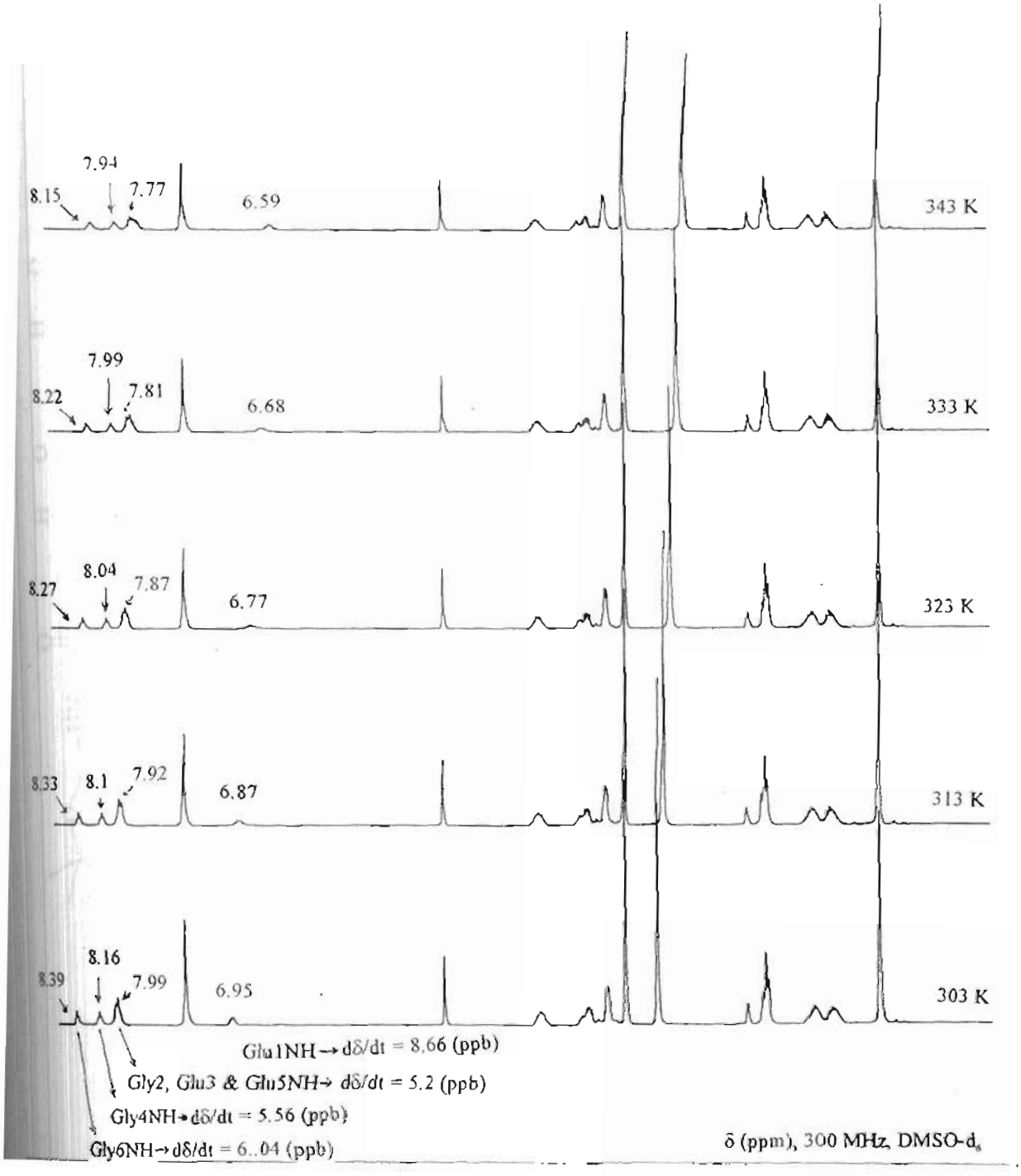

Variable temperature NMR plots of the hexapeptide (46)

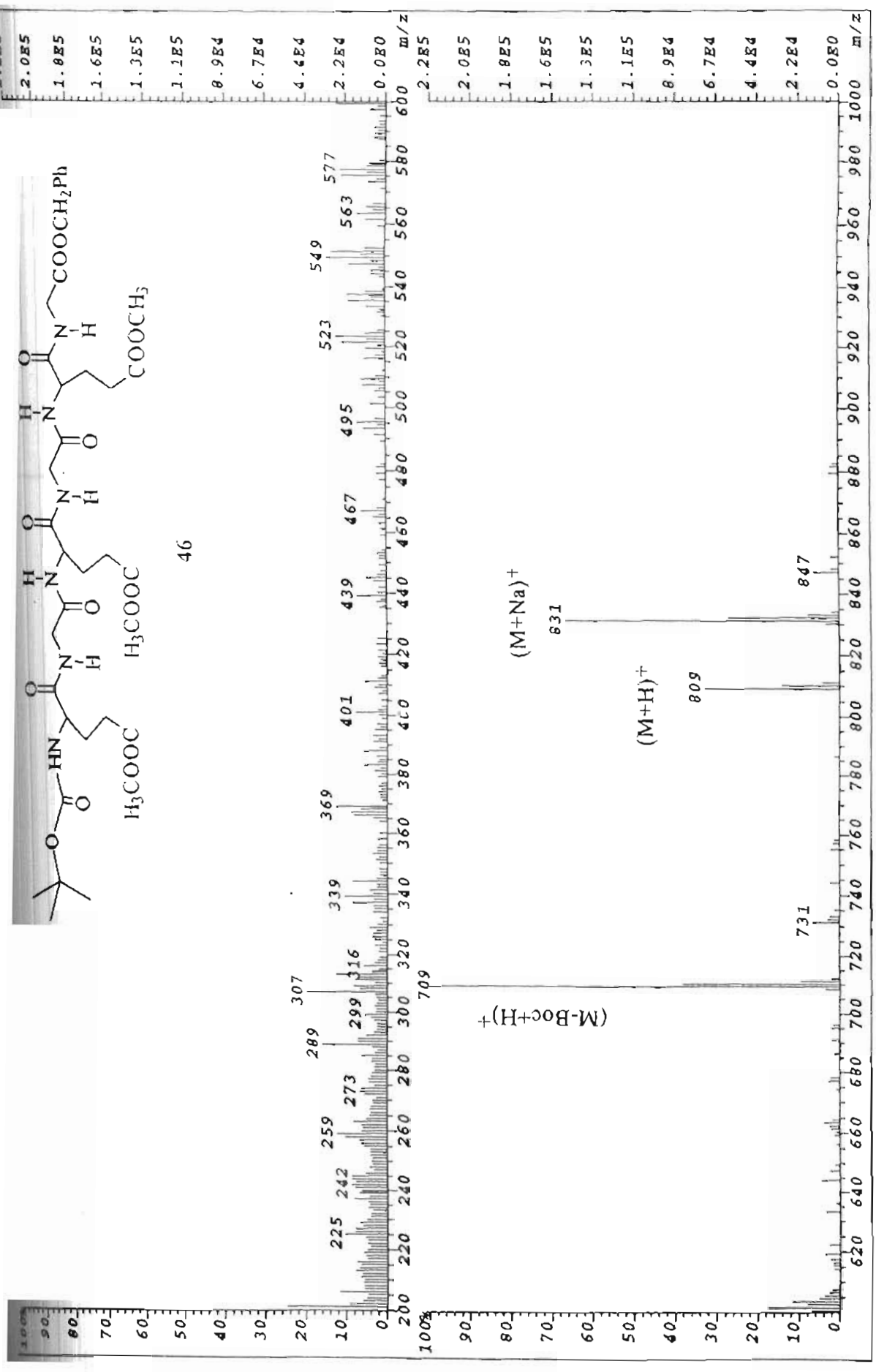

FAB mass spectrum

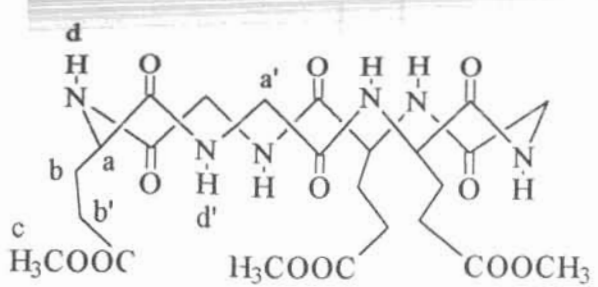

δ (600 MHz, DMSO-d 6)

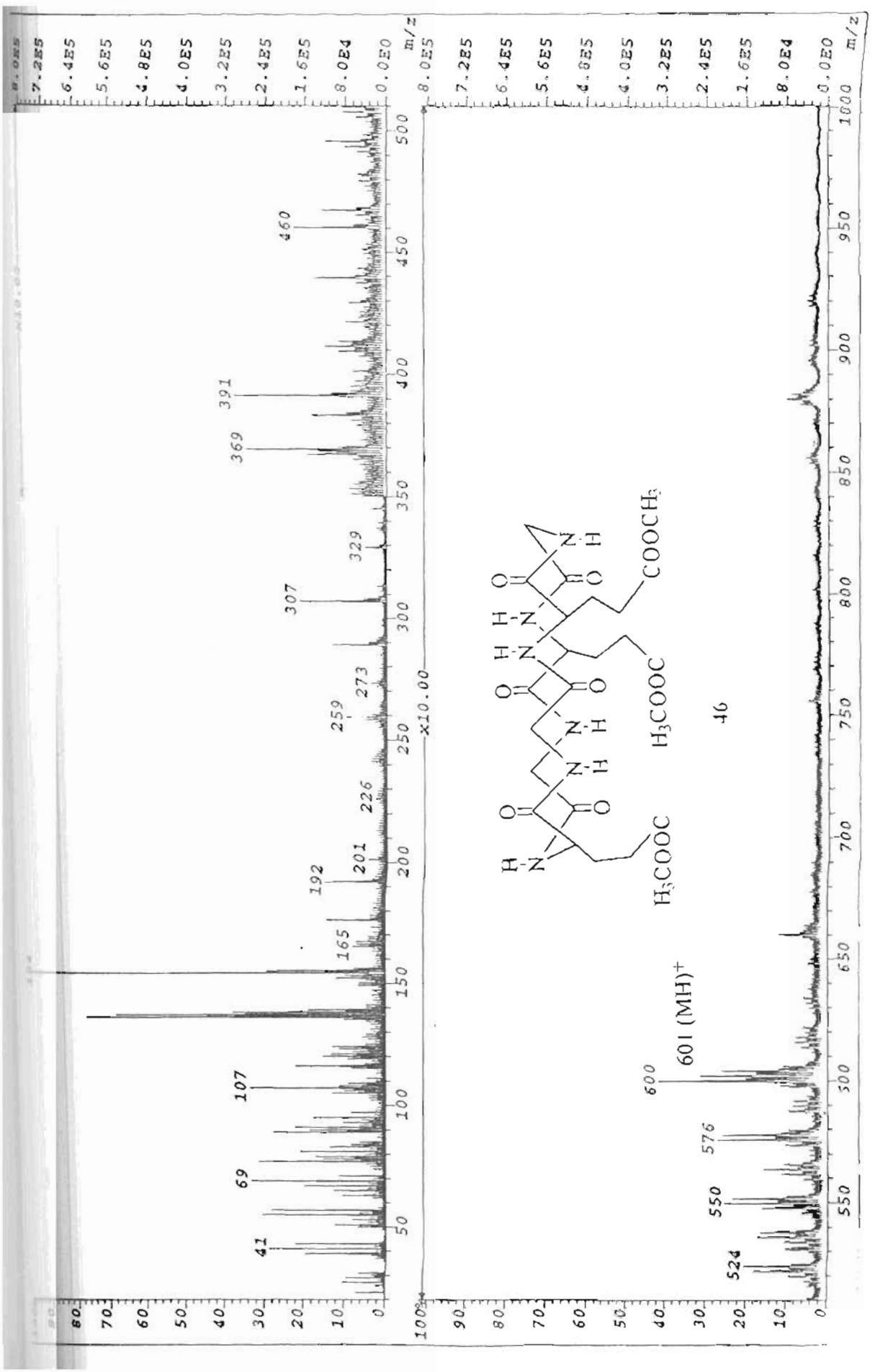

FAB mass spectrum

I.G. REFERENCES

1) G. R. Desiraju, *Angew. Chem. Int. Ed. Engl.*, **1995**, 34, 2311-2327.

2) G. M. Whitesides, E. M. Simanek, J. P. Mathias, C. T. Seto, D. N. Chin, M. Mammen and D. M. Gordon, *Acc. Chem. Res.*, **1995**, 28, 37-44.

3) a) R. Wyler, J. de Mendoza and J. Rebek Jr., *Angew. Chem. Int. Ed. Engl.*, **1993**, 32, 12, 1699-1701. b) N. Branda, R. Wyler, J. Rebek Jr., *Science*, **1994**,263,1267-1268. c) R. S. Meissner, J. Rebek Jr., J. de Mendoza, *Science*, **1995**, 270, 1485-1488.

4) a) M. R. Ghadiri, J. R. Granja, R. A. Milligan, D. E. McRee and N. Khazanovich, *Nature*, **1993**, 366, 324-327, b) M. R. Ghadiri, J. R. Granja and L. K. Buehler, *Nature*, **1994**, 369, 301-304. c) R. Granja and M. R. Ghadiri, *J. Am. Chem. Soc.*, **1994**, 116, 10785-10786. d) J. D. Hartgerink, J. R. Granja, R. A. Milligan and M. R. Ghadiri, *J. Am. Chem. Soc.*, **1996**, 118, 43-50. e) H. S. Kim, J. D. Hartgerink and M. R. Ghadiri, *J. Am. Chem. Soc.*, **1998**, 120, 4417-4424. f) K. S. Akerfeldt, J. D. Lear, Z. R. Wasserman, L. A. Chung and W. F. DEGrado, *Acc. Chem. Res.*, **1993**, 26, 191-197

5) D. Ranganathan, C. Lakshmi and I. L. Karle, *J. Am. Chem. Soc.*, **1999**,

J. J. Wolff, F. Gredel, T. Oeser, H. Irngartinger and H. Pritzkow, *Chem. Eur. J.*, **1999**, 5, 1, 29-38.

H. H. Cady and A. C Larson, *Acta.Cryst.*, **1965**, 18, 485-496.

K. B Borisenko, K. Zauer and I. Hargittai, *J. Phys. Chem.*, **1995**, 99, 13808-13813.

S. R. Byrn, D. Y. Curtin and I. C. Paul, *J. Am. Chem. Soc.*, **1972**, 94, 3, 890-898.

A. Kraft and R. Frohlich, *J. Chem Soc. Chem. Commun.*, **1998**, 1085-1086.

a) C. B. Aakeroy, D. P. Hughes and M. Nieuwenhuyzen, *J. Am. Chem. Soc.*, **1996**, 118, 10134-10140. b) S. Coe, J. J Kane, T. L. Nguyen, L. M. Toledo, E. Wininger, F. W. Fowler and J. W. Lauher, *J. Am. Chem. Soc.*, **1997**, 119, 86-93. c) J. C. MacDonald and G. M. Whitesides, *Chem. Rev.*, **1994**, 94, 2383-2420. d) X. Cheng, Q. Gao and R. D. Smith, *J. Org. Chem.*, **1996**, 61, 2204-2206. e) J. P. Mathias, E. E. Simanek and G. M. Whitesides, *J. Am. Chem. Soc.*, **1994**, 116, 4326-4340.

G. DE With and S. Harkema, *Acta. Cryst.*, **1977**, B33, 2367-2372

D. S. Lawrence, T. Jiang and M. Levett, *Chem. Rev.*, **1995**, 95, 2229-2260.

14) N. Kimizuka, T. Kawasaki, K. Hirata and T. Kunitake, *J. Am. Chem. Soc.*, 1998, 120, 4094-4104.

15) Chia-Yu Huang, L. A. Cabell and E. V. Anslyn, *J. Am. Chem. Soc.*, **1994**, 116, 2778-2792.

16) O. M. Yaghi, H. Li and T. L. Groy, *J. Am. Chem. Soc.*, **1996**, 118, 9096-9101.

17) S. J. Geib, C. Vicent, E. Fan and A. D. Hamilton, *Angew. Chem. Int. Ed. Engl.*, **1993**, 32, 1, 119-121.

18) J. A. Zerkowski, J. C. MacDonald, C. T. Seto, D. A. Wierda and G. M Whitesides, *J. Am. Chem. Soc.*, **1994**, 116, 2382- 2391.

19) a) F.M. Brodsky, *Science*, **1988**, 242, 1396 - 1402. b) G. S. Payne, *J. Membrane Biol.*, **1990**, 116, 93 - 105. c) J. H. Keen, *Annu. Rev. Biochem.* **1990**, 59, 415 - 438. d) E. Ungewickell, *Current Biol* , **1999**, 9, 1, R32 - 35.

20) J. G. Krause, S. Kwon, and B. George, *J. Org. Chem.*, **1972**, 37, 12, 2040 - 2042.

21) H. D. K. Drew and H. H. Hatt, *J. Chem. Soc.*, **1937**, 16 - 26

22) *J. Chem. Soc., Perkin Trans. 1* , **1996**, pp 1542

23) CA. 50: 4848b, *Compt. rend.* **1955**, 240. 2324 - 6.

24) a) R. Mayer, *Chem Ber*, 1956, **89**, 1443. b) F. Petru and V.Galik, *Chem Listy*.1957, **51**, 2371.

25) T. J. Katz, and W. Slusarek, *J. Am. Chem. Soc.*, **1980**. 102, 3, 1058 - 1063.

26) S. Ranganathan, K. M. Muraleedharan, D. Bhattacharya, and D. Kundu, *J. Indian. Chem. Soc.*, **1998**, 75, 10 - 12, 583 - 589. and references therein.

27) S. Ranganathan, K. M. Muraleedharan, P. Bharadwaj, and K. P. Madhusudanan, *J. Chem. Soc. Chem. Commun.*, **1998**, 2239 - 2240.

28) a) P. Braquet, *Ginkgolides-Chemistry, Biology, Pharmacology and Clinical Perspectives*, J. R. Prous Science Publishers, Barcelona, **1988**, vol. 1, p.xv. b) E. J. Corey, A. Y. Gavai, *Tetrahedron Lett.*, **1989**, 30, 6959. c) E. J. Corey, M.-C. Kang, M. C. Desai, A. K. Ghosh and I. N. Houpis, *J. Am, Chem. Soc.*,**1988**, 110, 649. d) D. Luca and P. Magnus, *J. Chem. SocPerkin. Trans 1*, **1991**, 2661.

29) CA. 52: 6299c; *Chem. listy.*, **1957**, 51, 2371 - 2373.

30) a) E. R. Boyko, and P. A. Vaughan, *Acta. Cryst.*, **1964**, 17, 152 - 158. b) H. Meier, Eu. Muller, and H. Suhr, *Tetrahedron*, **1967**, 23, 3713 - 3721. c) V. H. Meir, J. Heiss, H. Suhr, and Eu. Muller, *Tetrahedron*, **1968**, 24, 2307 - 2325. d) E. Heilbronner, B. Kovac, W. Nutakul, A. D. Taggart, and R. P. Thummel, *J. Org. Chem.*, **1981**, 46, 5279 - 5284. e) J. S. Siegel,

Angew. Chem. Int. Ed. Engl., **1994**, 33, 17, 1721 - 1723. f) H. B. Burgi, K. K. Baldridge, K. Hardcastle, N. L. Frank, P. Gantzel, J. S. Siegel, and J. Ziller, *Angew. Chem. Int. Ed. Engl.*, **1995**, 34, 13/14, 1454 - 1456. g) R. Durr, O. D. Lucchi, S. Cossu, and V. Lucchini, *J. Chem. Soc. Chem. Commun.*, **1996**, 2447 - 2448. h) A. Stanger, N. Ashkenazi, R. Boese, D. Blaser, and P. Stellberg, *Chem. Eur. J.*, **1997**, 3, 2, 208 - 211.

31) a) R. Neidlein, S. Throm, *Arch. Pharm. (weinheim, Ger.)*, **1980**, 313, 572. b) Von. R. Neidlein, A. Bischer and W. Kramer, *Helvetica chemica acta.*, **1990**, 73, 8, 2147 - 2156.

32) L. R. Kelland, G. Abel, M. J. McKeage, M. Jones, P. M. Goddard, M. Valenti, B. A. Murrer and K. R. Harrap, *Cancer Res.*, **1993**, 53, 2581 - 86.

PART II.

MOLECULAR DISASSEMBLY BY ZINC EJECTION AS A STRATEGY AGAINST HIV MATURATION: A MODEL STUDY

II.A. INTRODUCTION

The metal promoted self assembly of ligands, described in the previous section, forms a continuity to endeavours described here[II.C].

In general, assembly and dis-assembly are integrated in biological systems to bring about a specific function, such as endocytosis, described previously. In events promoted by metal ions, this would mean an exchange process, controlled by kinetic and thermodynamic factors. Since ligand dispositions are linked to the oxidation states of metal ions, only those ions that are redox inactive can play such a role, that is, in assembly and dis assembly that requires invariance in ligand distributions. Zn^{II} Ions with a d^{10} profile and having an invariant tetrahedral valency have been found, in recent years, to play a pivotal role in several critical biological processes, which involve the crucial ligand metal exchange process.

The work described in this section, complements and completes studies of biological systems that operate on an association $\rightleftharpoons$ dissociation mechanism. As stated in II.B. The [CCXX] boxes present in proteins are ideal for the study of the above reversible process, by thiol $\rightleftharpoons$ disulfide exchange mechanisms. A search for such [CCXX] boxes in proteins brought to light, the very recent reports pertaining to the inactivation of the HIV virus by removal of zinc from two [CCXX] boxes present in one of the constituent proteins NCp7, by exchange with redox systems of the type Ar-S-S-Ar. This suggested that redox coupled designs can be very effective in zinc removal from key pervasive enzymes, thus making them ineffective.

The above notion has been studied and substantiated. The basic Ar-S-S-Ar system was modified to bring additional stabilization of the transition state relating to the key thiol⇌disulfide process. This was done by the preparation of a series of Ar-S-S-Ar composites with a wide range of proteinous amino acids [coded amino acids] and tethered systems. The ability to remove zinc was then tested on RNA polymerase enzyme, an $\alpha\alpha\beta\beta\sigma$ composite, universally involved in all transcription processes and having two zinc atoms harbored in [CCXX] boxes present in each in the β and β segments. The consequences of zinc removal from this enzyme, as a function of the inhibition of the trancription of calf thymus DNA was monitored. Excellent inhibition was observed with several of the compounds prepared.

The present work has shown, for the first time ever, that enzymes having zinc in their [CCXX] boxes can be deactivated by redox composites having suitable ligands.

II.B. BACKGROUND

Metal ions serve a variety of functions in proteins, the important ones of which are to enhance the structural stability of the protein conformation required for biological functions and to take part in the catalytic processes of enzymes. Metal ions can activate chemical bonds and make them more amenable to reactions.They can take part in control mechanisms by specifically altering or stabilizing macromolecular conformations on binding. Metal ions can also take part in redox reactions.

Zinc and Zinc Fingers:

Amongst the first row of transition metals, zinc is second only to iron in terms of abundance and importance in biological systems. As a d^{10} metal ion, Zn^{2+} is not susceptible to ligand field stabilization effects, nor does it exhibit biologically relevant redox reactivity. Nevertheless, the co-ordination chemistry of zinc is as versatile as the metal ion functions in biology, and this is governed to a great degree by the metal ligands.

The ionic radius of Zn^{2+} is 0.74A°, compared to 0.64A° for Ca^{2+}, 0.65A° for Mg^{2+} and 0.53A° for Fe^{3+} and has borderline hardness.[1] Hence, unlike calcium and magnesium, zinc likes to be co-ordinated by the relatively soft donor functions in a protein environment such as cysteine thiolate and histidine

imidazole and exhibit variation in number, charge, structure and amino acid composition, depending on the structural, catalytic, or regulatory role.

Interest in zinc as an integral part of small protein domains began in 1985 with the discovery of the classical zinc finger motif - a 30 amino acid sequence motif in the protein transcription factor IIIA from the toad *xenopus laevis*. This zinc finger motif is defined by two cysteine and two histidine residues that ligate a zinc ion (arranged: Cys X_{2-4} Cys X_{12} $HisX_{3-5}$ His, where X represents any amino acid) and three conserved hydrophobic residues (Fig II.B.1)

The repeated nature of this motif is a feature common to all proteins containing classical zinc fingers, but the number of repeats varies widely among the proteins ranging from 2 (the *Drosophila* protein Tramtrack) to 37 (the *Xenopus* protein xfin). Since these motifs have been observed in a very large number of eukaryotic protein sequences, the zinc finger appears to be a wide spread structural motif for nucleic acid recognition. GAL4, GATA-1, Nucleocapsid, Hormone (Oestrogen) receptor, Carbonic anhydrase (Carbonic dehydratase) II, Carboxy peptidase A and Metallothionein are few examples of zinc finger proteins Fig II.B.2 - 6 shows the structures of zinc finger domains in few enzymes, solved by NMR and/or crystallographic data.[2]

To date, more than 200 different cDNA sequences have been found to encode zinc finger motifs, amounting to more than 1200 individual zinc fingers.

Indeed, it has been estimated that between 300 and 700 human genes (nearly 1% of the human genome) encode zinc finger containing proteins.

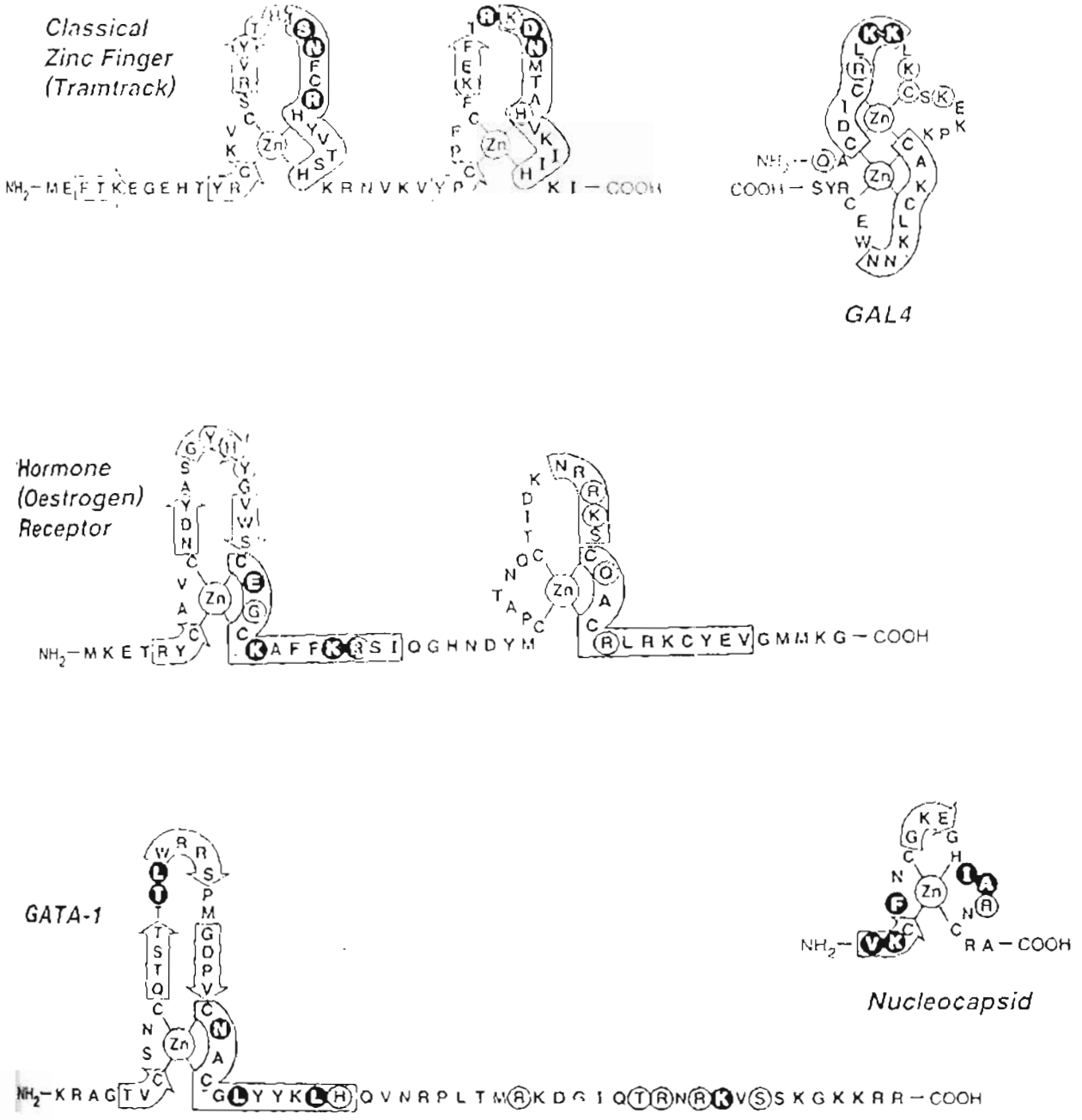

Fig. I.B.1. Classes of zinc containing DNA-binding motif, showing the pattern of zinc co-ordination. The protein sequence is indicated by the one-letter code. Shaded regions fold to form α helices. Arrows indicate β-strands. Residues that contact DNA are circled (phosphate contacts in white; base contacts in black)

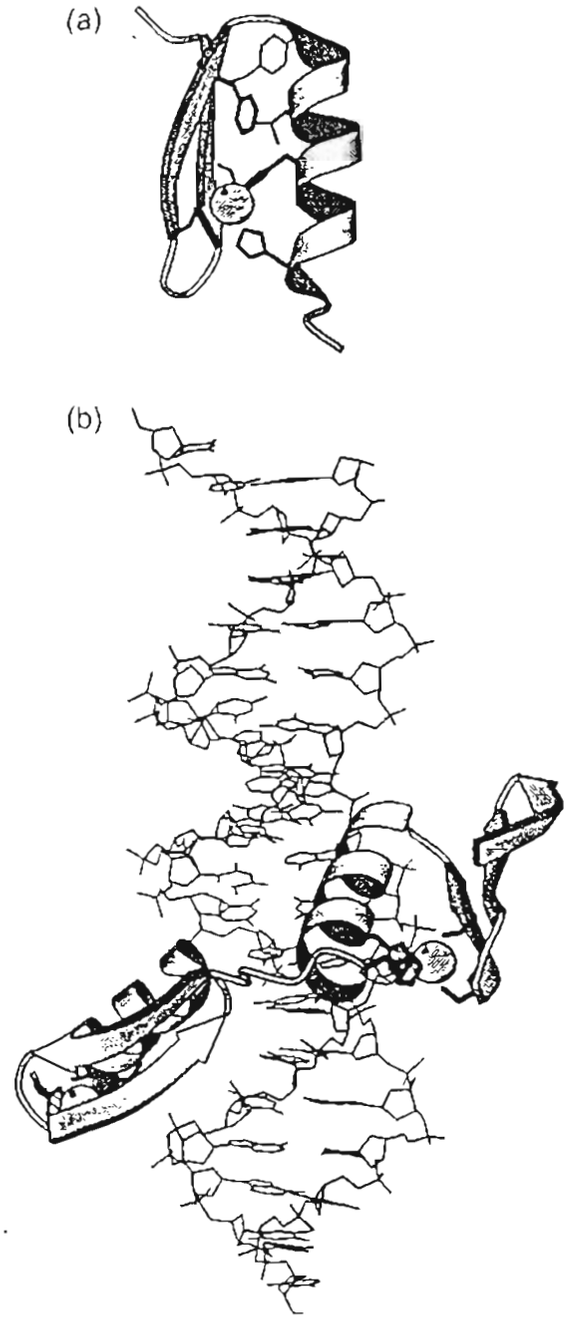

Fig. II.B.2. a) The solution structure determined by NMR spectroscopy, of the second of three classical zinc finger motifs in the yeast transcription factor SW15. The zinc ions and ligands are shown. [D. Neuhaus et. al, *J. Mol. Biol.* 1992, 228, 637 - 651]. b) The crystal structure of the two classical zinc finger motifs of the fruit fly transcription factor Tramtrack in complex with DNA. [L. Fairall et. al, *Nature*, 1993, 366, 483 - 487]

Fig. II.B.3 The structure of the zinc finger domain of the *Xenopus* Xfin protein, as determined by solution NMR methods [Le et. al, *Science*, 1989, 245, 635 - 637]

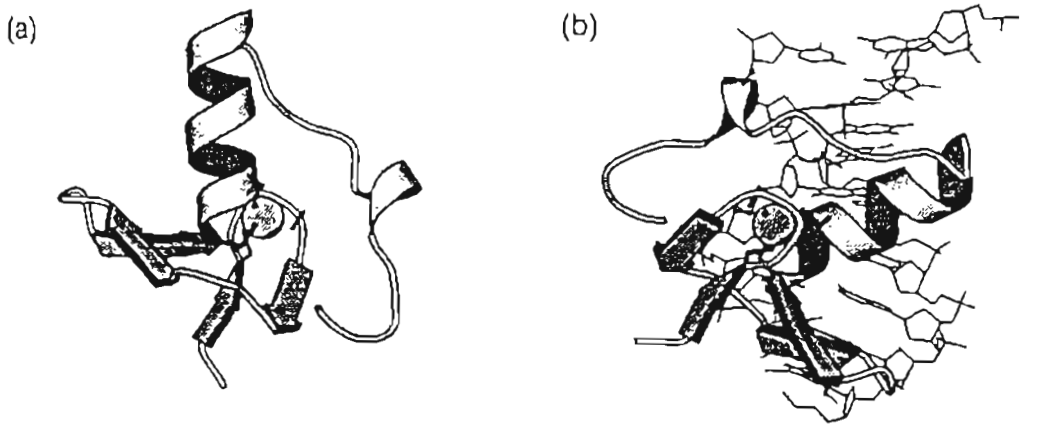

Fig. II.B.4. a) The structure of the DNA-binding domain of GATA-1 taken from b) the NMR structure of the domain complexed with DNA [J. G. Omichinski et. al, *Science*, 1993, 261, 438 - 446]

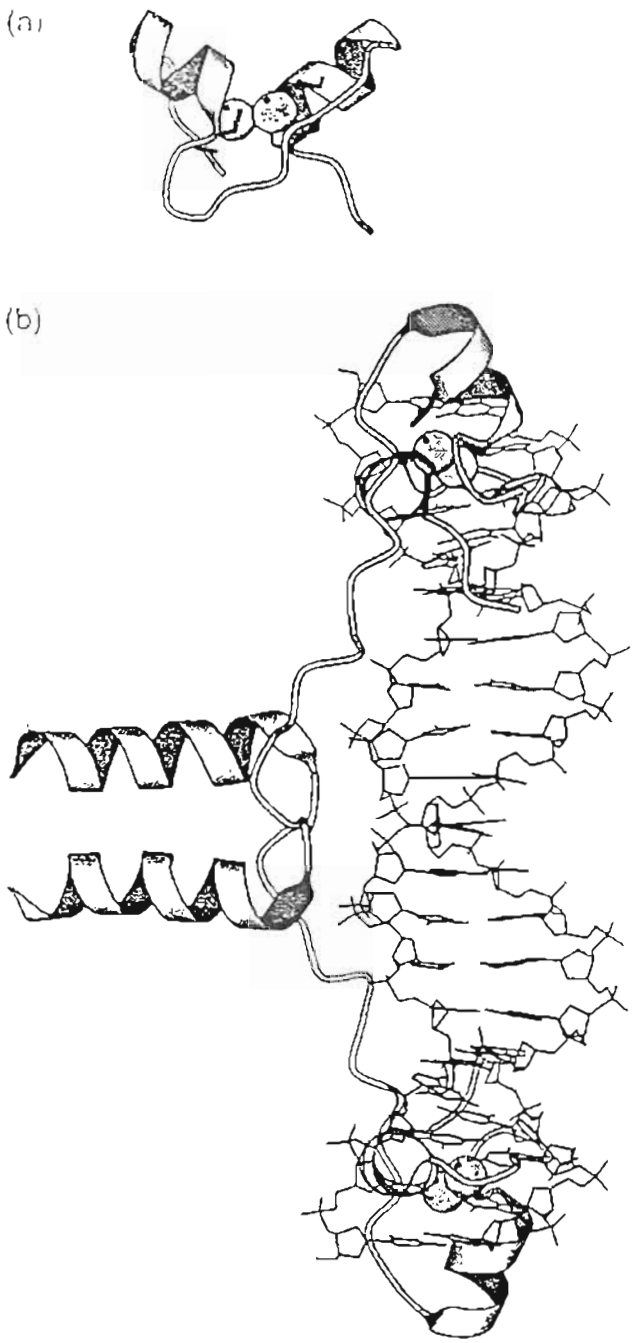

Fig. II.B.5. Crystal structures of a) the cysteine-rich DNA-binding module of the yeast transcription factor GAL4, showing the zinc ions and ligands, and b) a dimer of the complete DNA-binding domain from the yeast transcription factor GAL4 in complex with DNA [R. Marmorstein et. al, *Nature*, 1992, 356, 408 - 414]

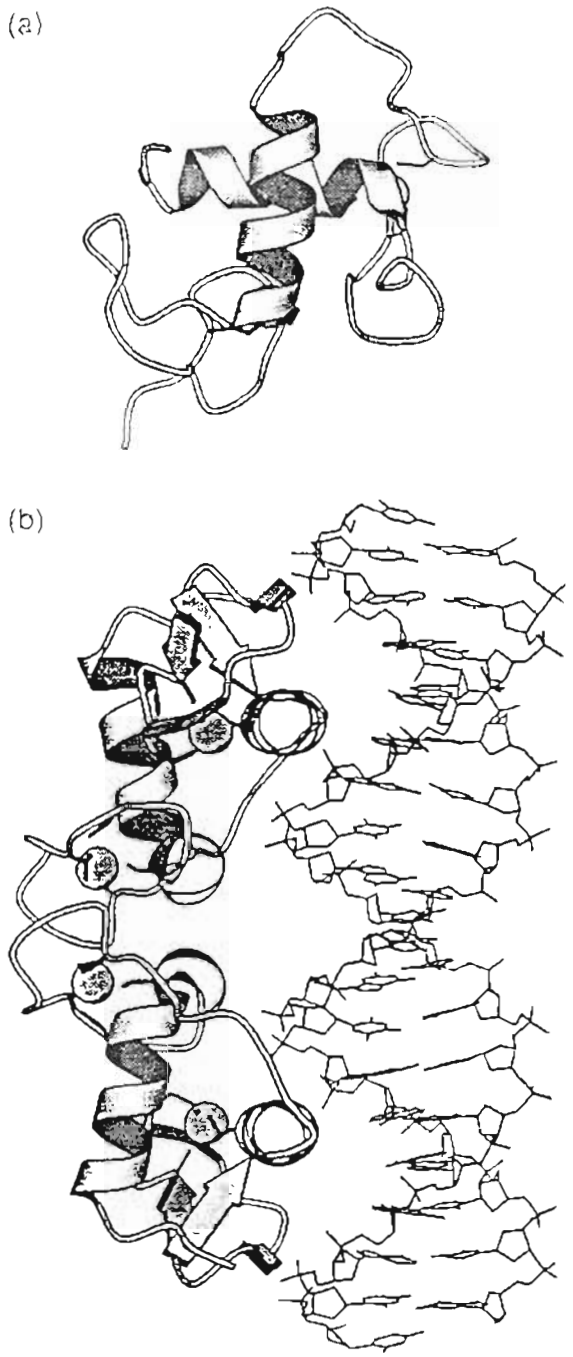

Fig. II.B.6. a) The solution structure determined by NMR spectroscopy, of the DNA-binding domain from the human estrogen receptor containing two class II zinc-binding motifs that are folded to form a single structural unit. [J. W. R. Schwabe et. al, *Nature*, 1990, 348, 458 - 461]. b) The crystal structure of a dimer of the DNA-binding domain from the human estrogen receptor in complex with DNA [J. W. R. Schwabe et al, *Cell*, 1993, 75, 567 - 578]

Engineering of zinc finger domains.

Given the *ubiquitous occurrence of zinc in biological systems, it* immediately follows as to how the engineering of a metal binding site or removal of a metal ion from the active site, could be used as a tool in the design of structurally and functionally modified proteins.

The extensive information available pertaining to zinc fingers has made the possibility of the detection of CCHH, CCCH, CCCC [C = Cysteine; H = Histidine] boxes in proteins or their genomic precursors and then transfer them to zinc binding domains for protein modification. The power of this approach is illustrated in Fig. II.B.7.[3] The metal free finger peptide (a) is chemically modified with a fluorophore. In this situation, the fluorophore is in a polar environment, involving minimum emission. On addition of zinc, the zinc finger is instantly constituted (b) using the [CCHH] box. This brings the helix close to the β sheet and here the fluorophore is in a nonpolar environment, resulting in a great enhancement of fluorescence emission. The method has been used to detect Zn^{2+} at concentrations less than 10^{-6} M. This discovery is significant since the Zn^{2+} is unresponsive to the usual methods of analysis like spectroscopy and redox monitoring. The process is reversible.

Zinc finger motifs could find application in the design of folded protein structures. This has been elegantly demonstrated by the folded design shown in Fig. II.B.8 of immunoglobulin by insertion of Zn in a [HHHC] box[4].

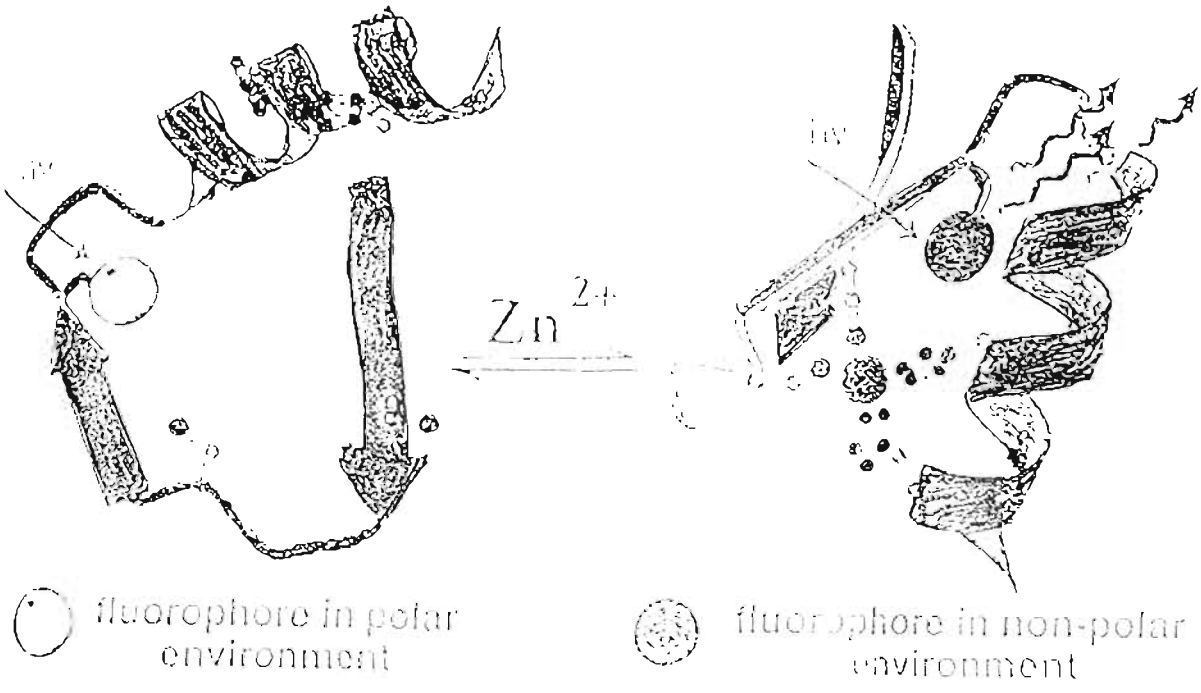

Fig. II.B.7.

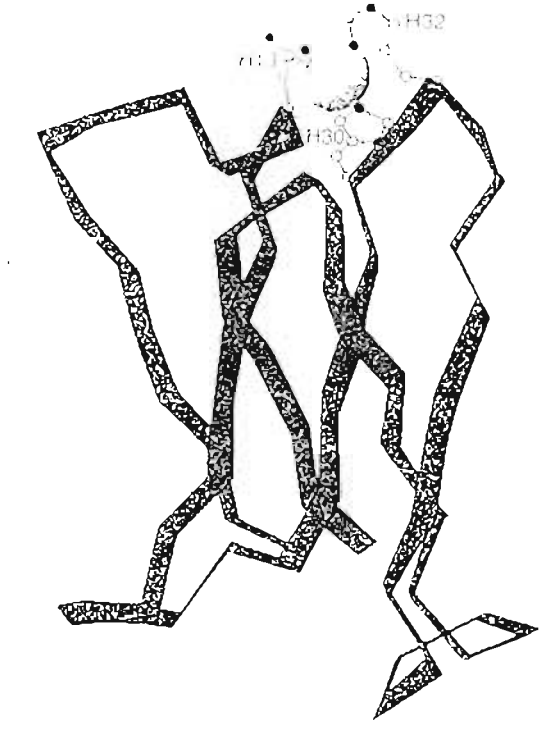

Fig. II.B.8.

The hormone insulin contains 3 disulfide bridges and two histidines. Endeavours to inscribe a zinc finger moiety in insulin has led to the presence of the finger using the B chain alone.[5]

Of direct relevance to the present work is the nucleocapsid protein, harboring two zinc finger motifs which play a pivotal role in the packaging of the AIDS virion.[6] Two [CCHC] domains are contained in HIV-1 p7 nucleocapsid protein (NCp7), which is a maturational proteolytic product of the Pr 55^{gag} precursor polyprotein. Interestingly, the [CCHC] motif is conserved in all onco and lenti retroviruses. While, still a part of the Pr 55^{gag} (GAG) precursor, the fingers function in selection and packaging of viral RNA in to budding virions After the p7 NC protein is fully processed from the gag precursor in the mature viruses, the fingers are required for completion of reverse transcription during the initial injection of target cells. Thus here, the highly conserved [CCHC] box performs essential roles in multiple phases of the HIV-1 replication cycle, which makes it an attractive target in AIDS chemotherapy.

In the last few years, agents that can efficiently remove zinc from the finger domains have been explored from this vantage.[6] In the present work, a series of dithio benzamides have been prepared as agents for the removal of zinc by exchange interaction. These are described in the next section.

RNA Polymerase - Structure and Function

Gene therapy, being one of the important medicinal tools envisaged for the 21st century, necessitates the development of compounds that can interfere with information-function system at various levels. Such compounds are believed to be effective in the treatment of various hereditary diseases, where the selective switching on or off of a gene can rectify the genetic abnormality. Since this part of the thesis deals with the inhibition studies on RNA polymerase, the key enzyme involved in gene expression, a brief outline on its structure and function is appropriate, which is given below.

Gene expression involves the sequential transfer of genetic information encoded as the sequences of the triplet codons on DNA to the 20 letter alphabets of amino acids, through the intermediacy of RNA. Transcription - the first and the foremost event in these processes, involves the synthesis of an RNA molecule complementary to a selected segment of DNA, and is catalyzed by the enzyme called DNA dependent RNA polymerase or RNA polymerase.[7] Transcription is undertaken exclusively by RNA polymerase, but not indiscriminately by the enzyme; other proteins like activators and repressors, whose function is to regulate transcription, determines whether a particular gene available to be transcribed or not.

The best characterized RNA polymerase are those of eubacteria, of which *li* is a typical case. It consist of four different kinds of sub units, namely α, and σ, *with molecular weights, 36512, 150619, 144162 and 70136 daltons* ectively.[8] The enzyme can exist in two distinct, but catalytically active forms ely core polymerase, having the sub unit composition $\alpha_2\beta\beta'$ and the oenzyme, which is the core polymerase associated with the σ factor (i.e. $\beta\beta'\sigma$). Although both these two forms are capable of catalyzing transcription, y holoenzyme can specifically bind and initiate transcription from promoters.[9] is the σ factor, which enables the holoenzyme to recognize and specifically nd to the promoters, compared to the non specific binding by the core olymerase.[10]

The DNA binding property of the polymerase is attributed to the β' ubunit because of its high affinity to DNA and other poly anions.[11] An additional rgument for this is the negative result that the sub assembly $\alpha_2\beta$ does not bind to NA in a filter binding assay, where as the corepolymerase ($\alpha_2\beta\beta'$) can bind to NA.[11] Moreover several bacterial mutants in which the RNA polymerase have impaired DNA binding contain altered β subunits, indicating the role of this subunit in DNA binding.[12] The β and β' subunits each contains an atom of bound zinc that plays both catalytic and structural roles in the enzyme. [13] Analysis of the

amino acid sequences of the enzyme subunits have indicated the presence of a DNA binding 'zinc finger' motif in β' [11].

II.C. PRESENT WORK

In the previous section, the use of metals to bring about molecular assembly was illustrated with gold. In recent times, the importance of metal ions in bringing about assembly is being increasingly recognized as an important strategy to control and regulate diverse processes. In biological systems, as was illustrated with clathrins, metal ions play an increasing role in the assembly. Assembly and disassembly are required in biological processes. Metals and metal ions can bring about these, in the sense that such metal complexes which brings about an assembly, can be disassembled by exchange processes

Amongst metals, zinc has been demonstrated to play a very vital role in biological reactions by virtue of the fact that zinc complexes are redox inactive and exhibit uniformly a tetrahedral disposition of valencies. Because of this, it has become possible to use this metal in non-covalent assembly and disassembly processes. Exploration of the role of zinc in biology, as was described in the previous section, mainly arose from the discovery of the zinc finger motif - modules having zinc in a dithiolate environment and having ~30 residues. Such fingers have been shown by X-ray crystallography to make direct contacts with code bases in the DNA, thereby playing a pivotal role in the initiation of transcription. Soon, the zinc finger concept was generalized and found application in diverse ways. Thus, close positioning of [CCXX] (X = Cys or His)

in protein sequences were predicted and proved to form zinc complexes which could be monitored by the resulting peptide - protein reorganization. Therefore, the reading frame of either a DNA or protein sequence can be used to identify such boxes and could be, with confidence, used as a design in molecular ordering. This aspect has been illustrated in the previous section. Exploration of these aspects in this laboratory have led to the preparation of minimal zinc finger motif and to highlight the importance of thiol $\rightleftarrows$ disulfide by exchange reactions in chemistry and biology.[15]

The genesis of the present work pertains to very recent reports on the fact that, in the maturation of HIV virus, a 55 residue protein called nucleocapsid protein (NCp7) plays a very important role in the proper packaging of the HIV RNA. Viral RNA, which provides all the information for its function can be packaged only if this protein is present. The sequence of this protein is presented in Chart II.C.1(A). The protein contains two zinc finger modules. Concerted efforts to remove zinc from these efficiently, led to identification of disulfides of the type B as useful agents to disrupt the NCp7 conformation by removal of the two zinc present, thus making the protein inoperative and there by the packaging of virions in the HIV virus very defective and dysfunctional.[16]

Several aspects of this was interesting from vantage described in the previous sections coupled with expertise available in this laboratory.

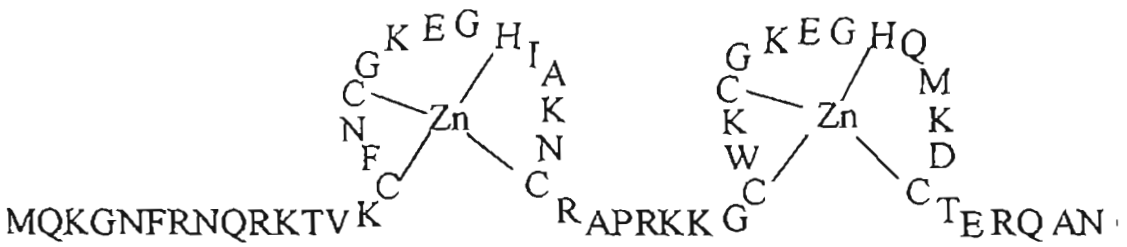

(A)

Amino acids are indicated by standard one letter codes.

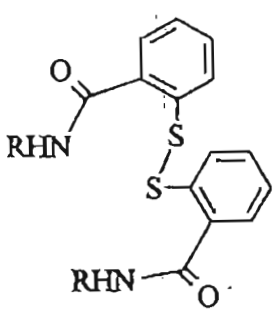

(B)

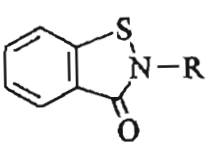

(C)

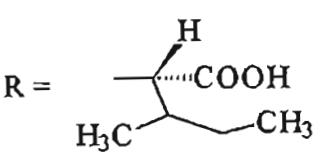

Chart II.C.1.

The efficiency with which zinc was removed from A by B (Chart II.C.1) strongly suggested exchange mechanisms as envisaged in Chart II.C.2, wherein compound B could react with an appropriate [CCXX] box present, to form the octahedral complex which could breakup, effecting an oxidation in the [CCXX] box with concomitant removal of B and its presence as a zinc complex. The rationalization of the overall processes in this manner brings to focus, the redox parity of the S-S system present in A and B. Therefore, it was considered desirable to prepare a series of compounds that are related to B and to study their efficiency in the removal of zinc from [CCXX] boxes present in key biological enzymes that harbour zinc.

We chose to design the redox up take systems present in compounds like B (Chart II.C.1) to link with diverse amino acid residues on the one hand and the zinc finger motifs on the other. This is an important factor in design, particularly when dealing with protein systems, that has not been recognized so far. It was envisaged that, in the removal of zinc from [CCXX] boxes by exchange processes involving compounds of the type B, the amino acid side chains could play a major role by stabilizing the transition state by interaction, with similar residues present in the zinc protein - enzyme. In the zinc finger domain, the importance of these interactions have been recognized in the function of the zinc finger motif. The efficiency with which zinc complexes can be prepared from a [CCXX] box made it interesting to generate these, in an exchange process

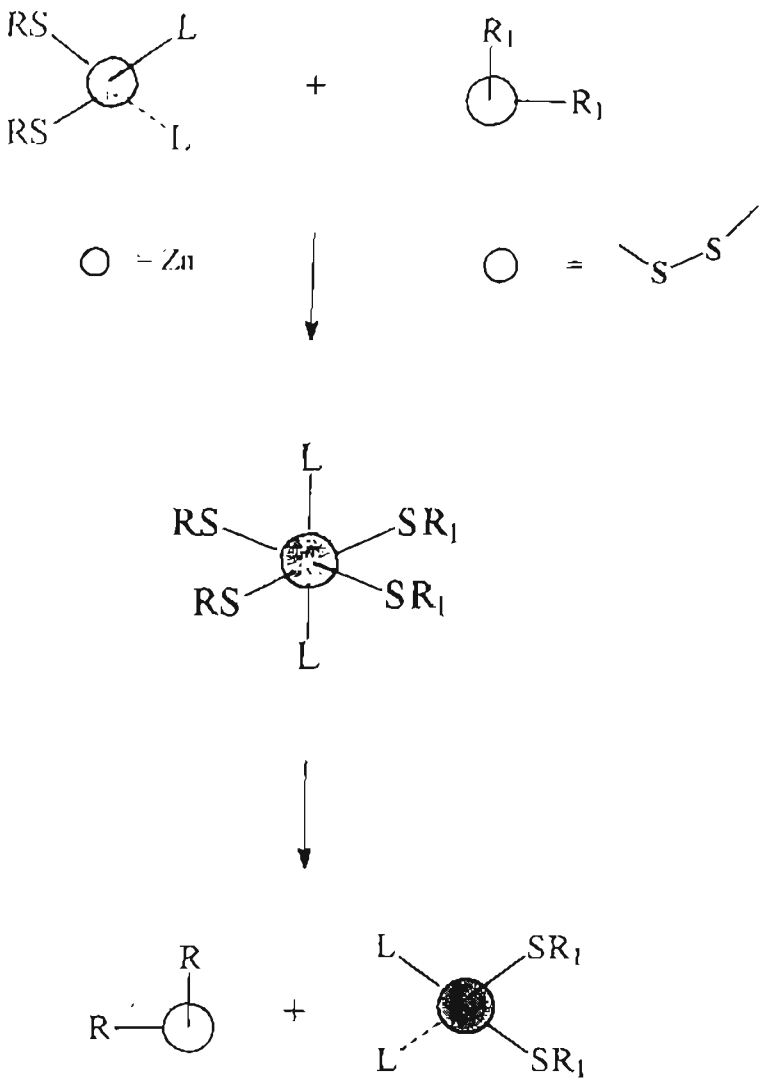

Chart II.C.2.

leading to minimalistic zinc finger motifs. This could be accomplished in principle by attachment of a histidine residue to the redox system shown in B, which could result in a [CCHH] box, that could very effectively harbour the zinc and the process, being energy facile could lead to the development of very efficient reagents to remove zinc from [CCXX] boxes present in proteins.

In the present work, the novelties incorporated in the design, was sought to be coupled with examination of its efficiency on an enzyme, which has a pervasive importance in all life systems. The enzyme, RNA polymerase was chosen by virtue of its role in the making of an RNA transcript from the genome, which would in turn be translated to the protein. The RNA polymerase activity of several systems have been shown to be a composite of four protein subunits, called α, β, β' & σ. The β and the β' units have been shown to posses one [CCXX] box each, that harbor zinc, possibly with the formation of two zinc fingers.[13] The presence of these units in their metal bound configurations is essential for the action of the composite enzyme RNA polymerase and are most likely related to the initiation of the transcription. In this sense, the generality of S-S redox systems, that can participate in exchange processes, as a strategy for the removal of zinc, could be of generalized importance when illustrated with RNA polymerase, since, the results from such studies would be of importance to

the application to other systems containing not only zinc ions in their [CCXX] boxes, but to other metal ions as well.

The redox system envisaged for exchange studies was the key disulfide flanked by two aromatic rings, to which appropriate ligands could be attached by means of the ortho carboxyl groups present (Chart II.C.1).

The required dithiobis-carboxylic acid (**1**) was prepared in excellent yields by the coupling of diazotized anthranilic acid with Na_2S_2 as reported[17]. The transformation of **1** to the 2,2'-dithiodibenzoyl chloride **2** was achieved by refluxing it in thionyl chloride for 24 h. The acid chloride thus prepared could be stored for further use under strict protection from moisture.

The coupling of **2** with aminoacid ligands shown in Charts II.C.3, II.C.4 and II.C.7 were accomplished by treatment with freshly prepared aminoacid methyl ester followed by purification of the product by column chromatography.

Thus, the methyl esters of Ala, Aib, Val, Pro, Phe and Met, afforded the expected bis-amides in yields respectively, **3** (25%), **4** (24%), **5** (63%), **6** (43%), **7** (36%), **8** (75%) (Chart II.C.3). The variation observed in the yields is largely attributed to purification procedures. The structural assignments for **3 - 8** have been fully supported by spectral and analytical data. Interestingly, the mass spectrum invariably exhibited peaks corresponding to MH^+ along with that corresponding to the uptake of one Na^+. An interesting and valuable observation

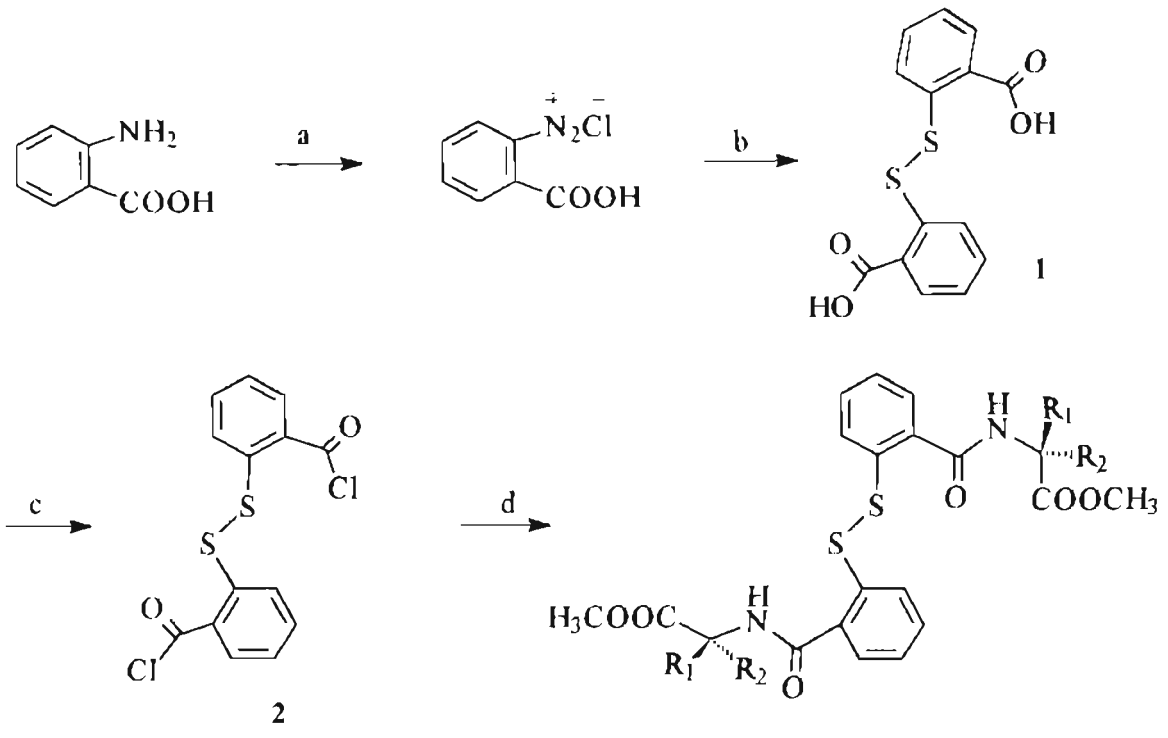

a) $NaNO_2$, HCl, 0 - 5°C, b) Na_2S_2, c) $SOCl_2$, reflux, d) H_2N-(AA)-$COOCH_3$, Et_3N

	R_1	R_2	AA	(%)
(3)	CH_3	H	Ala	25
(4)	CH_3	CH_3	Aib	24
(5)	$(CH_3)_2CH$	H	Val	63
(6)	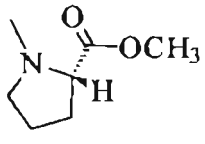		Pro	43
(7)	CH_2Ph	H	Phe	36
(8)	$CH_3SCH_2CH_2$	H	Met	75

Chart II.C.3.

was the presence of base peak in all these compounds corresponding to clean fragmentation around the S-S bond. The fact that these were actually generated in the mass spectrometer is evidenced by the fact that, they appeared uncomplexed with the proton as is always the case with parent ions.

Surprising results were obtained in all amino acids that have a proton source in the side chain. They afforded product arising from cleavage of the S-S bond, with concomitant participation of the peptide NH, resulting in the formation of isothiazolidene-3-ones. In the case of tyrosine and threonine, the normal bis products could also be obtained.

Thus, the reaction of TyrOMe and ThrOMe with the acid chloride **2**, followed by work up, resulted in the formation of, respectively, the bis-Tyr compound **10** (19%) and the Tyr-isothiazolidene-3-one **9** (29%), the bis-Thr compound **12** (31%) and the Thr-isothiazolidene-3-one **11** (59%) [Chart II.C.4].

The structural assignments for **9** - **12** are fully supported by spectral and analytical data. Having the bis-amino acid compounds as well as the isothiazolidene-3-ones arising from S-S cleavage at hand, it was possible to delineate the characteristic spectral features that could result in their identification. In their FAB mass spectrum, the bis compounds arising from tyrosine and threonine, **10** and **12**, afforded protonated mass peaks and those complexed with sodium ions. They invariably contained, as stated previously,

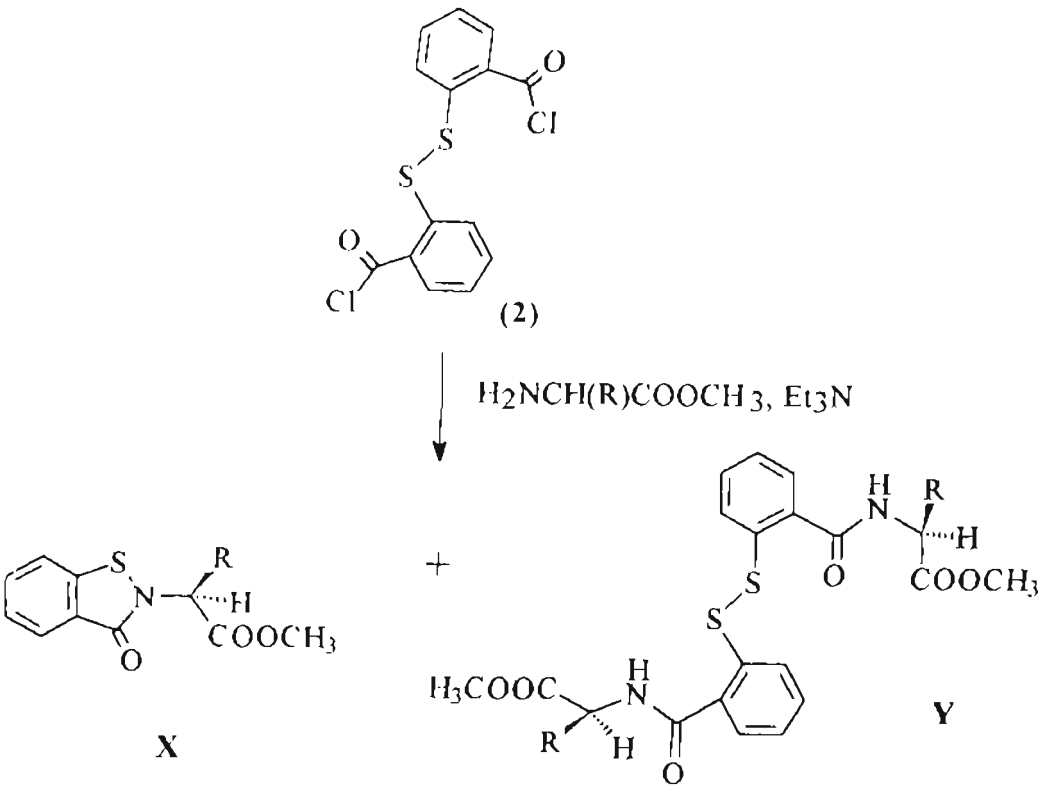

R	AA	X (%)	Y (%)
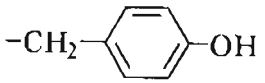	(Tyr)	**9** (29)	**10** (19)
$-CH(CH_3)OH$	(Thr)	**11** (59)	**12** (31)
$-CH_2OH$	(Ser)	**13** (41)	–
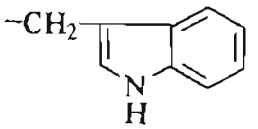	(Trp)	**14** (25)	–
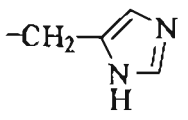	(His)	**15** (56)	–

Chart II.C.4.

base peaks corresponding to clean repture of the S-S bonds. In sharp contrast, the isothiazolidene-3-ones from these amino acids, namely, 9 and 11 gave peaks corresponding to the mass with a proton. A characteristic feature that distinguishes the bis-amino compounds from the isothiazolidene-3-ones is the appearance of the Cα proton, in the NMR spectrum. In the case of all bis-amino compounds, this proton appeared as a multiplet in the vicinity of 4.5 ppm, whereas the equivalent proton in the isothiazolidene-3-ones invariably appeared significantly down shifted by ~1 ppm to appear in the clear region in the NMR, corresponding to ~5.5 ppm. This factor could unambiguously distinguish the bis-amino compounds from isothiazolidene-3-ones. The isolation of the isothiazolidene-3-ones 9 and 11 is significant in the sense that although the formation of such compounds have been speculated in the fragmentation of the dithia compounds of the type described here (Chart II.C.1,C), they have never been isolated pure and completely characterized. Further, it is considered that the formation of systems like these would involve a nucleophilic attack by the amide nitrogen on the dithia bonds, resulting in the S-S cleavage to isothiazolidene-3-one on the one hand and the corresponding -SH compound on the other. This mechanism would envisage loss of 50% of the starting compound. The fact that, in the case of threonine, not only the isothiazolidene-3-one was secured in 59%, but also, the bis-threonine compound was isolated in 31%, would require a

revision of this mechanistic proposition. It is proposed, as shown in Chart II.C 5, that, *in the cases where there is a proton source available in the side chain, the* protonated intermediate undergoes rupture to give the isothiazolidene-3-one on the one hand and the -SH species on the other. We believe the process to operate in a cyclic form by the transformation of the SH compound by oxidation to the dithia compound and thereby this mechanism could account to as much as 100% yields of isothiazolidene-3-ones.

Dithia redox systems such as presented here having amino acid ligands with a free carboxyl group has been studied for their stability in water as stated previously.[16] Such a study has shown that cleavage, as envisaged here do take place by presence of another species, which, without any structural support was earlier assigned to the isothiazolidene-3-one In the present work, this has been confirmed by isolation and characterization of such compounds. Further, the importance of isothiazolidene-3-ones as drug prospect is discussed in the later part of this work.

The structural assignment for the novel isothiazolidenes **9** and **11** are additionally supported by their X-ray structures. The tyrosine compound (**9**) crystallized from acetonitrile - chloroform (1:1). The X-ray structure of this compound and selected inter atomic parameters are presented in Fig. II.C.1 and Table II.C.1 respectively. The ORTEP diagram in Fig. II.C.1 clearly brings about

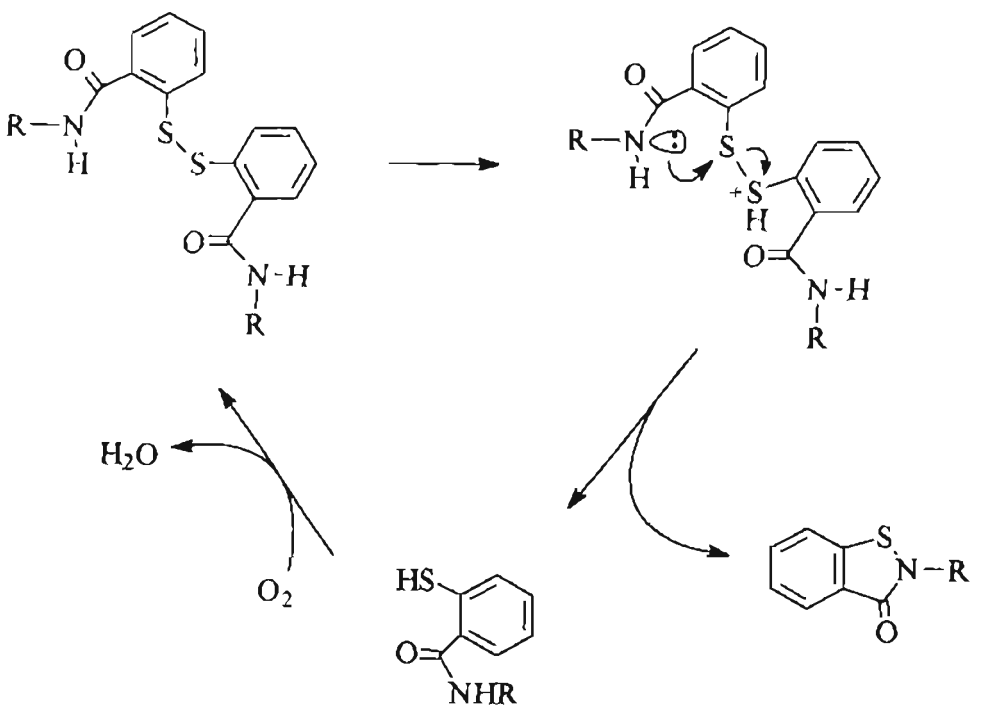

Chart II.C.5.

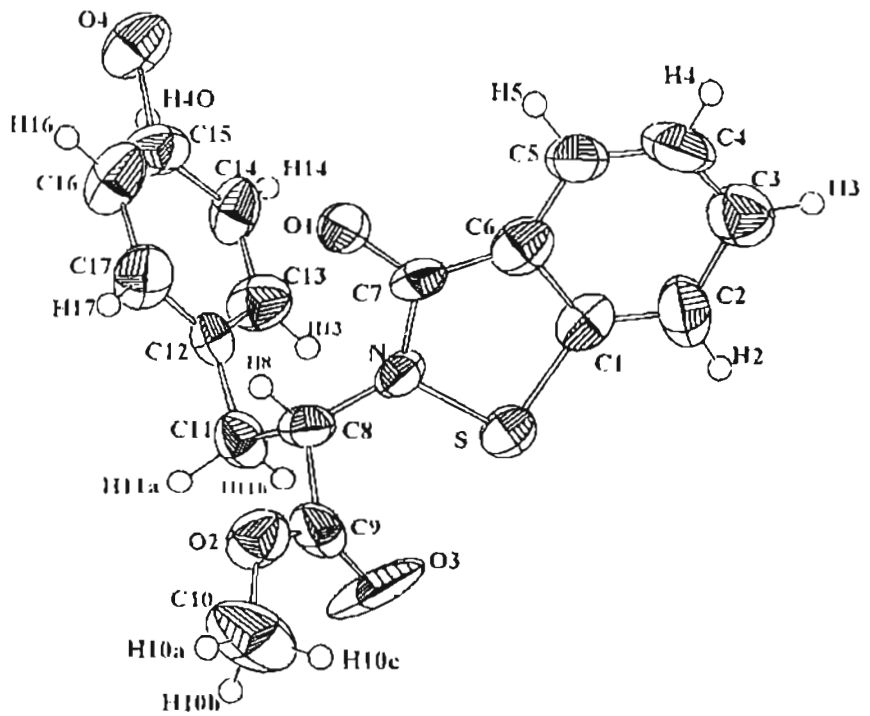

Fig. II.C.1. Crystal structure of **9**

Table II.C.1. Inter atomic parameters from the crystal data of **9**

Bond Distances	(Angstroms)
S-N	1.74(4)
S-C1	1.74(7)
N-C7	1.32(7)
N-C8	1.37(4)
O1-C7	1.31(5)
O2-C9	1.26(6)
O2-C10	1.45(4)
O3-C9	1.18(6)
O4-C15	1.45(3)
C1-C2	1.30(4)
C1-C6	1.45(6)
C2-C3	1.51(8)
C3-C4	1.46(7)
C4-C5	1.31(5)
C5-C6	1.43(8)
C6-C7	1.40(4)
C8-C9	1.58(3)
C8-C11	1.6(1)
C11-C12	1.46(3)
C12-C13	1.40(7)
C12-C17	1.34(6)
C13-C14	1.35(3)
C14-C15	1.45(6)
C15-C16	1.30(7)
C16-C17	1.43(4)

Bond Angles	(degrees)
N-S-C1	91(3)
S-N-C7	114(2)
S-N-C8	122(4)
C7-N-C8	124(3)
C9-O2-C10	119(4)
S-C1-C2	126(4)
S-C1-C6	109(2)
C2-C1-C6	124(5)
C1-C2-C3	119(5)
C2-C3-C4	115(3)
C3-C4-C5	121(6)
C4-C5-C6	123(4)
C1-C6-C5	116(3)
C1-C6-C7	112(5)
C5-C6-C7	132(4)
N-C7-O1	121(3)
N-C7-C6	113(3)
O1-C7-C6	126(5)
N-C8-C9	114(2)
N-C8-C11	115(4)
C9-C8-C11	108(4)
O2-C9-O3	130(3)
O2-C9-C8	112(3)
O3-C9-C8	118(4)
C8-C11-C12	111(5)
C11-C12-C13	121(3)
C11-C12-C17	122(4)
C13-C12-C17	117(3)
C12-C13-C14	121(4)
C13-C14-C15	119(4)
O4-C15-C14	117(4)
O4-C15-C16	121(4)
C14-C15-C16	122(2)
C15-C16-C17	117(4)
C12-C17-C16	124(4)

the nonplanar nature of the molecule with an orthogonal disposition of the tyrosine aromatic residues with respect to the near planar benzoisothiazolidene -3-one system. The S-N bond, which could receive electrons, concomitant with zinc in its removal from appropriate [CCXX] boxes, is however exposed.

The threonine compound **11** also crystallized well from acetonitrile -chloroform (1:1). The crystal structure of **11** and the selected inter atomic parameters are presented in Fig. II.C.2 and Table II.C.2. Here again, it appears that the ligand is out of plane with reference to the near planar benzoisothiazolidene-3-one system.

An interesting and potentially useful observation was that, the bis-threonine compound showed enhanced propensity for the uptake of sodium ions in the mass spectrometer. This compound, having a large number of oxygen atoms in side chains and with a defined cavity could, in principle, show good ionophore properties.

The reaction of the bis acid chloride (**2**) with amino acids having a proton source in the side chain, namely, serine, tryptophan and histidine afforded only the isothiazolidene-3-ones in respectively **13** (41% yield), **14** (25%yield) and **15** (56% yield) [Chart II.C.4]. The structures of all these compounds are confirmed fully on the basis of spectral and analytical data. They uniformly exhibited the 1 ppm downfield shift of the Cα proton, characteristic for these compounds. The

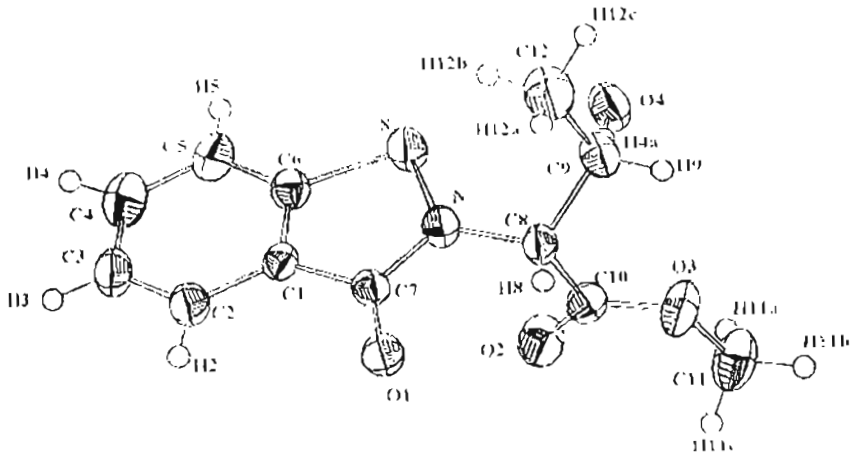

Fig. II.C.2. Crystal structure of **11**

Table II.C.2. Inter atomic parameters from the crystal data of **11**

Bond Distances (Angstroms)		Bond Angles	(degrees)
S-N	1.716(4)	N-S-C6	90.4(2)
S-C6	1.741(5)	S-N-C7	115.7(3)
N-C7	1.380(6)	S-N-C8	121.7(3)
N-C8	1.458(6)	C7-N-C8	120.5(4)
O1-C7	1.224(6)	C10-O3-C11	117.2(4)
O2-C10	1.205(6)	C2-C1-C6	120.4(5)
O3-C10	1.320(6)	C2-C1-C7	126.2(4)
O3-C11	1.463(7)	C6-C1-C7	113.4(4)
O4-C9	1.454(7)	C1-C2-C3	117.7(5)
C1-C2	1.406(7)	C2-C3-C4	121.2(6)
C1-C6	1.383(7)	C3-C4-C5	121.2(6)
C1-C7	1.464(7)	C4-C5-C6	117.1(5)
C2-C3	1.383(8)	S-C6-C1	111.8(4)
C3-C4	1.406(9)	S-C6-C5	125.7(4)
C4-C5	1.386(9)	C1-C6-C5	122.5(5)
C5-C6	1.391(8)	N-C7-O1	123.3(4)
C8-C9	1.554(7)	N-C7-C1	108.4(4)
C8-C10	1.531(7)	O1-C7-C1	128.2(5)
C9-C12	1.528(9)	N-C8-C9	113.4(4)
		N-C8-C10	109.9(4)
		C9-C8-C10	111.1(4)
		O4-C9-C8	107.7(4)
		O4-C9-C12	109.4(5)
		C8-C9-C12	112.1(5)
		O2-C10-O3	125.3(5)
		O2-C10-C8	124.6(5)
		O3-C10-C8	110.0(4)

formation of the histidine side chain containing benzoisothiazolidene-3-one is significant. This stable compound is obtained in ~ 60% yields and show significant activity in the removal of zinc from RNA polymerase (vide infra). Consequently, compound **15** has great potential to develop as an efficient and stable agent for the removal of zinc from [CCXX] boxes contained in biological systems. Of further interest is the fact that the transformation of the histidine containing systems like **15** to reduced zinc uptake systems at the expense of the enzyme, would represent the transformation of one [CCXX] box to another and the latter goes to a zinc finger prototype.

A detailed study of a series of compounds having a common redox system in the form of a Ar-S-S-Ar unit, with reference to the efficiency in the removal of zinc from the NCp7 protein - which has two zinc fingers and the process related to the nonproliferation of the virus - has shown that the p-sulfonylamide derived from 2 is one of the most efficient agents.[6c] In the continuing efforts to design better reagents that could show a propensity for the universal removal of zinc from [CCXX] boxes, it was considered desirable to incorporate the earlier design namely, the presence of an α amino acid to this particular redox system. As shown in Chart II.C.6, the sulfonylamide **16**, prepared from **2** and sulfanilamide was coupled with BocGlu(γOMe) to generate the bis compound **17**. The structural assignment of **17** is supported by spectral and analytical data. The

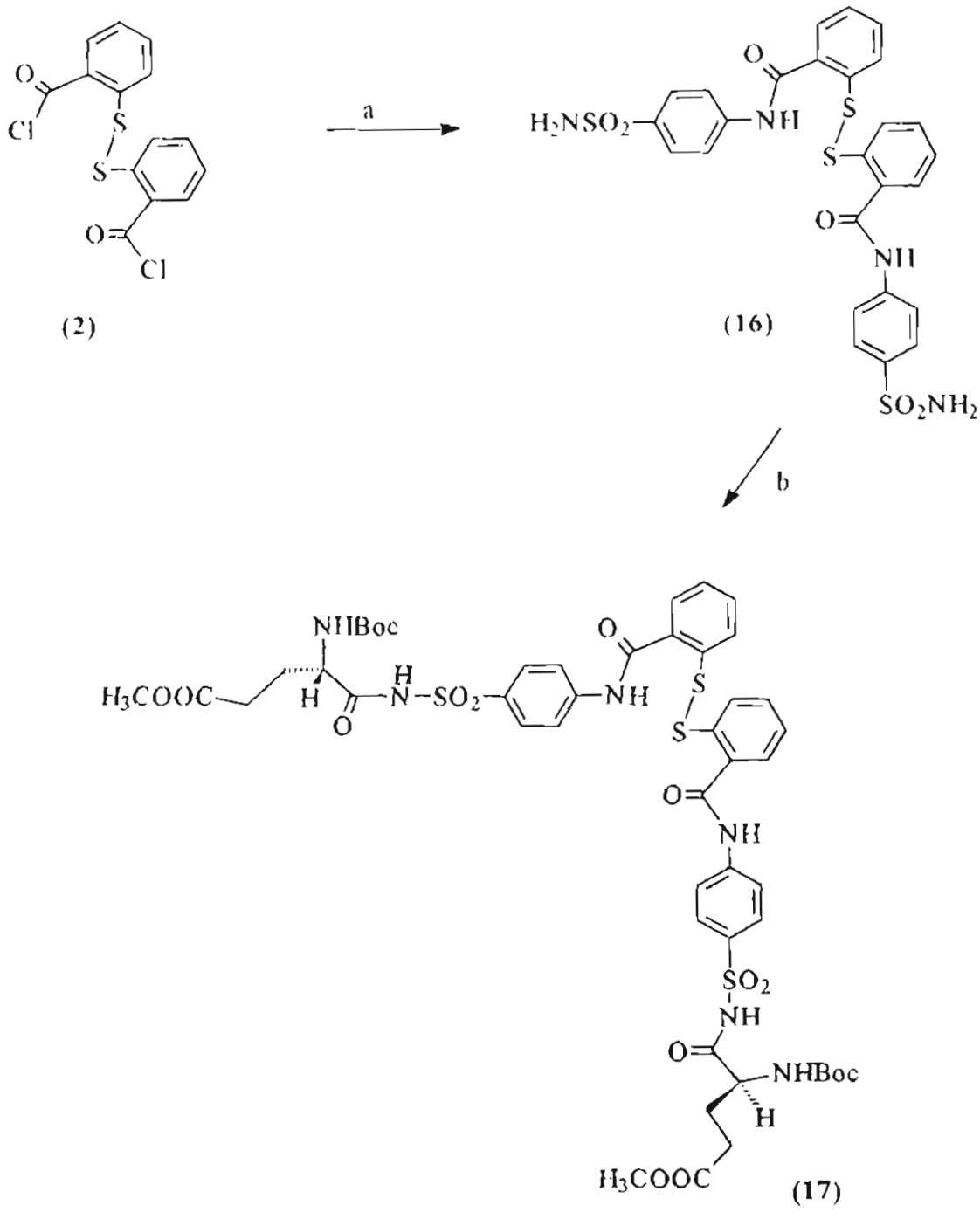

a) Sulfanilamide, Py. b) BocGlu(γOMe)OH, DCC, DMF.

Chart II.C.6.

coupling is noteworthy here, since, it involves the formation of a peptide bond using a charge depleted amino group of a sulfonamide unit. The design is good as seen by the fact that compound **17** was shown to be a very efficient remover of zinc from RNA polymerase (vide infra).

Steric aspects with thiol ⇌ disulfide exchange processes (Chart II.C.2) of the type discussed here, has not hitherto given attention. All the reagents which have been tested against NCp7 are derived from the common redox Ar-S-S-Ar system, harbouring two ligand amide appendages in the ortho positions. Efforts to secure crystal structures of these systems represented by many examples from our own work has been so far not successful. However, as shown in Charts II.C.3, II.C.4, and II.C.6, the ligands are spread out to accommodate the S-S orthogonal dihedral angle and should offer considerable steric hindrance in the transition state. Consequently, it was envisaged in the present work to tether the ortho carboxyl groupings of the redox system with a single chain, thus, reducing the steric requirements considerably, of the composite.

Two attempts were made in this direction, namely, the reaction of **2** with cystinedimethyl ester and that with orthophenylene diamine. Both occasions, in principle can lead to such tethered systems.

The reaction of the acid chloride **2** with freshly prepared CystinediOMe afforded three compounds, namely, the desired tethered system **20**, and

fragmentation products **18** and **19** (Chart II.C.7). The structural assignments from **18** - **20** are supported by spectral and analytical data. Further, compound **19** crystallized well from ethylacetate-hexane and the X-ray crystal structure of this compound is presented in Fig. II.C.3. A most interesting aspect of the crystal structure is that the unit cell consisted of a heterodimer arising from strong hydrogen bonding of the nearly cis oriented amides to form an 8 ring noncovalent assembly as shown. Such dimer formation is also seen in the mass spectrum of the compound, which showed a significant peak corresponding to dimer assembly at 475 $(2M+H)^+$. The RNA polymerase inhibition studies showed however that compound **20**, where the redox system is tethered exhibited only a week activity.

The fragmentation of **20** to **18** and **19** is explained in Chart II.C.8. It is proposed that, probably due to the steric constraints imposed on the system, fragmentation occurs via formation of a dehydro ala on the one hand and an S-S cleavage on the other, and these, by processes, which are explained earlier, readily could be transformed in to **18** and **19**.

Entirely divergent results were seen on treatment of **2** with orthophenylene diamine (Chart II.C.9). Of importance is the formation of the isothiazolidene-3-one derivative (**21**), which now carry an orthoaminophenyl grouping on the amide nitrogen. Most interestingly, the reaction also afforded the

fragmentation products **18** and **19** (Chart II.C.7). The structural assignments from **18** - **20** are supported by spectral and analytical data. Further, compound **19** crystallized well from ethylacetate-hexane and the X-ray crystal structure of this compound is presented in Fig. II.C.3. A most interesting aspect of the crystal structure is that the unit cell consisted of a heterodimer arising from strong hydrogen bonding of the nearly cis oriented amides to form an 8 ring noncovalent assembly as shown. Such dimer formation is also seen in the mass spectrum of the compound, which showed a significant peak corresponding to dimer assembly at 475 $(2M+H)^+$. The RNA polymerase inhibition studies showed however that compound **20**, where the redox system is tethered exhibited only a week activity.

The fragmentation of **20** to **18** and **19** is explained in Chart II.C.8. It is proposed that, probably due to the steric constraints imposed on the system, fragmentation occurs via formation of a dehydro ala on the one hand and an S-S cleavage on the other, and these, by processes, which are explained earlier, readily could be transformed in to **18** and **19**.

Entirely divergent results were seen on treatment of **2** with orthophenylene diamine (Chart II.C.9). Of importance is the formation of the isothiazolidene-3-one derivative (**21**), which now carry an orthoaminophenyl grouping on the amide nitrogen. Most interestingly, the reaction also afforded the

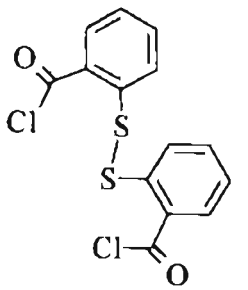

(2)

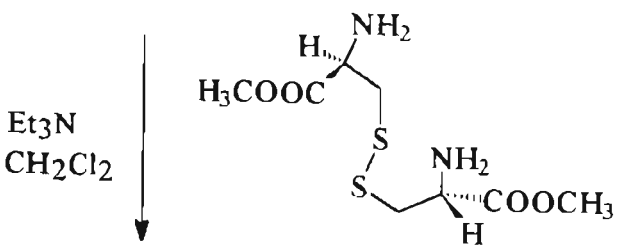

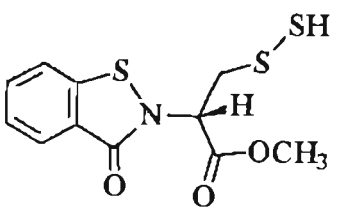

18

+

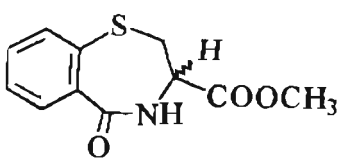

19

+

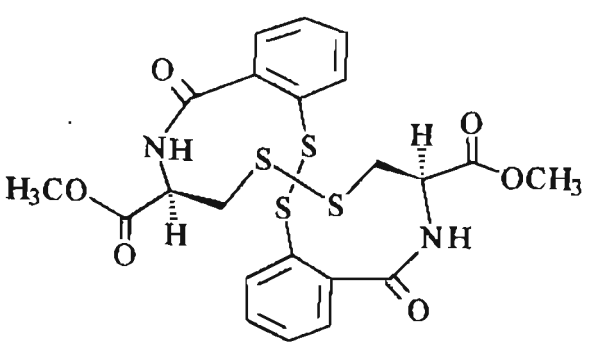

20

Chart II.C.7.

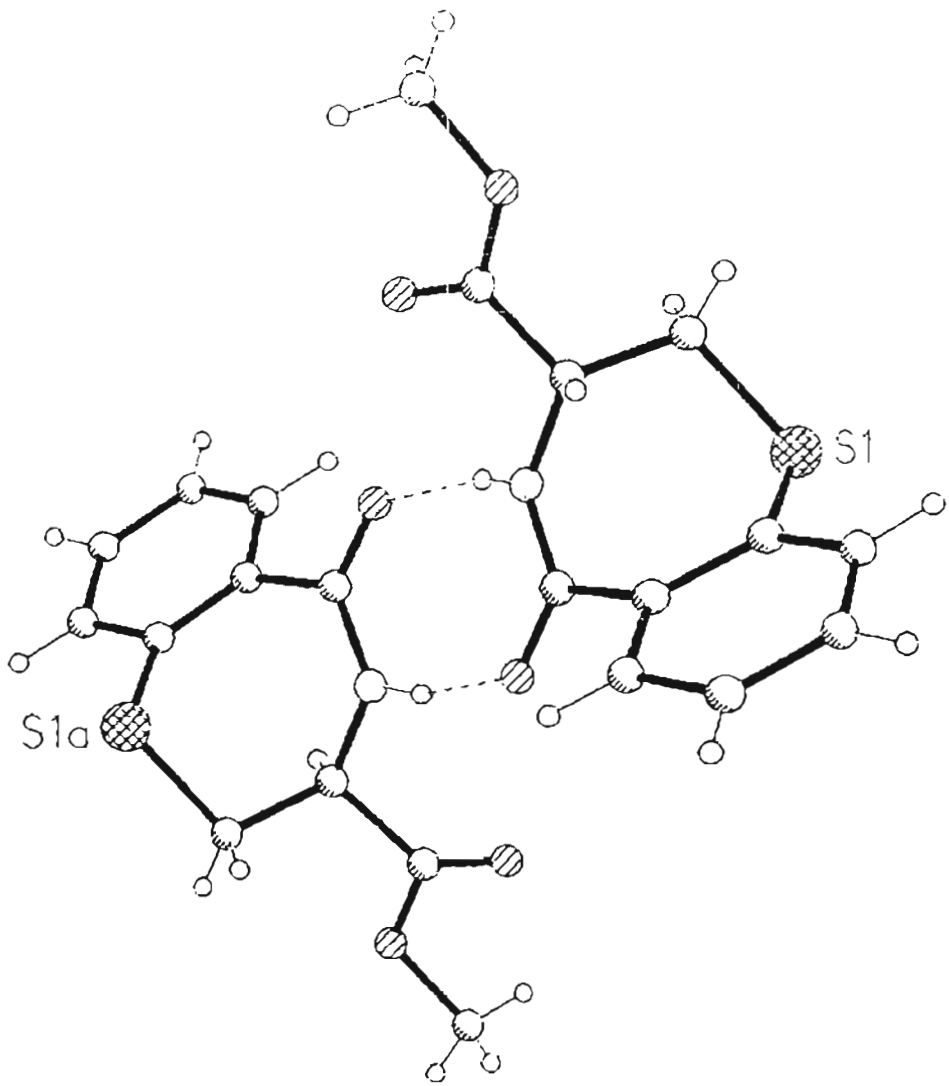

Fig. II.C.3. Crystal structure of **19** as hydrogen bonded dimer

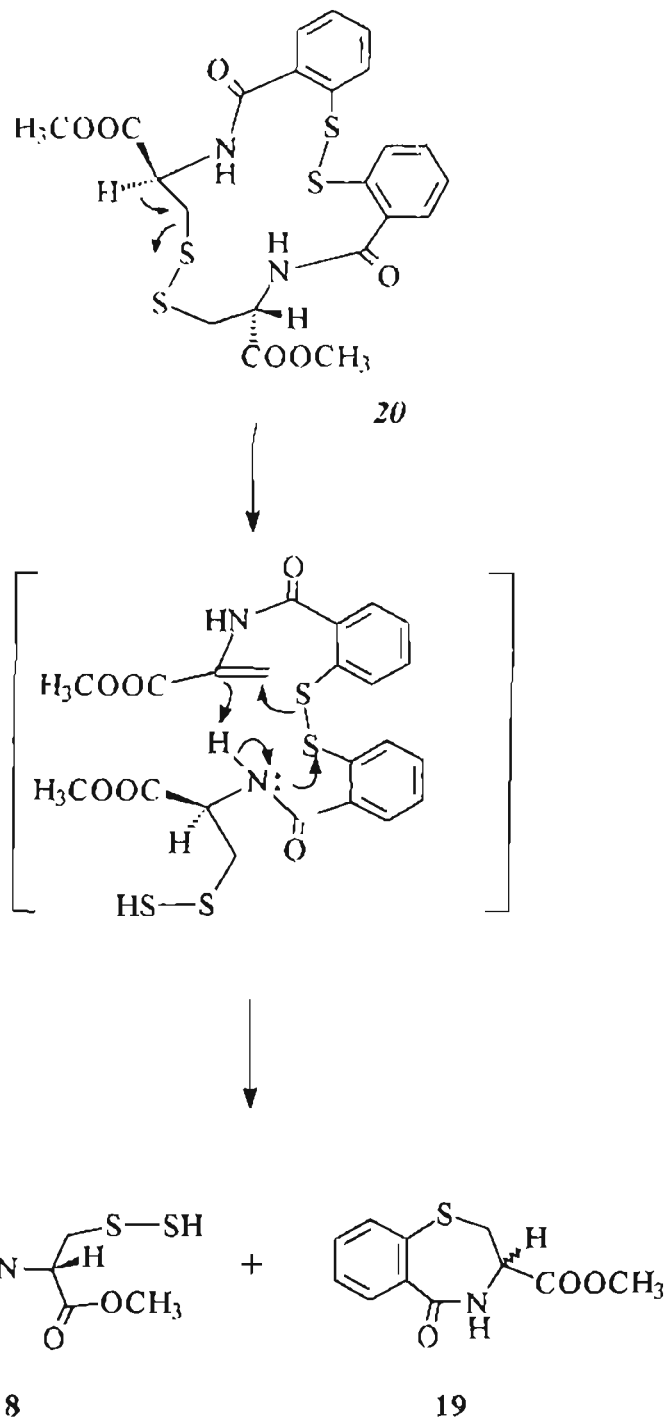

20

18 **19**

Chart II.C.8.

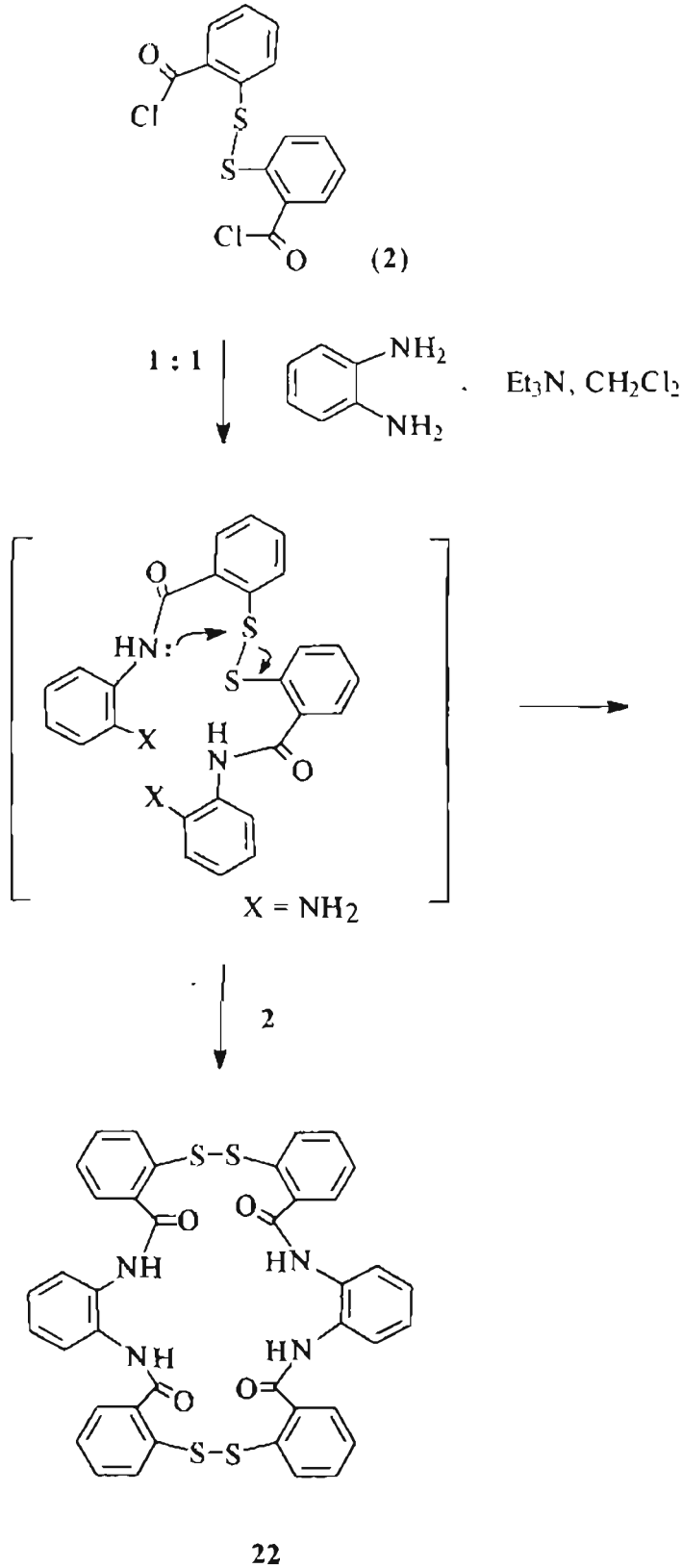

Chart II.C.9.

2+2 symmetrical adduct **22** in 5% yield. The structural assignment for **21** is supported by spectral and analytical data and by X-ray crystallography. The X-ray structure of this compound with selected inter atomic parameters are presented in Fig. II.C.4 and Table II.C.3. The X-ray structure of **21** is noteworthy. Unlike the other two examples (**9** & **11**), the molecule **21** is nearly planar. An unexpected feature of this is the proximal alignment of the amino group to the sulfur atom, rather than the expected hydrogen bond formation with the carbonyl grouping of the isothiazolidene-3-one system. The compound awaits detailed studies pertaining to its efficacy as an agent for removal of zinc. The structural assignment for **22** is principally on the basis of mass spectra, which showed a parent ion at 756. The structural profile of this compound is interesting in that, with in the confines of a Ar-S-S-Ar periphery, the cavity is highly programmed to the uptake of ions possessing as it does, four rigidly aligned peptide groupings.

An assessment of the efficiency of the compounds described thus far pertaining to the removal of zinc from RNA polymerase is presented in the next section. From this, it can be concluded that the design has given rise to very promising members that could be expected to show pervasive and significant activity in the removal of zinc from [CCXX] boxes which are present in diverse biological systems

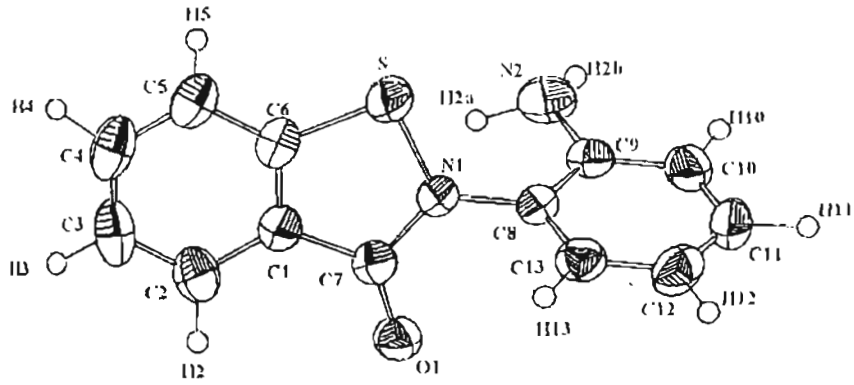

Fig. II.C.4. Crystal structure of **21**

Table II.C.3. Inter atomic parameters from the crystal data of **21**

Bond Angles	(degrees)
N1-S-C1	90.5(1)
S-N1-C7	116.3(2)
S-N1-C8	118.7(2)
C7-N1-C8	125.0(3)
S-C1-C2	126.5(3)
S-C1-C6	111.3(2)
C2-C1-C6	122.2(3)
C1-C2-C3	116.9(3)
C2-C3-C4	121.4(4)
C3-C4-C5	121.4(3)
C4-C5-C6	118.3(3)
C1-C6-C5	119.8(3)
C1-C6-C7	113.9(3)
C5-C6-C7	126.3(3)
N1-C7-O1	123.6(3)
N1-C7-C6	108.0(3)
O1-C7-C6	128.4(3)
N1-C8-C9	119.4(3)
N1-C8-C13	119.2(3)
C9-C8-C13	121.4(3)
C8-C9-C10	119.6(3)
C9-C10-C11	119.5(3)
C10-C11-C12	120.9(3)
C11-C12-C13	120.5(3)
N2-C13-C8	121.8(3)
N2-C13-C12	120.1(3)
C8-C13-C12	118.0(3)

Bond Distances	(Angstroms)
S-N1	1.712(3)
S-C1	1.741(4)
N1-C7	1.375(4)
N1-C8	1.437(4)
N2-C13	1.395(4)
O1-C7	1.222(4)
C1-C2	1.391(5)
C1-C6	1.387(5)
C2-C3	1.383(6)
C3-C4	1.384(6)
C4-C5	1.378(5)
C5-C6	1.391(4)
C6-C7	1.465(4)
C8-C9	1.392(5)
C8-C13	1.391(4)
C9-C10	1.380(5)
C10-C11	1.384(5)
C11-C12	1.377(5)
C12-C13	1.395(5)

II.D. TRANSCRIPTION INHIBITION STUDIES BY REMOVAL OF ZINC VIA EXCHANGE FROM E *coli* RNA POLYMERASE

The course of transcription of Calf thymus DNA by E *coli* RNA polymerase was monitored with the redox (S-S) amino acid composites (**3** - **8**, **10**, **12**, **16**, **17** & **20**) and with isothiazolidene-3-ones (**11**, **14** & **15**), whose formation is explained in Charts II C.3, II.C.4, II.C.6 and II.C.7.

Additionally, the removal of zinc from RNA polymerase by **12** was monitored by fluorescence studies.

Materials and methods

The enzyme aliquots after admixing with the drugs were incubated for 15 minutes and then dialyzed overnight. A general transcription assay was then carried out in a medium which contain ^{3}H UTP in addition to other nucleotides. The amount of radio active UTP incorporated in the transcribed RNA was monitored by scintillation counter and the count when compared to that obtained on using native enzyme gave the percentage loss of activity.

A mixture containing 0.8 μM solution of either the redox (S-S) amino acid composite or the isothiazolidene-3-one (5 μL from 8 μM stock in methanol) and 0.4 μM of E *coli* RNA polymerase (5 μL from 4 μM stock) in 1x transcription

buffer [a] (5 µL) and 35 mL milliQ water was incubated for 0.5 h. and dialyzed [b] overnight to remove the unbound chelator.

4 x transcription assay mixture [c] (10 µL) was diluted with 10µL of milliQ water and admixed with 20 µL of the dialyzed enzyme-chelator composite. The mixture was incubated for 20 minutes and spotted on to a D81 filter paper strip,[d] which was precoated with EDTA to arrest further transcription. The filter paper strips were allowed to air dry for 3 hours, washed successively with 5% Na_2HPO_4 solution (3 x 200 mL, 10 min each), distilled water (2 x 200 mL, 5 min each) and then with ethanol (2 x 75 mL). The strips were then dried under an IR lamp, put in the scintillation fluid[e] and noted the count in the scintillation counter. The count given by the native enzyme is taken as 100% and the relative value shown by the inhibited enzyme gave the percentage loss of activity.

For fluorescence studies, **12**, having the threonine ligand was chosen because it exhibited most favourable fluorescence profile. The fluorescence profile of a solution of 5 µM of **12** and 2.5 µM enzyme was monitored as a function of time.[f] The decrease in fluorescence intensity was used as a measure of the removal of zinc.

Results and discussion.

The results from the interaction of RNA polymerase with the redox amino acid composite as well as the isothiazolidene-3-one are presented in a graphical

format in Fig. II.D.1. For comparison purposes, the activity with out the reagent is taken as 100% and results from other experiments are made based on this standard. The results from normal chelating agents like EDTA and o-phenanthroline are also presented in Fig. II.D.1 at concentrations, but at much higher ($\sim 10^{-4}$)

Initial studies were done with higher concentrations of the reagent (15 mM), where total inhibition of transcription was seen. The effect of zinc removal on transcription profile has been studied. Of the two zinc atoms present in the enzyme, one could be removed rather easily, leading to a mono zinc depleted modified enzyme which still showed ~35% of original activity[18]. The removal of both zinc atoms require rather drastic conditions and the resulting totally zinc depleted enzyme does not show any transcription activity. This is pictorially represented in Fig. II.D.2. Fig II.D.1 is constructed based on the activity of the chelator to effect zinc depletion, and this, as could be seen, varies from 5% in the case of threonine compound (**11**) to 62% in the case of **17** and 56% in the case of Tyrosine containing compound (**10**). The value of 62% inhibition exhibited by **17** represents removal of one zinc from the enzyme. This limit is interestingly supported by the fact that both the alanine compound (**3**) and the methionine compound **8** effected inhibition in this range, but at a 10 fold increased concentration.

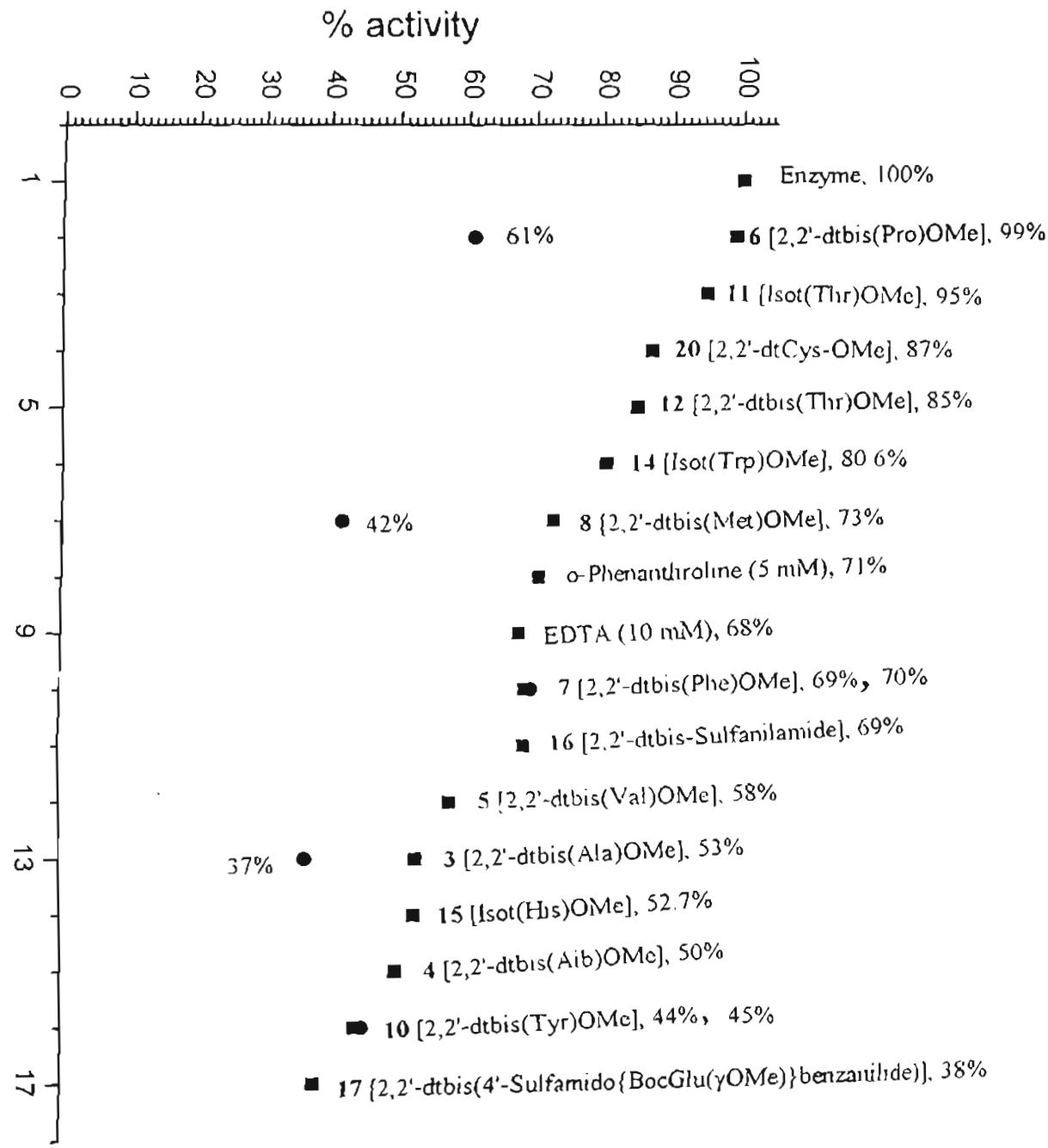

Fig. II.D. 1. Results of RNA polymerase inhibition studies with dithiobenzamides and isothiazolidene - 3-ones

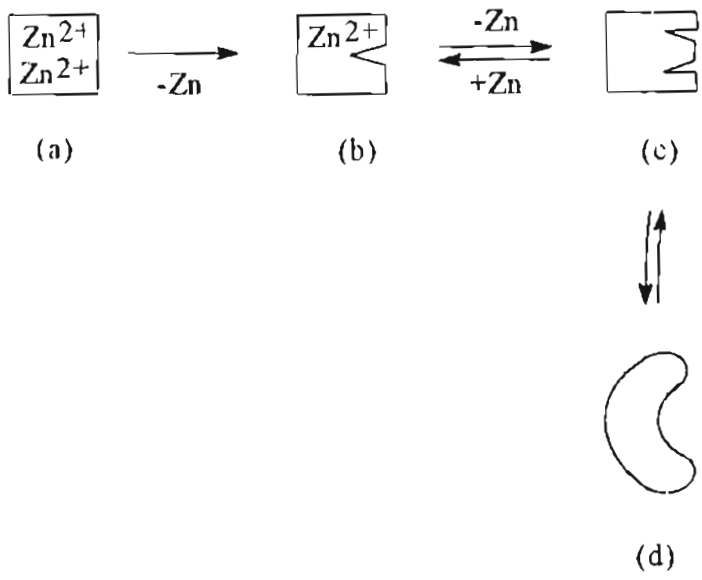

(a) Active enzyme

(b) Mild chelation with EDTA for 5h- Less active enzyme

(c) Strong chelation with o-Phenanthroline for 3h - Inactive enzyme

(d) Strong chelation with o-Phenanthroline for 5h - Inactive and denatured enzyme

Fig. П.D. 2.

A striking observation from Fig. II.D.1 is that the chelators studied here are far superior in the removal of metal, compared to the traditional agents like EDTA and o-phenanthroline. Even at enhanced concentrations ($\sim 10^4$), they were not able to effect significant removal of the metal.

As shown in Charts II.C.4 & II.C.5, the dithia compounds can fragment, leading to isothiazolidene-3-ones. In studies relating to the removal of zinc from HIV NCp7 protein, It has been shown that analogs, having free carboxyl groups, in water, at higher pH ranges, give rise to substantial amounts of isothiazolidene-3-ones.[16] Further, such studies with the HIV NCp7 protein has shown that, both the dithia compound, and isothiazolidene-3-ones are effective in the removal of zinc, although a comparative study has shown that the dithia compounds showed a superior profile. Some support of this can be seen from Fig. II.D.1, where dithia Thr compound (**12**) exhibited marginal increased inhibition, compared to isothiazolidene-3-one (**11**).

The fragmentation of dithia compounds under biological conditions is a drawback in developing these as ideal inhibitors. On the other hand, the isothiazolidene-3-ones are stable and therefore compounds of this class which show inhibition would be better candidates in the development of efficient inhibitors. In the present work, this aspect has found a satisfactory solution, since the histidine compound (**15**) which has an isothiazolidene-3-one type structure

exhibited high inhibition (47%) This observation is of interest for two reasons. As stated earlier, the interaction of the histidine compound **15** with the [CCXX] boxes present in the enzyme could result, by an exchange processes, an oxidized enzyme and the reduced reagent, which would have now a minimalistic zinc finger prototype structure Indeed, this fact of formation of stable zinc compound may in fact account for the significant inhibition exhibited by this compound. Compound **15** therefore show promise as a suitable inhibitor.

Mass spectrometric investigations [16] have shown that, in the case of NCp7, interaction with redox compounds of the type B(Chart II.C.1), results in an initial complex, from which zinc as well as the ligand is expelled, resulting in the oxidation of [CCXX] box. The present finding can be well explained on the basis of a similar mechanism, where zinc containing [CCXX] boxes present in β / β' units of the enzyme could form complexes with the reagent, effecting the removal of the zinc as envisaged in Chart II.C.2.

Figure II.D.1 neatly devides the reagents studied in this work into two categories. Those which are on the left side of the traditional chelators (o-Phenanthroline & EDTA) and the others to the right of it. The former form a class having decreased capacity for inhibition of transcription process by RNA polymerase and the latter, a vastly enhanced inhibitory profile. It cannot be a coincidence that, whilst the better profile is shown by hydrophobic amino acid

derivatives (Phe, Val, Ala, Aib, Tyr), those which cannot belong to this category are not that effective.

In the design of reagent systems for the removal of zinc, the importance of the side chain was a consideration, since these could lead to transition state stabilization. The fact that hydrophobic amino acids are able to achieve such stabilization in comparison to the others indicate the importance of hydrophobic interaction in the vicinity of [CCXX] box that are present in RNA polymerase. Proline would appear as an exception to this generalization, since among those having hydrophobic appendages, this is an exception. This would indicate the importance of the peptide NH bond in the stabilization of the transition state.

The fluorescence studies pertaining to the zinc removal were limited to (12) due to consideration of the appropriate fluorescence profile.

As illustrated in section II.B, changes in fluorescence profiles could be used to monitor the thiol $\rightleftharpoons$ disulfide exchange processes. In Fig II.D.3 is presented the fluorescence profile of the enzyme on addition of an aliquot of compound **12**. The decrease in fluorescence is a clear indication of the transfer of metal to **12** which is associated with quenching processes, resulting in decreased fluorescence intensity.

The above study has shown that the design presented for the removal of from [CCXX] boxes present in diverse enzyme systems, could be

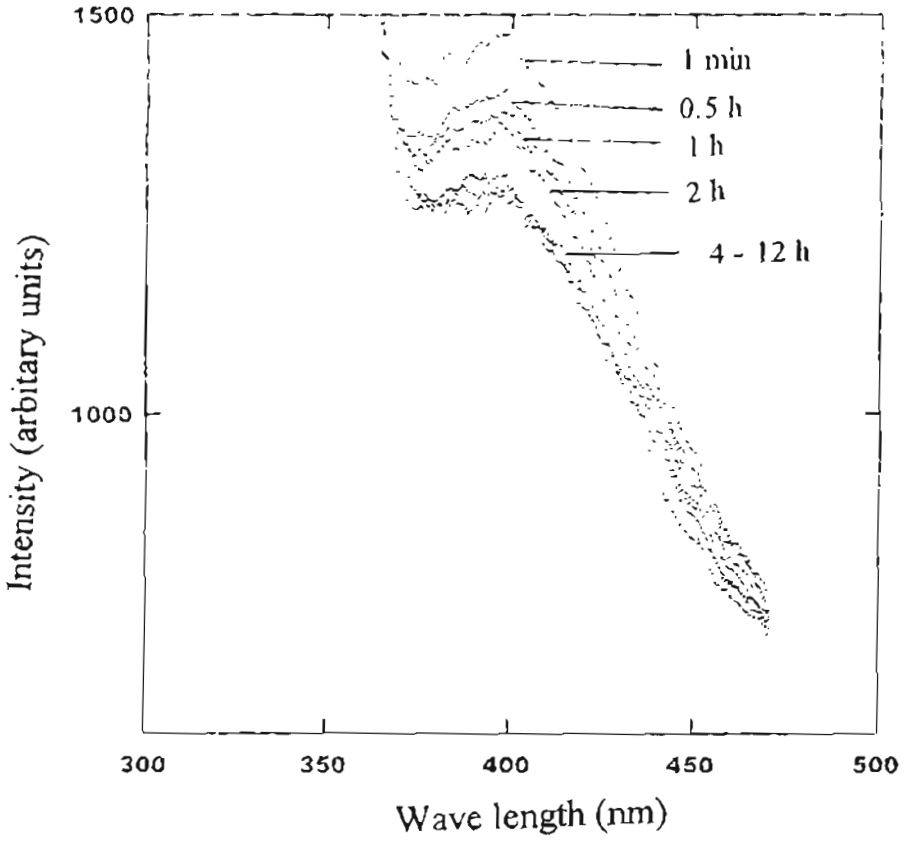

Fig. II.D. 3. Variation of fluorescence intensity of **12**, when emission from a mixture containing 5 μM of **12** and 2.5 μM of RNA polymerase in buffer [f] was monitored as a function of time.

generalized, leading to control of their activity, which in turn could be anticipated to have significant therapeutic significance.

Notes.

a. Composition of the 1xTranscription buffer:

50 mM Tris.HCl (pH 7.8); 0.1 mM EDTA; 0.1 mM DTT; 50 mM NaCl; 3 mM $Mg(OAc)_2$; BSA 25μg/mL.

b. Dialysis

i) Preparation of the dialysis tubings: Small pieces of dialysis tubing (10 -20 cm. 10 nos) were boiled in 250 mL of 2% $NaHCO_3$ solution for 10 min. They were then washed thoroughly with distilled water (4 x 100 mL) and again boiled for 10 min. in distilled water (200mL), allowed to cool and stored at 5°C.

ii) Composition of the dialysis buffer: Tris.HCl (pH 8), 10mM; Glycerol 5% (v/v); EDTA, 0.1 mM; DTT, 0.1 mM; NaCl, 50 mM.

c. Composition of the 1 x Transcription assay mixture: Tris.HCl (pH 8), 40mM; $MgCl_2$, 10mM; EDTA, 1mM; βME, 16 mM; ATP, 2 mM; CTP, 0.2 mM; GTP, 0.2 mM; UTP, 0.05mM; ^3H UTP. 50 mM. Calf thymus DNA, 1mg/mL. The solution was made up using milliQ water.

d. DE 81 filter paper strips were cut in 4 x 4 cm size, numbered at the corner using HB pencil and 100 μL of 50 mM EDTA solution was spotted on this. Gloves and forceps were used while handling. They were allowed to air dry.

e. Composition of the scintillation fluid: PPO, 4g; POPOP, 0.2g; *Naphthalene*, 60g; *Ethylene Glycol* 20 mL; Methanol 100 mL; Dioxane 880 mL.

f. Compound **12** showed a characteristic absorption at 325 nm and an emission at 395 nm. The fluorescence emission of **12** (5 μM), when admixed with a 2.5 μM solution of RNA polymerase in storage buffer [40 mM Tris.HCl, (Ph 8); 1 mM EDTA; 10 mM DTT; 100 mM NaCl and 50% Glycerol], was monitored as a function of time.

II.E. EXPERIMENTAL

All amino acids used were of L-configuration Melting points were recorded on a Fisher-Johns melting point apparatus and are uncorrected. Optical rotations were measured with an automatic JASCO polarimeter; concentrations are given in grams / 100 mL. Infra red spectra were recorded on a Perkin Elmer / 1600 - FT spectrometer either as neat liquids or as KBr pellets and prominent peaks are expressed in cm^{-1}. ^{1}H and ^{13}C NMR spectra were recorded on Bruker WM-300 NMR spectrometer. The chemical shifts are expressed in δ (ppm) with TMS at 0.000 as the internal reference. FAB MS were obtained on a JEOL SX-120 / DA - 6000 instrument using m-nitrobenzylalcohol as the matrix. C, H, N analysis was carried out in Vario EL elemental analyzer. Reactions were monitored wherever possible by TLC. Silica gel / G (Merck) was used for TLC and column chromatography was done on silica gel (100 - 200 mesh) columns, which were generally made from a slurry in hexane or a mixture of hexane and ethyl acetate. Products were eluted with a mixture of ethyl acetate / hexane. Dialysis tubings having 10 Kd cutof from Sigma were used in dialysis. Whatmann DE81 filter paper was used for spotting the transcription assay mixture. Radioactivity counts of the biological samples were measured using Packard 1500 TRI-CARB Liquid Scintillation counter.

I. Amino acid methyl esters: (General Procedure)

a) Dry HCl method.

Dry HCl was passed through a stirred suspension of the L-amino acid (Ser, Ala, Pro; 100 mmol) in dry MeOH (~75 mL) at room temperature until a clear solution was obtained and then at 0°C until saturation. The solvents were evaporated *in vacuo*, the residue crystallized from dry MeOH / Et_2O, filtered, washed with dry Et_2O and dried in vacuo over KOH to give the amino acid methyl ester hydrochloride in nearly quantitative yields.

In the case of SerOMe.HCl, the residue obtained after the removal of the solvent was redissolved in dry MeOH and again subjected to the passage of dry HCl for ~1 h at room temperature, followed by evaporation of the solvent and crystallization.

For the preparation of CysdiOMe.2HCl, a suspension of L-Cystine (17 mmol) in dry MeOH (125 mL) was subjected to the passage of dry HCl for 4 h at room temperature, the solution concentrated to ~30 mL *in vacuo*, refrigerated, filtered, crystallized from MeOH and dried.

In the case of histidine methyl ester dihydrochloride, a solution of L-histidine.HCl.H_2O (14.35 mmol) in dry MeOH (30 mL) was admixed with conc.H_2SO_4 (O.8 mL), refluxed for 2.5 h and subjected to a stream of dry HCl for 3 h, towards the end of which the product started separating as a white precipitate. The reaction mixture was refrigerated for 4 h, filtered, the residue

washed with hot MeOH (15 mL) under protection from moisture, filtered and the filtrate refrigerated overnight to afford HisOMe.2HCl, which was filtered and dried.

b) $SOCl_2$ Method.

Thionyl chloride (4 mL, 58 mmol) was added dropwise to stirred and ice cooled dry MeOH (35 mL), followed by L-amino acid (Phe, Tyr, Aib, Met, Thr, Trp; 50 mmol). The reaction mixture was allowed to attain room temperature, refluxed for 2 h, solvent evaporated and the residue on crystallization from dry MeOH / Et_2O gave the products in > 85% yields. In the case of Thr and Met, no refluxing was necessary.

II. 2,2' - Dithio dibenzoyl chloride (2)

a) Sodium disulfide.

To a stirred and refluxing solution of $Na_2S.2H_2O$ (15.5g, 0.135 mol) in water (37 mL), was added sulfur powder (4.25g, 0.135 mol). The mixture was left stirred until clear, admixed with 40% NaOH (12 mL), cooled in ice-salt bath and used in the following step.

b) 2,2' - dithiodibenzoic acid (1)

To an ice cooled and stirred solution of Na_2S_2 was added in drops, over 0.5 h, an ice - salt cooled solution of diazotized anthranilic acid - prepared by slow addition of ice cooled aqueous sodium nitrite (8.75g, 0.125 mol, 35 mL) to an

ice-salt cooled and stirred solution of anthranilic acid (16g, 0.117 mol) in conc. HCl (25 mL). The reaction mixture was allowed to attain room temperature, left stirred till nitrogen evolution ceased, acidified with conc.HCl, filtered, washed with water, admixed with 5% Na_2CO_3 (250 mL), filtered hot from sulfur, acidified with conc. HCl, filtered and dried to give 17g, (92%) of 2,2'-dithiodibenzoic acid.

M.p. : 284°C

IR (KBr) : 2996 (br), 1681, 1566, 1472

c) 2,2' dithiodibenzoyl chloride (**2**)

A mixture of 2,2'-dithiodibenzoic acid (2g, 6.53 mmol) and $SOCl_2$ (24 mL) was refluxed for 24 h, evaporated, the residue dissolved in CH_2Cl_2 (5 mL), evaporated *in vacuo*, triturated with dry hexane, filtered under protection from moisture, washed with dry hexane and dried over P_2O_5 to afford 1.5g of 2,2'-dithiodibenzoyl chloride.

Yield : 67%

M.p. : 148°C

IR (KBr): 1721, 1600, 1560.

^1H NMR ($CDCl_3$-DMSO-d6) δ 7.4 (t, 2H), 7.6 (t, 2H), 7.7 (d, 2H), 8.08 (d, 2H)

III. The reaction of 2,2'-Dithio dibenzoylchloride with α aminoacid methyl esters : isolation of 2,2'-Dithiodibenzoyl bis-aminoacid methyl esters [2,2'-dt(AA)-OMe] and (in some cases) N-(Benzoisothiazolidine-3-one) amino acid methyl esters [Isot(AA)OMe]. (General Procedure)

A solution of 2,2'-dithiodibenzoyl chloride (**2**) (1g, 2.915 mmol) in dry CH_2Cl_2 (25 mL) and 0.9 mL (6.413 mmol) of triethylamine were simultaneously added dropwise to an ice cooled and stirred solution of the free amine of the amino acid methyl ester [generated *in situ* by the addition of triethylamine (6.413 mmol) to an ice cooled and stirred suspension of the amino acid methyl ester hydrochloride (6.413 mmol) in dry CH_2Cl_2 (60 mL). [In the case of histidine methyl ester dihydrochloride, 12.8 mmol of triethylamine was used]. The reaction was left stirred for 48 h at room temperature, washed successively with cold saturated $NaHCO_3$ (3 x 10 mL), 2N H_2SO_4 (3 x 10 mL) and then with distilled water (1 x 10 mL) [In the case of Trp and His, acid wash was not done]. The organic layer was dried ($MgSO_4$), evaporated *in vacuo* and the residue chromatographed on a silica gel column using Hexane - EtOAc as eluent. When present, the Isot(AA)OMe eluted earlier to 2,2'-dt(AA)OMe.

IV. 2,2'-Dithiodibenzoyl bis-alanine methyl ester [2,2'-dtbis(Ala)-OMe] (3)

Prepared as per General procedure III.

Yield : 25%.

$[\alpha]_D^{20}$: - 10.00 (c 1, $CHCl_3$)

M.p. : 104 - 106°C

IR (KBr): 3306, 3012, 1749, 1651, 1545.

^{1}H NMR ($CDCl_3$) δ 1.56 (d, 6H, CH_3), 3.8 (s, 6H, $COOCH_3$), 4.7 - 4.8 (brm, 2H, CαHs), 6.76 - 6.78 (brd, 2H, NH), 7.2 - 7.77 (m, 8H, ArHs).

FAB MS (m/z) (%) : 477 (10) $(MH)^+$, 499 (5) $(M+Na)^+$, 238 (100) (M/2)

V. 2,2'-Dithiodibenzoyl bis-α-amino isobutyric acid methyl ester [2,2'-dtbis(Aib)-OMe] (4)

Prepared as per General procedure III

Yield : (24%)

M.p. : 178 - 180°C

IR (KBr): 3245, 2989, 1748, 1634, 1539.

^{1}H NMR ($CDCl_3$) δ 1.69 (s, 12H, CH_3s), 3.79 (s, 6H, $COOCH_3$), 6.76 (brs, 2H, NH), 7.2 - 7.76 (m, 8H, ArHs).

FAB MS (m/z) (%) : 527 (7) $(M+Na)^+$, 252 (100) (M/2)

Anal. Found: C, 57.55; H, 5.34; N, 4.80. Calc. for $C_{24}H_{28}N_2O_6S_2$: C, 57.14; H, 5.55; N, 5.55.

VI. 2,2'-Dithiodibenzoyl bis-Valine methyl ester [2,2'-dtbis(Val)-OMe] (5)

Prepared as per General Procedure III.

Yield : 63%.

M.p. : 148 - 150°C

$[\alpha]_D^{20}$: - 3.00 (c 1, $CHCl_3$)

IR (KBr): 3293, 2963, 1744, 1634, 1529.

^1H NMR ($CDCl_3$) δ 0.99 - 1.06 (m, 12H, CH_3s), 2.3 (m, 2H, CβHs), 3.79 (s, 6H, $COOCH_3$), 4.81 (m, 2H, CαHs), 6.63 (d, 2H, NHs), 7.21 - 7.78 (m, 8H, ArHs).

FAB MS (m/z) (%) : 533 (44) $(MH)^+$, 555 (10) $(M+Na)^+$, 266 (100) (M/2)

Anal. Found: C, 58.58; H, 6.01; N, 5.03 . Calc. for $C_{26}H_{32}N_2O_6S_2$: C, 58.64; H, 6.01; N, 5.26.

VII. 2,2'-Dithiodibenzoyl bis-Proline methyl ester [2,2'-dtbis(Pro)-OMe] (6)

Prepared as per General Procedure III.

Yield : 43%.

IR (neat): 2961, 1752, 1652, 1631, 1415

^1H NMR ($CDCl_3$) δ 1.88 - 2.32 (m, 8H, Cβ & $C\gamma H_2$s), 3.3 - 3.44 (m, 4H, $C\delta H_2$s), 3.79 (s, 6H, $COOCH_3$), 4.69 (m, 2H, CαH), 7.18 - 7.33 & 7.71 - 7.74 (m, m, 8H, ArHs)

FAB MS (m/z) (%) : 529 (59) $(MH)^+$, 551 (13) $(M+Na)^+$, 264 (100) (M/2)

VIII. 2,2'-Dithiodibenzoyl bis-Phe methyl ester [2,2'-dtbis(Phe)-OMe] (7)

Prepared as per General Procedure III.

Yield : (36%)

M.p. : 174 - 176°C

$[\alpha]_D^{20}$: +112.00 (c 1, $CHCl_3$)

IR (KBr): 3285, 3036, 1742, 1640, 1533.

^1H NMR ($CDCl_3$) δ 3.25 - 3.34 (m, 4H, $C\beta H_2s$), 3.78 (s, 6H, $COOCH_3$), 5.1 (m, 2H, CαHs), 6.57 (d, 2H, NHs), 7.15 - 7.74 (m, 16H, Phe ArHs+dithio ArHs), 7.75 (d, 2H, dithioArHs)

FAB MS (m/z) (%) : 629 (30) $(MH)^+$, 651 (7) $(M+Na)^+$, 314 (100) (M/2)

Anal. Found: C, 65.03; H, 5.05; N, 4.198 . Calc. for $C_{34}H_{32}N_2O_6S_2$: C, 64.96; H, 5.09; N, 4.45.

IX. 2,2'-Dithiodibenzoyl bis-methionine methyl ester [2,2'-dtbis(Met)-OMe] (8)

Prepared as per General Procedure III.

Yield : (75%)

M.p. : 206 - 208°C

$[\alpha]_D^{29}$: + 8.00 (c 1, $CHCl_3$)

IR (KBr): 3265, 3070, 1755, 1640, 1546.

^1H NMR ($CDCl_3$) δ 2.10 (s, 6H, $-SCH_3s$), 2.12 - 2.33 (m, 4H, $C\beta H_2s$), 2.63 (m, 4H, $C\gamma H_2s$), 3.81 (s, 6H, $COOCH_3$), 4.94 (m, 2H, CαHs), 6.93 (d, 2H, NHs), 7.24, 7.38, 7.57, 7.77 (t, t, d, d, 8H, ArHs).

FAB MS (m/z) (%) : 597 (48) $(MH)^+$,619 (11%) $(M+Na)^+$, 298 (100) (M/2)

Anal. Found: C, 51.90; H, 5.30; N, 4.28 . Calc. for $C_{26}H_{32}N_2O_6S_2$: C, 52.34; H, 5.37; N, 4.70.

X. N - [Benzo isothiazolidine-3-one] - tyrosine methylester [Isot(Tyr) -OMe] (9) and 2,2'-Dithiodibenzoyl bis-tyrosine methyl ester [2,2'-dtbis-(Tyr)-OMe] (10)

Prepared as per General Procedure III.

a) **[Isot(Tyr) -OMe] (9)**

Yield : (29%)

M.p. : 188 - 190°C

$[\alpha]_D^{29}$: - 63.00 (c 1, $CHCl_3$)

IR (KBr): 3421 (br), 3161, 1752, 1636, 1599, 1518, 1449.

^{1}H NMR ($CDCl_3$) δ 3.08 - 3.48 (dq, 2H, $C\beta H_2$), 3.76(s, 3H, $COOCH_3$), 5.75 (m, 1H, $C\alpha H$), 6.65 - 7.04 (dd, 4H, Tyr ArHs), 7.29, 7.54 & 7.94 (m, m, d, 4H, ArHs)

^{13}C NMR ($CDCl_3$) δ 36.78 (Cβ), 52.79 (Cα), 57.03 (-OCH3), 115.66 - 155.66 (C aromatic), 166.24 (-COO-), 170.25 (Ar-CO)

FAB MS (m/z) (%) : 330 (100) $(MH)^+$, 352 (7) $(M+Na)^+$ 659 (6) $(2M+H)^+$

Anal. Found: C, 61.89; H, 4.64; N, 3.98 . Calc. for $C_{17}H_{15}NO_4S$: C, 62.00; H, 4.56; N, 4.26.

b) **[2,2'-dtbis-(Tyr)-OMe] (10)**

Yield : (19%)

M.p. : 229 - 231°C

$[\alpha]_D^{29}$: + 28.00 (c 0.5, $CHCl_3$)

IR (KBr): 3366 (br), 3279, 3022, 1735, 1640, 1512, 1438.

^1H NMR ($CDCl_3$-$DMSOd_6$-D_2O) δ 3.14 (m, 4H, $C\beta H_2$s), 3.74 (s, 6H, $COOCH_3$), 4.80 (m, 2H, Cαhs), 6.73, 7.07 (dd, 8H, TyrArHs), 7.19 - 7.72 (m, 8H, ArHs), 8.01 (d, 2H, NH), 8.89 (s, 2H, OHs)

^{13}C NMR ($CDCl_3$) δ 35.56 (Cβ), 51.38 (Cα), 53.55 (-OCH3), 114.67 - 155.35 (C aromatic), 166.7 (-COO-), 171.36 (Ar-CO)

FAB MS (m/z) (%) : 661 (49) $(MH)^+$, 683 (10) $(M+Na)^+$, 330 (100) (M/2)

Anal. Found: C, 61.18; H, 4.84; N, 4.10 . Calc. for $C_{34}H_{32}N_2O_8S_2$: C, 61.81; H, 4.84; N, 4.24.

XI. N-[Benzo isothiazolidine-3-one]-threonine methylester [Isot(Thr) -OMe] (11) and 2,2'-Dithiodibenzoyl bis-threonine methyl ester [2,2'-dtbis-(Thr)-OMe] (12)

Prepared as per General Procedure III.

a) **[Isot(Thr) -OMe] (11)**

Yield : (59%)

M.p. : 144 - 146°C

$[\alpha]_D^{29}$: - 80.00 (c 0.5, $CHCl_3$)

IR (KBr): 3496 (br), 2992, 1732, 1670, 1450.

^1H NMR ($CDCl_3$) δ 1.24 (d, 3H, CH_3), 3.1 (brs, 1H, OH), 3.77 (s, 3H, $COOCH_3$), 4.72 (brs, 1H, CβH), 5.41 (d, 1H, CαH), 7.38 - 7.64 & 8.08 (m, d, 4H, ArHs)

^{13}C NMR ($CDCl_3$) δ 19.21 (Cγ), 52.86 (Cβ), 60.95 (Cα), 67.38 ($-OCH_3$), 120.1 - 142.1 (C aromatic), 166.8 (-COO), 169.42 (Ar-CO)

FAB MS (m/z) (%) : 268 (100) $(MH)^+$, 290 (21) $(M+Na)^+$ 535 (3) $(2M+H)^+$, 557 (2) $(2M+Na)^+$

Anal. Found: C, 54.08; H, 4.86; N, 5.01. Calc. for $C_{12}H_{13}NO_4S$: C, 53.93; H, 4.86; N, 5.24.

b) **[2,2'-dtbis- (Thr)-OMe] (12)**

Yield : (31%)

M.p. : 182 - 184°C

$[\alpha]_D^{29}$: - 40.00 (c 0.5, $CHCl_3$) ; UV λ_{max} ($CHCl_3$) 325 (ε, 10000) nm.

IR (KBr): 3527 (br), 3331, 2980, 1751, 1633, 1541, 1439, 1259

^1H NMR ($CDCl_3$) δ 1.31 (d, 6H, CH_3), 2.86 (brs, 2H, -OH), 3.79 (s, 6H, $COOCH_3$), 4.4 - 4.42 (brs, 2H, CβHs), 4.61 (d, 2H, CαHs), 4.75 (d, 2H, NH), 7.25, 7.4, 7.72 - 7.83 (t, t, m, 8H, ArHs)

^{13}C NMR ($CDCl_3$) δ 19.81 (Cγ), 51.78 (Cβ), 57.99 (Cα), 66.99 (-OCH_3), 125.29 - 137.15 (C aromatic), 167.5 (-COO), 170.71 (Ar-CO)

FAB MS (m/z) (%) : 537 (12) $(MH)^+$, 559 (12) $(M+Na)^+$, 268 (100) (M/2)

Anal. Found: C, 53.61; H, 5.20; N, 4.98 . Calc. for $C_{24}H_{28}N_2O_8S_2$: C, 53.73; H, 5.22; N, 5.22.

XII. N-[Benzo isothiazolidine-3-one] - serine methylester [Isot(Ser) -OMe] (13)

Prepared as per General Procedure III.

Yield : (41%)

M.p. : 153 - 155 °C

$[\alpha]_D^{29}$: + 4.00 (c 0.5, $CHCl_3$)

IR (KBr): 3466 (br), 3241, 2922, 1765, 1627, 1451, 1331

^1H NMR ($CDCl_3$) δ 3.2 (t, 1H, OH), 3.9 (s, 3H, $COOCH_3$), 4.1 - 4.4 (m, 2H, $C\beta H_2$), 5.4 (t, 1H, CαH), 7.35 - 7.72 & 8.15 (m, d, 4H, ArHs)

FAB MS (m/z) (%) : 254 (100) $(MH)^+$, 276 (7) $(M+Na)^+$

Anal. Found: C, 51.56; H, 4.25; N, 5.24. Calc. for $C_{11}H_{11}NO_4S$: C, 52.17; H, 4.34; N, 5.53.

XIII) N - [Benzo isothiazolidine-3-one] - tryptophan methyl ester [Isot(Trp) -OMe] (14)

Prepared as per General Procedure III.

Yield : (25%)

$[\alpha]_D^{30}$: - 75.00 (c 1, $CHCl_3$)

IR (neat) : 3420 (br), 3357 (br), 2930, 1748, 1663, 1552, 1453, 1308, 1240

^1H NMR ($CDCl_3$) δ 3.4 - 3.69 (dm, 2H, $C\beta H_2$s), 3.74(s, 3H, $COOCH_3$), 5.78 (m, 1H, $C\alpha H$), 7.12 - 8.01 (m, 9H, ArHs), 8.05 (s, 1H, indole NH)

^{13}C NMR ($CDCl_3$) δ 27.62 (Cβ), 52.8 (Cα), 55.97 (-OCH_3), 110.12 - 141.19 (C aromatic), 165.92 (-COO), 170.69 (Ar-CO)

FAB MS (m/z) (%) : 353 (66) $(MH)^+$, 375 (11) $(M+Na)^+$, 705 (4) $(2M+H)^+$

XIV. N - [Benzo isothiazolidine - 3 - one] - histidine methylester [Isot(His) -OMe] (15)

Prepared as per General Procedure III.

Yield : (56%)

M.p. : 240 - 242°C

IR (KBr): 3446 (br), 3025, 1650, 1455, 1340.

^1H NMR ($CDCl_3$-DMSO-d_6) δ 3.43 (m, 2H, $C\beta H_2$ merged with DMSO-d_6 water), 3.75 (s, 3H, $COOCH_3$), 5.62 (m, 1H, CαH), 6.73 (s, 1H, -N=CH), 7.38 (brs, 1H, imidazole NH), 7.48 (s, 1H, -C=CH), 7.64 & 7.94 (s, d, 4H, ArHs)

FAB MS (m/z) (%) : 304 (100%) $(MH)^+$

XV. Preparation of 2,2'-dithiobis-[4'-(sulfamoyl)-benzanilide] (16)

To 2.58g (14.99 mmol) of sulfanilamide in 50 mL of pyridine at 0 - 5°C was added in drops, 2g (5.83 mmol) of 2,2'-dithiodibenzoyl chloride (**2**) in 20 mL

of dry CH_2Cl_2. The mixture was stirred at 0 - 25°C for 18 h, filtered, the solid washed with 1N HCl (3 x 10 mL), water (3 x 10 mL) and dried, suspended in a mixture of DMF (20 mL) and EtOH (25 mL), filtered and precipitated from the filtrate with 9 mL of 5% $NaHCO_3$. The product was collected by filtration, washed with water and then with EtOH and dried to afford 1.2g (34%) of **16**

M.p. : 300°C

IR (KBr): 3373, 3265, 1661, 1600, 1526, 1317, 1175

^{1}HNMR ($CDCl_3$ - DMSO-d_6) δ 7.1 (s, 4H, SO_2NH_2), 7.31 - 7.46 (m, 4H, ArHs), 7.76 - 7.95 (m, 12H, ArHs), 10.7 (s, 2H, NH).

Anal. Found: C, 50.37; H, 3.57; N, 8.75. Calc. for $C_{26}H_{22}N_4O_6S_4$: C, 50.81; H, 3.58; N, 9.12.

XVI. 2,2' - Dithiobis [4'(sulfamido{Boc-Glu(γOMe)}) benzanilide] (17)

A solution of Boc-Glu(γOMe)OH (0.836g, 3.2 mmol) [prepared in two steps from Glu, (I.E, XXXII)] in dry DMF (30 mL) was admixed with DCC (0.725g, 3.52 mmol), left stirred for 5 minutes, admixed with 2,2'-dithiobis[4'-(sulfamoyl)benzanilide] (**16**) (0.984g, 1.6 mmol) in dry DMF (10 mL) and the reaction left stirred for 48 h. Solvents were evaporated in vacuo, the residue dissolved in $CHCl_3$ (150 mL), filtered, the filtrate washed successively with cold saturated $NaHCO_3$ (2 x 15 mL), 2N H_2SO_4 (2 x 15 mL), distilled water (1 x 10 mL), dried ($MgSO_4$) and chromatographed on silica gel using hexane -

EtOAc (1:2) as eluent to afford 0.5g of **17**. About 0.7g of unreacted **16** was recovered in the reaction

Yield : 98% (based on the starting material recovered)

M.p. : 113 - 115°C

$[\alpha]_D^{29}$: - 10.0 (*c* 0.5, $CHCl_3$)

IR (KBr): 3333, 2982, 1701, 1593, 1533, 1330, 1162

^1H NMR ($CDCl_3$) δ 1.41 (s, 18H, BocCH_3s), 1.67 - 2.10 (m, 4H, Glu CβH_2s), 2.32 - 2.35 (brs. 4H, Glu CγH_2s), 3.63 (s, 6H, COOCH_3), 4.34 (brs, 2H, CαHs), 5.13 (brs, 2H, -SO_2-NH-CO-), 5.29 (d, 2H, BocNH), 7.5 - 7.85 (m, 16H, ArHs), 8.3 (brs, 2H, NH).

FAB MS (m/z) (%) : 1123 (2%) $(M+Na)^+$

XVII. The reaction of 2,2'-dithiodibenzoyl chloride with Cystine-di-OMe: isolation of 18, 19 and 20

A solution of 2,2'-dithiodibenzoyl chloride (**2**) (1g, 2.915 mmol) in dry CH_2Cl_2 (30 mL) and triethylamine (0.9 mL, 6.4 mmol) were added dropwise simultaneously to an ice cooled and stirred solution of the diamine from CysdiOMe [generated in situ by the dropwise addition of triethylamine (0.9 mL, 6.4 mmol) to an ice cooled and stirred suspension of CysdiOMe.2HCl (1.1g, 3 mmol) in dry CH_2Cl_2 (70 mL)]. The reaction mixture was left stirred for four days at room temperature, washed successively with cold saturated $NaHCO_3$ (2 x

20 mL), 2N H_2SO_4 (2 x 20 mL), distilled water (1 x 20 mL), dried ($MgSO_4$), evaporated under reduced pressure and chromatographed on silica gel. Elution with hexane - *EtOAc (2:1)* gave ***18***, ***19*** and ***20***.

a) **18**

Yield : 3%

IR (neat): 3245, 2948, 1742, 1640, 1539, 1445, 1236

^{1}H NMR ($CDCl_3$) δ 3.44 - 4.04 (dd, 2H, $C\beta H_2$), 3.86 (s, 3H, $COOCH_3$), 5.37 (brs, 1H, $C\alpha H$), 7.6 (brs, 1H, -SH), 7.36 - 7.85 (m, 4H, ArHs)

FAB MS (m/z) (%): 302 (34) $(MH)^+$, 324 (5) $(M+Na)^+$, 268 [M - SH], 236 [M - (S-S-H)].

b) **19**

Yield : 17%

M.p. : 150 - 152°C

IR (KBr): 3191, 2962, 1755, 1661, 1458, 1384.

^{1}H NMR ($CDCl_3$) δ 3.03 (t, 1H, $C\beta Ha$), 3.62 (q, 1H, $C\beta Hb$), 3.78 (s, 3H, $COOCH_3$), 4.02 (m, 1H, $C\alpha H$), 6.84 (brs, 1H, NH), 7.41 - 7.69 (m, 4H, ArHs)

FAB MS (m/z) (%): 238 (100) $(MH)^+$, 260 (4) $(M+Na)^+$, 475 (15) $(2M+H)^+$ (hydrogen bonded dimer), 497 (1) $(2M+Na)^+$

Anal. Found: C, 56.057; H, 4.70; N, 5.66. Calc. for $C_{11}H_{11}NO_3S$: C, 55.69; H, 4.64; N, 5.9.

c) **20**

Yield : 31%

M.p. : 212 - 214°C

IR (KBr): 3279, 3063, 1742, 1640, 1539, 1337.

^{1}H NMR ($CDCl_3$) δ 3.52 (d, 4H, CβH$_2$s), 3.9 (s, 6H, $COOCH_3$), 4.94 (t, 2H, CαH), 6.0 (d, 2H, NH), 6.73, 6.97, 7.57, 7.98 (d, t, t, d, 8H, ArHs)

FAB MS (m/z) (%): 539 $(MH)^+$, 561 (6) $(M+Na)^+$

Anal. Found: C, 48.70; H, 4.08; N, 4.89. Calc. for $C_{22}H_{22}N_2O_6S_4$: C, 49.07; H, 4.08; N, 5.2.

XVIII. Reaction of 2,2'-dithiodibenzoyl chloride with ortho-Phenylene diamine: isolation of isothiazolidine-3-one (21) and the 2+2 adduct (22)

To stirred and ice cooled mixture of o-Phenylenediamine (0.157g, 1.45 mmol) and triethylamine (0.45 mL, 3.2 mmol) in dry CH_2Cl_2 (40 mL) was added 2,2'-dithiodibenzoyl chloride (0.5g, 1.457 mmol) in CH_2Cl_2 (20 mL) dropwise. The reaction mixture was left stirred at room temperature for 2 days, washed successively with cold saturated $NaHCO_3$ (2 x 15 mL), distilled water (1 x 15 mL), dried ($MgSO_4$), evaporated *in vacuo* and chromatographed on silica gel. Elution with hexane - EtOAc (1:1) afforded **21** and **22**.

a) **21**

Yield : 33%

IR (neat) 3434, 3336, 1681, 1635, 1504, 1458, 1334

^{1}H NMR ($CDCl_3$) δ 2.83 (brs, 2H, NH_2), 6.86, 7.26 (dq, 4H, ArHs), 7.45 - 7.67 & 8.1 (m, d, 4H, ArHs)

FAB MS (m/z) (%): 243 (100) $(MH)^+$, 485 (5) $(2M+H)^+$, 507 (1) $(2M+Na)^+$

b) **22**

Yield : 5%

M.p. : 215 (dec)

IR (KBr) : 3472, 1662, 1605, 1526, 1451, 1315

^{1}H NMR ($CDCl_3$ - DMSO-d_6) δ 7.24 - 8.19 (m, 24H, ArHs), 9.93 - 10.12 (brm, 4H, NHs)

FAB MS (m/z) (%): 757 (22) $(MH)^+$

II.F. SPECTRA

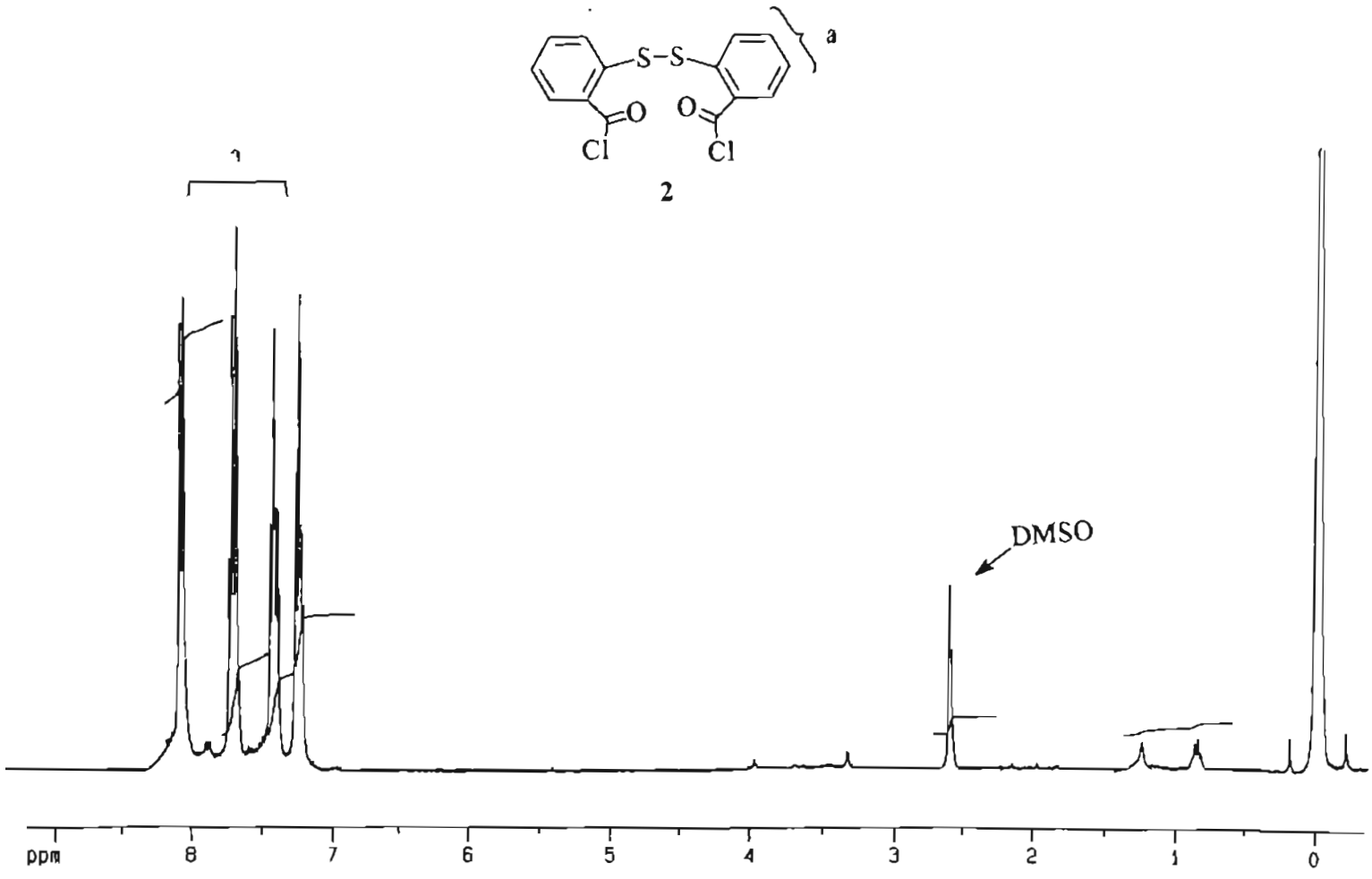

δ (300 MHz, $CDCl_3$ - DMSO-d_6)

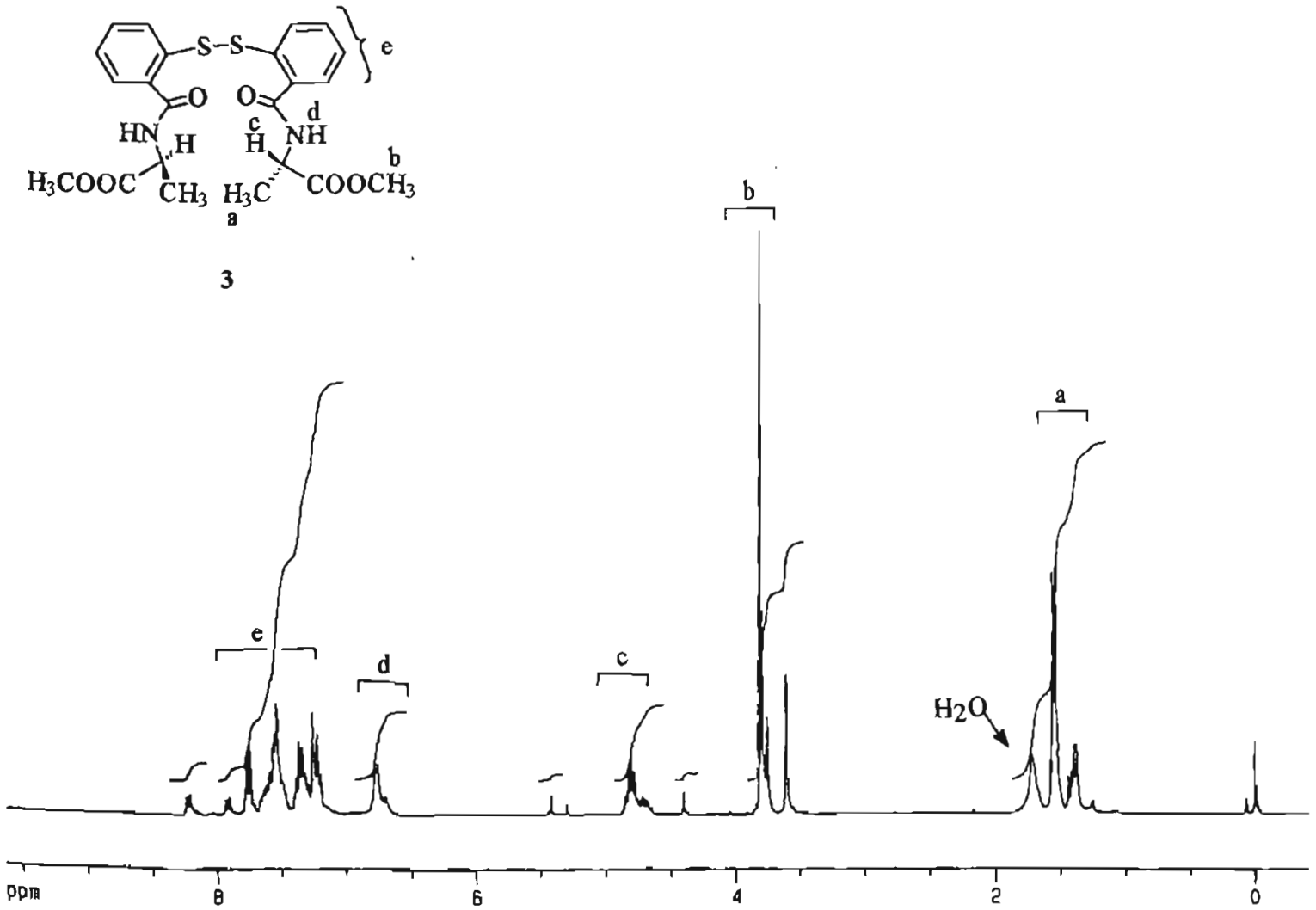

δ (300 MHz, $CDCl_3$)

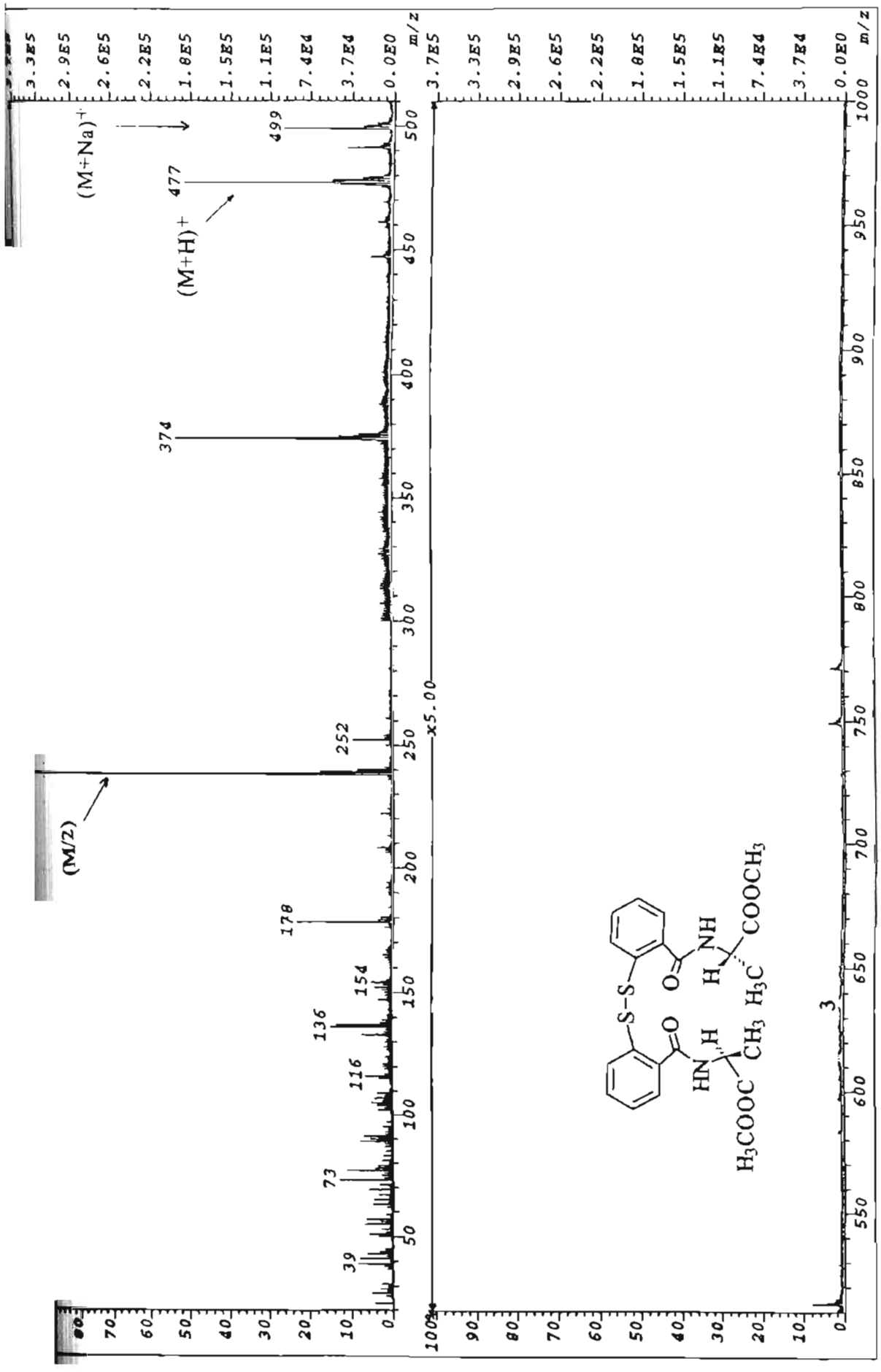

FAB mass spectrum

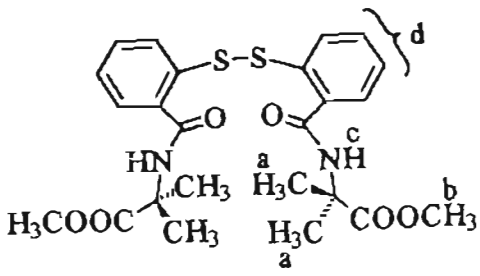

4

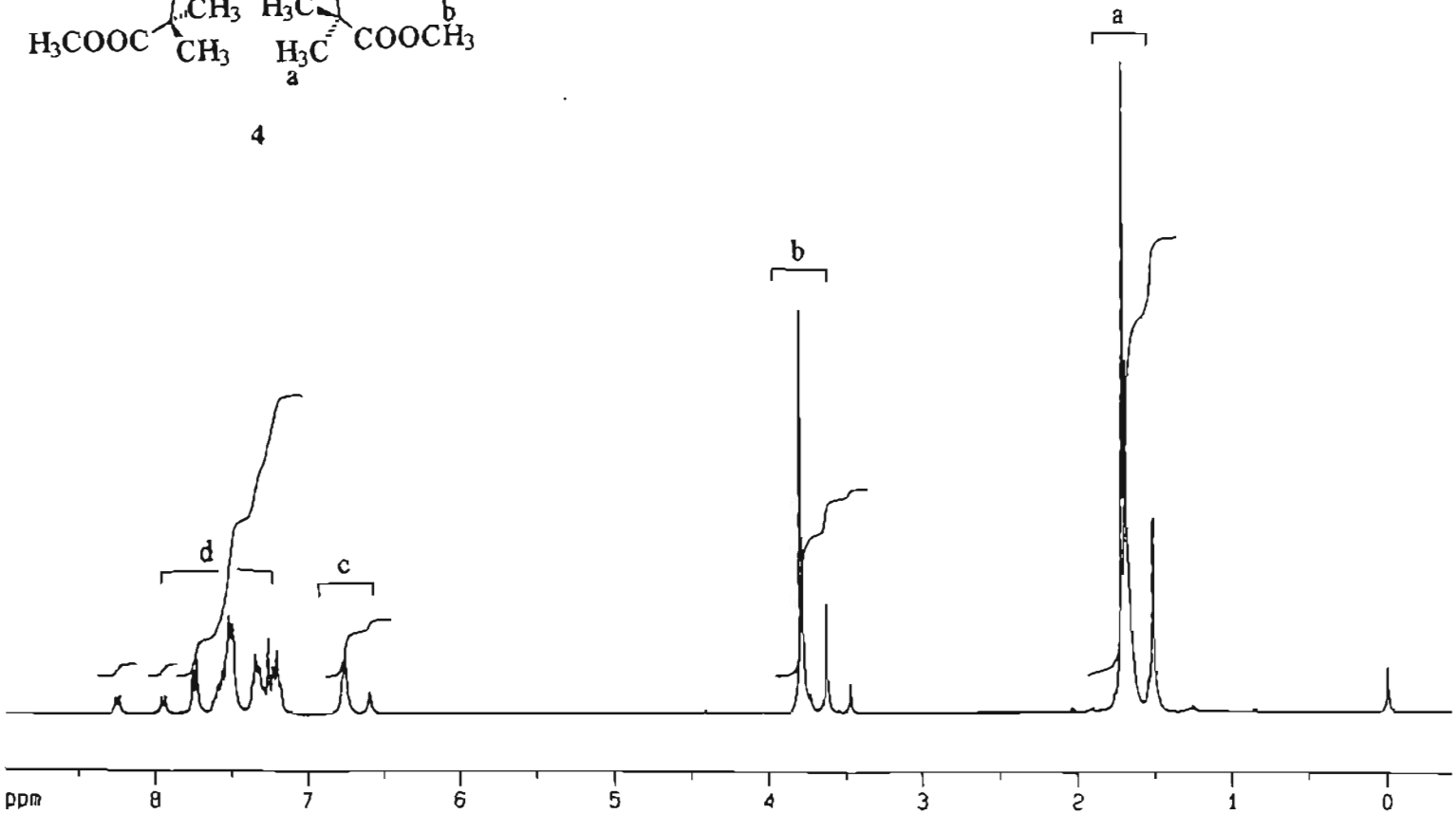

δ (300 MHz, $CDCl_3$)

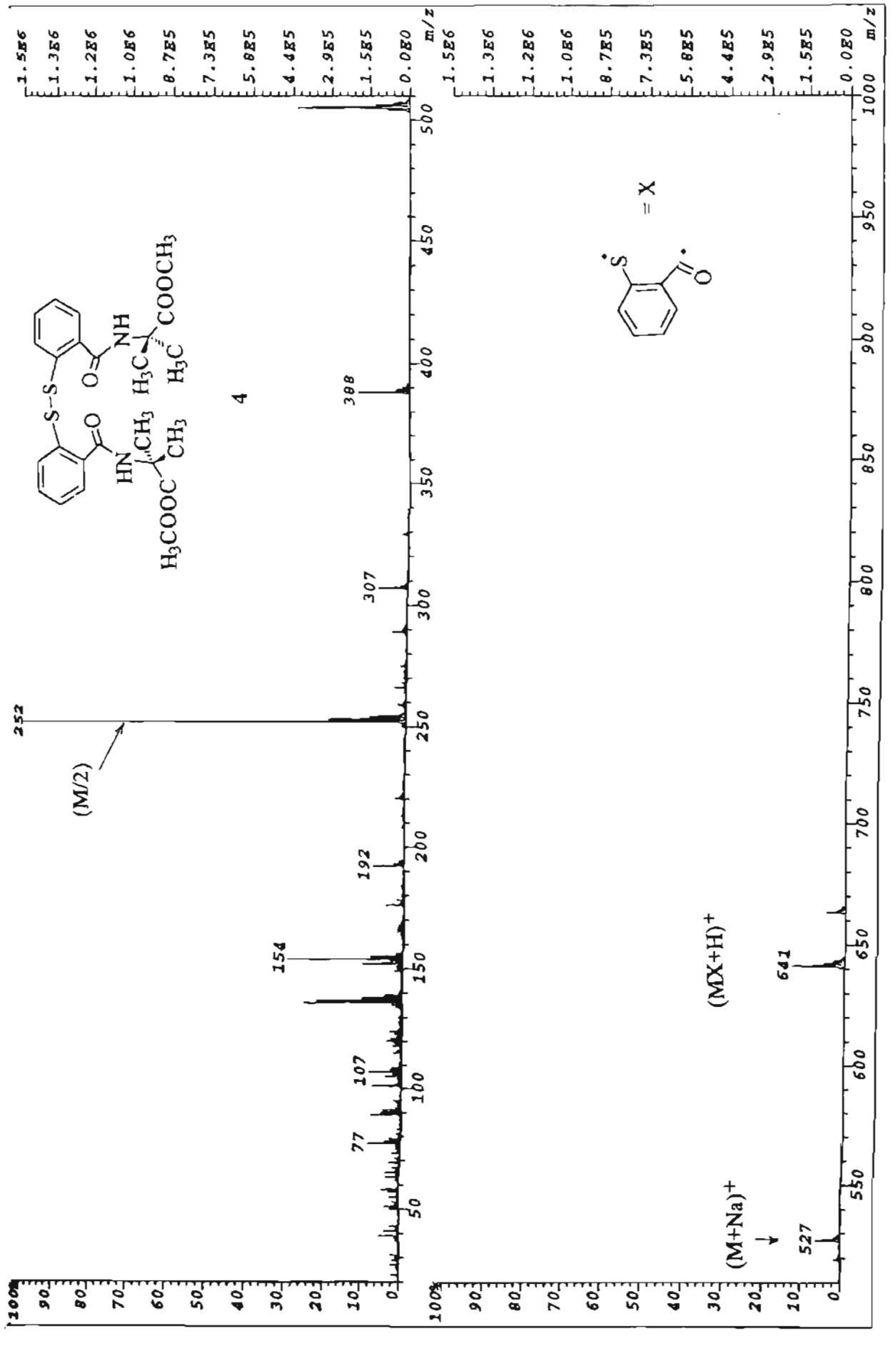

FAB mass spectrum

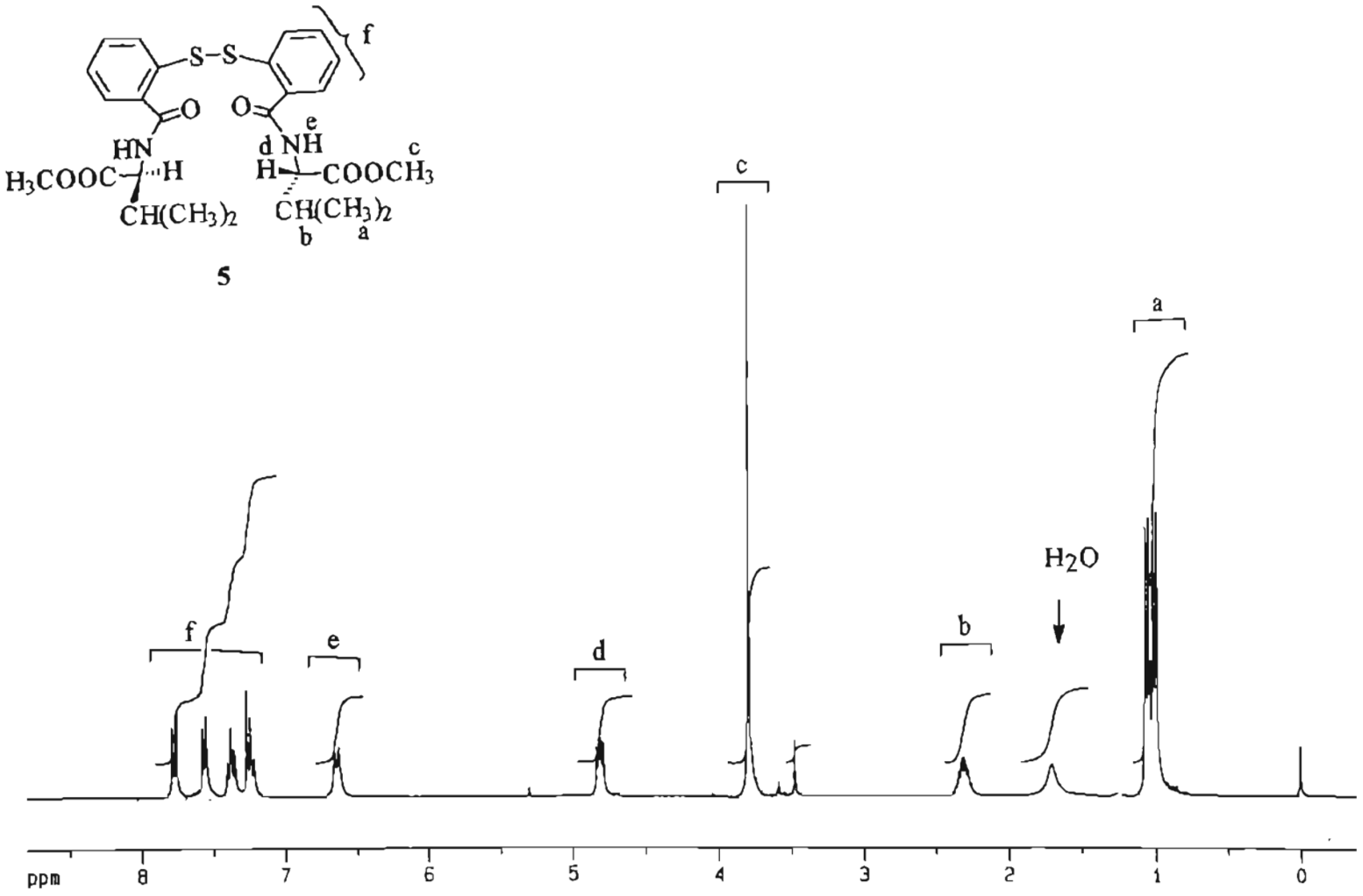

δ (300 MHz, $CDCl_3$)

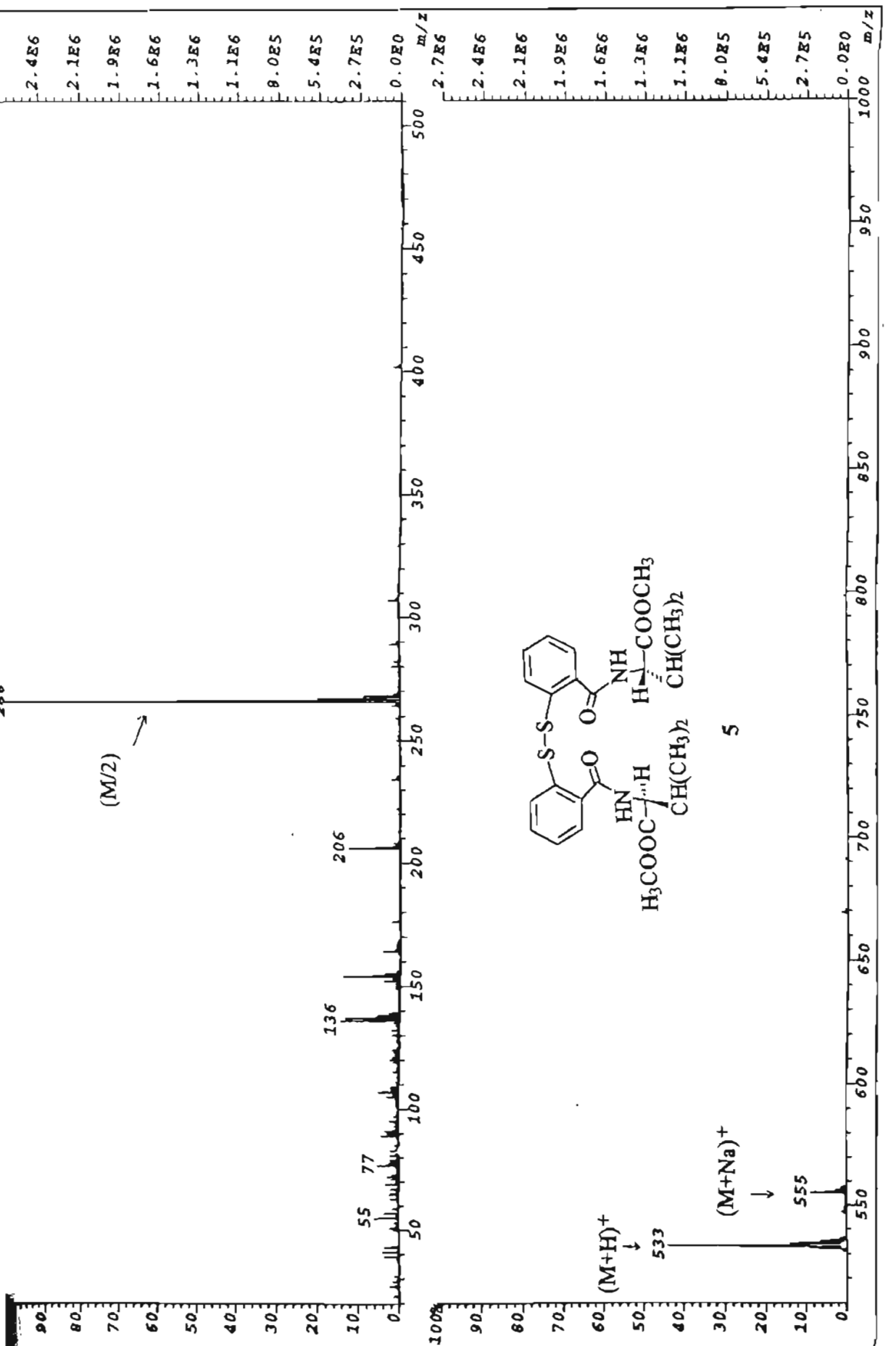

FAB mass spectrum

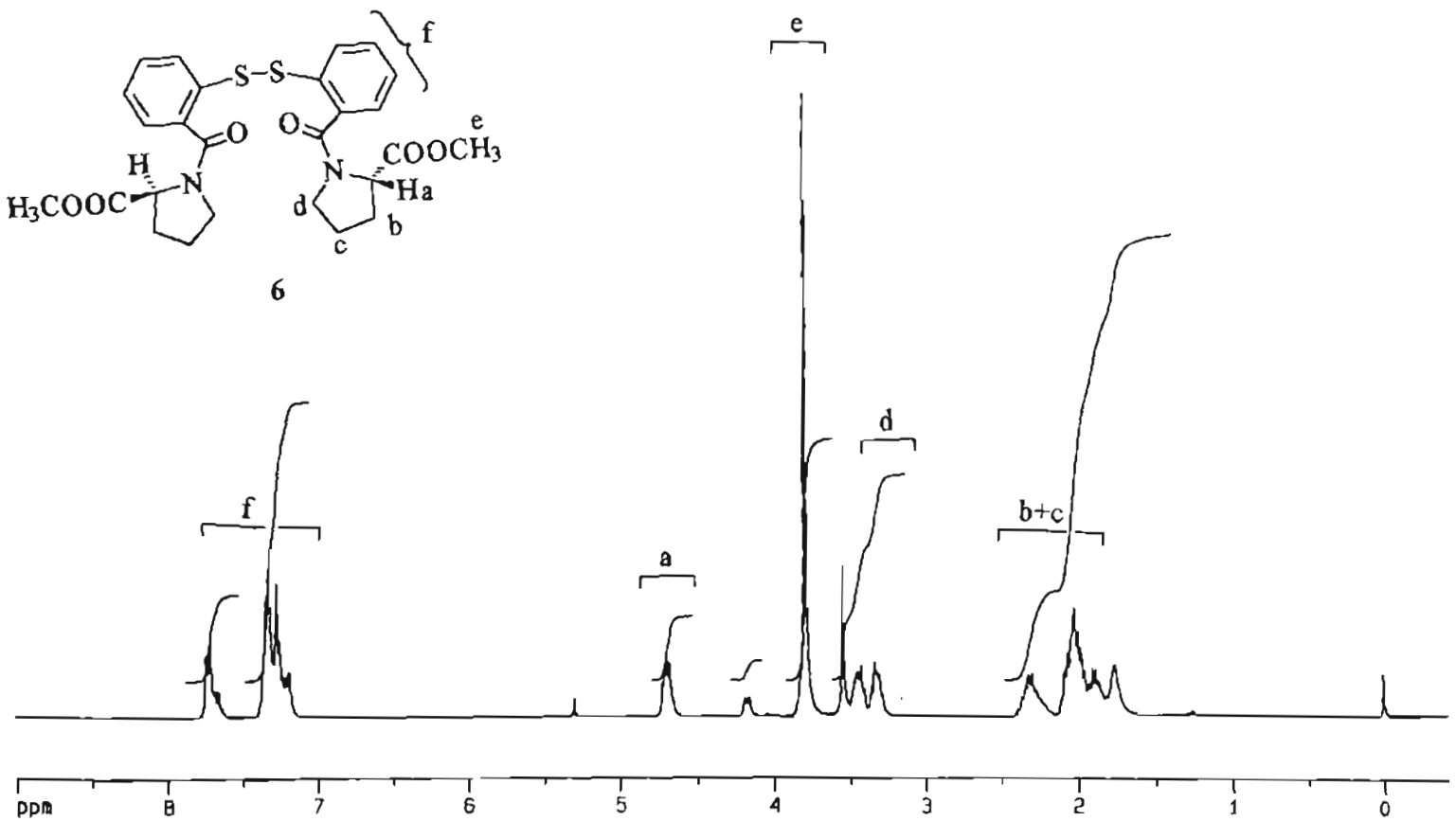

δ (300 MHz, $CDCl_3$)

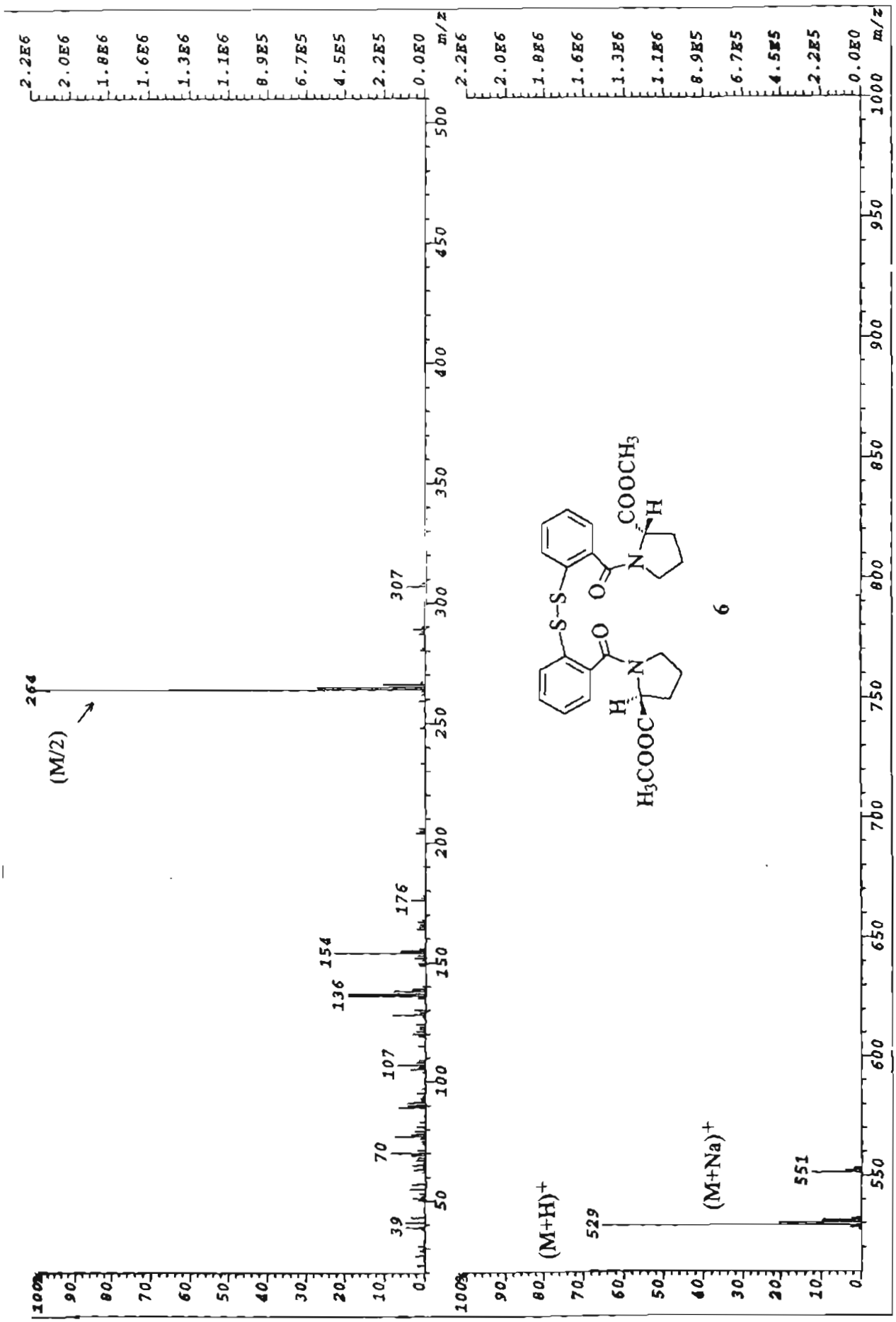

FAB mass spectrum

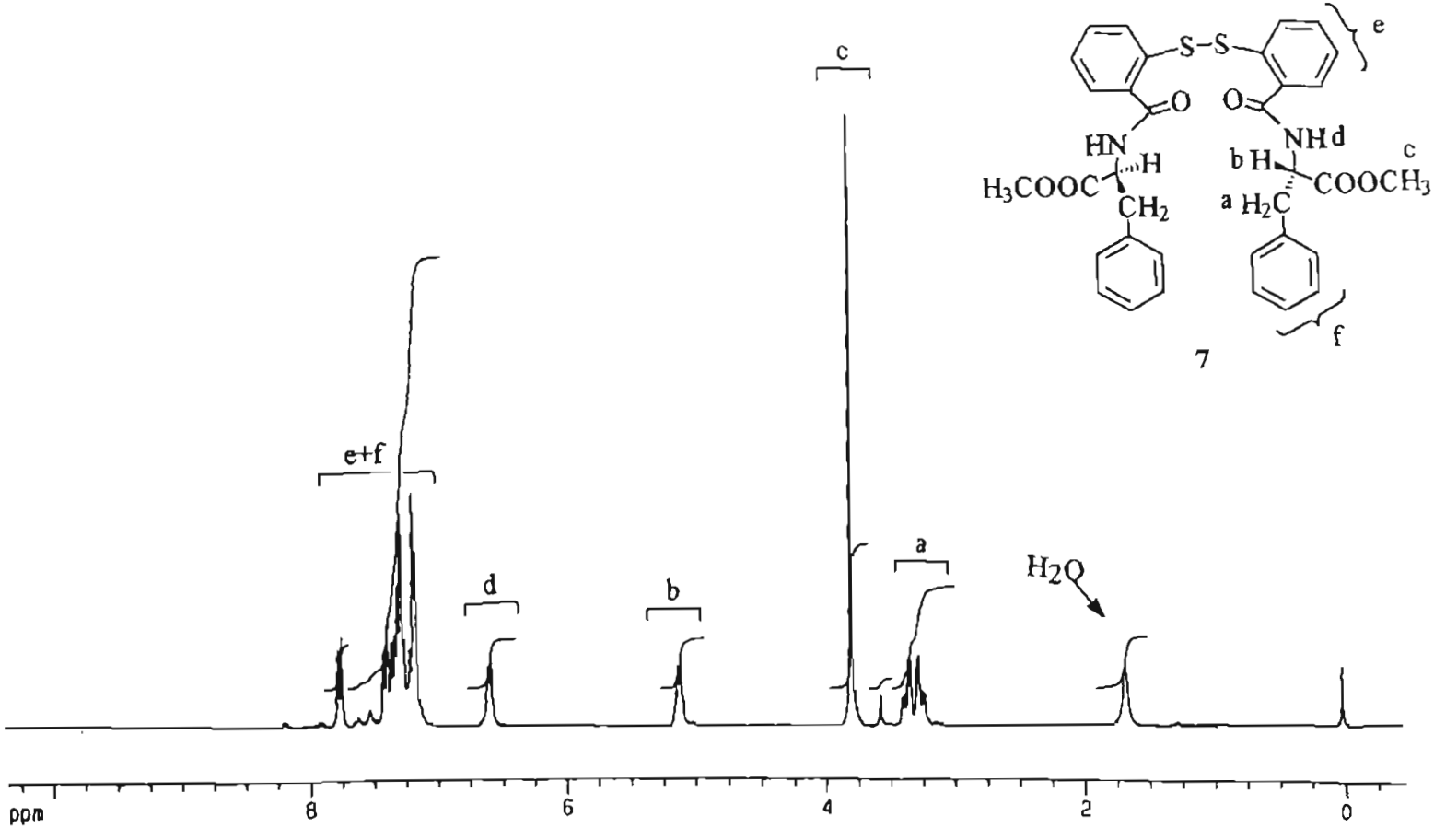

7

δ (300 MHz, $CDCl_3$)

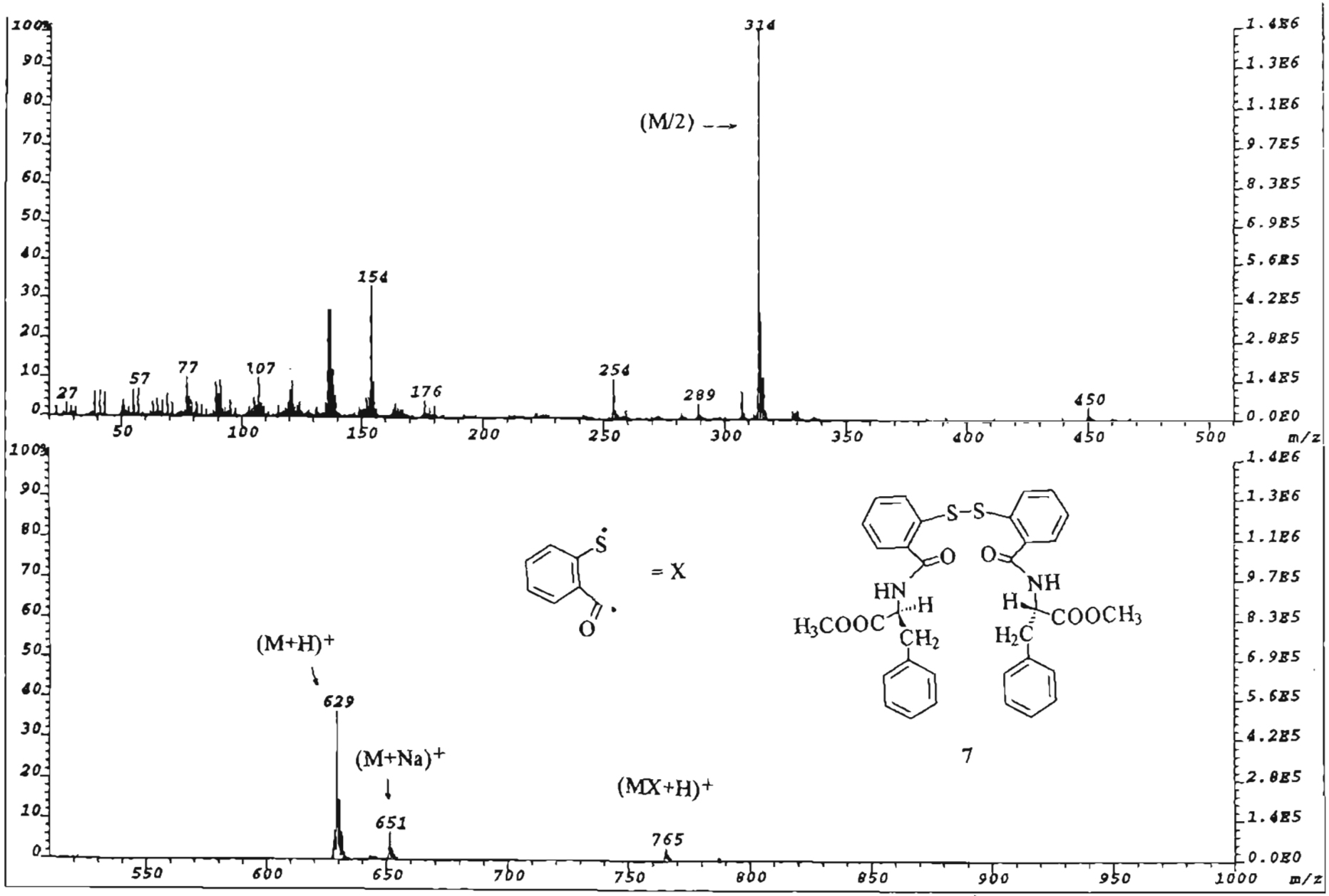

FAB mass spectrum

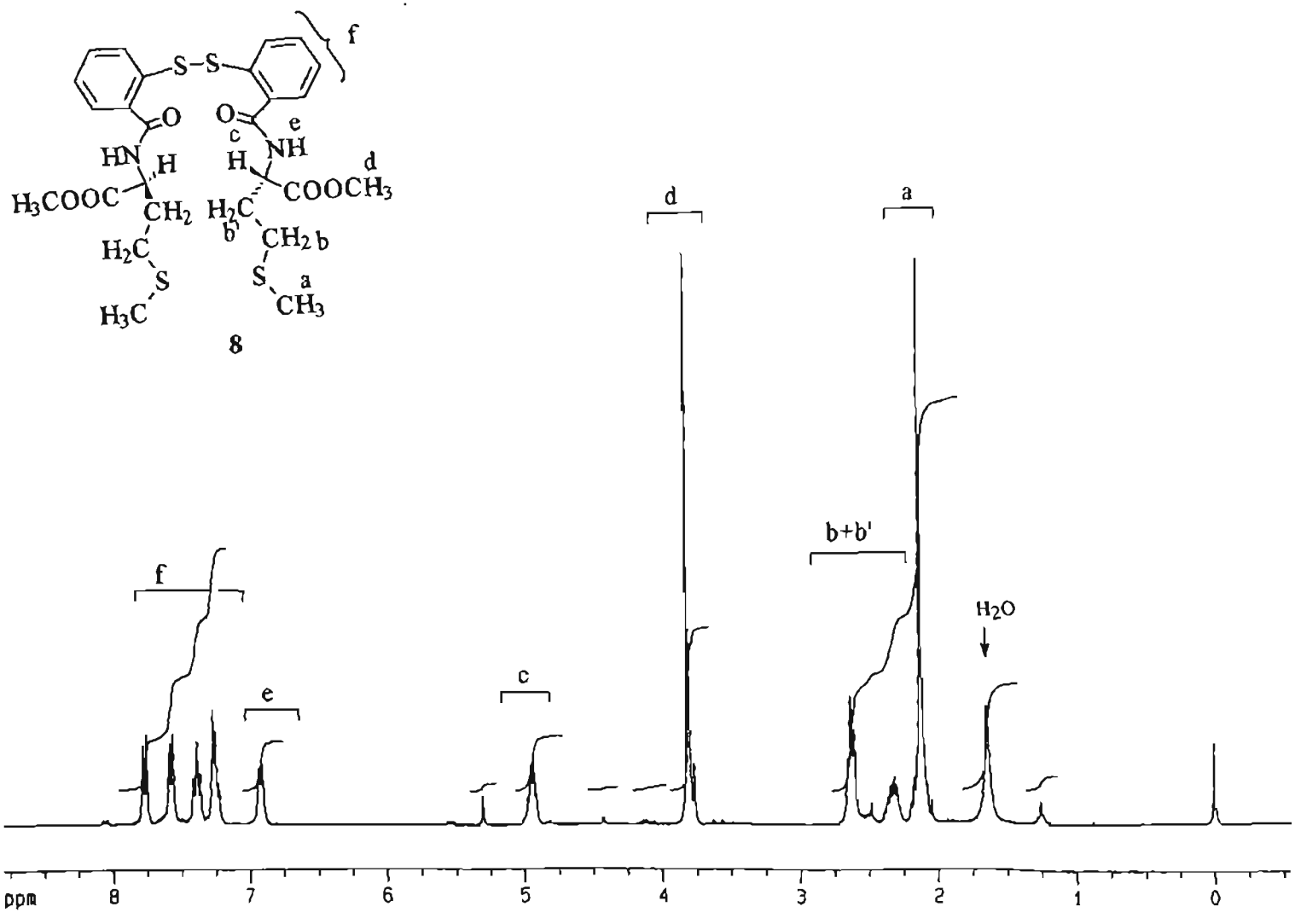

δ (300 MHz, $CDCl_3$)

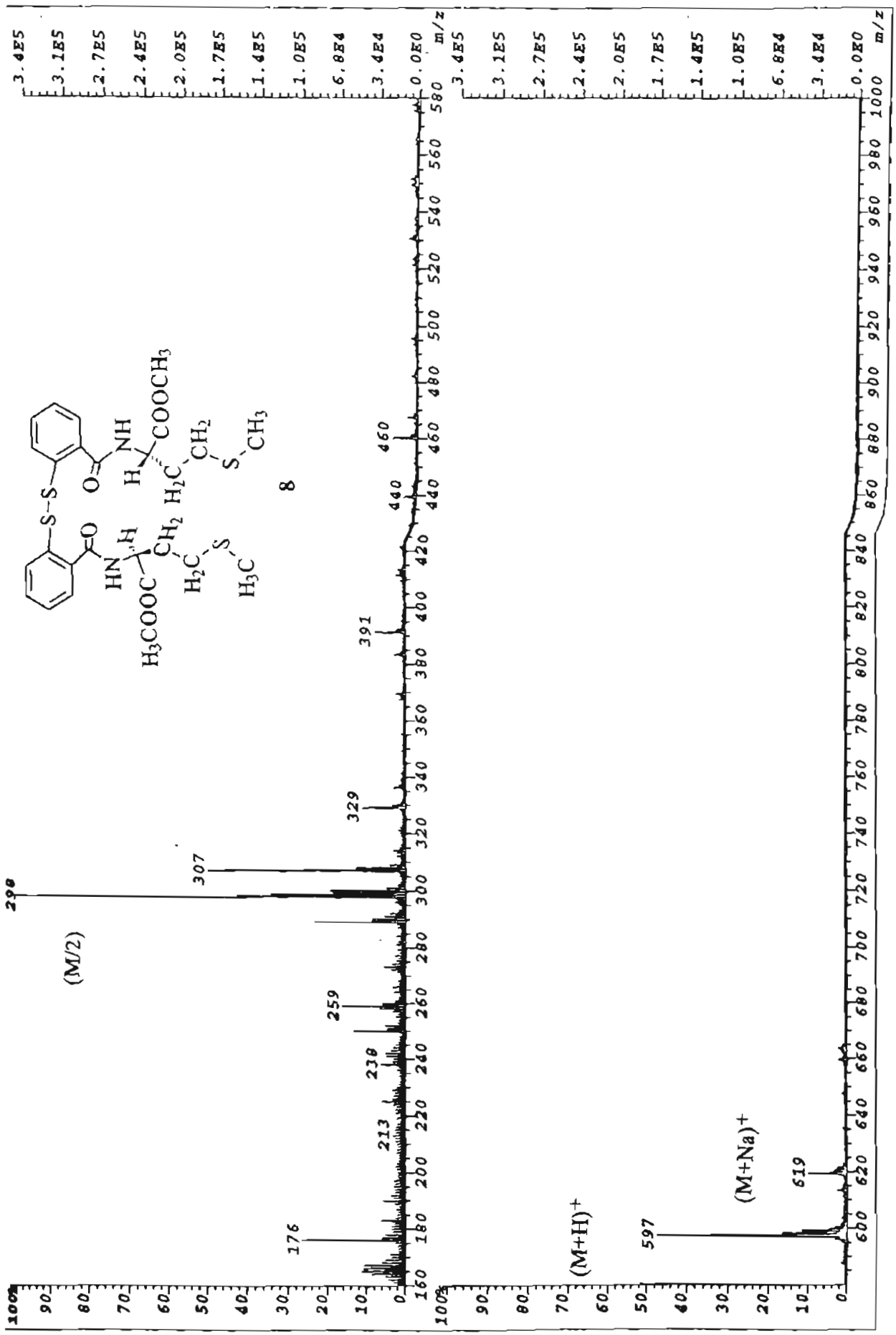

FAB mass spectrum

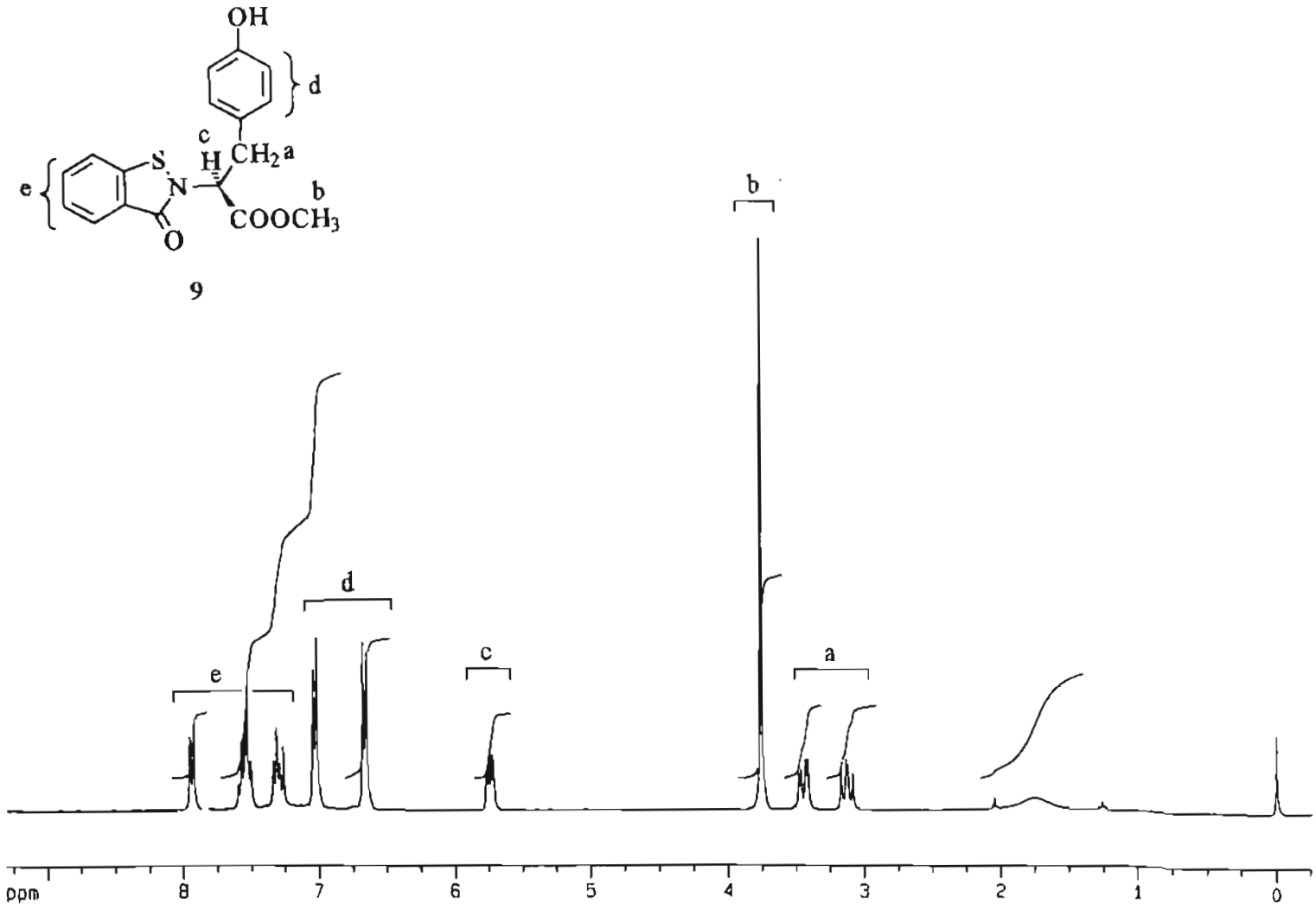

δ (300 MHz, $CDCl_3$)

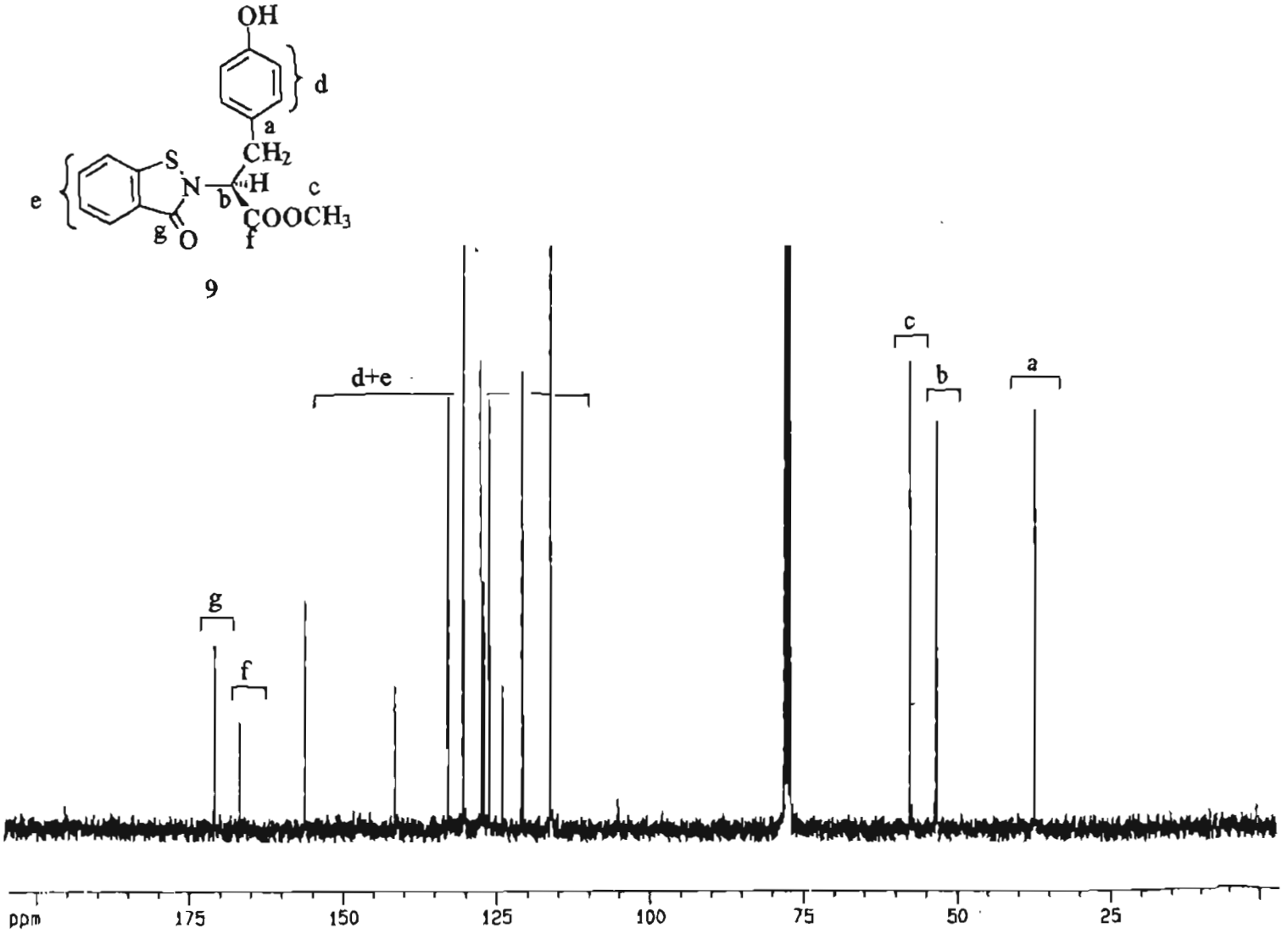

δ (300 MHz, $CDCl_3$)

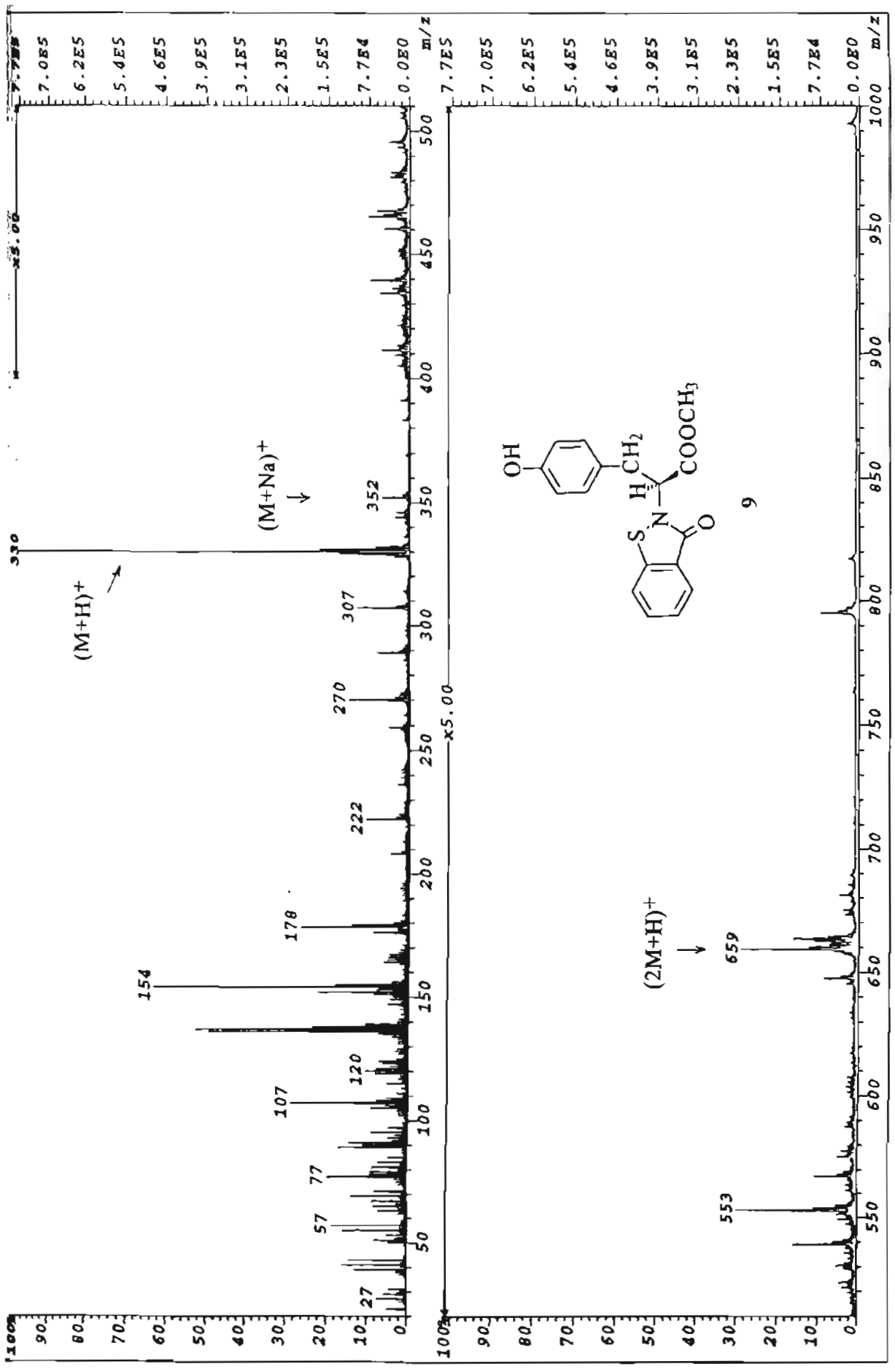

FAB mass spectrum

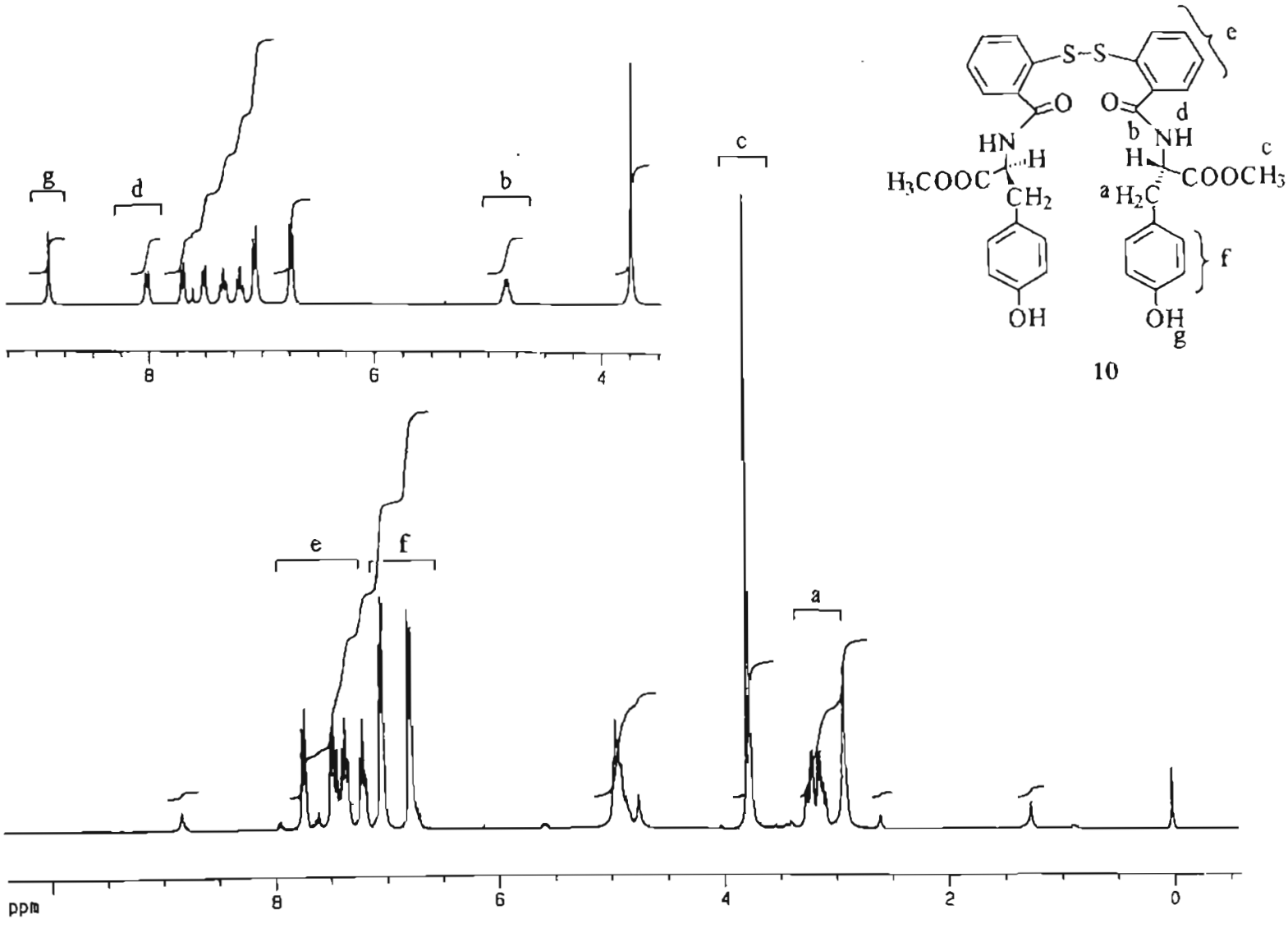

δ (300 MHz, $CDCl_3$)

10

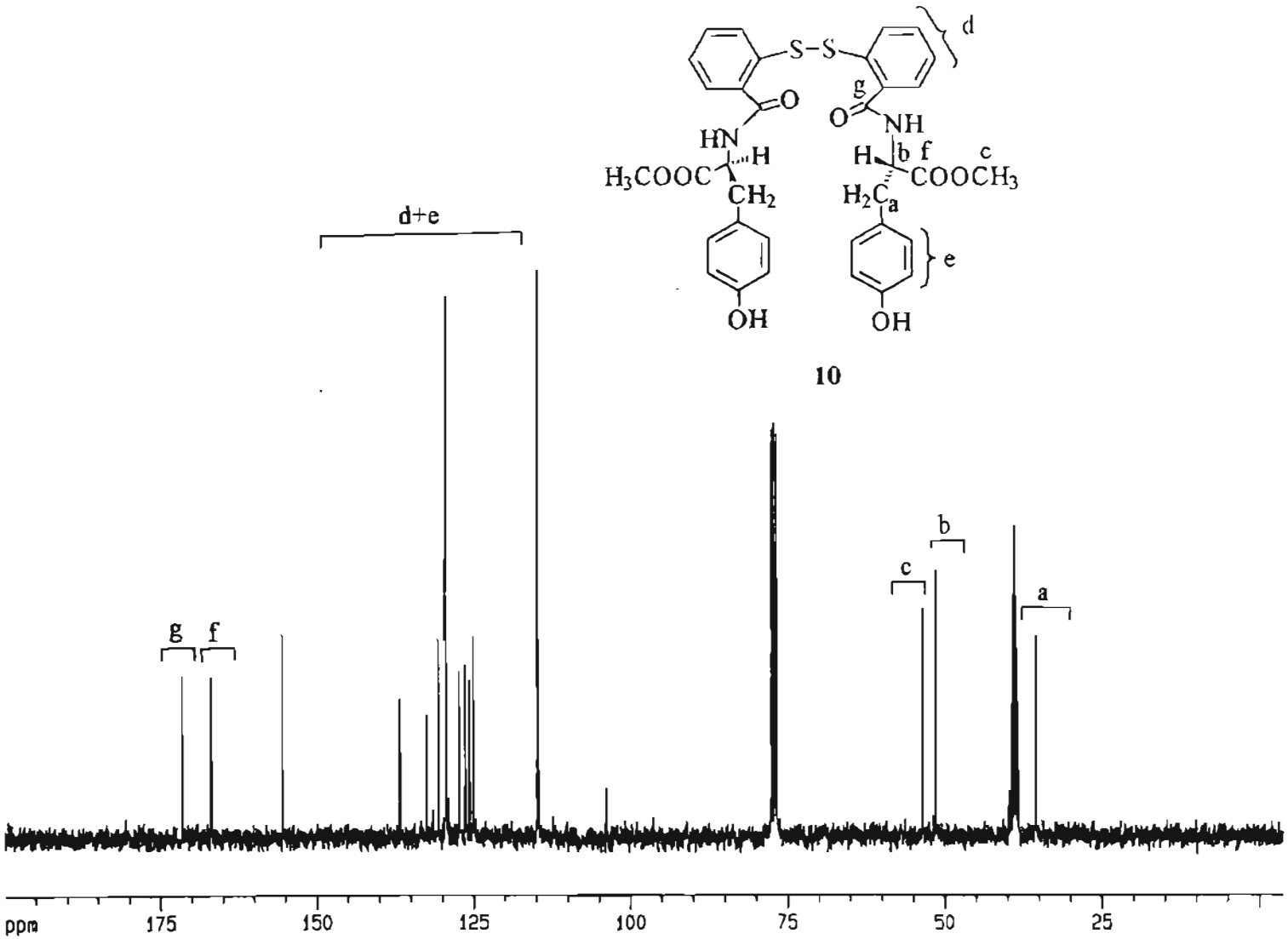

δ (300 MHz, $CDCl_3$ - DMSO-d_6)

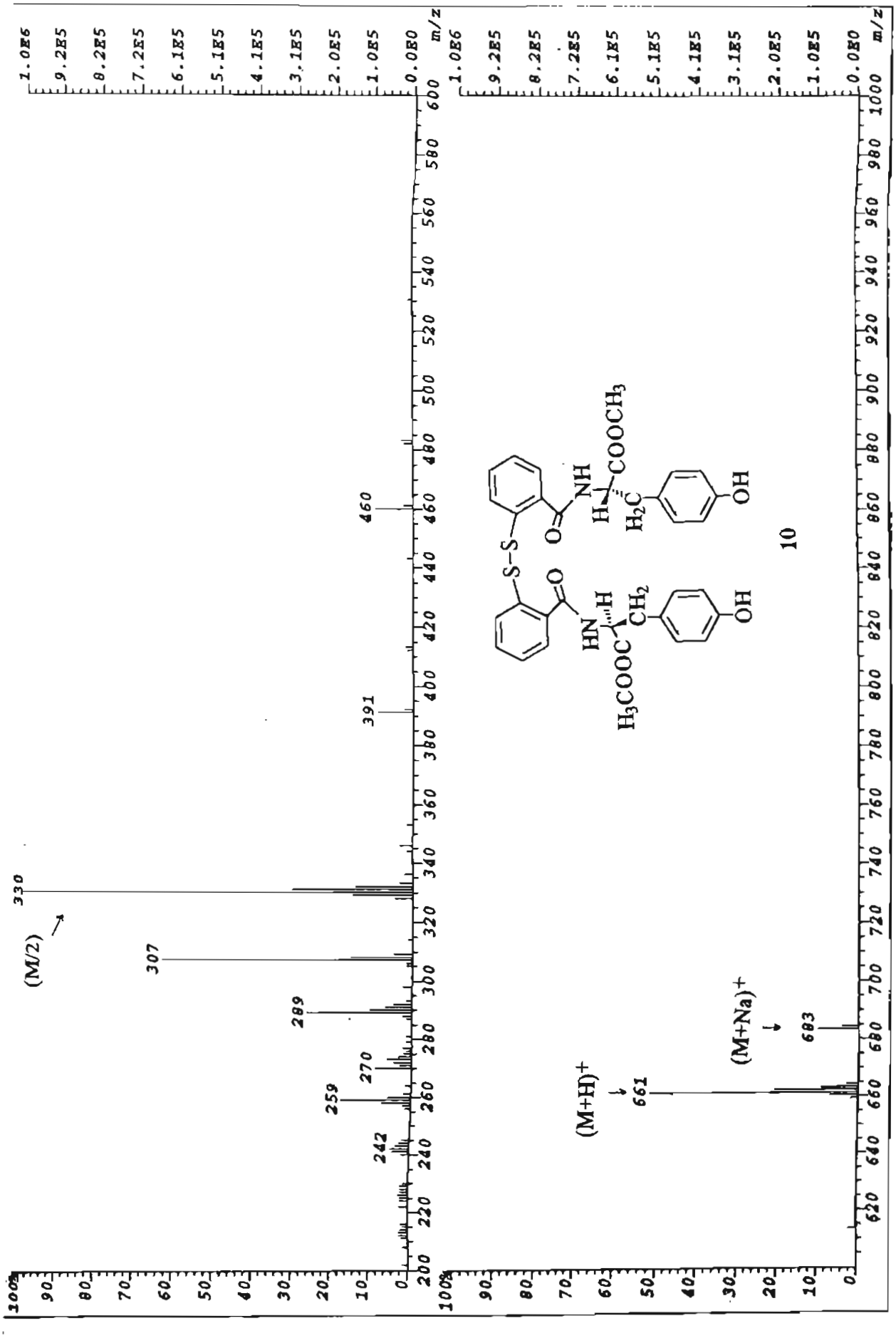

FAB mass spectrum

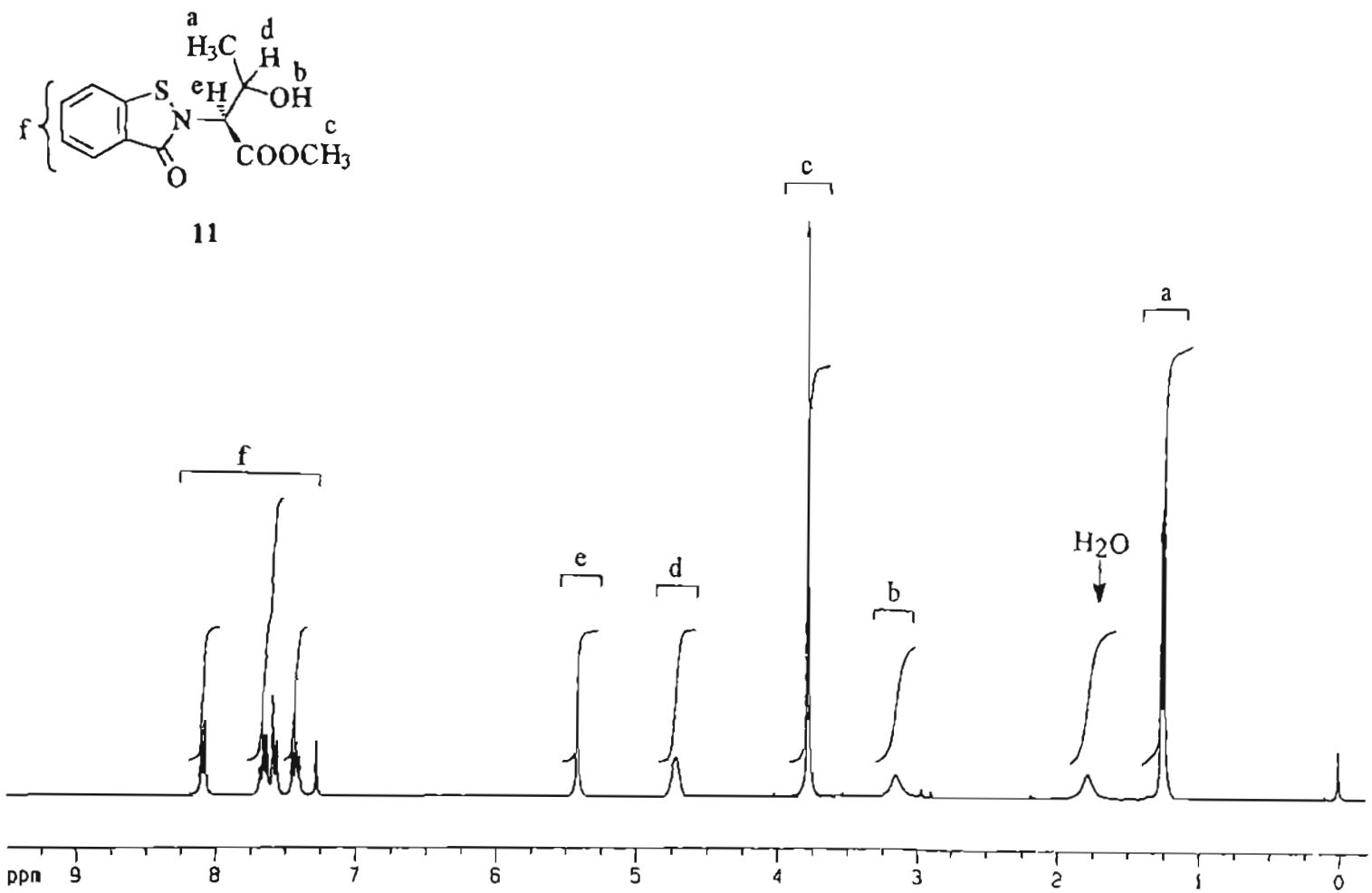

δ (300 MHz, $CDCl_3$)

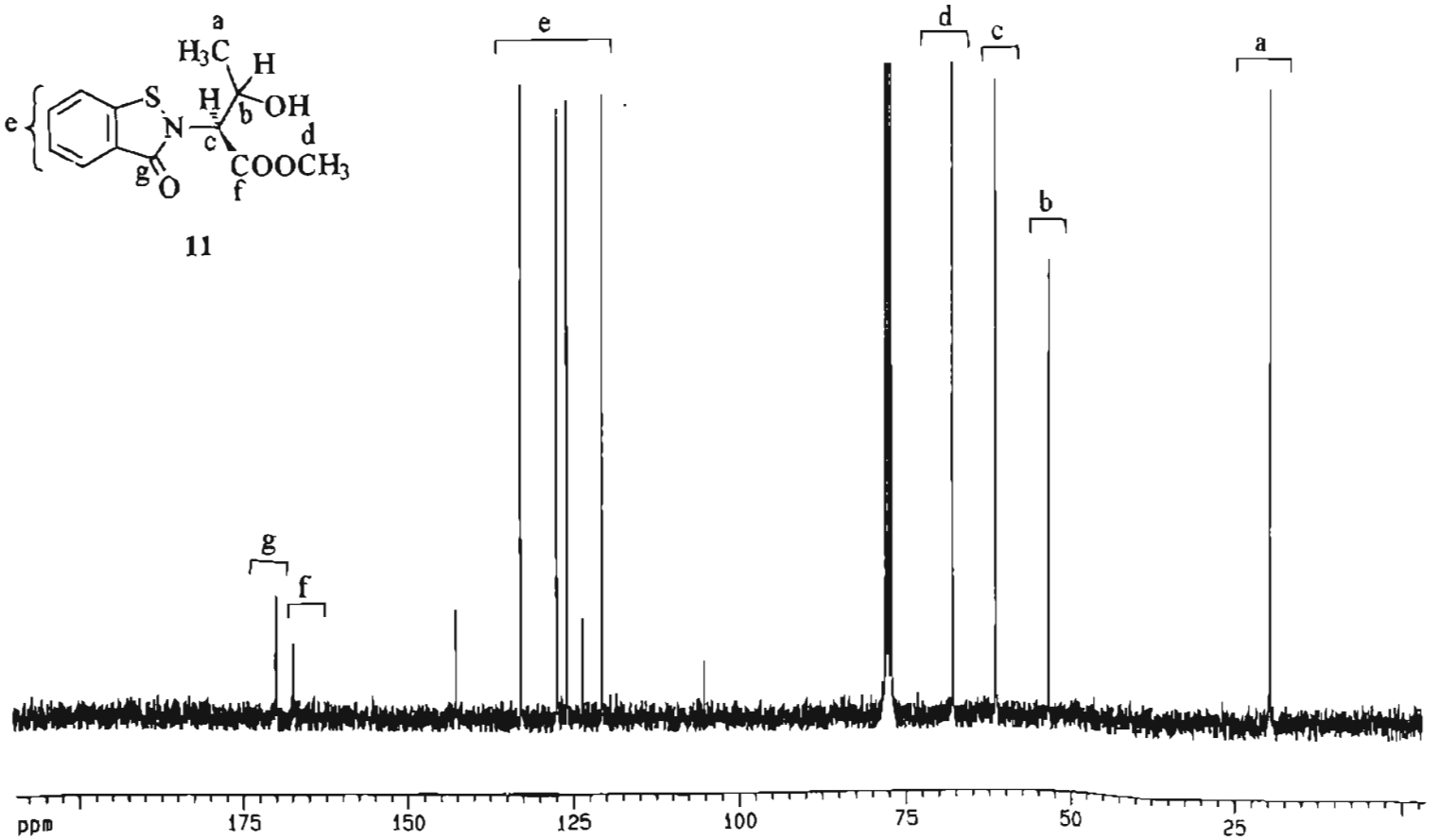

δ (300 MHz, $CDCl_3$)

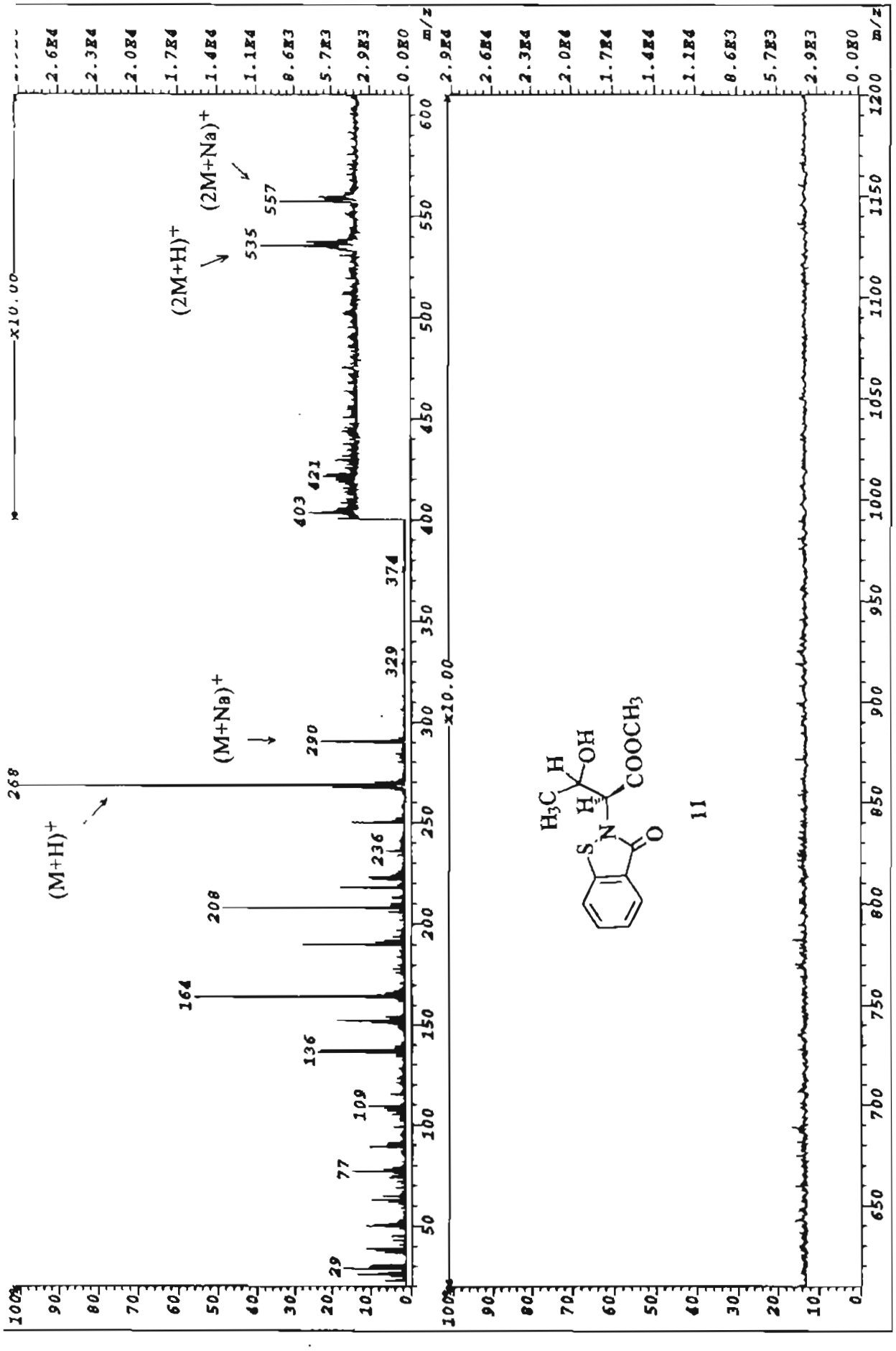

FAB mass spectrum

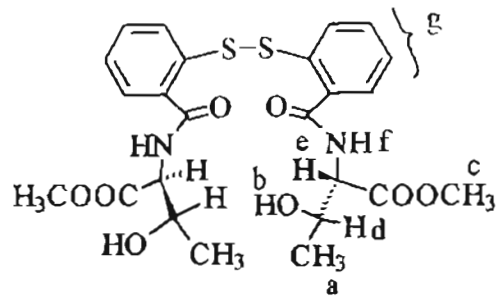

12

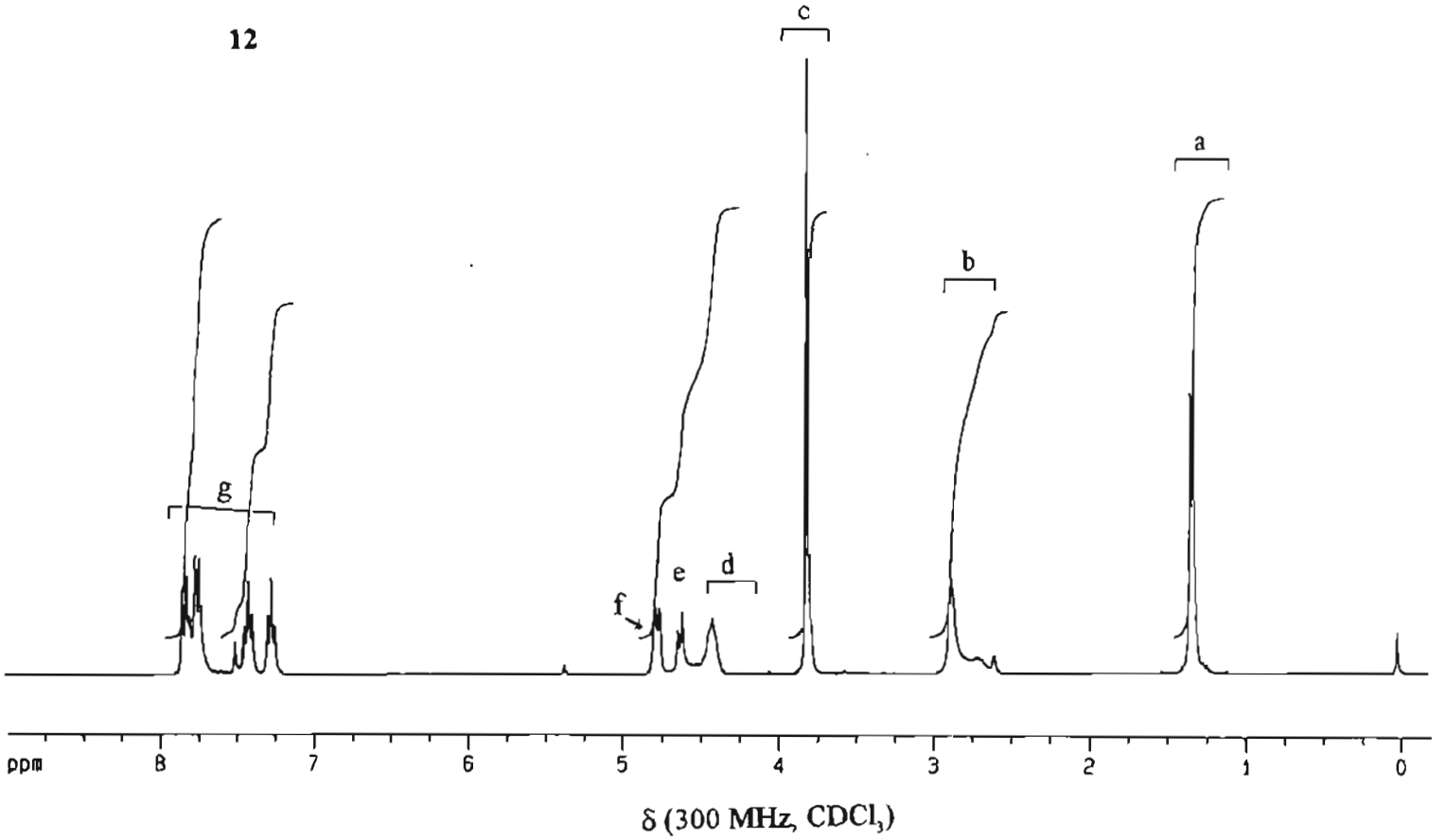

δ (300 MHz, $CDCl_3$)

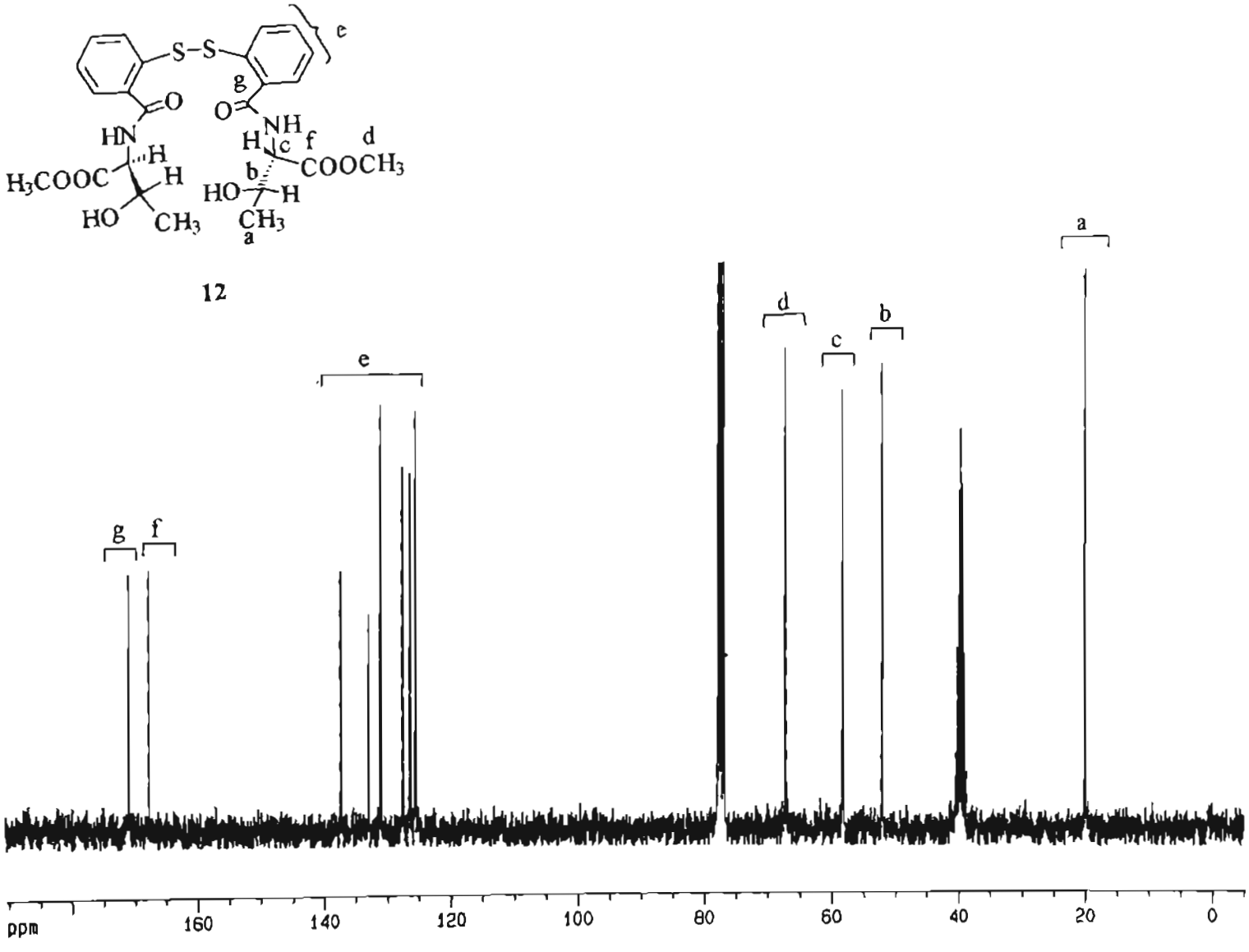

12

δ (300 MHz, $CDCl_3$ - DMSO-d_6)

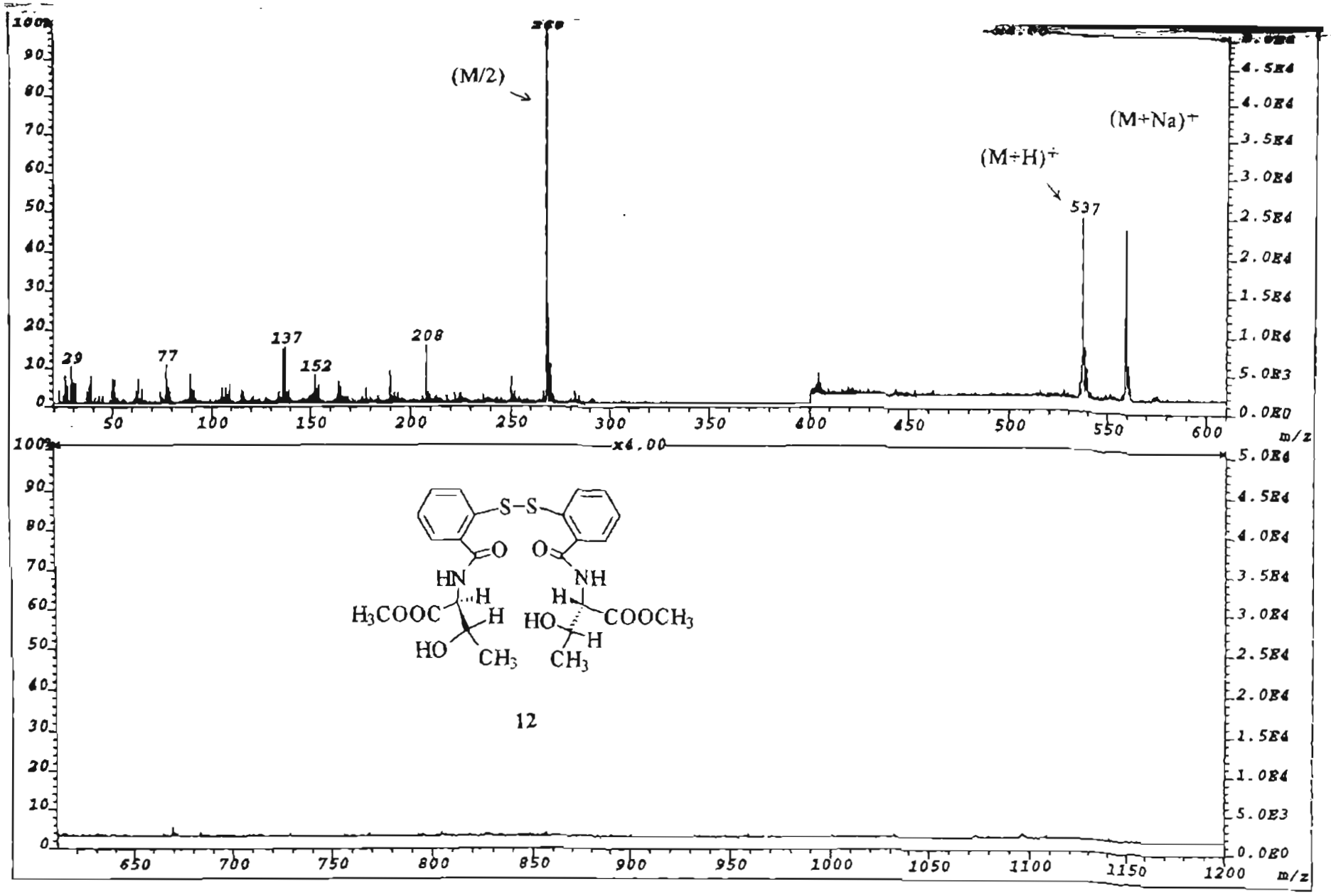

12

FAB mass spectrum

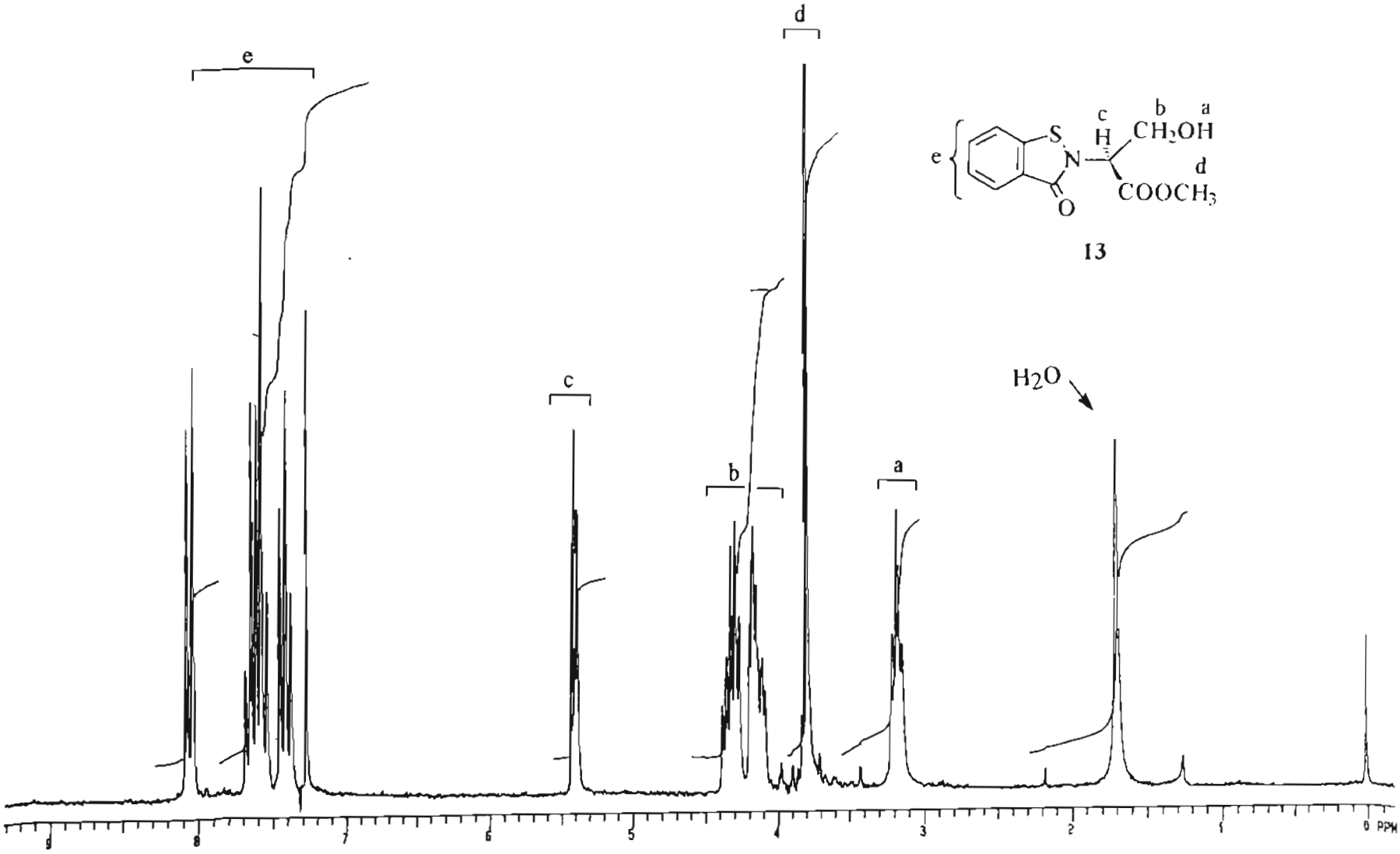

13

δ (200 MHz, $CDCl_3$)

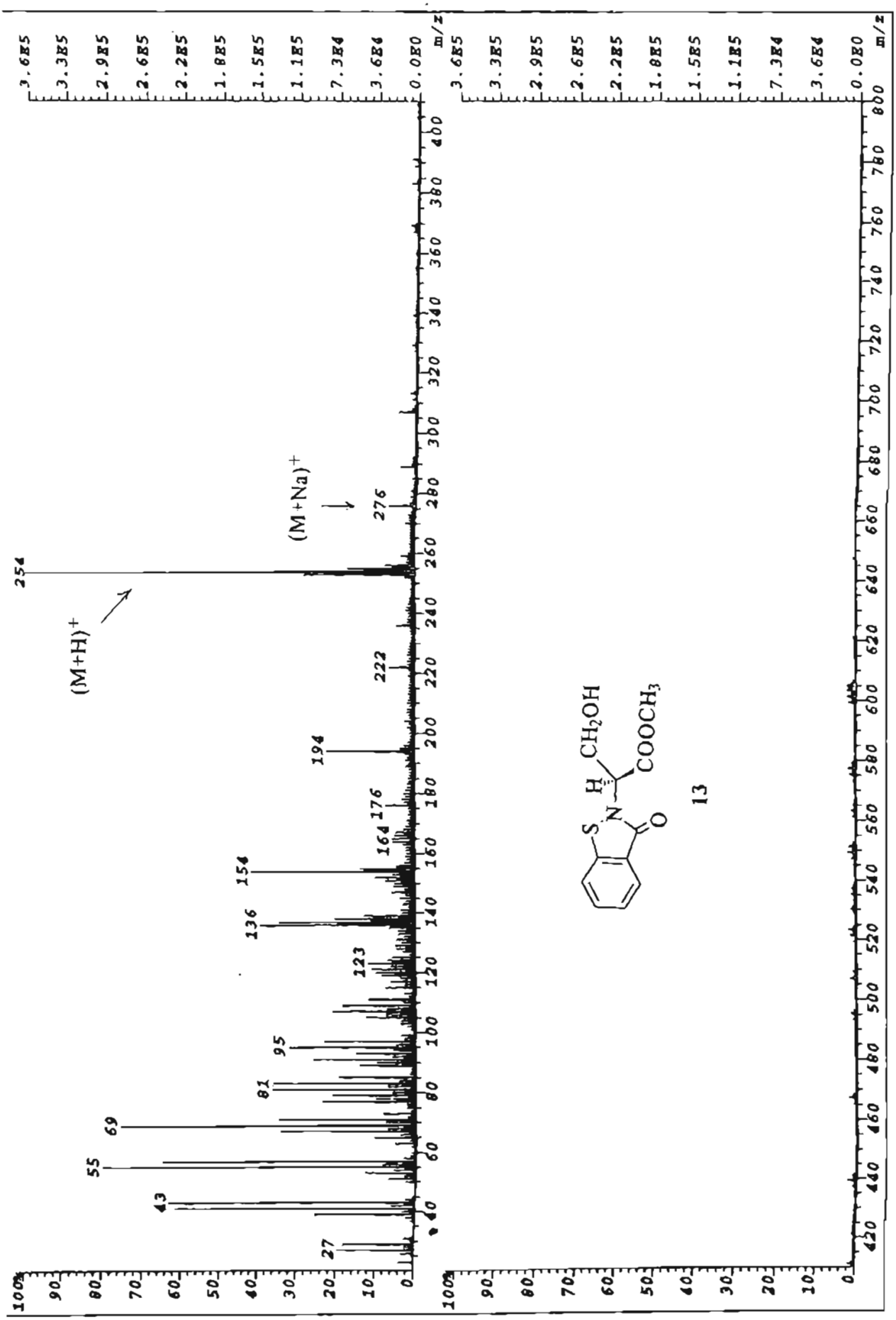

FAB mass spectrum

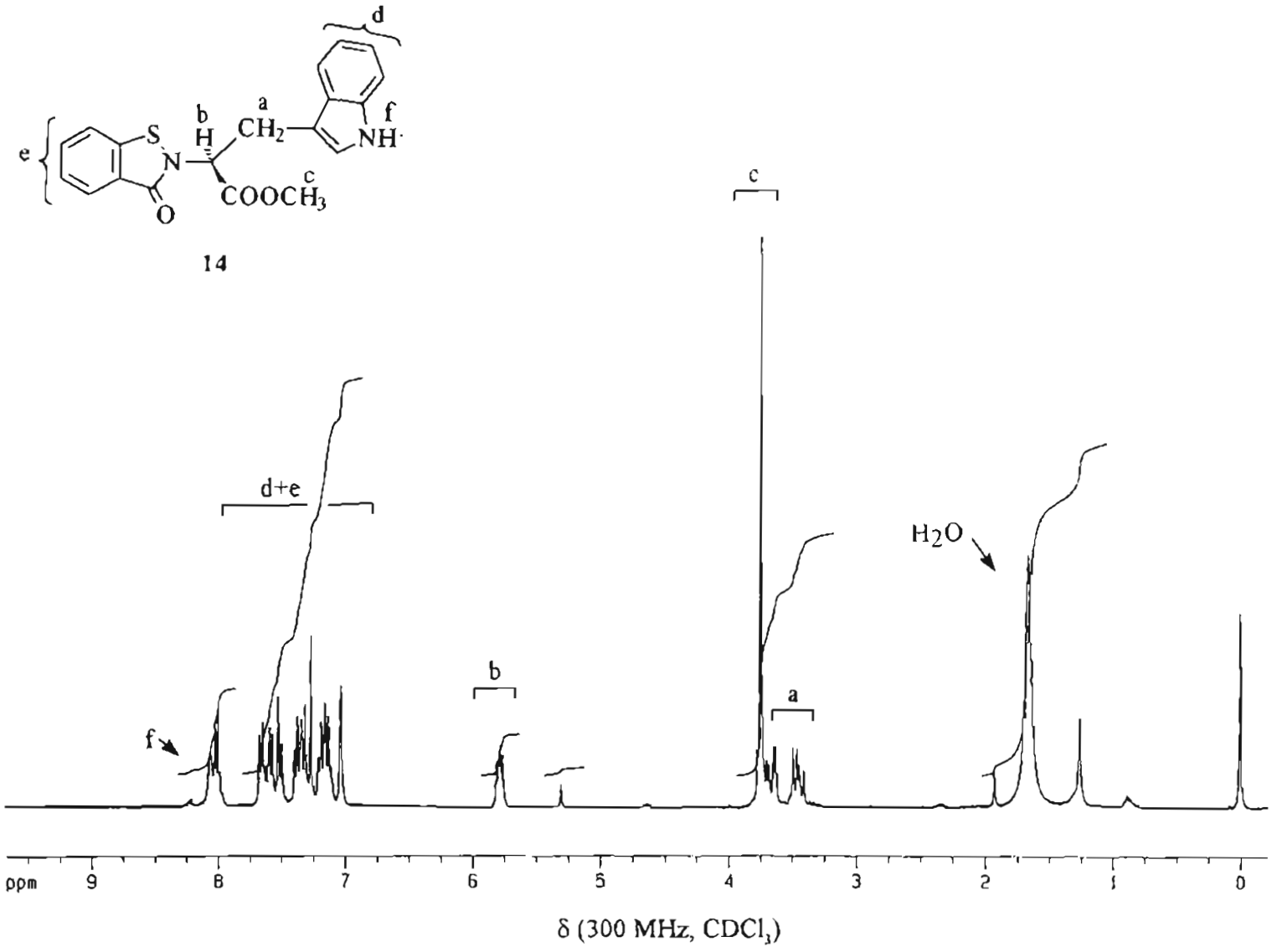

δ (300 MHz, $CDCl_3$)

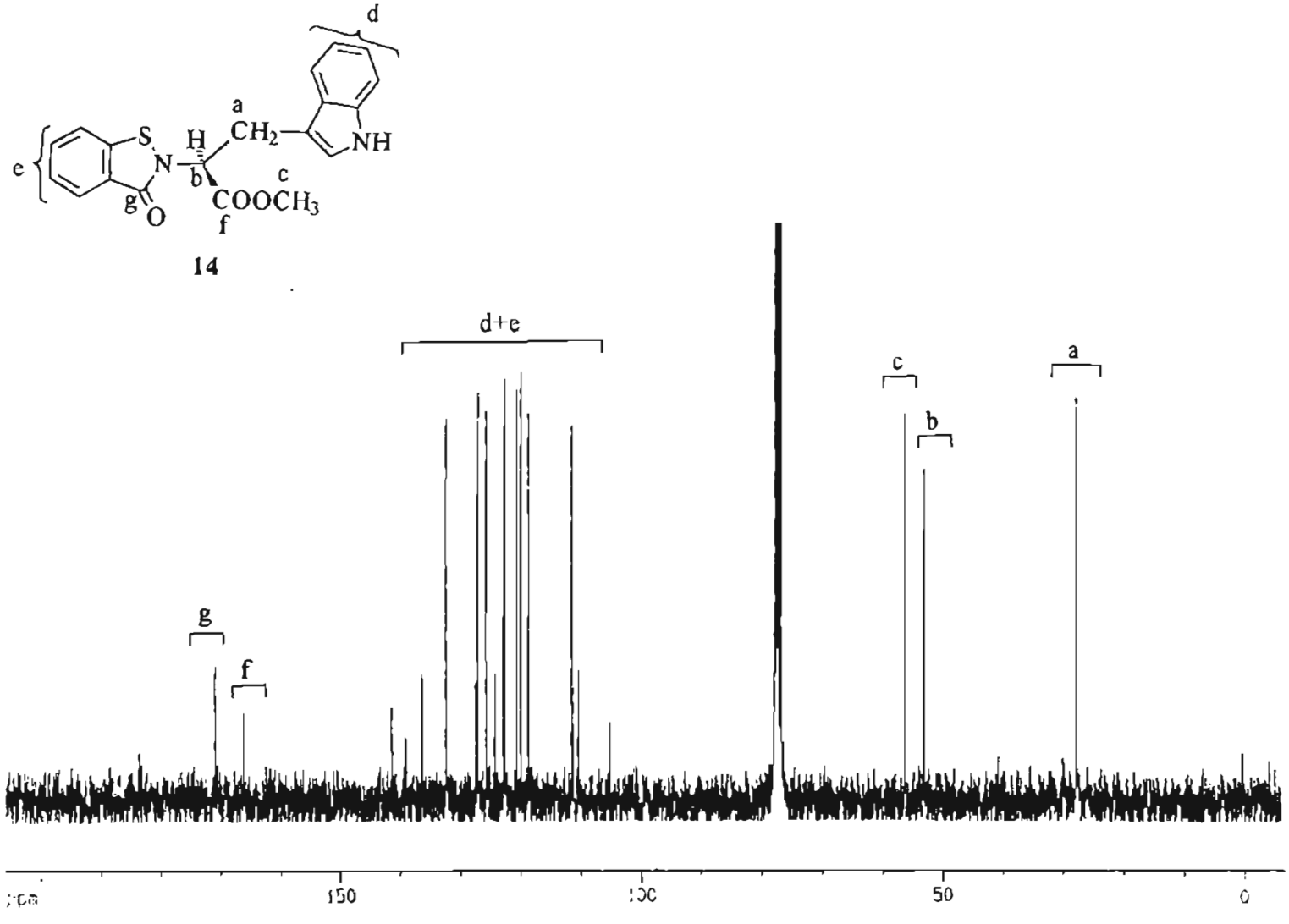
d
a
CH2
NH
S
N
H
b
c
COOCH3
f
e
g
O
14
d+e
c
a
b
g
f
150
100
50
0
δ (300 MHz, CDCl3)

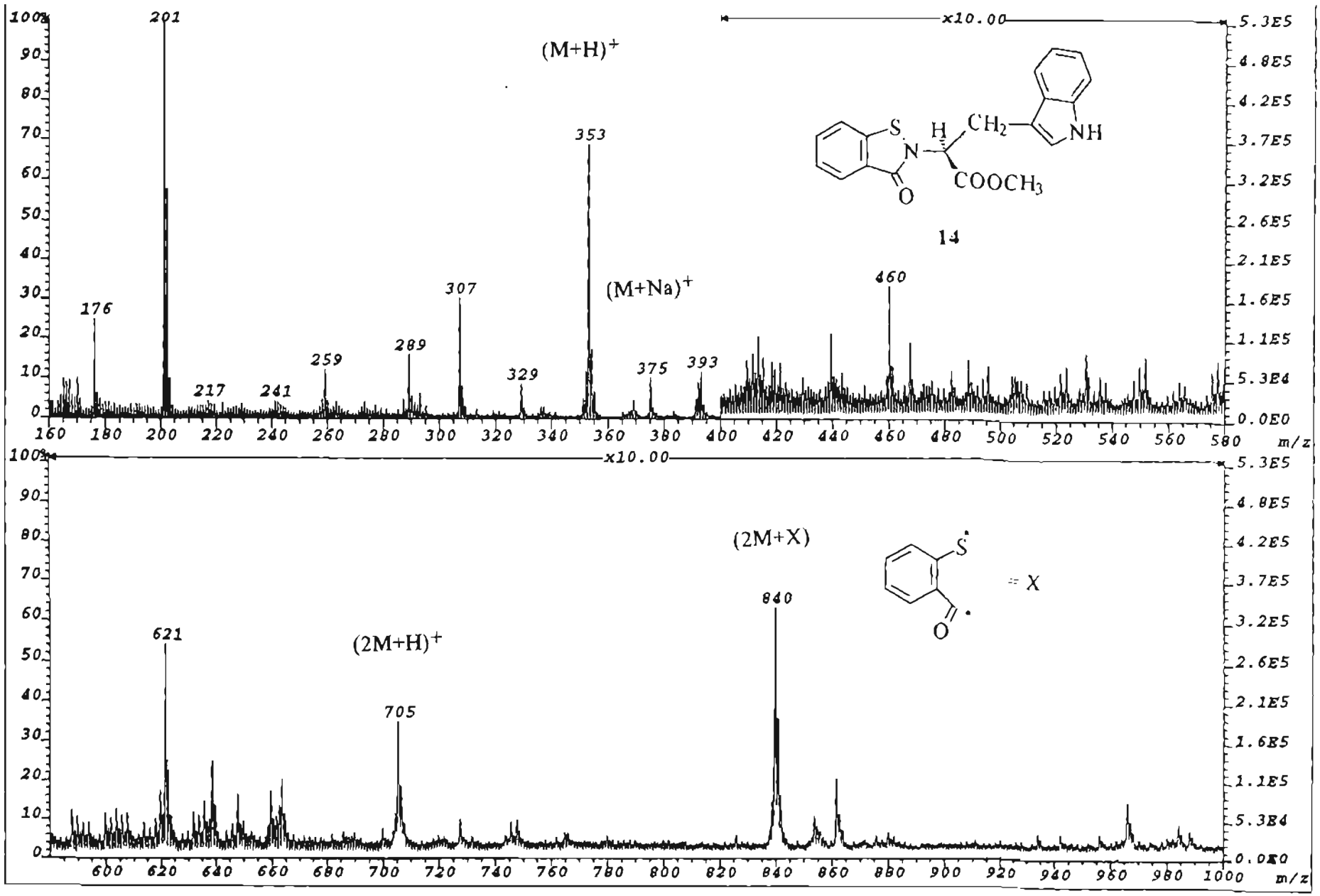

FAB mass spectrum

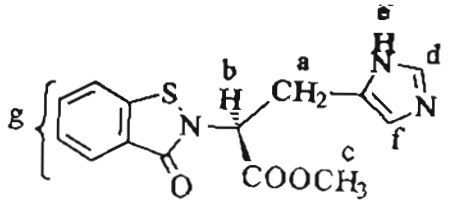

15

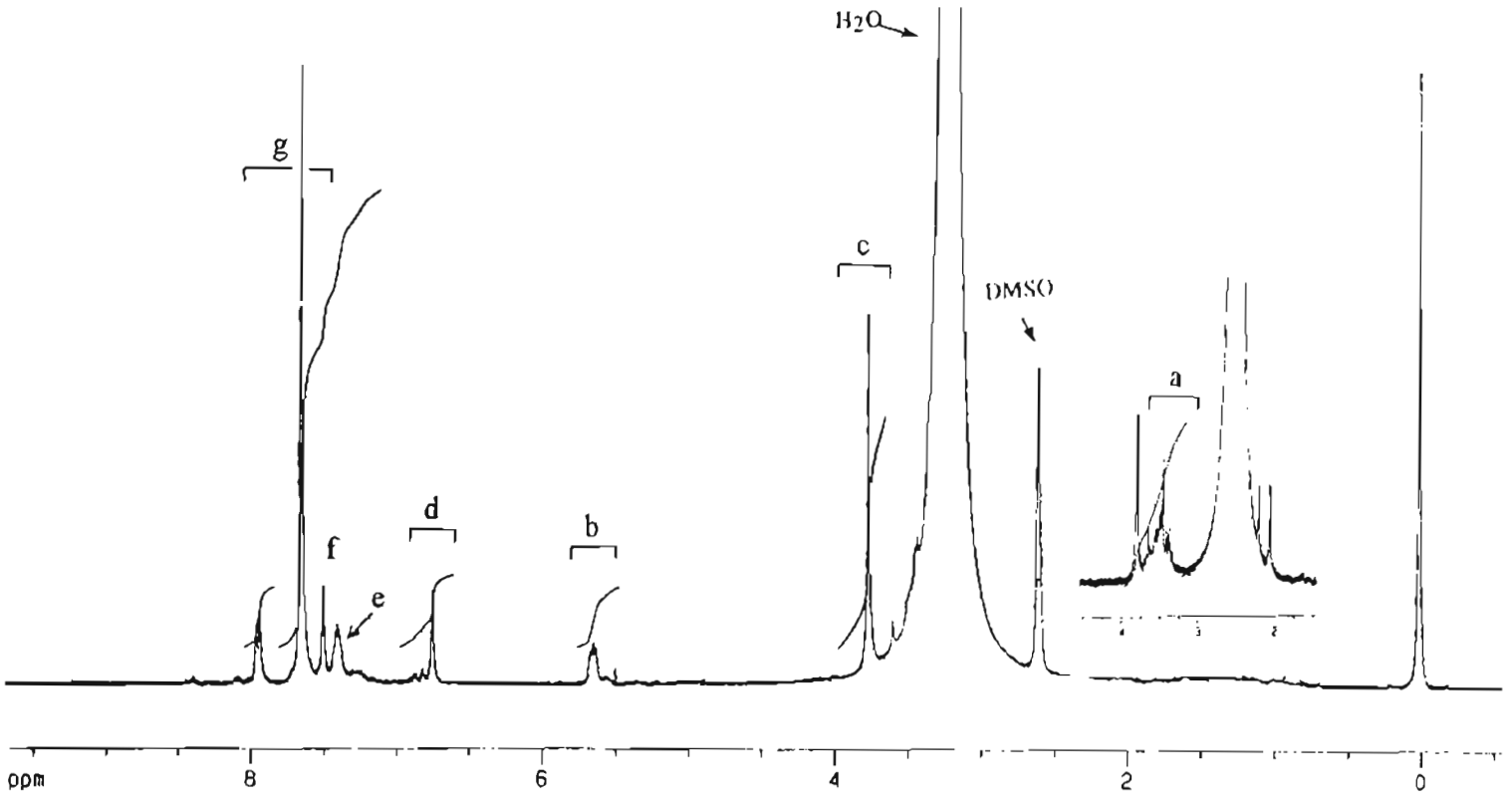

δ (300 MHz, $CDCl_3$ - DMSO-d_6)

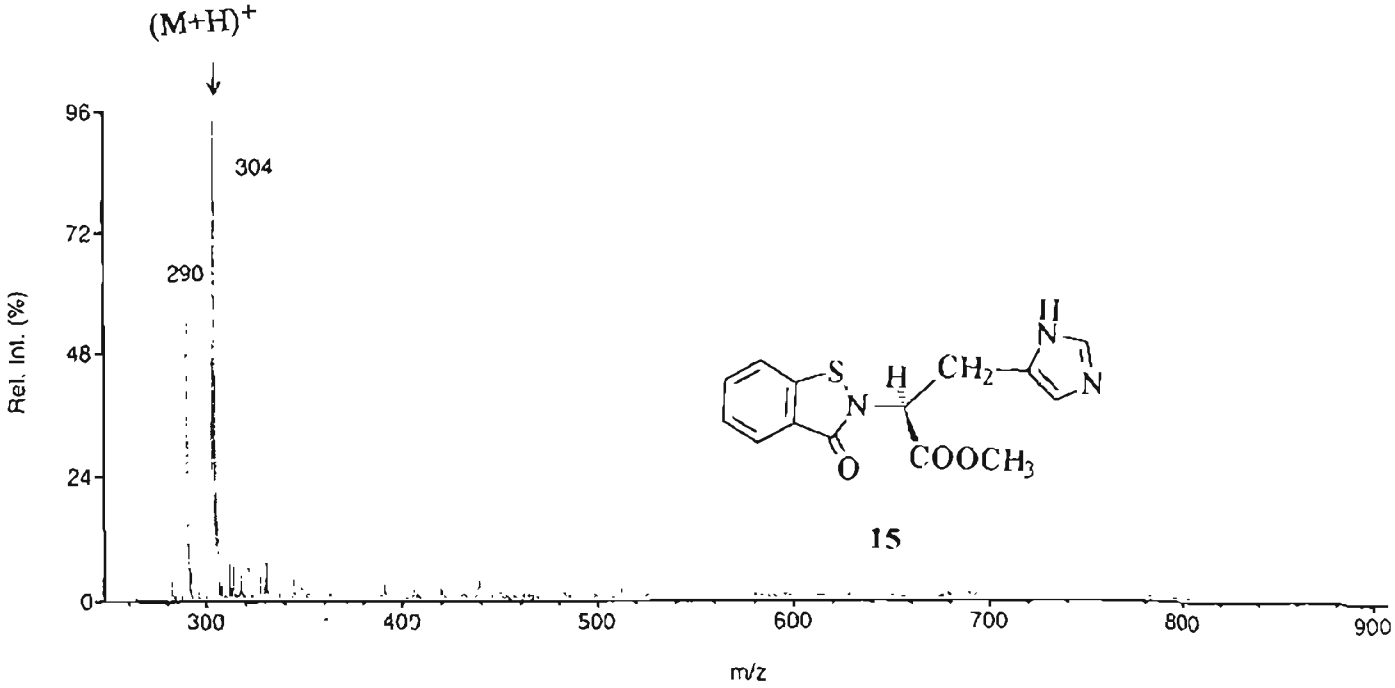

15

FAB mass spectrum

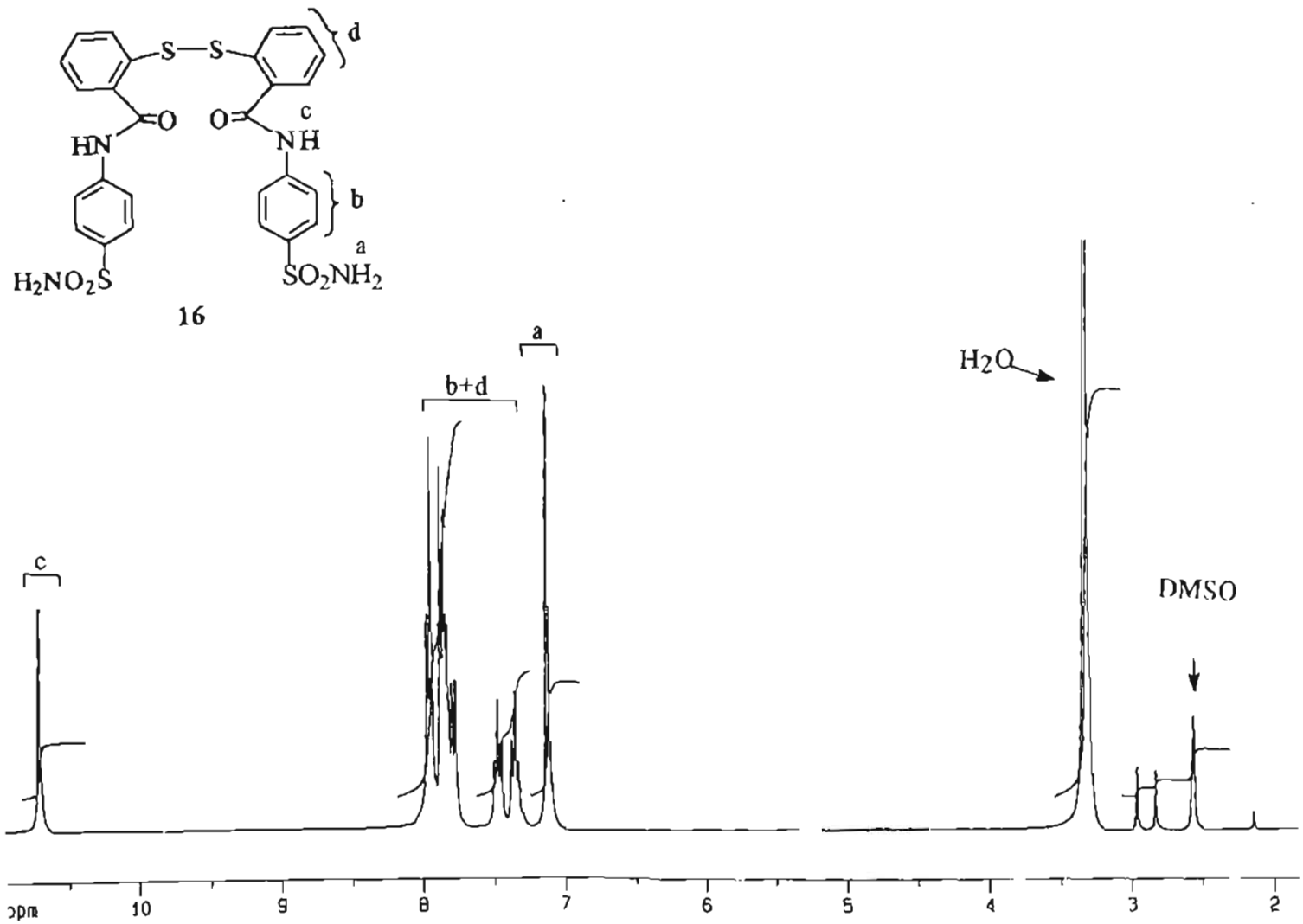

δ (300 MHz, DMSO-d_6)

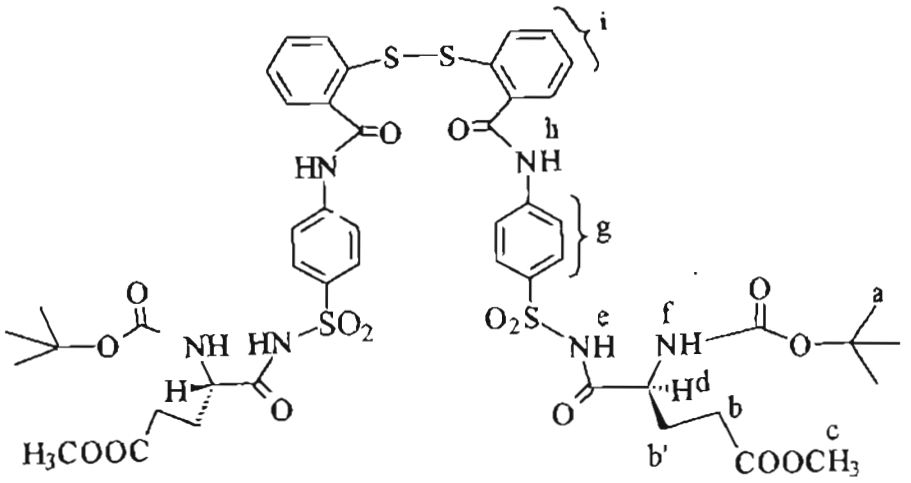

17

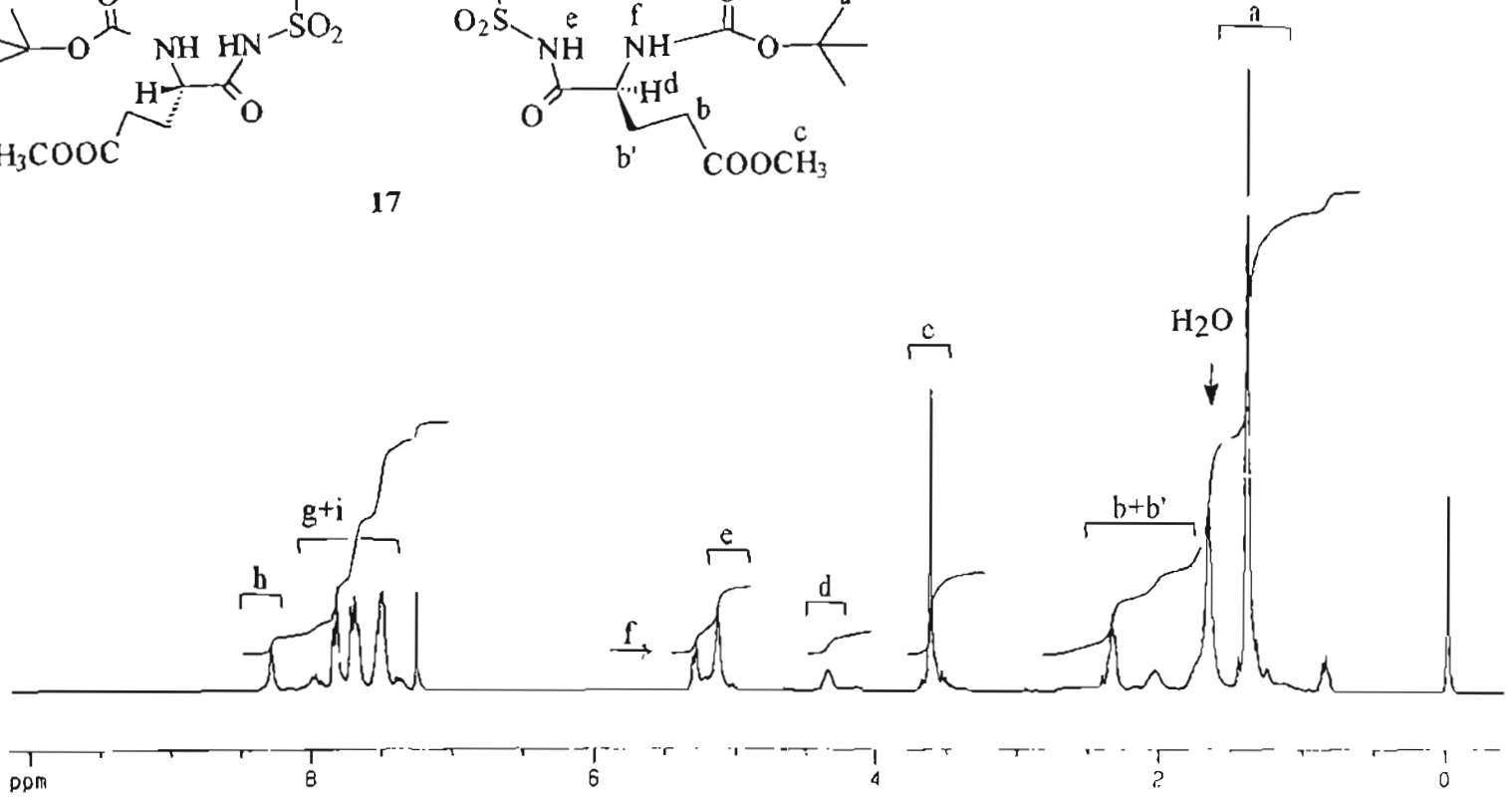

δ (300 MHz, $CDCl_3$)

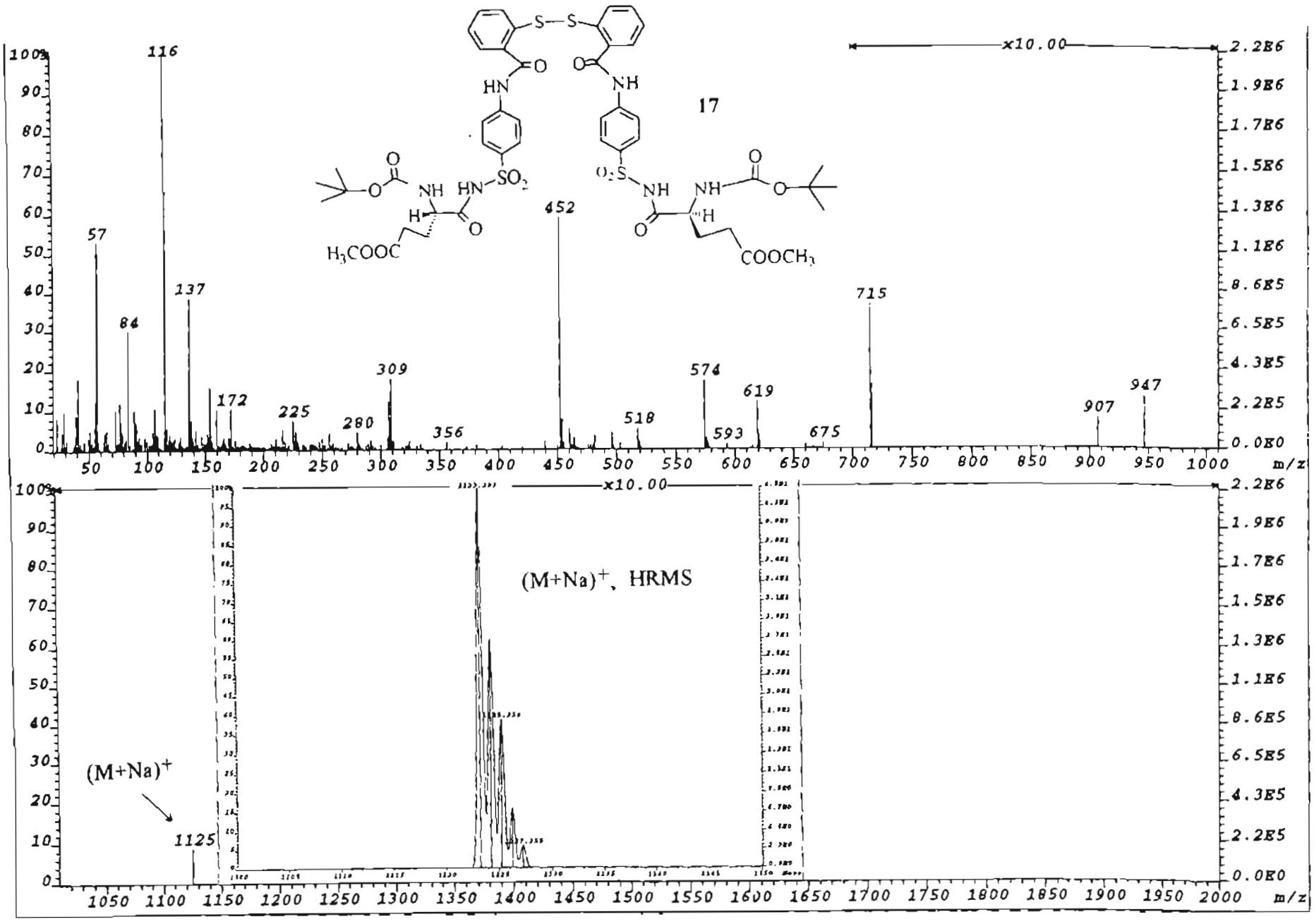

FAB mass spectrum

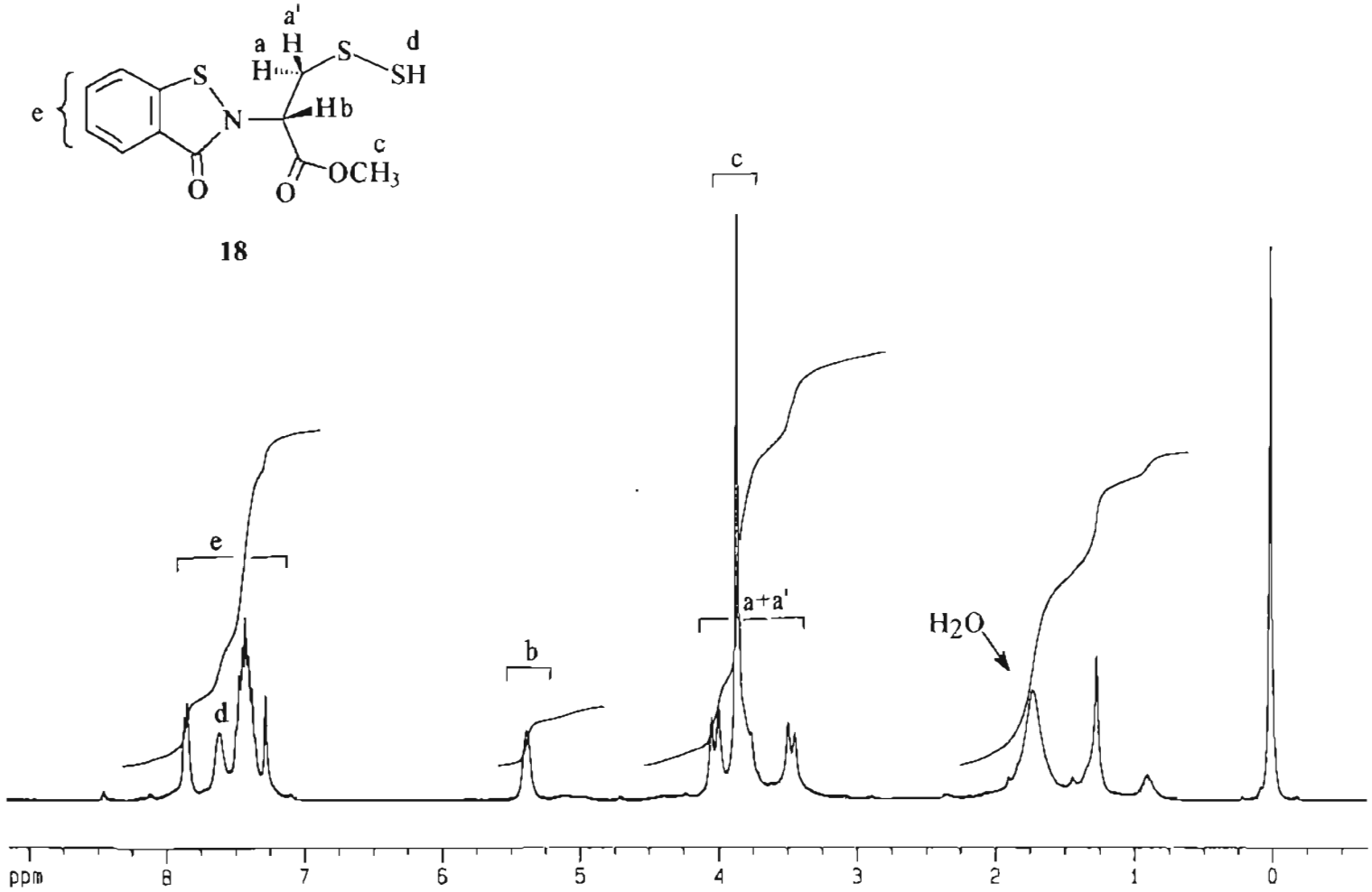

δ (300 MHz, $CDCl_3$)

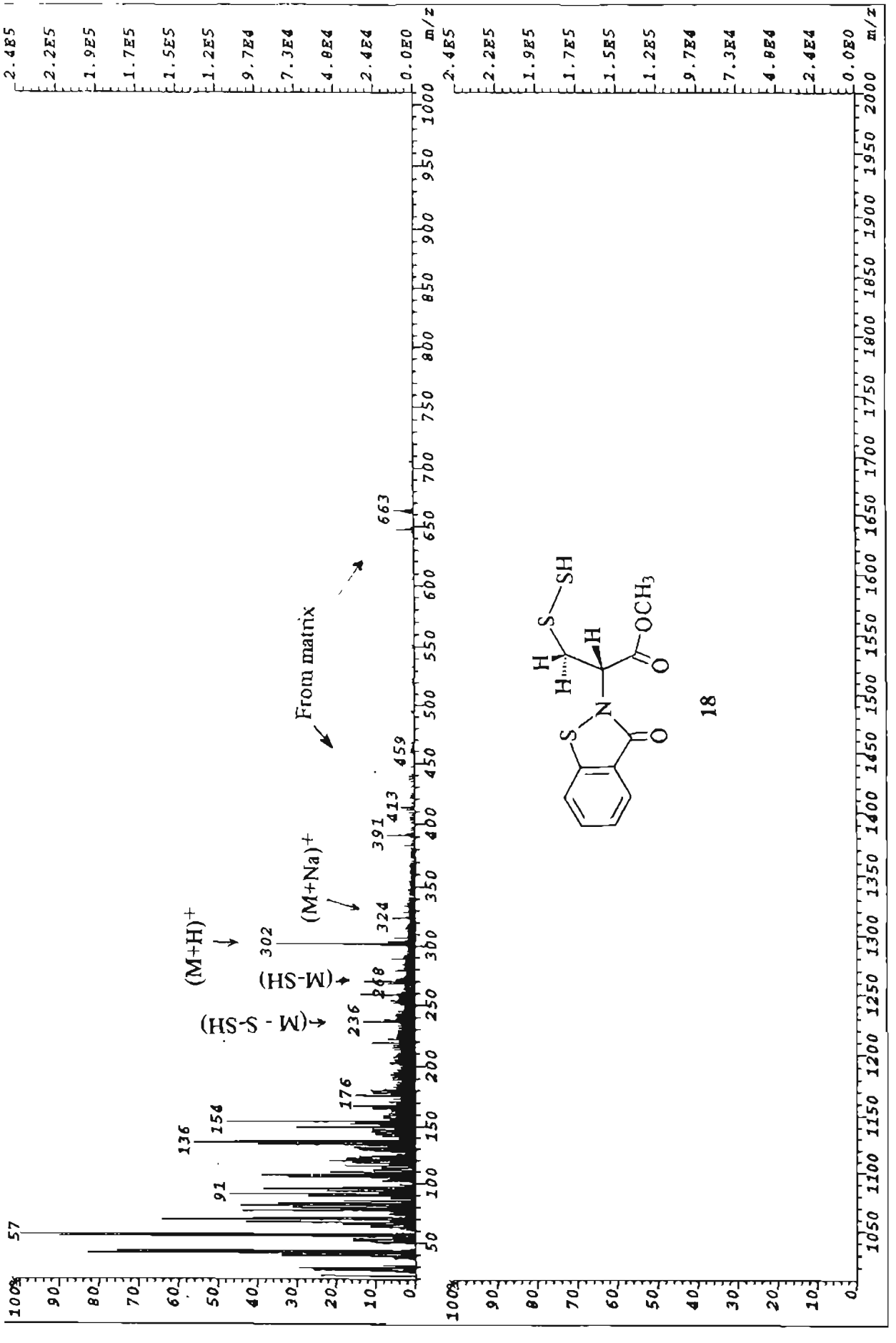

FAB mass spectrum

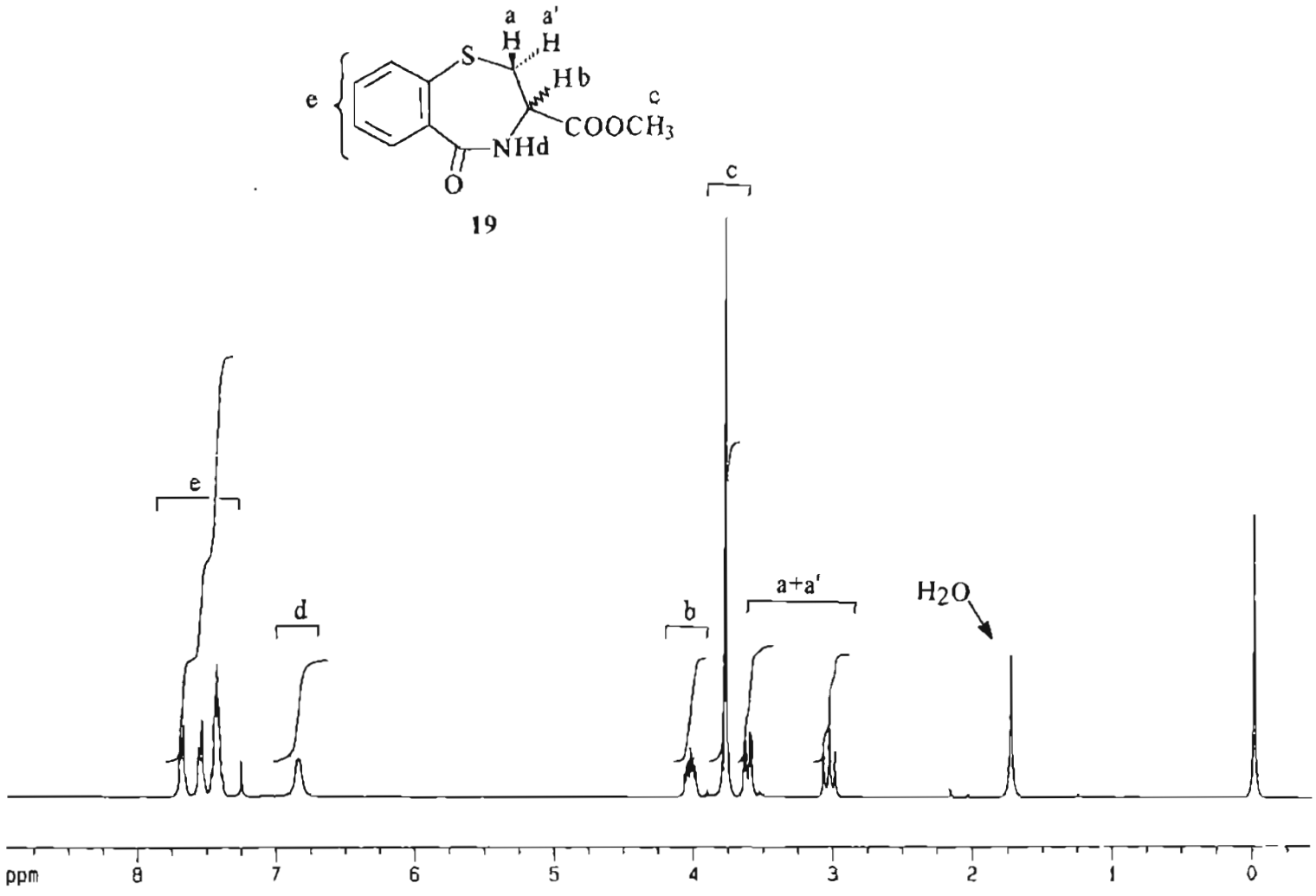

δ (300 MHz, $CDCl_3$)

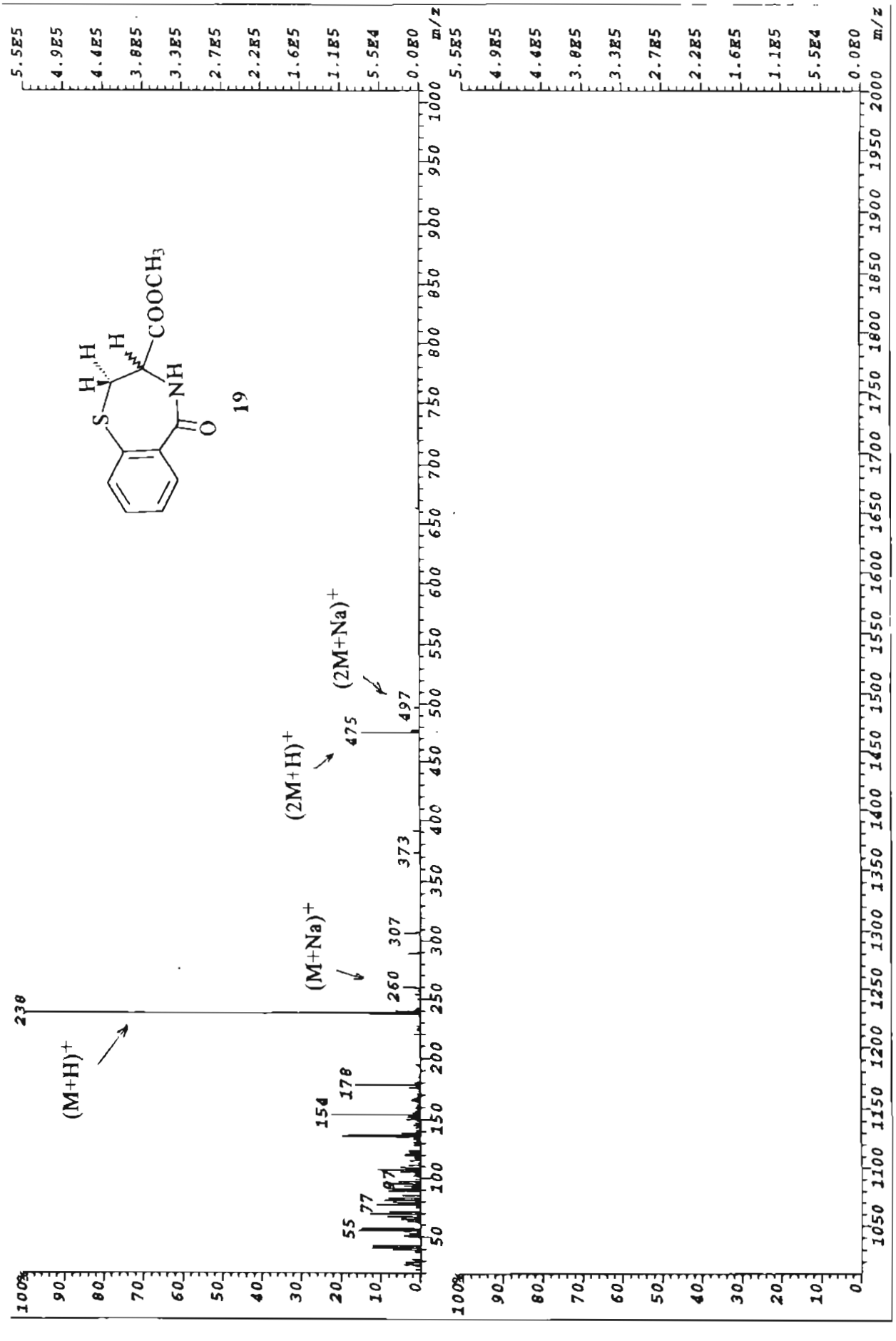

FAB mass spectrum

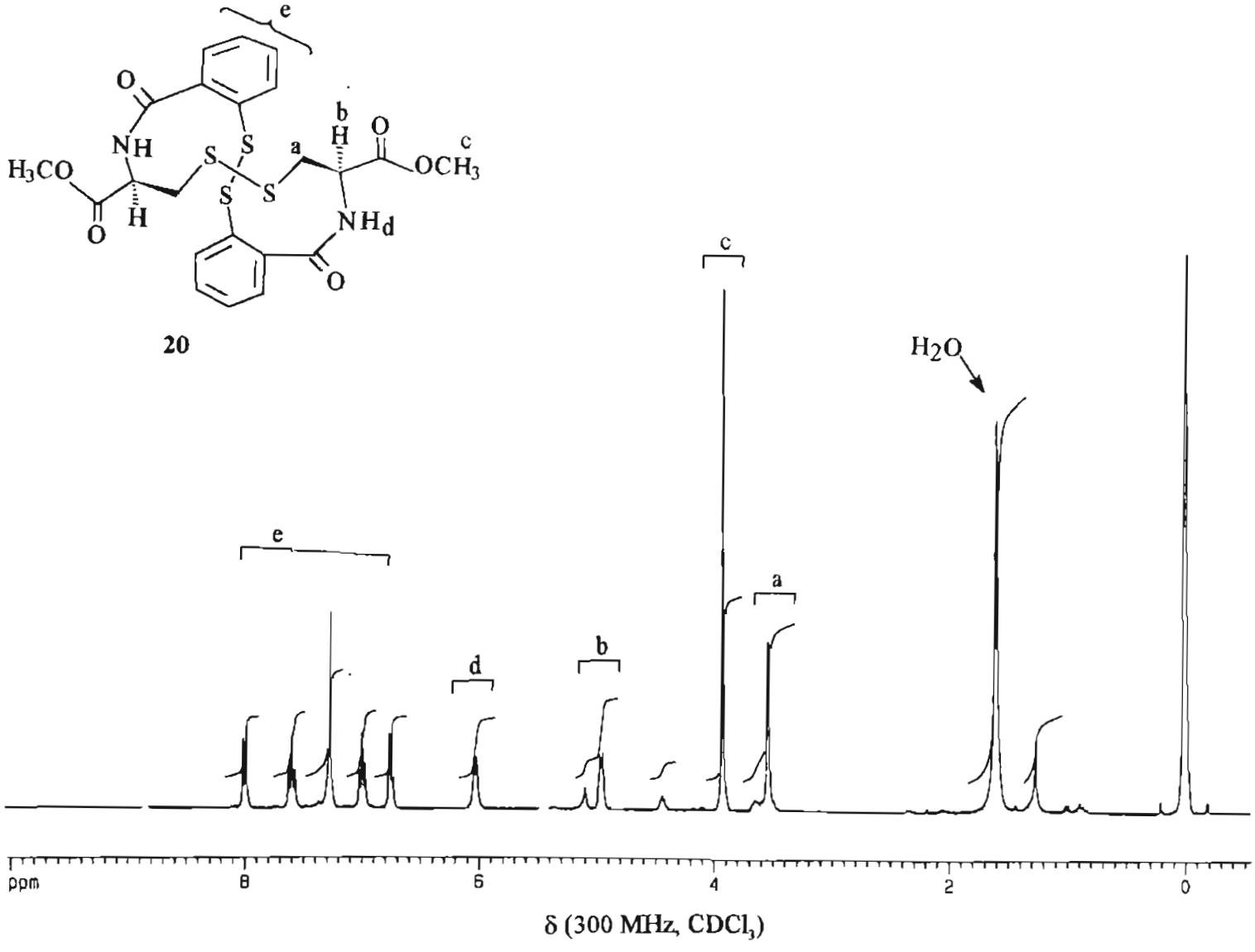

δ (300 MHz, $CDCl_3$)

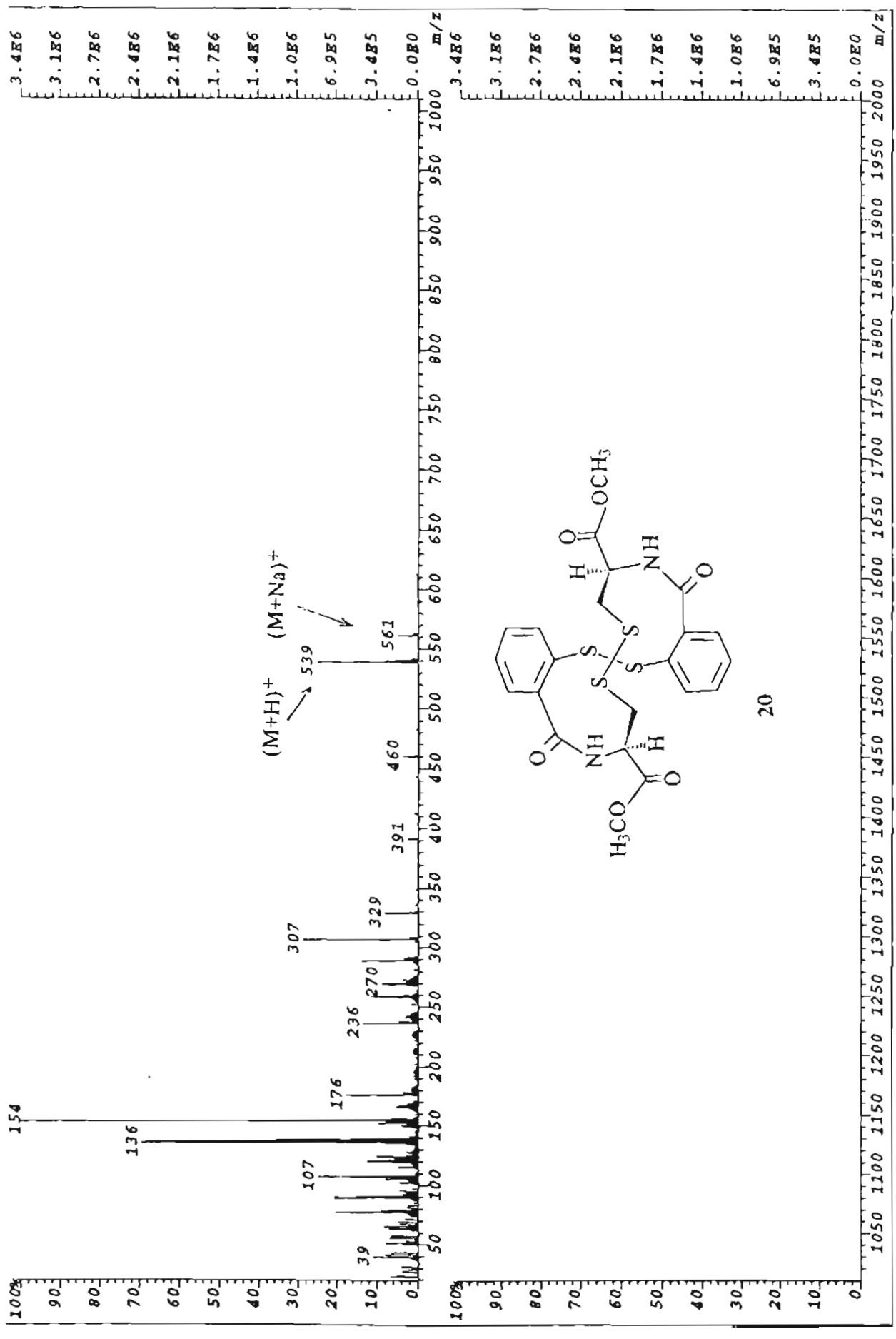

FAB mass spectrum

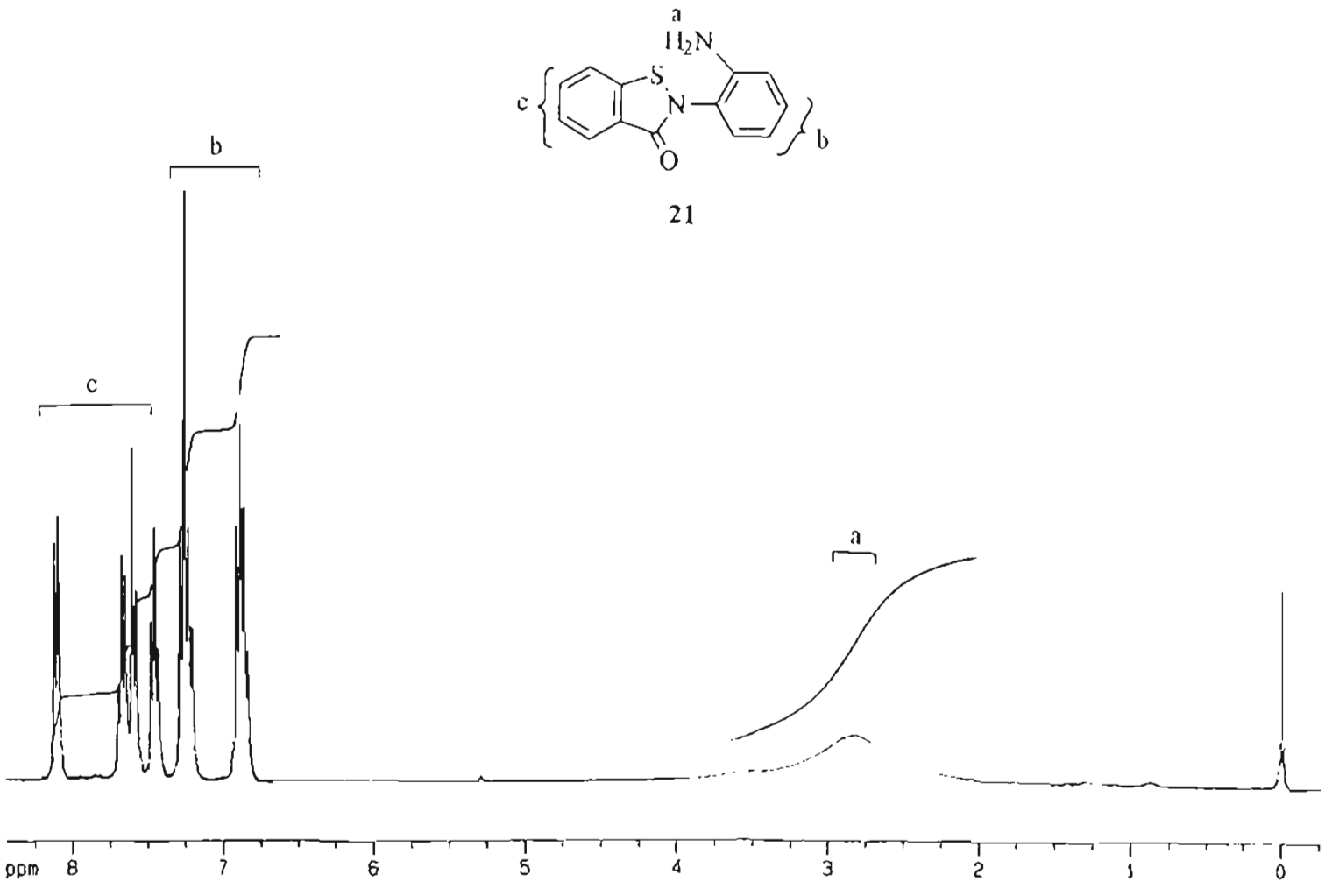

δ (300 MHz, $CDCl_3$)

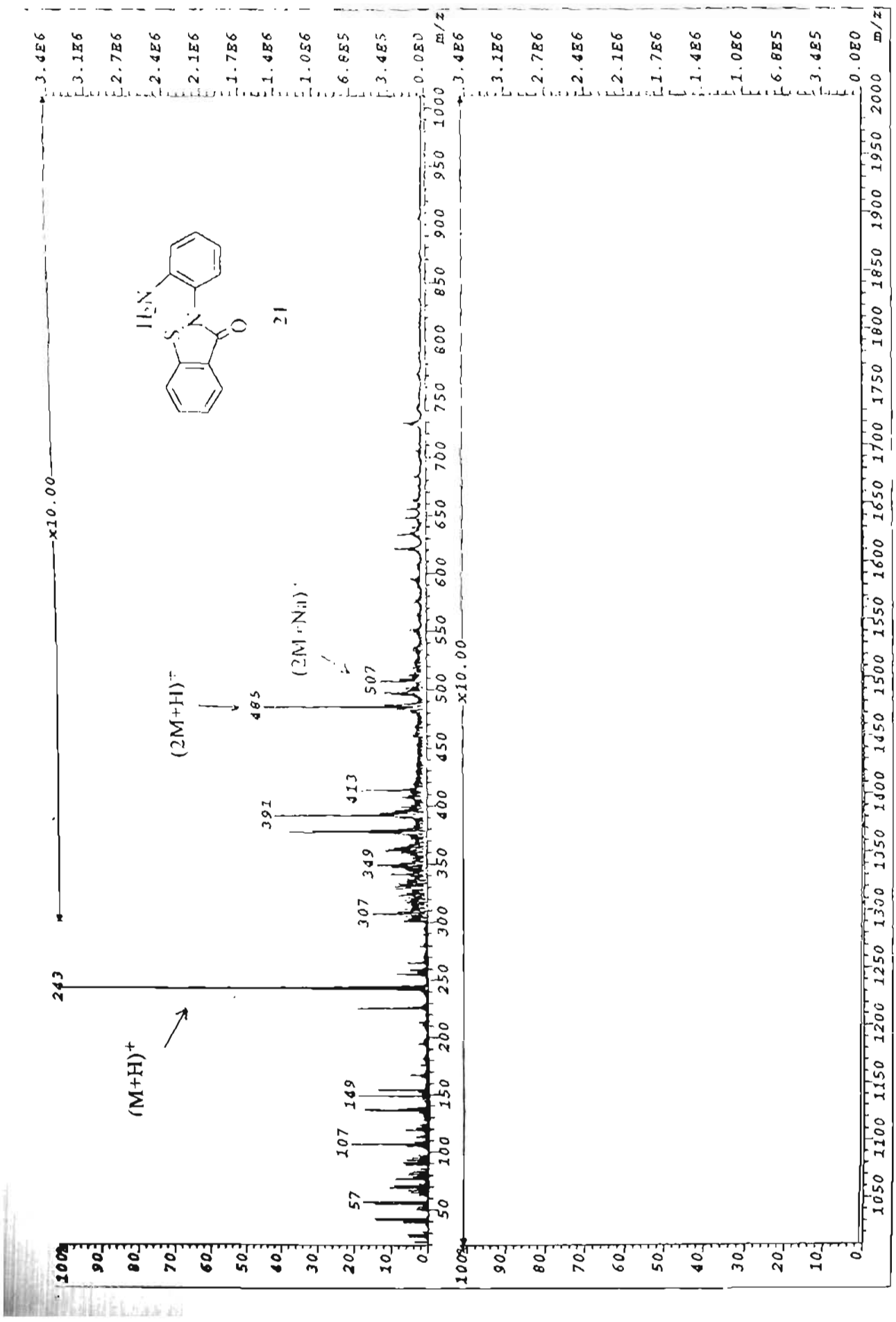

FAB mass spectrum

1) *Advances in Protein Chemistry*, vol 42, Academic Press, p283

2) *Encyclopedia of mol. Biol & Mol medicine* vol 6 - Zinc finger DNA binding motifs L. Fairall and J. W. R.. Schwabe, pp 327 - 336.

3) H. A. Godwin and J. M. Berg, *J. Am. Chem. Soc.*, **1996**, 118, 6514-15

4) Lynne Regan, *Tibs*, **1995**, 281 - 285

5) N. Jayaraman, Ph.D Thesis (**1993**), IIT Kanpur, India, p 103.

6) a) P. J. Tummino, J. D. Scholten, P. J. Harvey, T. P. Holler, L. M. Maloney, R. Gagliotti, J. Domagala and D. Hupe, *Proc. Natl. Acad. Sci. USA*, **1996**, 93, 969-973. b) W. R. Rice, J. A. Turpin, C. A. Shaeffer, L. Graham, D. Clanton, R. W. Buckheit Jr, D. Zaharevitz, M. F. Summers, A.Wallqvist and D. G. Covell, *J. Med. Chem*, **1996**, 39, 3606-3616. c) J. M. Domagala, J. P. Bader, R. D. Gogliotti, J. P. Sanchez, M. A. Stier, Y. Song, J. V. N. Vara Prasad, P. J. Tummino, J. Scholten, P. Harvey, T. Holler, S. Gracheck, D. Hupe, W. G. Rice and R. Schultz. *Bioorganic and Medicinal Chemistry*, **1997**, 5, 3, 569-579

7) R. A. Mooney and Robert Landick, *Cell*, **1999**, 98, 687 - 690

8) a) R. R. Burgess, *J. Biol. Chem*, **1969**, 244, 6168-6176

b) P. H. von Hippel, D. G. Bear, W. D. Morgan and J. A. Mc Swiggen, *Ann. Rev. Biochem*, **1984**, 53, 389-446

9) R. R. Burgess, A. A. Travers, J. J. Dunn and E. K. F. Bautz, *Nature*, **1969** 221, 43-46.

10) D. Hinkle and M. Camberline, *J. Mol. Bio*, **1972**, 70, 157-185

11) W. Zillig, K. Zechel, D. Rabussay, M. Schachner, V. S. Sethi, P. Palm, A. Heil and W. Seifert, *Cold Spring Harbor Symp.* Quant Biol, **1971**, 35, 47-58

12) a) S. R. Panny, A. Heil, M. Mazur, P. Palm, W. Zillig, S. Z. Mindlin, T. S. Ilyma and R. B. Khesin, *FEBS Lett*, **1974**, 48, 241-245 b) M. Suguira, K. Segawa, K. Yoshinaga, F. Yu, N. Ito, S. Yashuda and Y. Hirota, *Biochem, Biophys. Res.Commun*, **1977**, 76, 739-745

13) a) M. C. Scrutton, C. -W. Wu and D. A. Golthwait, *Proc. Natl. Acad. Sci. USA*, **1971**, 68, 2497-2501 b) D. Chatterji and F. Y. -H. Wu, *Biochemistry*, **1982**, 21, 4651-4656. c) D. Solaiman and F. Y. -H. Wu, *Biochemistry*, **1984**, 23, 6369-6377

14) D. Chatterji and K. Guruprasad, *Curr. Sci*, **1988**, 57, 376-377

15) S. Ranganathan and N. Jayaraman, *J. Chem. Soc. Chem. Commun.*, **1991**, 934

16) J. A. Loo, T. P. Holler, J. Sanchez, R. Gogliotti, L. Maloney, and M. D. Reily, *J. Med. Chem.* **1996**, 39, 4313-4320

17) P. V. Ramachandran, Ph.D Thesis, **1983**, p 170, IIT Kanpur, India.

18) S. Mayalagu, M. Putturajan, D. Chatterji, *Gene*, **1997**, 190, 77 - 85.